The Role of Inflammation in Vascular Function and Pregnancy Outcome in the Pregnant Stroke Prone Spontaneously Hypertensive Rat

Heather Yvonne Small BSc (Hons), MRes

This being a thesis submitted for the degree of Doctor of Philosophy (PhD) in the Institute of Cardiovascular and Medical Sciences, University of Glasgow, August 2016

BHF Glasgow Cardiovascular Research Centre

Institute of Cardiovascular and Medical Sciences

College of Medical, Veterinary, and Life Sciences

University of Glasgow

Author Declaration

I declare that this thesis has been written by myself and is a record of research performed by myself with the exception of the following experiments. Where an independent operator was required for quantification of histology, Hannah Morgan (Institute of Cardiovascular and Medical Sciences) was this operator for uteroplacental sections in Chapter 3 and 4 and Sheon Mary (Institute of Cardiovascular and Medical Sciences) and Dr. Shana Coley (Institute of Infection, Immunity & Inflammation) were the operators for the kidney sections in Chapter 6. Wire myography of WKY mesenteric arteries in Chapter 3 was carried out by Hannah Morgan (Institute of Cardiovascular and Medical Sciences). Urinary electrolyte and metabolite analysis in Chapter 6 was carried out by Elaine Butler (Institute of Cardiovascular and Medical Sciences). Kidney sections in Chapter 6 were visualised using the Leica Aperio slide scanner by Clare Orange (University Pathology Unit). Running and preliminary analysis of capillary electrophoresis mass spectrometry of urine samples in Chapter 6 was carried out together with Sheon Mary (Institute of Cardiovascular and Medical Sciences).

Any contribution from others has been clearly referenced and reproduced with permission. This work has not been submitted previously for a higher degree and was supervised by Professor Christian Delles and Dr. Delyth Graham.

Acknowledgments

Firstly, I am very grateful to my supervisors: Professor Christian Delles and Dr. Delyth Graham. I am thankful for the many opportunities that have been afforded to me during this PhD. Thank you for your ever present support and wisdom which has guided me to completing this thesis. Equally as important, thank you to the British Heart Foundation for making my PhD possible through their financial support.

Thank you to everyone in the Glasgow Cardiovascular Research Centre and West Medical Building who I have had the pleasure of working with over the last four years. A special mention to the Graham/McBride group for your guidance during Thursday morning lab meetings. In particular, thank you to Elisabeth Beattie for her patience in teaching me myography and invaluable help organising all of the animal studies. Thank you to Christine, Charlie and the BHF GCRC biological services team for all your assistance. Thank you to Professor Tomasz Guzik and Ryszard Nosalski for their time and patience in teaching me flow cytometry and in helping me to analyse the results. Finally, shout out to #team313 (past and present members) for all the laughs, hugs and coffee.

I would like to dedicate this thesis to my amazing friends and family. Thank you for always being there for me when I needed you. Special credit to my mum, my sister and my ever-patient husband who have lived through every high and low of this PhD with me.

“So stick to the fight when you're hardest hit—

It's when things seem worst that you must not quit.”

An Excerpt from Don’t Quit by John Greenleaf Whittier.

This poem is in the public domain.

Table of Contents

Author Declaration 2
Acknowledgments 3
Table of Contents 5
List of Figures 9
List of Tables 12
Abbreviations, Acronyms & Symbols 13
Presentations, Published Work, Awards and Prizes 17
Summary 22
Chapter 1 Introduction 26
1.1 The Cardiovascular System 26
1.1.1 Blood Pressure Regulation 31
1.1.2 Mechanisms of Vascular Contraction and Relaxation 36
1.2 Cardiovascular Disease 41
1.2.1 Hypertension 41
1.3 Inflammation & Hypertension 49
1.3.1 Activation of the Innate Immune System in Hypertension 52
1.3.2 Natural Killer Cells 52
1.3.3 Tumor Necrosis Factor α (TNFα) 58
1.4 Animal Models of Hypertension 65
1.5 Pregnancy & the Cardiovascular System 73
1.5.1 Cardiovascular System Adaptation to Pregnancy in Humans and Rodents 73
1.5.2 Mechanisms of Pregnancy-Dependent Cardiovascular Remodelling in Humans and Rodents 76
1.5.3 Blood Pressure during Pregnancy in Humans and Rodents 77
1.6 Animal Models of Human Pregnancy 81
1.6.1 Placentation in Humans and Rats 81
1.6.2 Pregnancy-Dependent Uterine Artery Remodelling During Pregnancy in Humans and Rodents 84
1.7 Hypertensive Disorders of Pregnancy 92
1.7.1 Pregnancy as a Cardiovascular Stress Test 92
1.7.2 Pregnancy-Specific Hypertensive Disorders 94
1.7.3 Chronic Hypertension during Pregnancy 96
1.7.4 Rodent Models of Hypertensive Disorders of Pregnancy 99
1.8 The SHRSP as a Model of Chronic Hypertension during Pregnancy 102
1.8.1 Deficient Uterine Artery Remodelling in the SHRSP 102

1.9 Hypothesis & Aims....104
Chapter 2 General Materials & Methods....105
2.1 General Laboratory Practice....105
2.2 Animals....106
2.2.1 Animal Strains....106
2.2.2 Animal Housing....106
2.3 Animal Procedures....106
2.3.1 Time Mating....106
2.3.2 Metabolic Cage....107
2.3.3 Radiotelemetry Probe Implantation....107
2.3.4 Tissue Collection Protocols....108
2.4 Gene expression....109
2.4.1 Ribonucleic Acid (RNA) Extraction....109
2.4.2 Reverse Transcription Polymerase Chain Reaction (RT-PCR)....110
2.4.3 Quantitative Polymerase Chain Reaction (qPCR)....112
2.5 Western blot....114
2.5.1 Protein Extraction for Western Blot....114
2.5.2 Western Blot....115
2.5.3 Membrane Blocking & Antibody Incubation....115
2.5.4 Western Blot Development & Analysis....116
2.6 Histology....116
2.6.1 Tissue Preparation for Histology....116
2.6.2 Haematoxylin and Eosin Stain....116
2.6.3 Threshold Quantification of Staining Using Image J....117
2.7 Statistical Analysis....117
Chapter 3 Characterisation of the SHRSP as a Rat Model of Chronic Hypertension in Pregnancy....119
3.1 Introduction....119
3.2 Materials & Methods....121
3.2.1 Animals....121
3.2.2 Identification of Implantation Sites using Evans' Blue....121
3.2.3 Enzyme Linked Immunosorbent Assay (ELISA)....122
3.2.4 Polymerase Chain Reaction (PCR)....122
3.2.5 Western Blot for Cleaved Capsase-3....123
3.2.6 Histology....123
3.3 Results....124
3.3.1 Maternal Adaptation to Pregnancy in the SHRSP and WKY....124
3.3.2 Placental Biology is Altered in Pregnant SHRSP....132
3.3.3 Blastocyst Implantation is Not Impaired in the SHRSP....138

3.3.4 Resorption frequency is increased in SHRSP 138
3.3.5 Fetal and Placental Growth is Not Restricted in the SHRSP 139
3.4 Discussion 141
Chapter 4 Excess TNFα Signalling Plays a Central Role in Deficient Uterine Artery Function in the SHRSP 145
4.1 Introduction 145
4.2 Materials & Methods 146
4.2.1 Etanercept Treatment 146
4.2.2 Radiotelemetry Probe Implantation 146
4.2.3 Doppler Ultrasound 147
4.2.4 Placental Tissue Explants 149
4.2.5 TNFα Measurement in Plasma, Urine and Explant Media using Enzyme Linked Immunosorbent Assay (ELISA) 149
4.2.6 Pressure Myography 149
4.2.7 Wire Myography 150
4.2.8 Periodic acid-Schiff Stain 150
4.2.9 Quantitative PCR (qPCR) for *Tnfr1* Expression 151
4.2.10 Western Blot for Phosphorylated NFκB 151
4.3 Results 151
4.3.1 Tumor Necrosis Factor α (TNFα) is a Promising Target Molecule in Pregnant SHRSP 151
4.3.2 Etanercept Reduces Systolic Blood Pressure in the SHRSP 153
4.3.3 Etanercept Improves Placenta and Litter Size in the SHRSP 155
4.3.4 Etanercept Improves Uterine Artery Function in Pregnant SHRSP 158
4.3.5 Etanercept Affects the TNFα Pathway in the Placenta 162
4.4 Discussion 164
Chapter 5 The Role of Natural Killer Cells in SHRSP Pregnancy 168
5.1 Introduction 168
5.2 Materials & Methods 169
5.2.1 Etanercept Treatment 169
5.2.2 Flow Cytometry 169
5.2.3 Immunohistochemistry for Granzyme B 171
5.2.4 Cytokine Array 171
5.2.5 Cell Free DNA (cfDNA) Isolation from Placental Explant Media 172
5.3 Results 172
5.3.1 CD3- CD161+ NK Cells are increased in the Maternal Circulation and Placenta in Pregnant SHRSP 172
5.3.2 CD3- CD161+ NK Cells are a Source of Excess TNFα in the Maternal Circulation and Placenta in Pregnant SHRSP 174

5.3.3 Etanercept Reduces the Population of CD3- CD161+ NK Cells in the Placenta of Pregnant SHRSP 179
5.3.4 Etanercept Treatment Reduces CD161 Expression and Granzyme B Production in NK cells from the Placenta of Pregnant SHRSP. 182
5.3.5 Peptide Array Demonstrates that Placenta from SHRSP is a Site of Global Inflammation 184
5.3.6 The Placenta from SHRSP Reveals Increased Shedding of DNA 188
5.4 Discussion 188
Chapter 6 Kidney Dysfunction and Urinary Peptidomics in Pregnant SHRSP ... 193
6.1 Introduction 193
6.2 Materials & Methods 195
6.2.1 Animals 195
6.2.2 Histology 195
6.2.3 Urinary Peptidomics 196
6.2.4 Quantitative PCR (qPCR) for *Umod* Expression 199
6.3 Results 199
6.3.1 The SHRSP Kidney is increased in Size Relative to the WKY but does not Exhibit Histological Abnormalities 199
6.3.2 The Urinary Peptidome is altered during Pregnancy and between WKY and SHRSP 204
6.3.3 Uromodulin is increased in the Urine and Kidney of Pregnant SHRSP relative to WKY 210
6.4 Discussion 212
Chapter 7 General Discussion 215
Appendix I: Laboratory-Prepared Solutions 223
Appendix II: Sacrifice Protocol Sheet 226
Appendix III: 788 urinary peptides altered between WKY and SHRSP 227
Appendix IV: 123 urinary peptides altered between WKY and SHRSP at all time points (NP, GD12 and GD18) or GD12 & GD18 only 233
Appendix V: Sequenced peptides list 237
References 240

List of Figures

Figure 1-1: The Cardiovascular System. 27
Figure 1-2: The Structure of a Vessel. 29
Figure 1-3: Baroreceptor Reflex Regulating Blood Pressure. 33
Figure 1-4: The Renin Angiotensin Aldosterone System (RAAS). 35
Figure 1-5: G_q Coupled Receptor Phospholipase C Mechanism of Vascular Smooth Muscle Cell Contraction. 38
Figure 1-6: The 2014 Update on the Paige Mosaic Model of Hypertension. 45
Figure 1-7: The Effects of Sex Hormones on Blood Pressure Regulation. 48
Figure 1-8: The Main Cell Types Involved from the Innate and Adaptive Immune System in Hypertension. 51
Figure 1-9 The Natural Killer (NK) Cell-Target Cell "Zipper" in Humans. 54
Figure 1-10: Summary of TNFα Signalling through TNFR1. 60
Figure 1-11: TNFα Levels and Blood Pressure Regulation. 62
Figure 1-12: Tumor Necrosis Factor-α in Vascular Dysfunction. 64
Figure 1-13: Genealogy of the Stroke Prone Spontaneously Hypertensive Rat. 70
Figure 1-14: Characteristics of the Stroke Prone Spontaneously Hypertensive Rat. 71
Figure 1-15: Blood Pressure Profile of Normotensive Pregnancy and Pregnancy Associated with Hypertensive Complications. 78
Figure 1-16: Blood Pressure Profile in the normotensive WKY rat and the Stroke prone Spontaneously Hypertensive Rat (SHRSP). 80
Figure 1-17: Comparative Placentation between Rodents and Humans. 83
Figure 1-18: The Uterine Circulation in Humans and Rodents 85
Figure 1-19: Mechanisms of Uterine Spiral Artery Remodelling. 88
Figure 1-20: Known and Hypothetical Mechanisms of Pregnancy-Induced Uterine Artery Remodelling. 91
Figure 1-21: Pregnancy as a Cardiovascular Stress Test. 93
Figure 1-22 The Pathology of Pre-eclampsia. 95
Figure 1-23 Abnormal Uterine Artery Remodelling in Response to Pregnancy in the Stroke Prone Spontaneously Hypertensive Rat (SHRSP) 103
Figure 2-1 Arteries used for myography studies: 109
Figure 2-2 Example results from Agilent RNA quality control for WKY placenta. 110
Figure 3-1 Nifedipine treatment does not improve uterine artery structure or function in the SHRSP. 120
Figure 3-2 Maternal weight gain over pregnancy is reduced in the SHRSP relative to the WKY. 126
Figure 3-3 Heart and kidney weight are increased in SHRSP relative to the WKY. 127
Figure 3-4 SHRSP exhibit features of left ventricular hypertrophy during pregnancy. 129
Figure 3-5 Maternal plasma biomarkers associated with hypertensive pregnancy are altered in the SHRSP. 131
Figure 3-6 qPCR markers for placental layers. 134
Figure 3-7 Placental markers of hypoxia are increased in placenta from pregnant SHRSP. 135
Figure 3-8 The SHRSP placenta at GD18 exhibits increased free blood and cell death. 136
Figure 3-9 The SHRSP placenta exhibits premature glycogen cell loss from the junctional zone. 137

Figure 3-10 Blastocyst implantation is not altered in the SHRSP relative to the WKY.....138
Figure 3-11 Example of a fetal resorption. 139
Figure 3-12 Fetal and placental weight is not altered in the SHRSP relative to the WKY.....140
Figure 4-1: Representative ultrasound image of the uterine artery used for Doppler measurements. 148
Figure 4-2 TNFα is increased in the SHRSP relative to the WKY. 152
Figure 4-3: Etanercept treatment significantly reduces systolic blood pressure from GD 12-21 of pregnancy in the SHRSP. 154
Figure 4-4: Etanercept treatment significantly improves glycogen cell loss from the placenta and litter size in the SHRSP. 156
Figure 4-5: Maternal, fetal and placental weight are unaffected by etanercept treatment in the SHRSP. 157
Figure 4-6 Etanercept treatment improves uterine artery function in pregnant SHRSP but not structure. 159
Figure 4-7 Etanercept treatment does not alter third-order mesenteric artery function in the SHRSP. 160
Figure 4-8 Etanercept treatment improves uterine artery blood flow in pregnant SHRSP.....161
Figure 4-9 Etanercept Treatment Alters the TNFα signalling pathway in the Placenta. 163
Figure 5-1 CD3- CD161+ natural killer cells are significantly increased in pregnant SHRSP.....174
Figure 5-2 CD161+ cells are a source of excess TNFα in pregnant SHRSP maternal circulation and placenta. 176
Figure 5-3 TNFα producing CD161+ cells are increased in a pregnancy dependent manner in SHRSP.....177
Figure 5-4 TNFα production from CD3+ cells and other CD45+ cells is not significantly different between WKY and SHRSP.....178
Figure 5-5 Flow cytometry panel in maternal blood from pregnant WKY, SHRSP and SHRSP treated with etanercept. 180
Figure 5-6 Flow cytometry panel in placenta from pregnant WKY, SHRSP and SHRSP treated with etanercept. 181
Figure 5-7 Etanercept reduces granzyme B-producing CD161+ cells in the SHRSP placenta. 183
Figure 5-8 Granzyme B positive cells are increased in placenta from SHRSP....184
Figure 5-9 Representative array for WKY, SHRSP and SHRSP treated with etanercept.....186
Figure 5-10 The array profile is altered in GD18 placenta from SHRSP relative to WKY and SHRSP treated with etanercept. 187
Figure 5-11 Cell free DNA is increased in media of placental explants from SHRSP relative to WKY. 188
Figure 6-1 Normal renal structural and functional changes in response to pregnancy.....193
Figure 6-2 The urinary peptidome. 195
Figure 6-3 Kidney size is increased in non-pregnant and pregnant (GD18) SHRSP relative to WKY. 200
Figure 6-4 Glomeruli distribution is altered in non-pregnant and pregnant (GD18) SHRSP relative to WKY. 201
Figure 6-5 The SHRSP does not show histological abnormalities in the glomeruli or vessels of the kidney 203

Figure 6-6 Contour plots for peptide mass fingerprint in WKY and SHRSP at pre-pregnancy (NP), gestational day (GD) 12 and 18. 205
Figure 6-7 Venn diagram for various comparisons. 206
Figure 6-8 Principal component analysis of 123 differentially expressed peptides in WKY and SHRSP at pre-pregnancy (NP), gestational day (GD) 12 and 18. 208
Figure 6-9 Heat map analysis of 123 differentially expressed peptides in WKY and SHRSP at pre-pregnancy (NP), gestational day (GD) 12 and 18. 209
Figure 6-10 Urinary uromodulin peptides are increased in the SHRSP relative to WKY in a pregnancy-dependent manner. 211
Figure 6-11 Gene expression of *Umod* in kidney tissue from WKY and SHRSP pre-pregnancy (NP) and gestational day (GD) 18. 212
Figure 7-1 Excess TNFα in pregnant SHRSP is central to the pathology in this model.....215
Figure 7-2 PubMed hits comparing search terms for "pre-eclampsia/preeclampsia" and "chronic hypertension pregnancy".....222

List of Tables

Table 1-1 Classification of Arteries. 31
Table 1-2 Molecular Mechanisms of Endothelium-Dependent Vasorelaxation. ... 40
Table 1-3 JNC-8 Guidelines for Blood Pressure Classification in Adults ≥18. 42
Table 1-4 Existing Inbred Rat Models of Hypertension 67
Table 1-5 Physiological Adaptation of the Maternal Cardiovascular System in Humans and Rodents. 75
Table 1-6 Drugs to treat chronic hypertension in pregnancy. 98
Table 3-1 Raw maternal weights recorded over gestation in the WKY and SHRSP 126
Table 3-2 Resorption frequency is increased in SHRSP at GD14 and GD18. 139
Table 4-1 Etanercept reduces the frequency of SHRSP with spontaneous pregnancy loss 156
Table 6-1 Number of differentially expressed peptides between WKY and SHRSP at different gestational time point comparisons 207

Abbreviations, Acronyms & Symbols

α	Alpha
ß	Beta
δ/Δ	Delta
γ	Gamma
µg	Microgram
µl	Microliter
ACE	Angiotensin converting enzyme
ACOG	American College of Obstetricians and Gynaecologists
ANP	Atrial natriuretic peptide
ANOVA	Analysis of variance
ARRIVE	Animal Research: Reporting of In Vivo Experiments
BCA	Bicinchoninic Acid Assay
PVDF	Polyvinylidene fluoride
BHF	British Heart Foundation
BNP	Brain natriuretic peptide
BP	Blood pressure
Ca^{2+}	Calcium ion
$CaCl_2$	Calcium chloride
cDNA	Complementary deoxyribonucleic acid
CE-MS	Capillary electrophoresis-mass spectrometry
cfDNA	Cell free DNA
CHAMPS	Cardiovascular health after maternal placental syndromes study
CHIPS	Control of Hypertension in Pregnancy Study
Cl^-	Chloride ion
Clr	C-lectin type receptor
CNS	Central nervous system
CO	Carbon monoxide
CO_2	Carbon dioxide
COMT	Catechol-O-methyl transferase
COX	Cyclooxygenase
CSE	Cystathionine γ-lyase
Ct	Threshold cycle
CV	Cardiovascular
CVD	Cardiovascular disease
DAB	3,3'-diaminobenzidine
DAG	Diacylglycerol

Dahl S	Dahl salt sensitive rat model
DBP	Diastolic blood pressure
dCt	Delta Threshold Cycle
dH_2O	Distilled water
DNA	Deoxyribonucleic acid
dNTPs	Deoxynucleotides
DOCA	Deoxycorticosterone acetate
ECM	Extracellular matrix
EDHF	Endothelium derived hyperpolarising factor
EDTA	Ethylenediamine tetra-acetic acid
ELISA	Enzyme linked immunosorbent assay
ENaC	Epithelial sodium channel
eNOS	Endothelial nitric oxide synthase
FBS	Fetal bovine serum
G	Gauge
GD	Gestational day
GFR	Glomerular filtration rate
GWAS	Genome wide association study
H^+	Hydrogen ion
H_2O_2	Hydrogen peroxide
H_2S	Hydrogen sulphide
HBSS	Hanks' buffered saline solution
HCl	Hydrochloric acid
HO-1	Heme oxygenase 1
HR	Heart rate
HRP	Horse radish peroxidase
HRT	Hormone replacement therapy
IFNγ	Interferon gamma
IgG	Immunoglobulin G
IHC	Immunohistochemistry
IL	Interleukin
ILC	Innate lymphoid cell
ILC3	Group 3 innate lymphoid cell
IP_3	Inositol triphosphate
ITAM	Immunoreceptor tyrosine-based activation motifs
ITIM	Immunoreceptor tyrosine-based inhibitory motifs
K^+	Potassium ion
KCl	Potassium chloride

KH_2PO_4	Potassium dihydrogen orthophosphate
LH	Lyon Hypertensive rat
L-NAME	L-nitro-arginine methyl ester
M	Molar
MAPK	Mitogen-activated protein kinase
Mg^+	Magnesium ion
$MgCl_2$	Magnesium chloride
$MgSO_4$	Magnesium sulphate
MHC	Major Histocompatibility Complex
miRNA	MicroRNA
ml	Millilitre
MLCK	Myosin light chain kinase
mM	Millimolar
mmHg	Millimetres of mercury
MMP	Matrix metalloproteinases
mRNA	Messenger RNA
Na^+	Sodium ion
NaCl	Sodium chloride
$NaHCO_3$	Sodium bicarbonate
Na_2HPO_4	Disodium phosphate
NFW	Nuclease free water
ng	Nanogram
NHS	National Health Service
NICE	National Institute for Health and Care Excellence
NK cell	Natural killer cell
NK-T cell	Natural killer- T cell
nNOS	Neuronal nitric oxide synthase
NO	Nitric oxide
NZGH	New Zealand Genetically Hypertensive rat
^oC	Degrees Celsius
PAI-1	Plasminogen activator inhibitor 1
PBS	Phosphate buffered saline
PCR	Polymerase chain reaction
PGL_2	Prostaglandin E2
PIP_2	Membrane phospholipid
PPARγ	Peroxisome proliferator-activated receptor γ
PSS	Physiological salt solution
qPCR	Quantitative polymerase chain reaction

RAAS	Renin angiotensin aldosterone system
RIN	Ribonucleic acid integrity number
RIPA	Radioimmunoprecipitation assay buffer
RNA	Ribonucleic acid
ROS	Reactive oxygen species
RPF	Renal plasma flow
rpm	Revolutions per minute
RT-PCR	Reverse transcriptase PCR
RUPP	Reduced uterine perfusion pressure
SBH	Sabra Hypertensive Rat
SBP	Systolic blood pressure
SCID	Severe combined immunodeficiency
SDS	Sodium dodecyl sulfate
SEM	Standard error of the mean
sEng	Soluble endoglin
sFLT-1	Soluble fms related tyrosine kinase-1
SHR	Spontaneously hypertensive rat
SHRSP	Stroke prone spontaneously hypertensive rat
SR	Sarcoplasmic reticulum
SV	Stroke volume
TBS	Tris buffered saline
TBS-T	Tris buffered saline - Tween
T_c	Cytotoxic T cell
T_h	Helper T cell
TLR	Toll like receptor
TNFα	Tumor necrosis factor alpha
TPR	Total peripheral resistance
TReg	Regulatory T cell
UK	United Kingdom
UMOD	Uromodulin
USA	United States of America
VSMC	Vascular smooth muscle cell
WKY	Wistar-Kyoto rat

Presentations, Published Work, Awards and Prizes

Abstracts for Oral Presentation

Small HY, Nosalski R, Morgan H, Beattie E, Guzik T, Graham D, Delles C. Council on Hypertension Meeting, Orlando, America, 14-17 Sep 2016. *The role of TNFa and natural killer cells in deficient uterine artery function and adverse pregnancy outcome in the stroke prone spontaneously hypertensive rat.*

Small HY, Nosalski R, Morgan H, Beattie E, Guzik T, Graham D, Delles C. Centre for Trophoblast Research Annual Meeting, University of Cambridge, UK, 11-12 Jul 2016. *TNFa and natural killer cells are involved in adverse pregnancy outcome in the stroke prone spontaneously hypertensive rat.*

Small HY; Invited speaker. Lumps and Bumps Meeting, University of Nottingham, UK, 20-21 Jun 2016. *The role of natural killer cells in adverse pregnancy outcome in the stroke prone spontaneously hypertensive rat: lessons from cancer biology?*

Small HY, Nosalski R, Morgan H, Beattie E, Guzik T, Graham D, Delles C. 26th European Meeting on Hypertension and Cardiovascular Protection, Paris, France, 10-13 Jun 2016. *Inhibition of TNFa signalling using etanercept improves deficient uterine artery remodelling and pregnancy outcome in the stroke prone spontaneously hypertensive rat.*

Mary S, **Small HY**, Coley S, Mischak H, Mullen W, Delles C. 26th European Meeting on Hypertension and Cardiovascular Protection, Paris, France, 10-13 Jun 2016. *Investigation of urinary peptidome over pregnancy in rodent model of hypertension.*

Morgan H, **Small HY**, Beattie E, McBride MW, Graham D. 26th European Meeting on Hypertension and Cardiovascular Protection, Paris, France, 10-13 Jun 2016. *Transcriptomic changes in early pregnancy-associated uterine artery remodelling in the stroke prone spontaneously hypertensive rat.*

Small HY, Nosalski R, Morgan H, Beattie E, Guzik T, Graham D, Delles C. Roger Wadsworth Presentation, Scottish Cardiovascular Forum, Belfast, UK, 6 Feb 2016.

The role of TNFa and natural killer cells in deficient uterine artery function and adverse pregnancy outcome in the stroke prone spontaneously hypertensive rat.

Small HY, Morgan H, Beattie E, Delles C, Graham D. Centre for Trophoblast Research Annual Meeting, University of Cambridge, UK, 13-14 Jul 2015. *Characterising Pregnancy in the Stroke Prone Spontaneously Hypertensive Rat: A Novel Model of Deficient Uterine Artery Remodelling.*

Small HY, Delles C, Graham D. Scottish Cardiovascular Forum, Edinburgh, UK, 2 Feb 2015. *Abnormal Water Balance During Pregnancy in the Stroke Prone Spontaneously Hypertensive Rat.*

Abstracts for Poster Presentation

Sheikh A, **Small HY**, Currie G, Delles C. 26th European Meeting on Hypertension and Cardiovascular Protection, Paris, France, 10-13 Jun 2016. *Systematic review of microRNAs in preeclampsia identifies a number of common pathways involved with the disease.*

Small HY, Nosalski R, Morgan H, Beattie E, Guzik T, Graham D, Delles C. British Society for Cardiovascular Research, Manchester, UK, 6-7 Jun 2016. *The role of TNFa and natural killer cells in deficient uterine artery function and adverse pregnancy outcome in the stroke prone spontaneously hypertensive rat.*

Small HY, Morgan H, Delles C, Graham D. 25th European Meeting on Hypertension and Cardiovascular Protection, Milan, Italy, 12-15 Jun 2015. *Abnormal water balance and kidney function during pregnancy in the stroke prone spontaneously hypertensive rat.*

Small HY, Morgan H, Delles C, Graham D. 25th European Meeting on Hypertension and Cardiovascular Protection, Milan, Italy, 12-15 Jun 2015. *Placental dysfunction in the pregnant stroke prone spontaneously hypertensive rat.*

Small HY, Morgan H, Delles C, Graham D. 8th International Diabetes, Hypertension, Metabolic Syndrome & Pregnancy Conference, Berlin, Germany, 15-

18 Apr 2015. *Placental dysfunction and adverse pregnancy outcome in the pregnant stroke prone spontaneously hypertensive rat*.

Small HY, Beattie E, Graham D, Delles C. 83rd European Atherosclerosis Society Congress, Glasgow, UK, 22-25 March 2015. *Deficient pregnancy-dependent uterine artery remodelling is independent of chronic hypertension in the stroke prone spontaneously hypertensive rat*.

Small HY, Morgan H, Delles C, Graham D. Scottish Cardiovascular Forum, Edinburgh, UK, 2 Feb 2015. *Placental dysfunction in the pregnant stroke prone spontaneously hypertensive rat*

Published Work

Mary S*, **Small HY***, Siwy J, Mullen W, Delles C. Altered urinary peptidome in the pregnant stroke prone spontaneously hypertensive rat identifies an increase in uromodulin. Manuscript submitted. *Joint first authors

Small HY, Akehurst C, Sharafetdinova L, McBride MW, McClure JD, Robinson S, Carty D, Freeman D, Delles C. HLA gene expression is altered in whole blood and placenta from women who later developed preeclampsia. J Physiol Genom. (Under Revision).

Small HY, Cornelius DC, Guzik T, Delles C. Natural killer cells in placentation and cancer: Implications for Hypertension during Pregnancy. Placenta. (Under Revision).

Small HY, Nosalski R, Morgan H, Beattie E, Guzik T, Graham D, Delles C. The role of TNFα and natural killer cells in uterine artery function and adverse pregnancy outcome in the stroke prone spontaneously hypertensive rat. Hypertension. 2016;68(5).

Sheikh A, **Small HY**, Currie G, Delles C. Systematic Review of Micro-RNA Expression in Pre-Eclampsia Identifies a Number of Common Pathways Associated with the Disease. PLoS One. 2016;11(8): e0160808.

Small HY, Morgan H, Beattie E, Griffin S, Indahl M, Delles C, Graham D. Abnormal uterine artery remodelling in the stroke prone spontaneously hypertensive rat. Placenta. 2016;37:34-44.

Small HY, Currie GE, Delles C. Prostasin, proteases, and preeclampsia. J Hypertens. 2016;34:193-5.

Akehurst C*, **Small HY***, Sharafetdinova L, Forrest R, Beattie W, Brown CE, Robinson SW, McClure JD, Work LM, Carty DM, McBride MW, Freeman DJ, Delles C. Differential expression of microRNA-206 and its target genes in preeclampsia. J Hypertens. 2015;33:2068-74. *Joint first authors

Small HY, Montezano AC, Rios FJ, Savoia C, Touyz RM. Hypertension Due to Antiangiogenic Cancer Therapy with Vascular Endothelial Growth Factor Inhibitors: Understanding and Managing a New Syndrome. Can J Cardiol. 2014;30:534-43

Awards

European Society of Hypertension Young Investigator Travel Award, Jun 2016.

British Society of Cardiovascular Research Young Investigator Travel Award, Jun 2016.

Simon Wolff Young Trainee Award, Jul 2015

Flow Cytometry UK Young Trainee Award, Jun 2015.

Graham Wilson Award, Apr 2015.

European Atherosclerosis Society Young Fellowship Travel Award, March 2015.

Prizes

Top Trainee Oral Abstract awarded by the American Council on Hypertension, 15 Sep 2016.

Basic Science Poster Prize awarded by the British Society of Cardiovascular Research/British Atherosclerosis Society, 7 Jun 2016.

Roger Wadsworth Memorial Prize awarded by the Scottish Cardiovascular Forum, 6 Feb 2016.

Poster Prize awarded by the Scottish Cardiovascular Forum, 2 Feb 2015.

Summary

During pregnancy, the maternal cardiovascular system undergoes major adaptation. One of these changes is a 40-50 % increase in circulating blood volume which requires a systemic remodelling of the vasculature in order to regulate maternal blood pressure and maximise blood supply to the developing placenta and fetus. These changes are broadly conserved between humans and rats making them an appropriate pre-clinical model in which to study the underlying mechanisms of pregnancy-dependent cardiovascular remodelling. Whilst women are normally protected against cardiovascular disease; pregnancy marks a period of time where women are susceptible to cardiovascular complications. Cardiovascular disease is the leading cause of maternal mortality in the United Kingdom; in particular hypertensive conditions are among the most common complications of pregnancy. One of the main underlying pathologies of these pregnancy complications is thought to be a failure of the maternal cardiovascular system to adapt.

The remodelling of the uterine arteries, which directly supply the maternal-fetal interface, is paramount to a healthy pregnancy. Failure of the uterine arteries to remodel sufficiently can result in a number of obstetric complications such as preeclampsia, fetal growth restriction and spontaneous pregnancy loss. At present, it is poorly understood whether this deficient vascular response is due to a predisposition from existing maternal cardiovascular risk factors, the physiological changes that occur during pregnancy or a combination of both. Previous work in our group employed the stroke prone spontaneously hypertensive rat (SHRSP) as a model to investigate pregnancy-dependent remodelling of the uterine arteries. The SHRSP develops hypertension from 6 weeks of age and can be contrasted with the control strain, the Wistar Kyoto (WKY) rat. The phenotype of the SHRSP is therefore reflective of the clinical situation of maternal chronic hypertension during pregnancy. We showed that the SHRSP exhibited a deficient uterine artery remodelling response with respect to both structure and function accompanied by a reduction in litter size relative to the WKY at gestational day (GD) 18. A previous intervention study using nifedipine in the SHRSP achieved successful blood pressure reduction from 6 weeks of age and throughout pregnancy; however uterine artery remodelling and litter size at GD18 was not

improved. We concluded that the abnormal uterine artery remodelling present in the SHRSP was independent of chronic hypertension. From these findings, we hypothesised that the SHRSP could be a novel model of spontaneously deficient uterine artery remodelling in response to pregnancy which was underpinned by other as yet unidentified cardiovascular risk factors.

In Chapter 1 of this thesis, I have characterised the maternal, placental and fetal phenotype in pregnant (GD18) SHRSP and WKY. The pregnant SHRSP exhibit features of left ventricular hypertrophy in response to pregnancy and altered expression of maternal plasma biomarkers which have been previously associated with hypertension in human pregnancy. I developed a protocol for accurate dissection of the rat uteroplacental unit using qPCR probes specific for each layer. This allowed me to make an accurate and specific statement about gene expression in the SHRSP GD18 placenta; where oxidative stress related gene markers were increased in the vascular compartments. The majority of SHRSP placenta presented at GD18 with a blackened ring which encircled the tissue. Further investigation of the placenta using western blot for caspase 3 cleavage determined that this was likely due to increased cell death in the SHRSP placenta. The SHRSP also presented with a loss of one particular placental cell type at GD18: the glycogen cells. These cells could have been the target of cell death in the SHRSP placenta or were utilised early in pregnancy as a source of energy due to the deficient uterine artery blood supply. Blastocyst implantation was not altered but resorption rate was increased between SHRSP and WKY; indicating that the reduction in litter size in the SHRSP was primarily due to late (>GD14) pregnancy loss. Fetal growth was not restricted in SHRSP which led to the conclusion that SHRSP sacrifice part of their litter to deliver a smaller number of healthier pups.

Activation of the immune system is a common pathway that has been implicated in the development of both hypertension and adverse pregnancy outcome. In Chapter 2, I proposed that this may be a mechanism of interest in SHRSP pregnancy and measured the pro-inflammatory cytokine, TNFα, as a marker of inflammation in pregnant SHRSP and WKY and in the placentas from these animals. TNFα was up-regulated in maternal plasma and urine from the GD18 SHRSP. In addition, TNFα release was increased from the GD18 SHRSP placenta as was the expression of the pro-inflammatory TNFα receptor 1 (*Tnfr1*). In order to

investigate whether this excess TNFα was detrimental to SHRSP pregnancy, a vehicle-controlled intervention study using etanercept (a monoclonal antibody which works as a TNFα antagonist) was carried out. Etanercept treatment at GD0, 6, 12 and 18 resulted in an improvement in pregnancy outcome in the SHRSP with an increased litter size and reduced resorption rate. Furthermore, there was an improved uterine artery function in GD18 SHRSP treated with etanercept which was associated with an improved uterine artery blood flow over the course of gestation. In Chapter 3, I sought to identify the source of this detrimental excess of TNFα by designing a panel for maternal leukocytes in the blood and placenta at GD18. A population of CD3- CD161+ cells, which are defined as rat natural killer (NK) cells, were increased in number in the SHRSP. Intracellular flow cytometry also identified this cell type as a source of excess TNFα in blood and placenta from pregnant SHRSP. I then went on to evaluate the effects of etanercept treatment on these CD3- CD161+ cells and showed that etanercept reduced the expression of CD161 and the cytotoxic molecule, granzyme B, in the NK cells. Thus, etanercept limits the cytotoxicity and potential damaging effect of these NK cells in the SHRSP placenta.

Analysing the urinary peptidome has clinical potential to identify novel pathways involved with disease and/or to develop biomarker panels to aid and stratify diagnosis. In Chapter 4, I utilised the SHRSP as a pre-clinical model to identify novel urinary peptides associated with hypertensive pregnancy. Firstly, a characterisation study was carried out in the kidney of the WKY and SHRSP. Urine samples from WKY and SHRSP taken at pre-pregnancy, mid-pregnancy (GD12) and late pregnancy (GD18) were used in the peptidomic screen. In order to capture peptides which were markers of hypertensive pregnancy from the urinary peptidomic data, I focussed on those that were only changed in a strain dependent manner at GD12 and 18 and not pre-pregnancy. Peptide fragments from the uromodulin protein were identified from this analysis to be increased in pregnant SHRSP relative to pregnant WKY. This increase in uromodulin was validated at the SHRSP kidney level using qPCR. Uromodulin has previously been identified to be a candidate molecule involved in systemic arterial hypertension but not in hypertensive pregnancy thus is a promising target for further study.

In summary, we have characterised the SHRSP as the first model of maternal chronic hypertension during pregnancy and identified that inflammation mediated by TNFα and NK cells plays a key role in the pathology. The evidence presented in this thesis establishes the SHRSP as a pre-clinical model for pregnancy research and can be continued into clinical studies in pregnant women with chronic hypertension which remains an area of unmet research need.

Chapter 1 Introduction

1.1 The Cardiovascular System

The cardiovascular (CV) system is composed of the heart and vessels that form a rapid transport system delivering blood to the tissues of the body. Its vital role is highlighted by the fact that it is the first system to form and function in the developing embryo (1). Fundamentally, the CV system functions: as a convective transport system providing nutrients and washing away waste products; as a messenger system by delivery of hormones and bioactive molecules; and to regulate body temperature (1). The driving force which powers transport around the CV system is the heart. The heart is principally composed of four chambers: two muscular pumps, ventricles, and two reservoirs, atria. The right chambers of the heart perfuse the pulmonary circulation whilst the left chambers of the heart perfuse the systemic circulation. The heart is a muscle whereby contraction, thus ejection of blood, is known as systole followed by the relaxation of the ventricle allowing it to be filled with blood in diastole. Both right and left ventricles pump the same amount of blood synchronously but the left ventricle must eject blood at a much higher pressure to serve the distant systemic circulation. Thus, it is larger and more powerful than the right. Oxygenated blood enters from the pulmonary circulation where it is pumped into the systemic circulation via the aorta. Deoxygenated blood returns from the systemic circulation via the vena cava where it is then returned to the lungs by the pulmonary artery to be oxygenated once more (Fig 1-1).

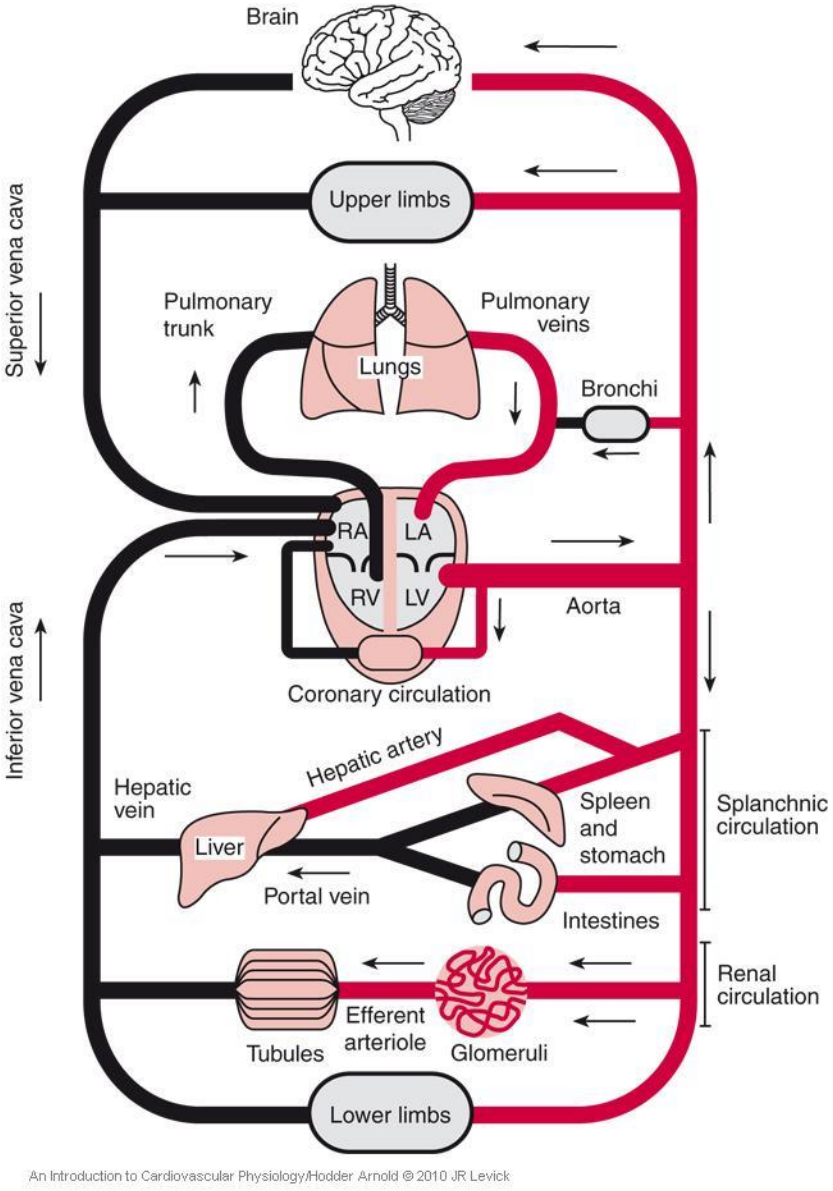

Figure 1-1: The Cardiovascular System.

The systemic and pulmonary systems are arranged in series i.e. they are reliant on the function of the other. The circulatory system delivers blood to the organs arranged in parallel i.e. their blood flow is not dependent on the blood flow of an upstream organ. This allows the cardiovascular system to adapt the blood supply dependent on the demand from a specific tissue. The exception to this role is the "portal" blood supply in the liver and kidney where the tissue additionally receives partially deoxygenated blood from other tissues in the body. Image from Levick (2010).

Cardiac output (CO) is defined as the volume of blood ejected by one ventricle in one minute. Cardiac output is therefore equal to stroke volume (SV) (the volume of blood ejected per heartbeat) multiplied by the heart rate (HR) (number of heart beats per minute): *CO = SV x HR*. Cardiac output is dynamic dependent upon the oxygen demand of the body (2). The blood from the heart is then distributed to tissues dependent upon this demand. A pressure gradient drives the movement of blood through the CV system. Blood pressure is measured in "millimetres of mercury" (mmHg) above atmospheric pressure after the original method of measuring blood pressure using a mercury column (3). Blood flow is pulsatile due to the contraction and relaxation of the ventricles in the heart. In the systemic arterial circulation, the initial ejection of blood by the left ventricle during systole is approximately 120 mmHg above atmospheric pressure. During diastole this falls to approximately 80 mmHg. Therefore "normal" blood pressure is defined as 120/80 mmHg (4).

The vasculature forms the "plumbing" of the CV system. Every vessel wall is composed of three layers: the tunica intima, the tunica media and the adventitia (Fig 1-2). Only capillaries do not have three layers and are principally composed of endothelial cells.

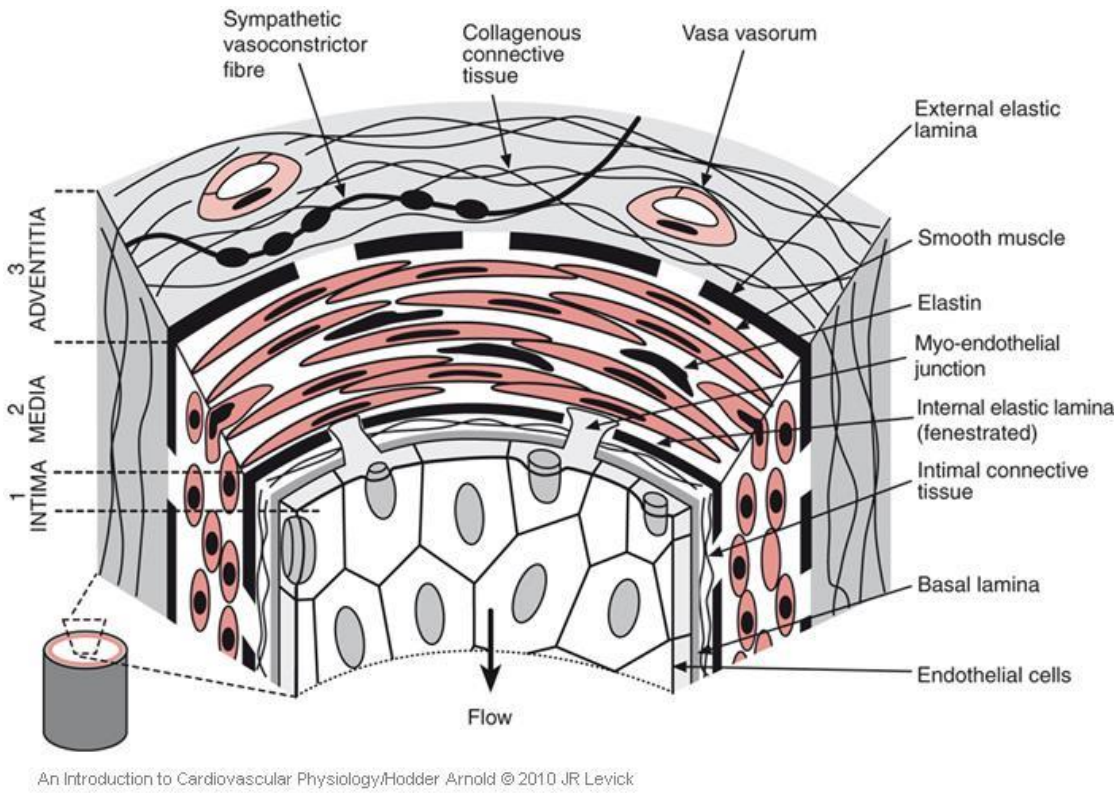

Figure 1-2: The Structure of a Vessel.

A vessel is normally composed of three layers. The innermost intima (1) is characterised by endothelial cells arranged on a thin layer of basement membrane (basal lamina & intimal connective tissue). This forms the main barrier to the blood and produces a number of vasoactive factors. The middle layer, media (2), is composed of smooth muscle cells in an elastin and collagen matrix contained within the internal and external lamina. Myoendothelial junctions through fenestrations in the internal elastic lamina facilitate contact between the intima and media. The outermost adventitia (3) is principally composed of collagenous connective tissue which attaches the vessel to its surroundings. Also within this outer layer, there are sympathetic fibre terminals which regulate vascular function and small vasa vasorum (vessels of vessels) which act to nourish the medial layer. Image from Levick (2010).

The arteries of the CV system are classified by their additional functions other than to carry blood (Table 1-1). Vessels are branched which functions to slow down the flow of blood for safe delivery to the tissues. To control the conductance of blood through the vessels there must also be resistance to restrict blood flow. Resistance is defined by Darcy's law of flow (5) where a vessel with high resistance needs a large difference in pressure to drive blood flow. Large, wide arteries require only a low drop in pressure to drive flow whereas smaller arterioles need a larger difference in pressure. The measurement of the amount of pressure difference needed to drive blood flow is known as the resistance index. Therefore, large arteries contribute only approximately 2% to total systemic resistance and the smallest arteries and arterioles contribute approximately 60% (1).

Table 1-1 Classification of Arteries.

Vessel	Example	Function	Wall/Lumen	Composition (%)
Elastic Artery	Aorta Iliac Artery Pulmonary Trunk	Elastin content allows the vessel to store mechanical energy ensuring continuous blood flow to the smaller vessels. Collagen prevents over-expansion.	2 mm/25 mm	Endothelium: 5 Smooth Muscle: 25 Elastin: 40 Collagen: 27
Conduit Artery	Brachial Radial Femoral Cerebral Coronary Uterine	Conduct flow from the large elastic arteries to the small arterioles. Thick wall prevents collapse at sharp bends. Rich sympathetic nervous innervation to alter the blood flow to different vascular beds.	1 mm/4 mm	
Arteriole		Site of high resistance vessels causing a major drop in blood pressure. These act to constrict or dilate to alter local blood flow.	30 μm/30 μm	Endothelium: 10 Smooth Muscle: 60 Elastin: 10 Collagen: 20

Table adapted from Levick (2010).

1.1.1 Blood Pressure Regulation

Blood pressure is the force of blood against the walls of the vessels. “Blood pressure” can refer to intraventricular blood pressure, systemic arterial blood pressure, capillary hydrostatic pressure or systemic venous return. For the purposes of this thesis, the generic term “blood pressure” will refer to systemic arterial blood pressure. Blood pressure is dynamic and varies with age, race, gender, circadian rhythm and transiently such as during periods of stress or standing. Therefore, a number of mechanisms are in place to regulate changes in blood pressure. These can be categorised into short term and long term changes.

Blood pressure equals cardiac output multiplied by total peripheral resistance (*BP = CO x TPR*) thus changing either cardiac output (*CO = SV x HR*, section 1.1) or total peripheral resistance directly affects blood pressure. Short term mechanisms of blood pressure regulation focus on altering total peripheral resistance as this is quicker and more effective than changing CO. Longer term mechanisms of blood pressure regulation adjust blood volume which predominantly affects CO (6).

The three main short term mechanisms of blood pressure control operate within seconds or minutes: baroreceptors, chemoreceptors or the central nervous system (CNS) ischemic response. All of these short term mechanisms act through the nervous system which is controlled by three main cardiac centres in the medulla: cardio-acceleratory centre (sympathetic), cardio-inhibitory centre (parasympathetic) and the vasomotor centre (sympathetic). Physiologically, short term fluctuations in blood pressure are predominantly regulated by the baroreceptors found in the carotid sinuses which adjoin to the glossopharyngeal nerve and the aortic arch which joins to the vagus nerve (1). The direct effects altering TPR by activation of the baroreceptors account for three quarters of the change whereas their neuroendocrine effect account for the remainder (Fig 1-3) (6). The other two mechanisms of short term blood pressure control, chemoreceptors (7) and the CNS ischemic response, are more relevant to acute changes such as clinical shock or asphyxia. The chemoreceptors are located in the small, highly vascularised carotid and aortic bodies, adjacent to the carotid sinus and aorta. Chemoreceptors are responsive to changes in levels of O_2, CO_2, pH and hyperkalaemia. Activation of the chemoreceptors increases blood pressure through tachycardia and vasoconstriction restoring SV and increasing total peripheral resistance. CNS ischemic response is activated by cerebral hypoxia leading to a powerful stimulation of the sympathetic system and noradrenaline release to increase blood pressure (8).

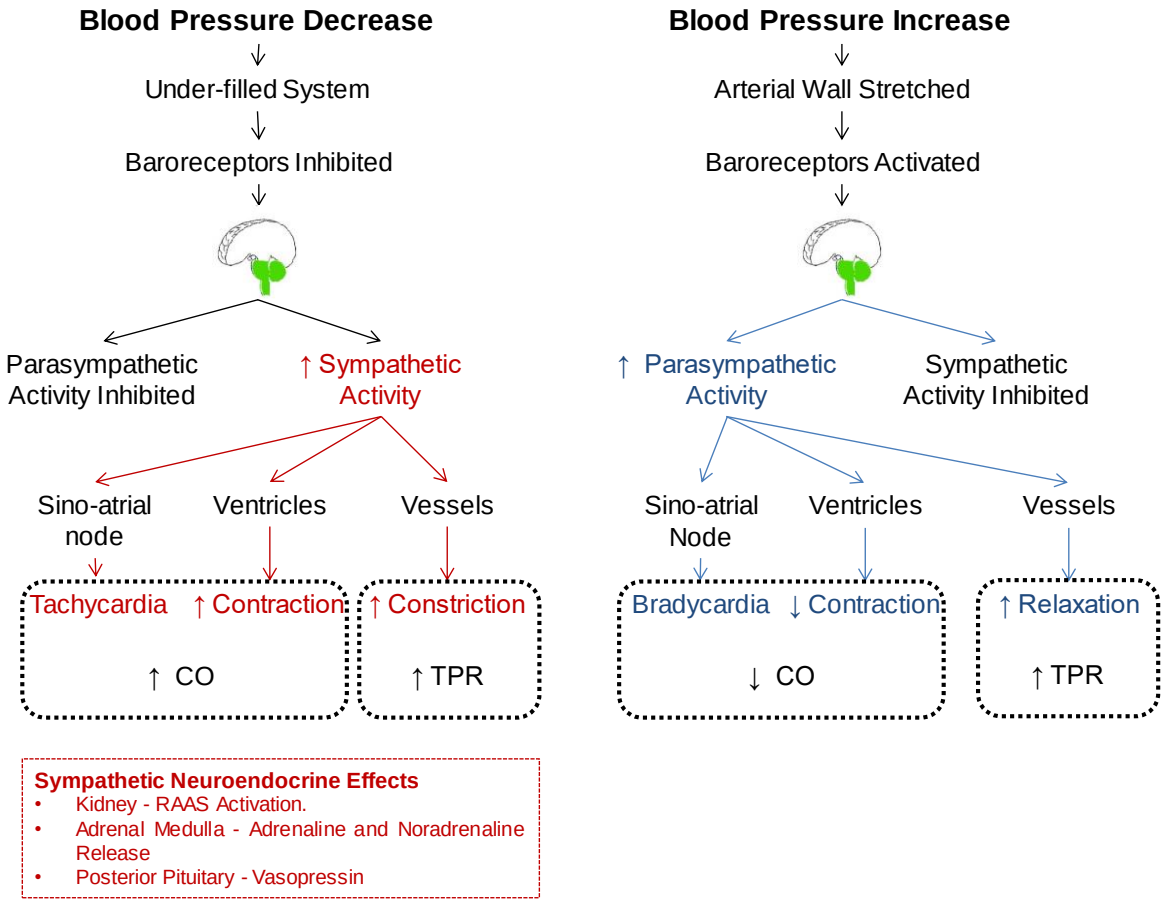

Figure 1-3: Baroreceptor Reflex Regulating Blood Pressure.

Increased sympathetic output leads to increased contractility of the heart through noradrenaline and adrenaline actions on β_1-adrenoreceptors and constriction of both the arteries and veins through α-adrenoreceptors. Venous constriction contributes to both increasing peripheral resistance and cardiac output by restoring venous return to the heart and increasing stroke volume. The parasympathetic system releases acetylcholine which acts through muscarinic receptors on the heart and vessels to reduce contractility and release nitric oxide causing vasorelaxation. CO: cardiac output, TPR: total peripheral resistance, RAAS: renin angiotensin aldosterone system.

Intermediate and long term control of blood pressure is mainly affected through peptides and hormones which act to alter blood volume through modifying sodium and fluid reabsorption at the kidney. An increase in arterial pressure results in a decrease in sodium and fluid resorption and an increase in sodium excretion; this is known as pressure natriuresis. The main peptides are: catecholamines, the renin angiotensin aldosterone system (RAAS), vasopressin and the natriuretic peptides. The intermediate neuroendocrine term effects of catecholamines are shown in Figure 1-3. The RAAS (Fig 1-4) is a major regulator of blood pressure; drugs which inhibit the RAAS pathway are currently the first line drug to be prescribed to hypertensive patients under 55 (9) and many monogenic forms of hypertension are due to mutations in this pathway (section 1.2.1.1) (10). Angiotensin II, the main active peptide of this pathway acts to increase blood pressure in three ways: by stimulating aldosterone production which promotes sodium and fluid retention thus increasing plasma volume, boosting sympathetic nervous system activity to induce systemic vasoconstriction and by stimulation of the thirst centres in the hypothalamus. Angiotensin II has its main effect on blood volume through stimulation of the mineralocorticoid hormone, aldosterone, from the adrenal cortex. Aldosterone acts through the mineralocorticoid receptors in the kidney to retain sodium and water at the expense of potassium and hydrogen ions (11). Vasopressin (also known as anti-diuretic hormone) is released by stimulation from angiotensin II as well as activation of arterial baroreceptors and osmoreceptors in the brain. Physiologically, vasopressin works at the kidney to balance water excretion to balance plasma volume and osmolality. When blood pressure is decreased, vasopressin concentration is stimulated above baseline levels to induce systemic vasoconstriction sparing the cerebral and coronary vessels and reducing urine output from the kidney.

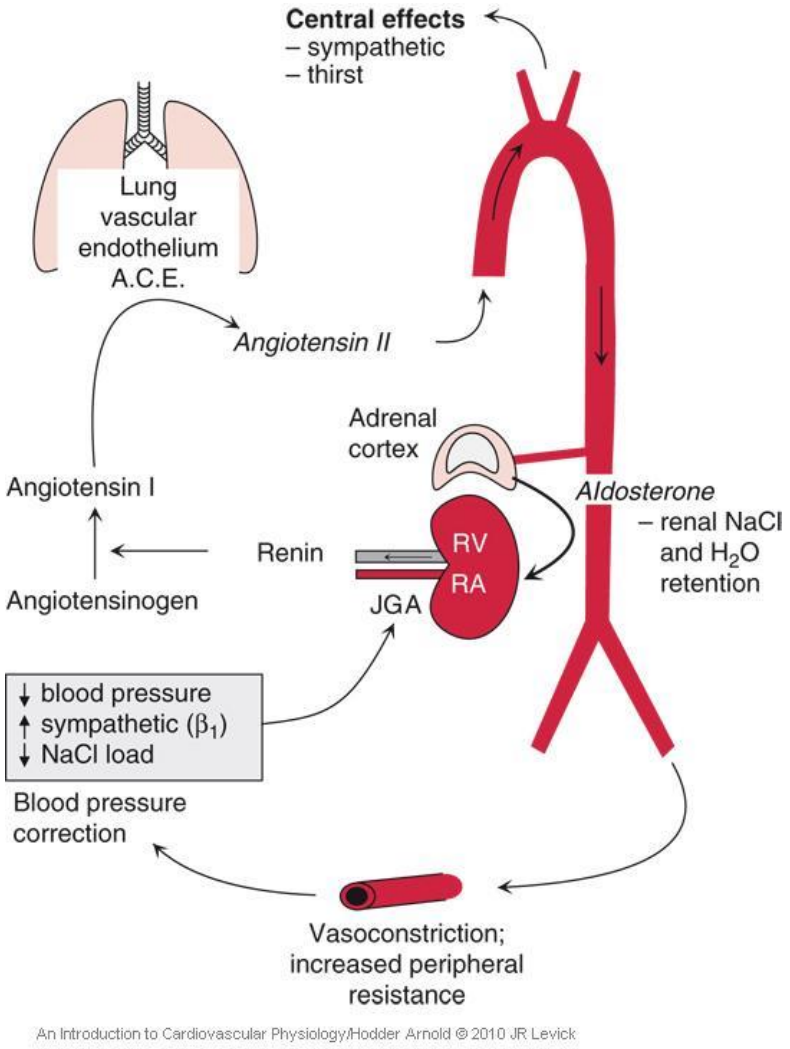

Figure 1-4: The Renin Angiotensin Aldosterone System (RAAS).

Renin is produced from specialised juxtaglomerular cells in the kidney. It catalyses the proteolytic cleavage of angiotensinogen to produce angiotensin I. Angiotensin I has limited activity until it is cleaved by angiotensin converting enzyme (ACE) expressed on the surface of endothelial cells into the active peptide angiotensin II. This process principally happens in the lung as it is the first expanse of endothelial cells reached by angiotensin I. Angiotensin II then goes on to stimulate the release of aldosterone from the adrenal cortex, directly stimulate vasoconstriction and increase sympathetic outflow. These combined mechanisms have the effect of increasing blood pressure. JGA: juxtaglomerular apparatus, RA: renal artery, RV: renal vein. Image from Levick (2010).

The natriuretic peptides, namely atrial natriuretic peptide (ANP) (12) and brain natriuretic peptide (BNP) (13), act to reduce blood pressure, thus are counter-regulatory to the RAAS system. ANP is the predominant physiological peptide with levels of BNP being greatly increased in heart failure. Pro-forms of ANP and BNP are released from specialised cardiomyocytes in either the atria or ventricles in response to increased cardiac filling pressure (14). These peptides reduce plasma volume by modest vasodilation binding to the vessels directly (15) and promoting salt and fluid loss at the kidney and transferring fluid from the plasma to the interstitial compartment (16). The inactive and active forms of ANP and BNP have promise as potential biomarkers for CV morbidity and mortality associated with hypertension (17).

Signalling pathways involving reactive oxygen species (ROS) are involved in both short and long term mechanisms of blood pressure regulation. ROS can be short-lived radicals such as superoxide ($\bullet O_2$) or more sTable non-radical derivatives such as H_2O_2. ROS are produced by all vascular cell types from a number of sources including: mitochondria, xanthine oxidase, uncoupled nitric oxide synthase and NADPH oxidase (18). Mice lacking ROS-generating enzymes have lower blood pressure than wild type animals and are resistant to the development of angiotensin II dependent hypertension (19). In the kidney, ROS promotes sodium retention resulting in an increase in blood pressure (20). However, the role of vascular derived ROS can have seemingly opposing effects. For example, an increase in $\bullet O_2$ results in increased vasoconstriction through scavenging of the vasodilator nitric oxide (21) but increased H_2O_2 has been shown to act as a vasodilator in some circumstances (22). Despite their paradoxical effects, it is well established that an imbalance derived from increased vascular ROS production and decreased clearance, known as oxidative stress, is associated with vascular pathology and an increase in blood pressure (23).

1.1.2 Mechanisms of Vascular Contraction and Relaxation

Vascular reactivity plays a central role in CV physiology. The sum of the resistance to blood flow across all of the systemic vasculature is known as the systemic vascular resistance or total peripheral resistance (TPR). The level of physiological TPR is determined by a balance between vasodilation, which reduces

TPR, and vasoconstriction which increases TPR. Dysregulation of the molecular mechanisms of vasoconstriction and dilation are central to CV disease.

1.1.2.1 Vasoconstriction

The physiology of the vascular smooth muscle cells (VSMC) is unique with regards to its molecular machinery which allows the vessels to fulfil a specific type of slow, sustained constriction. The contraction is initiated by a rise in intracellular calcium which can occur through depolarisation-dependent or independent mechanisms. This is determined by the size of the arteries and the balance of receptors expressed on the VSMC surface (24, 25). Most vasoconstrictor molecules act through receptors coupled to the G_q protein and subsequent activation of the phospholipase C signalling pathway (Fig. 1-5). Intracellular calcium release culminates in the activation of myosin light chain kinase (MLCK) which goes on to phosphorylate myosin. This allows myosin-actin interaction and induces contraction. In contrast to the sarcomeric structure of the skeletal muscle, myosin-actin bundles are organised into dense bodies disseminated across the VSMC. These are connected by intermediate filaments forming a contractile mesh which propagates contraction over the whole cell. The first phase of vasocontraction (30-60 seconds) is calcium dependent, however, a further tonic phase exists in VSMCs where the contraction is sustained through activation of RhoA kinase (26). Sympathetic stimulation is the major determinant of physiological vasoconstriction. Noradrenaline is released from sympathetic nerves where it diffuses across the neuromuscular junction and binds α1-adreoreceptors on the VSMC surface. The α1-adreoreceptor is a G_q protein coupled receptor and acts to induce contraction as shown in Fig. 1-5 Other molecules such as angiotensin II, endothelin-1 and adrenaline can also elicit vasocontraction through binding to their respective VSMC surface receptors.

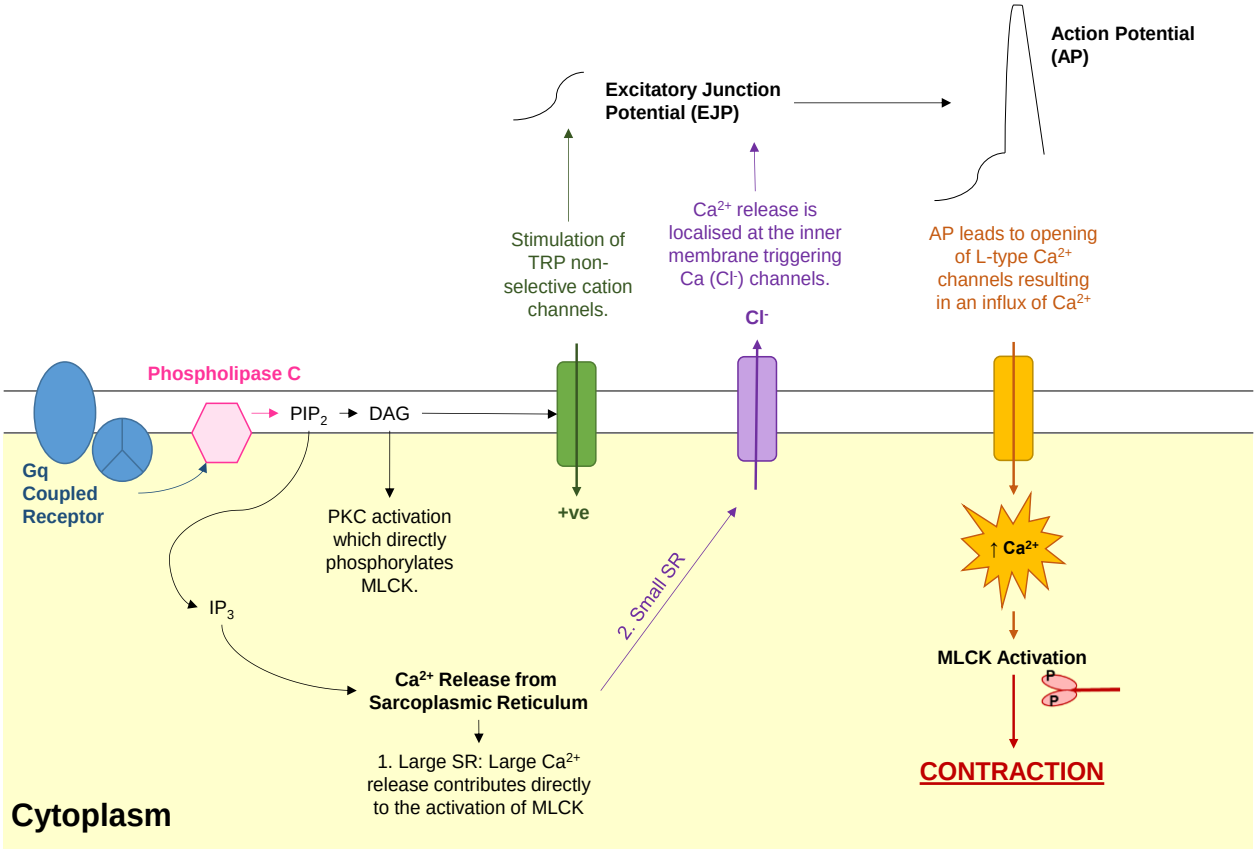

Figure 1-5: G_q Coupled Receptor Phospholipase C Mechanism of Vascular Smooth Muscle Cell Contraction.

G_q protein coupled receptors stimulate phospholipase C to split membrane phospholipid (PIP_2) into the second messengers diacylglycerol (DAG) and inositol triphosphate (IP_3). IP_3 triggers the release of calcium (Ca^{2+}) from the sarcoplasmic reticulum (SR). If the cell has a large SR, Ca^{2+} release is global and contributes directly to the activation of myosin light chain kinase (MLCK). If the cell has a small SR, Ca^{2+} release localised a the inner cell membrane triggers the opening of Ca^{2+} activated chloride (Cl^-) channels which results in depolarisation . DAG stimulates the opening of TRP non-selective cation channels leading to depolarisation and activates protein kinase C (PKC) which phosphorylates MLCK. Depolarisation leads to an action potential causing an influx of Ca^{2+} through L-type Ca^{2+} channels. These pathways converge on the phosphorylation and activation of MLCK which phosphorylates myosin leading to contraction of the smooth muscle cell.

1.1.2.2 Vasodilatation & the Role of the Endothelium

The contribution of the endothelium to vasodilatation is dependent upon vascular bed, species, age, gender and developmental stage (27). There are three major groups of vasoactive substances released by the vascular endothelium which act upon the vascular smooth muscle cells to elicit a relaxation response (Table 1-2). The molecular pathways responsible for endothelium dependent vasorelaxation exhibit a degree of redundancy. For example, in eNOS knockout mice (28) and in vessels from human subjects with CV disease where eNOS is impaired (29) another form of NOS enzyme, neuronal NOS (nNOS), is upregulated in the endothelium as a compensatory mechanism. Endothelial dysfunction, when these mechanisms of vasorelaxation are impaired, is a hallmark of many CV diseases and is positively correlated with adverse clinical outcomes (30). Excessive levels of inflammation (31) and/or oxidative stress (21) are considered to be two key drivers of endothelial dysfunction during disease by either direct damage of the endothelial layer itself or disruption of the molecular pathways detailed in Table 1-2.

Table 1-2 Molecular Mechanisms of Endothelium-Dependent Vasorelaxation.

Molecule	Enzyme	Mechanism of Relaxation in VSMCs
Nitric Oxide (NO)	Endothelial nitric oxide synthase (eNOS)	Stimulates guanylyl cyclase to produce cyclic GMP leading to activation of protein kinase G (PKG). PKG induces hyperpolarisation through activation of K^+ channels, promotes dephosphorylation of myosin, inhibits IP_3 mediated Ca^{2+} release and increases Ca^{2+} sequestration.
Prostaglandins (e.g. PGl_2)	Cyclooxygenase (COX)	Stimulates adenylate cyclase to produce cyclic AMP leading to activation of protein kinase A (PKA). PKA activation leads to hyperpolarisation through activation of K^+ channels.
Endothelial Derived Hyperpolarised Factor (EDHFs e.g. H_2O_2, CO, H_2S)	H_2O_2: catalase CO: heme oxygenase-1 (HO-1) H_2S: cystathionine-γ-lyase (CSE)	Lead to hyperpolarisation by activation of K^+ channels or Na+/K+ ATPase.

1.2 Cardiovascular Disease

CVD includes, but is not limited to, myocardial infarction, stroke, left ventricular hypertrophy, peripheral vascular disease and renal failure. CVD accounts for 27% of deaths in the United Kingdom (British Heart Foundation, 2015). Furthermore, approximately 10% of the population are living with CVD (British Heart Foundation, 2015). This is at great cost to the National Health Service (NHS) as, based on the British National Formulary; drugs for CVD make up 4 out of the 5 top prescribed drugs in the United Kingdom (NHS, 2011). Globally, CVD has been identified as a major disease burden worldwide as the leading cause of non-communicable disease death globally and projected to overtake infectious diseases as a cause of mortality and morbidity by 2030 (32). One underlying problem driving the increase in CVD is that known risk factors such as obesity, metabolic syndrome, atherosclerosis and hypertension are prevalent in the developed world. This thesis will focus on hypertension as a risk factor for CVD.

1.2.1 Hypertension

Hypertension is a chronic raised systemic arterial blood pressure that is defined as pathological at the level which causes an increased risk for adverse CV outcomes such as myocardial infarction or stroke. Hypertension is diagnosed by a SBP of 140 mm Hg or above and/or a DBP of 90 mmHg or above (Table 1-3). Hypertension is a “silent killer” as it is thought that as many as one third of people with hypertension do not know that they are affected as it occurs with few obvious symptoms (33). The only definitive way to know whether someone has hypertension is for the individual’s blood pressure to be measured. However, blood pressure measurement by a physician is not straightforward due to phenomena such as “white coat hypertension” (34). Recent NICE guidelines have supported the use of ambulatory blood pressure measuring to prevent misdiagnosis and the subsequent cost of unnecessary treatment (9). Untreated, hypertension can elicit major damage on the vital organs (35) which establishes it as a key risk factor for CVD. Hypertension is quantitatively the most important risk factor for CVD accounting for 13.5% premature deaths globally and approximately half of all cases of stroke (54%) and ischemic heart disease (47%) (36). In particular, its incidence has begun rapidly increasing in the developing world (37). A recent study carried out in the United Kingdom in 2014 assessed hypertension as a risk factor

for 12 different adverse CV outcomes in 1.25 million individuals (38). This study established blood pressure as an independent risk factor for CVD and showed that individuals with hypertension developed CVD 5 years earlier (95% CI 4.8 – 5.2) and their lifetime overall risk of CVD at 30 years of age was approximately 22% higher

Table 1-3 JNC-8 Guidelines for Blood Pressure Classification in Adults ≥18.

Classification	SBP (mmHg)		DBP (mmHg)
Normal	<120	AND	<80
Pre-Hypertension	120 – 139	OR	80 – 89
Stage 1 Hypertension	140 - 159	OR	90 - 99
Stage 2 Hypertension	≥160	OR	≥100

Table compiled by author.

In 5 – 10% of individuals with hypertension the increase in blood pressure is secondary to an underlying pathology such as a genetic mutation or primary aldosteronism. However, in most (90 – 95%), the cause of hypertension is unknown (essential or primary hypertension). Both primary and secondary hypertension present with great clinical heterogeneity. Blood pressure has a smooth bell-shaped distribution in the population which indicates that it is a net effect of multiple factors each with a small cumulative contribution (39). It is known that the dysregulation of blood pressure is a complex multifactorial disease with a number of known genetic and environmental factors.

1.2.1.1 Genetic Factors

Compelling evidence for a genetic component in blood pressure regulation comes from twin studies, adoptive studies and family studies. Hypertension has a heritability between 30 – 50 % (40) and this decreases with the individual's age at onset (41). Early twin studies showed increased concordance in blood pressure between monozygotic than dizygotic twins (42). These findings were supported by the Montreal adoption study which showed increased correlation of blood pressure in biological siblings relative to adopted siblings (43). Large family studies, for example from the long-running Framingham Heart Study, also reported heritability of long term systolic (57%) and diastolic blood pressure (55%) (44).

The advent of studying the contribution of specific genes in hypertension began with linkage analysis in large families with a monogenic cause of hypertension (secondary). These diseases are predominantly characterised by genes involved in the renal salt and fluid handling (45). For example, Liddle's Syndrome is caused by a gain of function mutation in the sodium channel, ENaC, which results in it not being degraded correctly by the ubiquitin proteasome and subsequent increase in salt and fluid resorption at the kidney (46). Whilst individuals with Mendelian forms of hypertension are in the small minority, knowledge of the genes involved has given rise to most of the candidate genes and drug approaches for current hypertension research and treatment. A number of studies have utilised knowledge generated from Mendelian forms of hypertension to inform candidate gene studies in humans with hypertension (47, 48).

The polygenic nature of hypertension was proposed in Paige's "Mosaic Theory" (49). This theory was recently updated by Padmanabhan, Caulfield and Dominiczak to incorporate the complexity of genetic interactions that have been uncovered in hypertension (Fig 1-6) (50). Modern research has focussed on large genome wide association studies (GWAS) to detect novel genetic variants (single nucleotide polymorphisms or SNPs) involved in hypertension. However, the contribution of such studies is presently small. Most hits from GWAS are in non-coding regions or in coding regions where the gene in question has a small effect on blood pressure making functional annotation difficult. However, there has been success in this area (51, 52) and with the advent of better bioinformatic resources and bigger datasets GWAS will have the ability to identify more target genes.

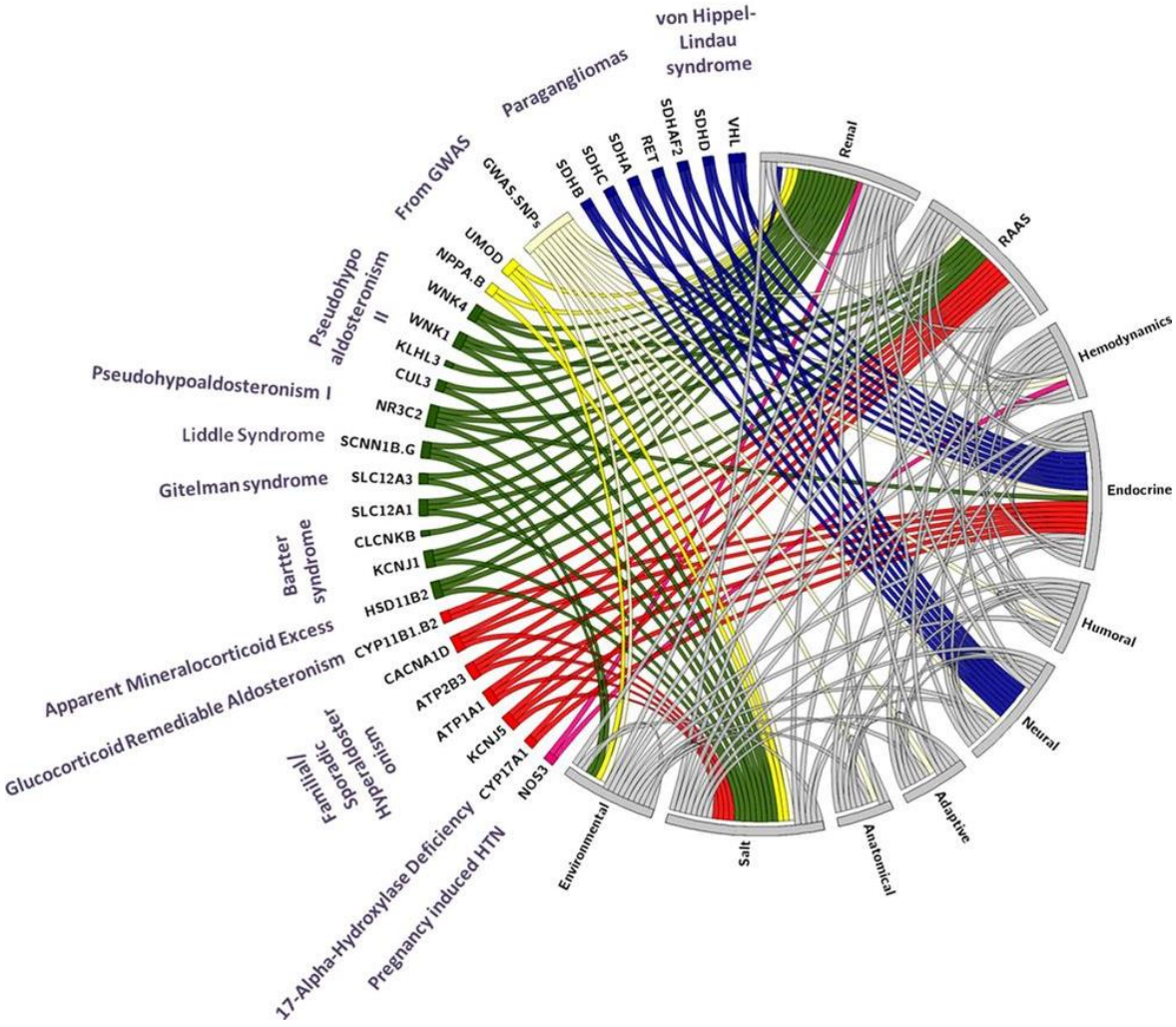

Figure 1-6: The 2014 Update on the Paige Mosaic Model of Hypertension.

The Paige model of hypertension was proposed in 1960 to explain the multifactorial nature of hypertension, inclusive of: genetic, environment, adaptive, neural, mechanical and hormonal mechanisms. The updated 2014 model builds on this theory by the addition of specific genes (coloured) and pathways (grayscale) which are now known to play a causal role in hypertension. Image from Padmanabhan, Caulfield and Dominiczak (2015).

1.2.1.2 Environmental Factors

Heritability studies take into account common genetic factors found in families but these individuals are also likely to have a shared environment. The environment-gene interaction in hypertension is known to be a large component of the disease process (53). For example, even Mendelian forms of hypertension with a strong genetic background are exacerbated by the environment of the individual. Women with a mutation in the mineralocorticoid (*MCR*) gene experience pregnancy-induced hypertension due to the significant rise in progesterone (54). The principal environmental factor affecting hypertension is dietary salt due to its effects on pressure natriuresis. Furthermore, stress, obesity, dyslipidaemia and insulin resistance have all been shown to have independent interactions with blood pressure (55). Another angle on gene-environment interactions is Barker's Hypothesis (56) which proposes that there is fetal genetic programming which takes place in response to the intrauterine environment which can predispose an individual to disease later in life. In keeping with this hypothesis, the blood pressure of offspring has been associated with maternal blood pressure during pregnancy (57, 58).

1.2.1.3 Sex Differences in Hypertension

Blood pressure differences between males and females add a further layer of complexity to the understanding of the development of hypertension. Premenopausal women tend to have lower blood pressure (59) and have a significantly reduced CV risk (60) than age-matched men. Estrogen is the main female sex hormone produced in three forms: estradiol (premenopausal), estrone (postmenopausal) and estriol (pregnancy). Estrogen, particularly estradiol, has predominantly vasoprotective effects (Fig 1-7). Testosterone is the main androgen or male sex hormone. In the vasculature, androgens have been found to have predominantly deleterious effects (Fig 1-7) however can also cause acute vasodilation (61). Increased maternal testosterone levels during pregnancy are associated with endothelial dysfunction in male but not female offspring (62). This is thought to be due to direct effects of testosterone on impaired placental development and vascular remodelling *in vivo* (63). Despite this, the cardio-protective phenotype in females is not as simple as the presence or absence of specific hormones. Postmenopausal women are not protected against CVD and

even have a slightly higher blood pressure than men (64) but supplementation with hormone replacement therapy (HRT) has not been shown to have any conclusively beneficial effects on the CVS in two large clinical trials (65, 66). Furthermore, testosterone is paradoxically reduced in chronic disease (67). This disconnection between physiology and epidemiological data requires further research to dissect these seemingly counter-intuitive results.

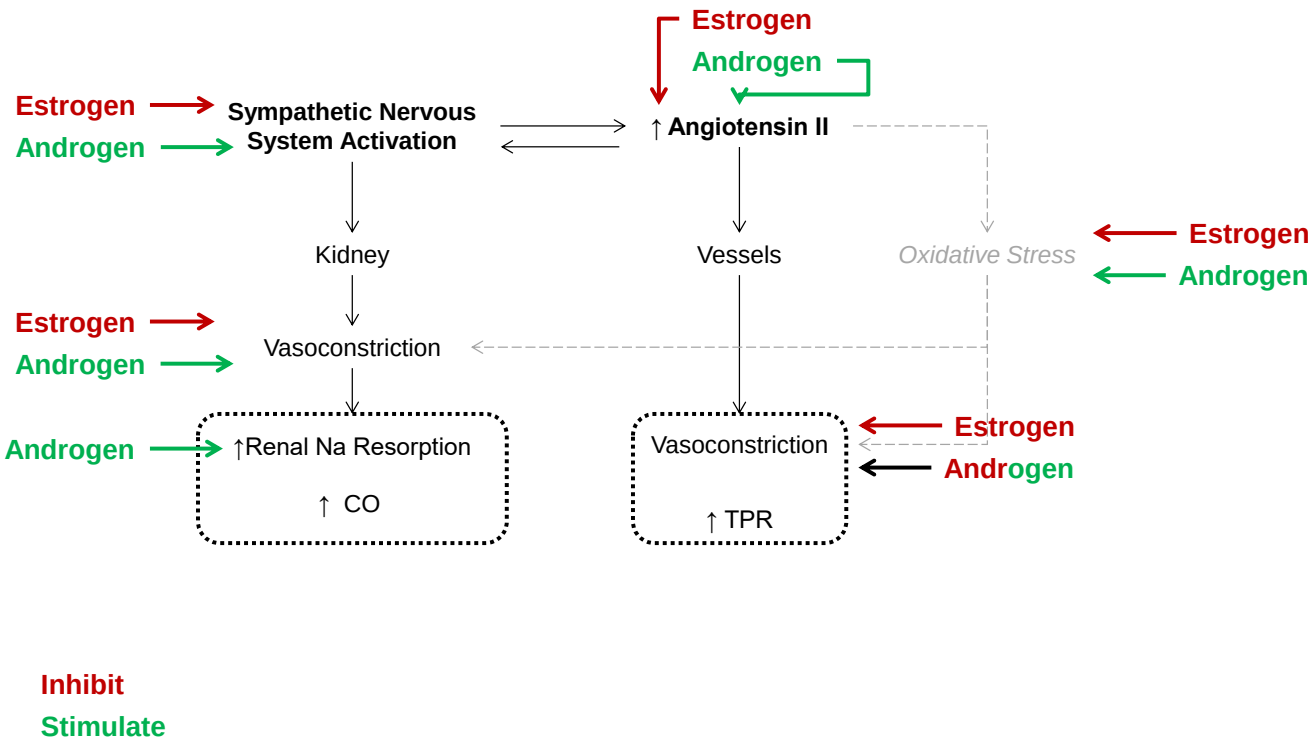

Figure 1-7: The Effects of Sex Hormones on Blood Pressure Regulation.

Estrogens tend to have cardioprotective effects and androgens tend to have deleterious effects; however the mechanisms are not well defined. Estradiol has been shown to attenuate sympathetic outflow induced by aldosterone however testosterone levels have been shown to correlate with noradrenaline release. Estrogens down-regulate components of the RAAS and the angiotensin II receptor 1 whereas androgens directly stimulate sodium reabsorption and increase angiotensinogen synthesis in the kidney. Estradiol has been shown to induce eNOS and acts as an antioxidant in the vasculature. Antioxidant therapy lowers blood pressure in male rats but not female rats suggesting that testosterone has pro-oxidant properties.

1.3 Inflammation & Hypertension

The immune system is composed of two specialised arms: the innate and adaptive. The innate immune system is the body's first line of defence and acts immediately to recognise "non-self" molecules or viral and bacterial markers such as double stranded RNA or coat molecules which it then destroys directly (e.g. phagocytosis) or indirectly through antigen presentation to cells of the adaptive immune system. Cells of the innate immune system include macrophages, dendritic cells and natural killer (NK) cells. Killing of target cells is principally carried out by the macrophages and NK cells whilst the dendritic cell predominantly acts as an antigen presenting cell. However, there is some overlap in these functions. The adaptive immune system, unlike the innate immune system is highly specific and begins to act several days after the advent of an infection. Effectors of the adaptive immune system are T and B cells.

Activation of the immune system, or inflammation, has been reported to be involved in the development and end-organ damage associated with hypertension since the 1960s (68). Early studies showed that immunosuppression by cortisone reduced blood pressure in a rat model of hypertension (69). More sophisticated work which followed in the next 20 years showed that the active Na^+ retaining mineralocorticoid deoxycorticosterone acetate (DOCA) and salt administration induced an increase in blood pressure in both wild type and athymic nude mice but this increase was only sustained in wild type mice (70). Furthermore, splenocytes from mice with DOCA induced hypertension transplanted into wild type mice caused an increase in blood pressure (71). In addition, leukocyte infiltration was seen in the heart, kidneys, adventitia and perivascular fat surrounding vessels from people with hypertension and in hypertensive animal models (68, 72, 73). This is associated with the increased expression of chemokines and adhesion molecules which recruit immune cells to these sites (68, 72, 73). An increase in ROS which can be produced from immune cells themselves as well as the sources discussed in section 1.1.1 results in the activation of oxidation sensitive pro-inflammatory transcription factors which stimulate the production of cytokines and adhesion molecules leading to further leukocyte recruitment (68).

Research focussing on the role of the adaptive immune system in the development of hypertension has benefited greatly in recent years with the development of RAG and SCID mouse models which lack T and B cells (74, 75). However, this thesis will focus on the role of the innate immune system where the mechanisms underlying blood pressure control are less well defined.

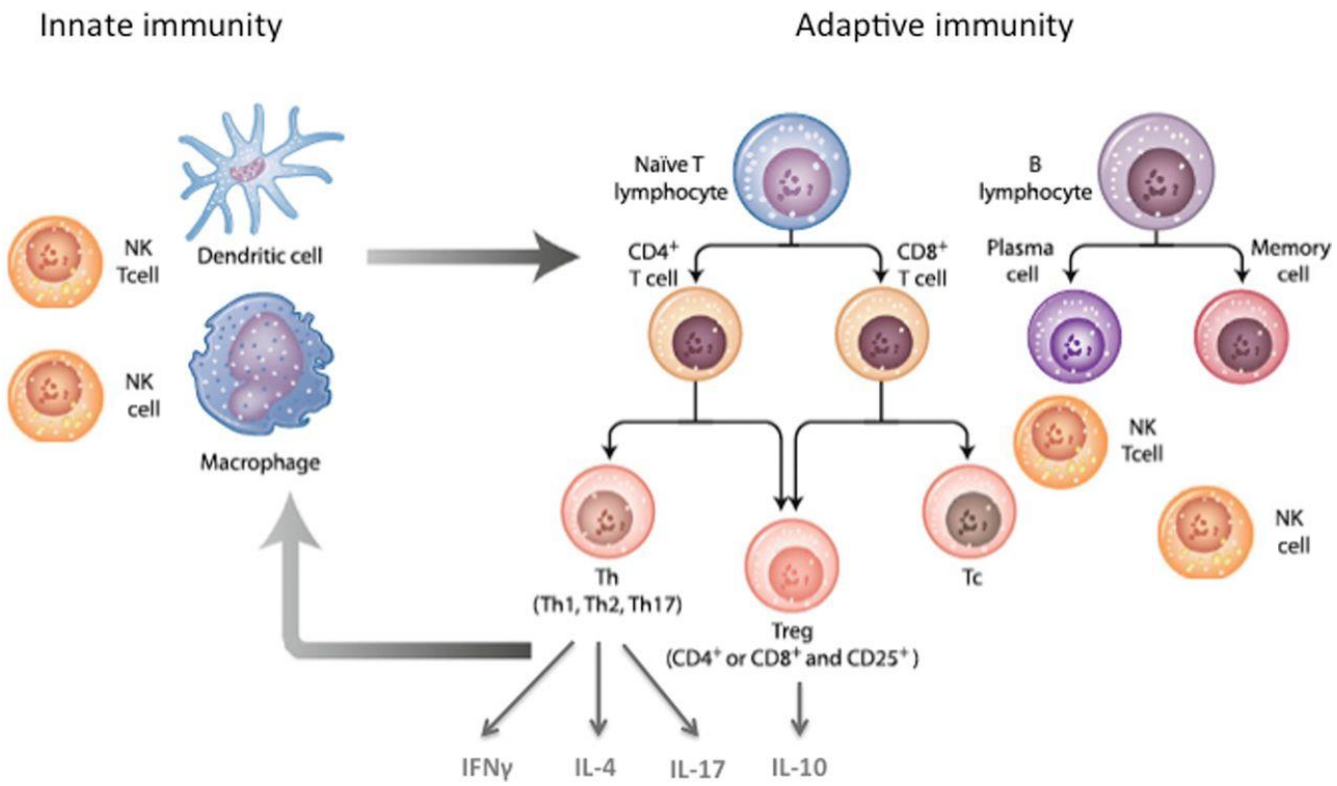

Figure 1-8: The Main Cell Types Involved from the Innate and Adaptive Immune System in Hypertension.

The key cell types from the innate immune system involved in hypertension are macrophages (principally a professional phagocyte but can also present antigens), dendritic cells (principally an antigen presenting cell but also a professional phagocyte) and natural killer (NK) and natural killer T cells (non-professional phagocytes). Cells of the innate immune system are linked to the adaptive immune system by antigen presentation or chemokine production with promotes leukocyte recruitment. T cells are mediators of cell based immunity. They can develop into either CD4+ helper T (Th) cells which assist the actions of other immune cells by releasing T cell cytokines or CD8+ cytotoxic T (Tc) cells which can recognise and kill target cells expressing specific antigens on their cell surface. Regulatory T cells (CD4+ or CD8+ and CD25+) act to suppress T cell activity at the end of an immune reaction and to prevent autoimmune T cell activity. B cells are mediators of humoral immunity. Plasma cells work in concert with Th cells to proliferate and produce antibodies to a specific threat. Memory B cells retain the information regarding a previous threat to allow it to produce a more rapid response with a greater production of antibodies upon secondary infection. Image adapted from Schiffrin (2014).

1.3.1 Activation of the Innate Immune System in Hypertension

Cells of the innate immune system (macrophages, dendritic cells and NK cells) are signalled by chemokine release and adhesion molecule expression from vessels or tissues under stress and/or injury (76). Mouse models where macrophages are functionally deficient or depleted are resistant to elevations in blood pressure induced by angiotensin II infusion and DOCA. They are also protected from end organ damage and vascular remodelling (77-79). However, the relative contribution of the reduction in blood pressure and a direct effect of knocking down the macrophage cells are not clear. Macrophages produce reactive oxygen species in response to angiotensin II stimulation therefore they could play a role directly in vascular remodelling and tissue damage induced by oxidative stress (80). With respect to dendritic cells, blockade of a specific type of antigen presentation which activates naïve T cells has also been shown to blunt the response to angiotensin II induced blood pressure increase in mice (81). The evidence for a role of the innate immune system in the development and end organ damage of hypertension is convincing. However, what is lacking is a mechanistic basis for such findings. Furthermore, this work has predominantly been carried out in preclinical models and lacks clinical translation. This thesis will focus on NK cells and their role in the development of hypertension.

Pro-inflammatory cytokines which are predominantly released from immune cells play a key role in hypertension associated damage by affecting tissues directly or indirectly by recruiting other immune cells (82). Some key examples are IL-6 which plays a role in the development of angiotensin II induced hypertension in a mouse model (83) and is positively associated with blood pressure in apparently healthy humans (84). Interferon-γ knockout mice are also protected from cardiac damage induced by angiotensin II induced hypertension (85). This thesis will focus on another pro-inflammatory cytokine, TNFα, and its role in the development of hypertension.

1.3.2 Natural Killer Cells

NK cells are large granular lymphocytes shown to demonstrate traits of both the innate and adaptive immune system (86). Among other functions, this group of cells possess spontaneous cytotoxic ability, acting as an effective defence

against infected and cancerous cells. They produce a number of cytokines which recruit and regulate cells of the adaptive immune system (87). NK cells are described as immune sentinels thus have a widespread distribution throughout the body. They are unique in that they are able to identify stressed or infected cells without binding major histocompatibility complex (MHC) or antibodies and therefore provide a rapid immune reaction. In most tissues, NK cells represent only a small percentage of the lymphocyte population, for example, 5-10% of the lymphocyte population in the spleen and 2-18% in human peripheral blood (88).

The potent cytotoxic ability of NK cells is regulated on three levels. Firstly, NK cells undergo an education process whereby only those that recognise "self" are promoted to having cytotoxic ability (89). Secondly, these cytotoxic cells are tightly regulated by a sophisticated system involving a complex of interactions between the target cell and either activating or inhibitory receptors on the NK cell surface (Fig 1-9). NK cell surface receptors classically recognise MHC class I ligands as "self" or when these are up-regulated due to stress, "dangerous self", or missing, "missing self", such as during infection or in cancerous cells. NK cells can also recognise cell adhesion or virally-derived molecules. Receptors on NK cells can be predicted to be either activating or inhibitory based upon a characteristic immune-receptor tyrosine-based activation or inhibitory motif; ITAM or ITIM respectively. These specialised domains are phosphorylated by Src kinases resulting in the recruitment of scaffolding proteins for further signal transduction in the case of ITAMs; or recruitment of protein phosphatases to turn off signalling in ITIMs (90). Finally, resting NK cells have a relatively low cytotoxic ability compared to "primed" NK cells. Priming involves a translational switch of the mRNA of cytotoxic molecules abundant in resting NK cells thus resulting in activation of the cytotoxicity (91). This is regulated by the cytokine microenvironment in which the NK cell is present; such as type-1 interferons, IL-12, IL-18 and IL-15 to varying degrees in humans and rodents (92). It can also be regulated by the close proximity of other immune cell types such as T cells, monocytes and dendritic cells (93-95).

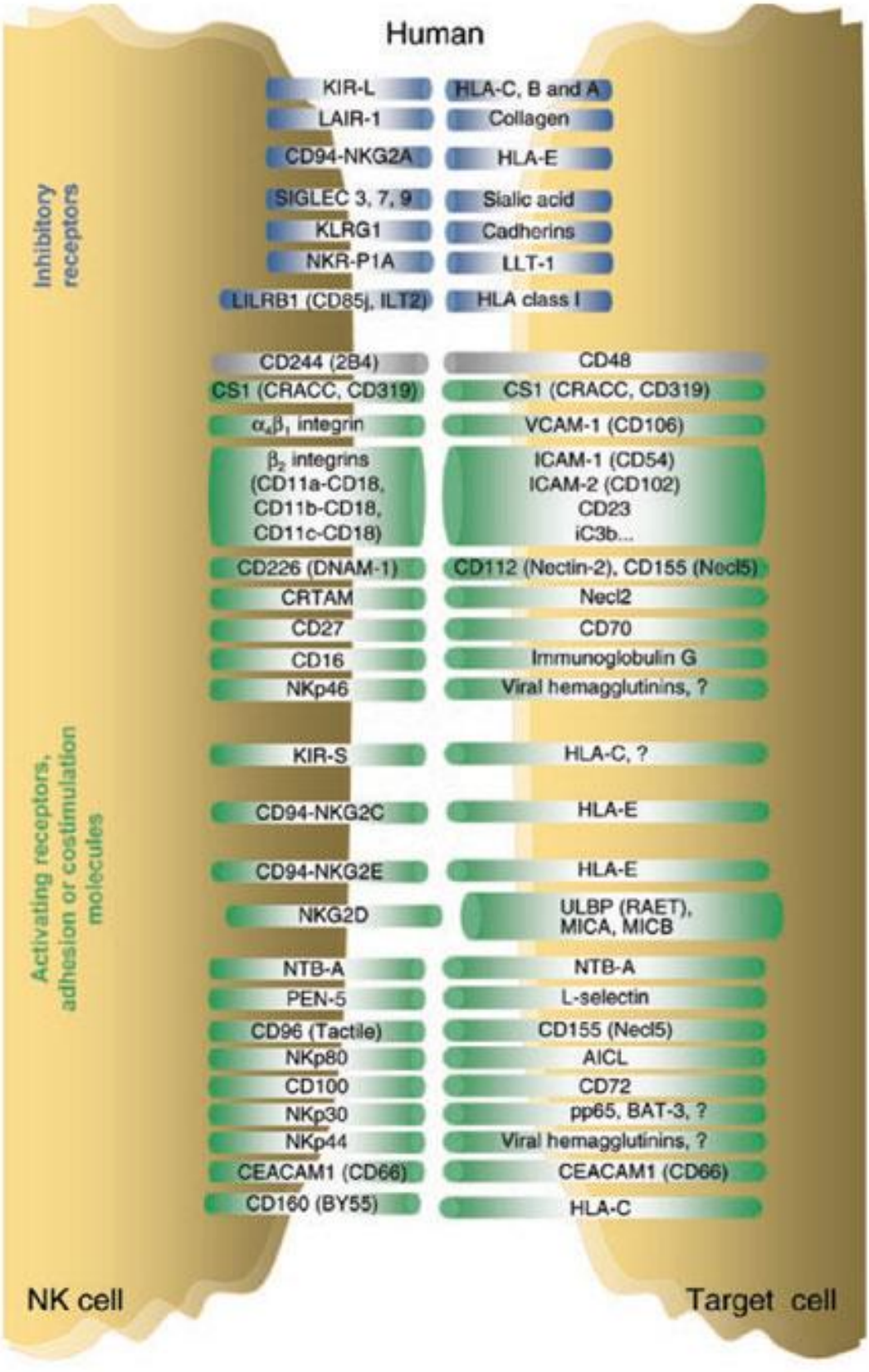

Figure 1-9 The Natural Killer (NK) Cell-Target Cell “Zipper” in Humans.

The evolution of potent cytotoxic ability is accompanied by an equally powerful control mechanism in NK cells. Activating receptors (green) predominantly recognise self “stress” ligands or infectious ligands. Inhibitory receptors (blue) predominantly recognise “self” ligands such as the human version of the major histocompatibility complex genes (the human leukocyte antigen (HLA) family) which prevent NK cells from damaging host tissue. Image adapted from Vivier *et al.* (2008).

1.3.2.1 NK Cell Receptors

Whilst the general regulatory mechanisms of NK cell surface receptors are conserved between humans and rodents; the identity of these receptors are not directly comparable. For example, CD56 the main extracellular marker of NK cell populations in humans is not expressed in rodents. Therefore, direct comparison of NK cell populations between rodents and humans requires care. Interspecies variation in cell surface receptors also exists between rats and mice. Additionally, further complexity exists as intraspecies variation is observed in different strains of laboratory mice (96). The NK cell receptors are mainly transcribed from the natural killer gene complex (NKC); this is located on chromosome 4 in rats, 6 in mice and 12 in humans (97-99).

1.3.2.2 Natural Killer Receptor Protein (Nkrp) Receptors

The first group of receptors to be identified which were selective for natural killer cells were the natural killer receptor protein 1 (Nkrp1) group, encoded by the killer-cell lectin-like receptor group b 1 (*Klrb*) genes found within the NKC. Nkrp1 receptors are a marker of commitment to the NK cell lineage and are expressed throughout development from immature to mature NK cells in rodents and humans (100). Nkrp1 receptors recognise “self” or “missing self” in an MHC-dependent manner by interacting with target cell C-type lectin-related molecules (Clr) (101, 102). There are 4 Nkrp1 members in the rat: Nrkp1-a, b, f and g. Nkrp1a and b are clustered on the proximal part of the rat NKC whereas Nkrp1f and g are found on the distal part. Nkrp1a (CD161) is currently the most widely used marker to identify natural killer cell populations in rats however CD161 is also known to be expressed on specific subsets of T cells and dendritic cells (103-105). Therefore, the accepted definition of rat NK cells is CD3- CD161+ to exclude T cells (CD3+). This classification has been used in the experiments presented in this thesis (Chapter 5). In mice, there are 7 family members: Nkrp1-a, b, c, d, e, f and g (106). The mouse Nkrp1-c, d, f and g are considered to be orthologues of the rat Nrkp1-a, b, f and g respectively (107). In contrast to the multiple Nkrp1 family members in rodents, there is only a single human NKRP1A (CD161) receptor. This shares 46% homology with rat Nkrp1 and 46-47% with mouse Nkrp1 receptors. CD161 expression is only limited to a subset of human NK cells whereas all rodent NK cells express CD161 (108). In humans, CD161 is up-regulated

by interleukin-12 (IL-12) (109) and binds lectin-like-transcript 1 which has an inhibitory function and supresses cytotoxic activity against the target cell (109-111). In parallel, humans also express KLRF1 genes which are thought to be evolutionarily related to the NKRP1 family and have an activating function (102).

Nkrp1a was first shown to be an activating receptor in rats in the 1980s, where antibodies to Nkrp1a induced the release of cytotoxic granules from NK cells (112). This mechanism was further developed in a rat natural killer cell line (RNK-16) where all Nrkp1 receptors were knocked out and the presence of Nkrp1a alone was sufficient to induce a significant rise in NK intracellular calcium (113). These knockout cells also had cytotoxic ability against a cancer cell line dependent upon the generation of phosphoinositide signalling (114). Nkrp1a activation also stimulates the release of pro-inflammatory interferon-γ (113). In contrast, Nkrp1b incubation inhibits the cytotoxic activity of the RNK-16 cell line (115). In the event of infection or genotoxic stress, the inhibitory Nkrp1b receptor is down-regulated (116). Due to its similar inhibitory function, human NKR-P1A is thought to be orthologous to Nkrp1b in rat. Furthermore, Nkrp1a and b have a high degree of intraspecies allelic variation in rats and this has led to the misclassification of "novel" Nrkp1 family members. The other Nkrp1 receptors in the rat, f and g, have only recently been characterised (105). Unlike Nkrp1a and b which have a high degree of sequence variability between strains of rat and between rats and mice, the sequences of Nkrp1f and g are highly conserved (117). Nrkp1f activation was shown to induce an increase in intracellular calcium and induce target cell lysis but not to the same degree as Nkrp1a. This suggests that Nrkp1f is not as potent an activating factor as Nrkp1a. Inhibitory Nkrp1g effectively reduced target cell lysis induced by both Nkrp1a and Nkrp1f and showed up-regulation of the ITIM downstream signalling cascade (105).

1.3.2.3 Pattern-Recognition Receptors

An evolutionary conserved mechanism exists in the innate immune system that allows broad recognition of molecular motifs derived from a potentially harmful external source such as glycoproteins or double stranded RNA from pathogens (pathogen associated molecular patterns or PAMPs) or an internal source such as modifications resulting from oxidative damage or necrosis (damage associated molecular patterns or DAMPs) (118). These motifs are recognised by an

evolutionary conserved group of receptors known as the toll-like receptors (TLRs) (119). Activation of TLRs in NK cells results in a signalling cascade which activates pro-inflammatory gene expression through the transcription factors NFκB and interferon regulatory factors (IRF) (120).

1.3.2.4 NK Cells in Hypertension & Vascular Dysfunction

The most prominent cytokines produced by the NK cell are interferon γ (IFNγ) and TNFα which function as an innate form of defence and to recruit cells of the adaptive immune system (121). In humans, TNFα and IFNγ work in concert to promote the cytotoxic ability of NK cells through up-regulation of the expression of intracellular adhesion molecule 1 (ICAM-1) on target cells (122). Uncontrolled release of these pro-inflammatory cytokines is a central cause of morbidity and mortality in autoimmune disorders (123, 124). In particular, NK cells have been shown to have a causative role in vascular pathology, hypertension and hypertensive end-organ damage through both secretion of pro-inflammatory cytokines and cytotoxic ability. NK cells possess the receptors to adhere to endothelial cells (87) and are a causative factor for endothelial damage as a result of viral infection (125) and transplantation (126). IFNγ receptor knockout mice are protected from end-organ damage from angiotensin II induced hypertension suggesting a role for IFNγ in angiotensin II induced vascular damage (85). Recently, Kossman *et al.* identified the source of this damaging IFNγ to be NK cells which become activated by IL-12 secreting monocytes in a positive feedback loop to potentiate endothelial dysfunction and increased oxidative stress in mouse aorta (127). TNFα blockade has also been shown to reduce angiotensin II induced cardiac damage (128, 129); yet the relative contribution of TNFα in the model proposed by Kossman *et al.* was not explored. The study by Kossman *et al.* also focussed on the aorta and did not assess effects on the resistance vessels which are predominantly involved in the regulation of blood pressure. The NKC has been identified as a susceptibility locus for L-NAME induced hypertension in C57BL/6 mice (130). Taherzadeh *et al.* exploited the genetic differences in the NKC between the C57BL/6 and BALB/C mouse strain showing that C57BL/6 mice had an increased propensity for hypertension and vascular remodelling. The authors then developed a congenic strain, BALB.B6-Cmvlr, where the C57BL/6 NKC is inserted on to a BALB/C background. The congenic strain developed significantly higher blood pressure than the BALB/C accompanied by an infiltration of NK cells

surrounding the mesenteric arteries. The BALB.B6-Cmvlr congenic also shows a significant increase in vascular remodelling and NK cell invasion in a balloon-model of vascular injury (131). These finding indicate that the NKC locus is involved in hypertension and vascular injury but the identification of which gene in the NKC is responsible or whether these findings are relevant clinically is yet to be shown. With respect to the model central to this thesis, the SHRSP, the role of NK cells has not been previously studied. However, non-specific activation of circulating NK cells has been shown in the related SHR strain and is thought to contribute to the significant age-related reduction in T cell mediated immunity in the SHR relative to the WKY (132).

1.3.3 Tumor Necrosis Factor α (TNFα)

Tumor necrosis factor α (TNFα) is a pleiotropic pro-inflammatory cytokine not normally detecTable in healthy individuals but is up-regulated in the event of an infection, inflammation or an autoimmune disorder (133). In the majority of published work on TNFα, it has been measured as a biomarker of inflammation. However, delineating the signalling mechanisms of TNFα remains an active area of research. TNFα is produced in a 26 kDa transmembrane form which can then be cleaved by metallopeptidase ADAM17 (also known as TNFα converting enzyme; TACE) into the 17 kDa soluble TNFα. Both the transmembrane and soluble forms of TNFα have distinct roles in the activation of target cells either by direct cell to cell contact or acting on remote sites respectively (134). In cells outside of the immune system, TNFα receptor 1 (TNFR1) is the major mediator of intracellular TNFα signalling (135) (Fig. 1-10).

TNFα signalling through TNFR1 induces apoptosis and a pro-inflammatory response in the target cell. This is primarily through the intracellular TNFR1 death domain (TNF-receptor associated death domain; TRADD) which can associate with other death domain containing proteins and initiate a signalling cascade for apoptosis (136). The TRADD also acts as a scaffold for the activation of the pro-inflammatory gene transcription factor, NF-κB. TRAF2 is associated with the TRADD (TNF receptor-associated factor 2) which recruits the enzyme I-κB kinase (IKK). IKK is then activated by RIP (receptor-interacting protein) serine/threonine kinase. Once IKK is activated it targets the regulatory subunit of NF-κB, I-κB, for destruction by the proteasome. NF-κB is then available to be phosphorylated and

translocates to the nucleus (137). TNFα also transiently stimulates JNK and the p38 signalling pathways which contribute to inflammation and apoptosis; activation of these pathways is only prolonged under apoptotic conditions (135).

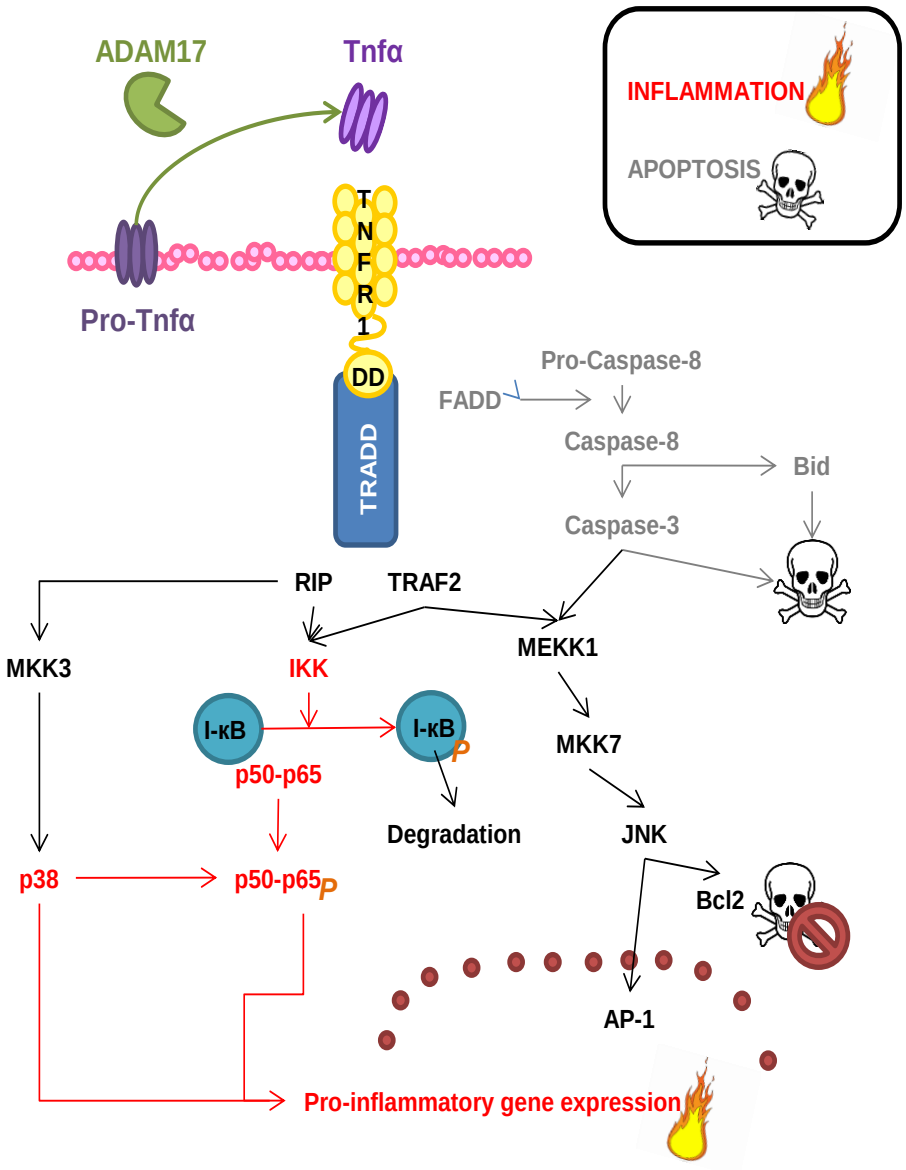

Figure 1-10: Summary of TNFα Signalling through TNFR1.

TNFR1 signalling converges on phosphorylation of the I-κB protein which binds and inhibits the nuclear localisation sequence of the pro-inflammatory NF-κB (p50-p65) transcription factor. Once I-κB is phosphorylated it is targeted for degradation by the proteasome. Secondly NF-κB (p50-p65) must also be phosphorylated itself by MAP kinases such as p38 to be fully activated for nuclear translocation. The stress-activated (SAPK)/C-Jun N-terminal kinase group (JNK) is activated by TNFR1 signalling. JNK translocates to the nucleus to enhance the activity of the activating protein-1 (AP-1) transcription factor. In response to TNFR1 activated JNK signalling, AP-1 transcribes genes involved in inflammation such as MCP-1 and E-selectin. The activation of p38 also stabilises mRNA of inflammatory cytokines IL-1 and IL-6. ADAM17: ADAM metallopeptidase 17, TRADD: TNF receptor associated death domain, FADD: Fas-Associated protein with Death Domain, RIP: receptor interacting protein, TRAF2: TNF receptor associated factor 2, MEKK1: MAP/Erk kinase kinase 1, MKK: MAP kinase kinase.

1.3.3.1 TNFα in Hypertension & Vascular Dysfunction

TNFα has been shown to play a role in blood pressure regulation. Modest increases in circulating levels of TNFα are associated with hypertension (138, 139) however large increases in TNFα such as in septic shock are associated with a sharp decrease in blood pressure and increased survival (140) (Fig 1-11). The effect of TNFα on blood pressure may also be determined by the source, location and type (acute or chronic) of inflammation which could explain the often variable and sometimes conflicting results for the effect of TNFα inhibitors on blood pressure in humans and pre-clinical models.

TNFα can control blood pressure through direct effects on the kidney (Fig. 1-11). TNFα is predominantly expressed by immune cells resident in the kidney but can also be produced by renal cells (141). Renal TNFα production is increased in response to increases in blood pressure, reactive oxygen species and angiotensin II (141). Increased TNFα production promotes leukocyte recruitment and activation which then results in more TNFα production and thus a self-perpetuating loop of inflammation. The principal cause of kidney damage elicited by TNFα is primarily through this mechanism of inflammation and through TNFα-dependent cell death pathways (Fig. 1-11). In addition, TNFα in the kidney is able to directly regulate salt and fluid balance through modifying the expression of components of the RAAS cascade (142, 143) and Na^+ transporters (144).

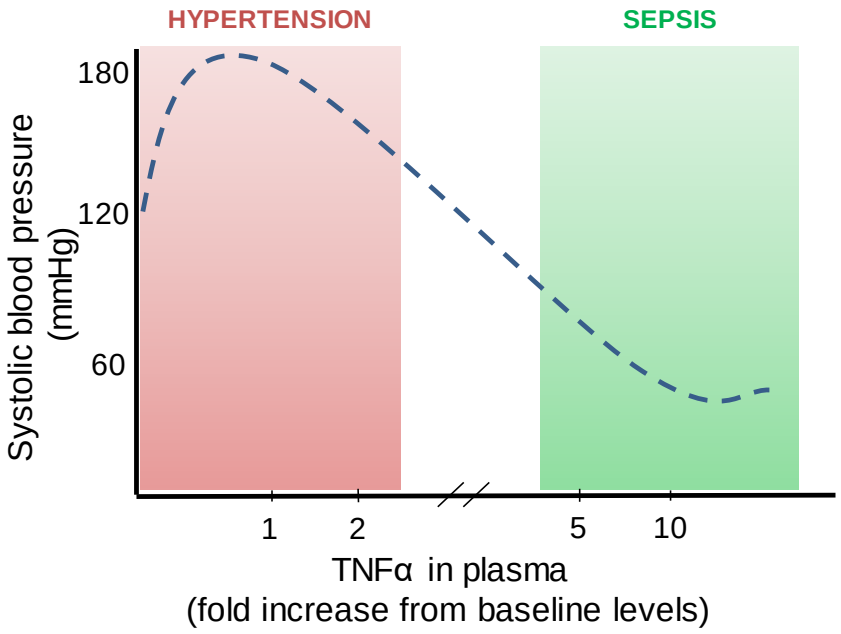

Figure 1-11: TNFα Levels and Blood Pressure Regulation.

Chronic increases in TNFα such as that seen in hypertension (red box) perpetuates increases in blood pressure and associated end-organ damage. However, an acute, large increase in TNFα such as in sepsis (green box) induces mechanism that acts to reduce blood pressure. In both situations, TNFα causes activation of the immune system. Figure adapted from Ramseyer & Garvin (2013).

TNFα signalling has also been shown to have direct deleterious effects on the vasculature in hypertension (Fig 1-12) (145). TNFα infusion induces a significant reduction in endothelial dependent relaxation in large and small arteries of both humans and rodents (146-148). In endothelial cells, TNFα diminishes the bioavailability of vasodilator NO through down-regulation of the expression of the eNOS pathway (149, 150) and through increased superoxide production which scavenges NO (151). TNFα pre-incubation also significantly reduces the vasodilatory effects of endothelium dependent hyperpolarising factor in omental arteries from pregnant women (152) and directly affects hyperpolarisation in endothelial cells from intact arteries from animal models (153). With respect to vasoconstriction, TNFα promotes endothelin 1 (ET-1) mRNA expression (154) and can alter VSMC calcium handling (155). TNFα induces endothelial cell activation through the expression of other pro-inflammatory cytokines leading to immune cell infiltration and a self-perpetuating vascular inflammation (156).

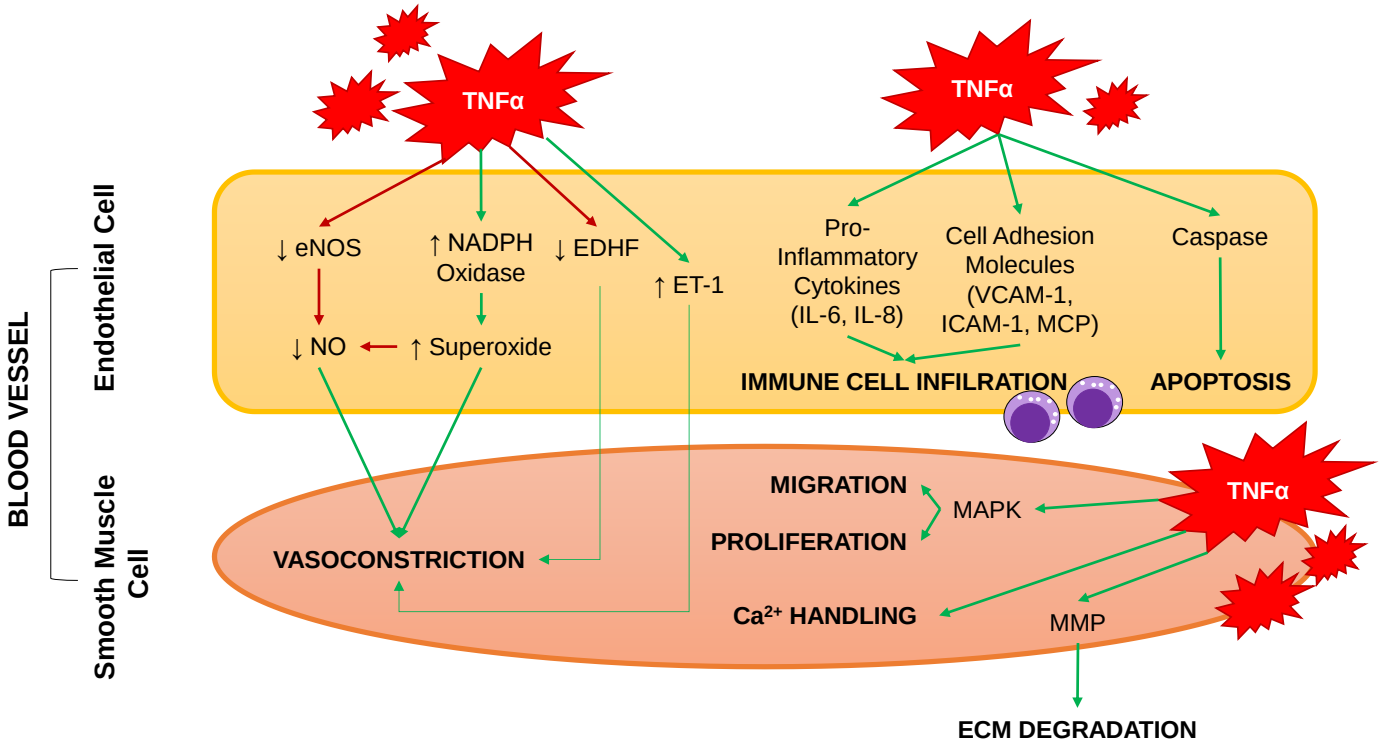

Figure 1-12: Tumor Necrosis Factor-α in Vascular Dysfunction.

TNFα induces endothelial cell dysfunction by reducing vasodilators NO and EDHF and enhancing vasoconstriction through ROS and ET-1 production. Endothelial cell activation is triggered through the expression of pro-inflammatory cytokines and adhesion molecules leading to immune cell recruitment and endothelial damage. TNFα plays a role in vascular remodelling through activation of MAP kinases that promote vascular smooth muscle cell proliferation and migration and matrix metalloproteinases (MMPs) which act to degrade the extracellular matrix (ECM). NO: nitric oxide, EDHF: endothelium derived hyperpolarizing factor, eNOS: endothelial nitric oxide synthase, ET-1: endothelin-1.

1.4 Animal Models of Hypertension

1.4.1.1 Animal Models

The use of animal models in research has steadily increased over the last decade; this has principally been due to an increase in the use of animals bred for specific genetic modifications (157). The attraction of animal models of human disease is that they allow the study of specific disease pathology and treatment *in situ*. Broadly, the ideal animal model of human disease would exhibit phenotypic similarities to the human condition, respond similarly to humans when treated with clinically relevant drugs and be easily reproducible. Animal models, specifically rodents, provide the researcher with an invaluable tool for studying complex diseases such as hypertension. Rodent models offer a number of advantages for study: they breed easily producing large litters, have a short lifespan allowing for relatively long-term and intergenerational studies and the ability to have environmental control. Animal models are excellent for studying human disease without additional complexity, however, this can also a disadvantage. For example, animal models are often inbred with a similar genetic background in a tightly regulated environment to produce consistent results. This is not the case for humans where the genetic background is diverse with many different environments. Furthermore, many animal studies do not take into account effects that may be gender specific or affect a certain group of people, for example, BMI or race. However, the use of both genders in animal experiments has now been addressed in recent guidelines from the National Institute of Health (158).

1.4.1.2 Rat Models of Hypertension

Rats are the leading animal model for hypertension research (159). There are a number of hypertensive rat models, which exhibit similarities to the human condition and provide a range of tools to complement the diversity of hypertensive disease seen. Examples of rat models currently in use employ surgically-induced hypertension (160), dietary hypertension (161), endocrine hypertension (162), neurogenic hypertension (163), psychogenic hypertension (164), chemically induced hypertension (165) or angiotensin II infusion induced hypertension.

A genetic rat model of hypertension incorporates two different methodologies: genotype driven or phenotype driven. The mouse is currently the model of choice for geneticists owing to extensive knowledge of the mouse genome and existing infrastructure for producing genetically modified animals. Despite this, genetically modified rat models for studying hypertension do exist such as the (mREN-2)27 transgenic rat (166). With the recent advent of new gene editing technologies such as CRISPR-Cas (167); inexpensive and straightforward genome editing will be more widely available in rats. Genotype-driven models are excellent for dissecting out a single gene in a mechanism of interest. One disadvantage is that, by definition, these models are more reflective of rare monogenic forms of hypertension. As discussed in section 1.2.1.1, essential hypertension of unknown cause accounts for the majority of cases of human hypertension. Essential hypertension is known to be polygenic with varying degrees of penetrance. This led researchers to develop phenotype-driven rat models. Using this approach, rats from an outbred strain are selected for the highest blood pressure and selectively bred through sequential brother x sister mating to produce a hypertensive inbred strain. Hypertensive animal models can also be selected to respond to a specific stimulus such as high salt or high fat. These inbred strains resemble the human phenotype of essential hypertension where one single gene does not account for the observed phenotype. There are a number of inbred hypertensive rat strains currently in use which are summarised in Table 1-4. The variety of strains available is helpful to validate findings from one strain to the other, for example, the hypertensive susceptibility locus found on rat chromosome 1 has been identified in four different rat models (168-171).

Table 1-4 Existing Inbred Rat Models of Hypertension

Name	Origin	SBP Adult Males (mmHg)	SBP Adult Females (mmHg)	Reference for SBP Values	Control Strain	Background Strain
Spontaneously Hypertensive Rat (SHR)	Kyoto, Japan (172)	185	163	(173)	Wistar-Kyoto (WKY)	Wistar-Kyoto (WKY)
Stroke Prone Spontaneously Hypertensive Rat (SHRSP)	Kyoto, Japan (174)	245	197	(175)	WKY	WKY
Milan Hypertensive Rat (MHS)	Milan, Italy (176)	163	SBP was not significantly different in females[1].	(177)	Milan Normotensive Rat	Wistar

[1] SBP of 163.7 ± 1.9 mmHg is given as an average of a group containing both male and female animals. The authors state there is no significant difference between male and female animals.

Dahl Salt Sensitive Rat (Dahl S)	Brookhaven, USA (178)	152	141	(179)[2]	Dahl Salt Resistant Rat	Sprague-Dawley
Lyon Hypertensive Rat (LH)	Lyon, France (180)	173	-	(181)	Lyon Normotensive Rat and/or Lyon Low Blood Pressure Rat	Sprague-Dawley
Sabra Salt Sensitive Rat (SBH)	Jerusalem, Italy (182)	186	157	(183) [3]	Sabra Salt Resistant Rat	Wistar
New Zealand Genetically Hypertensive Rat (NZGH)	Dunedin, New Zealand (184)	158	148	(185)	New Zealand Normotensive Rat	Wistar

SBP in the Table is given for adult animals 4-6 months of age. Table compiled by author.

[2] Dahl S rats were salt loaded (0.8 % NaCl in drinking water) for 2 weeks.

[3] Sabra Salt Sensitive Rats were salt loaded (0.1% NaCl in drinking water) for 4 weeks.

1.4.1.3 The Stroke Prone Spontaneously Hypertensive Rat

The spontaneously hypertensive rat (SHR) and stroke prone spontaneously hypertensive rat (SHRSP) were obtained by selective inbreeding of Wistar-Kyoto (WKY) rats in the laboratory of Okamoto and colleagues at the Kyoto University Faculty of Medicine, Japan (172, 174). Firstly, the SHR was developed by selective inbreeding of WKY with high systolic blood pressure in 1963 (172). The SHR blood pressure begins to spontaneously increase from 4 weeks of age reaching an SBP in males of 180-200 mmHg relative to 130 mmHg in the contrasting WKY strain (186). In 1971, the SHR was divided into three sub-strains (A - C); where sub-strain A consistently exhibited higher SBP and an increased propensity for cerebrovascular disease. Inbreeding of offspring from sub-strain A produced the SHRSP (Fig 1-13).

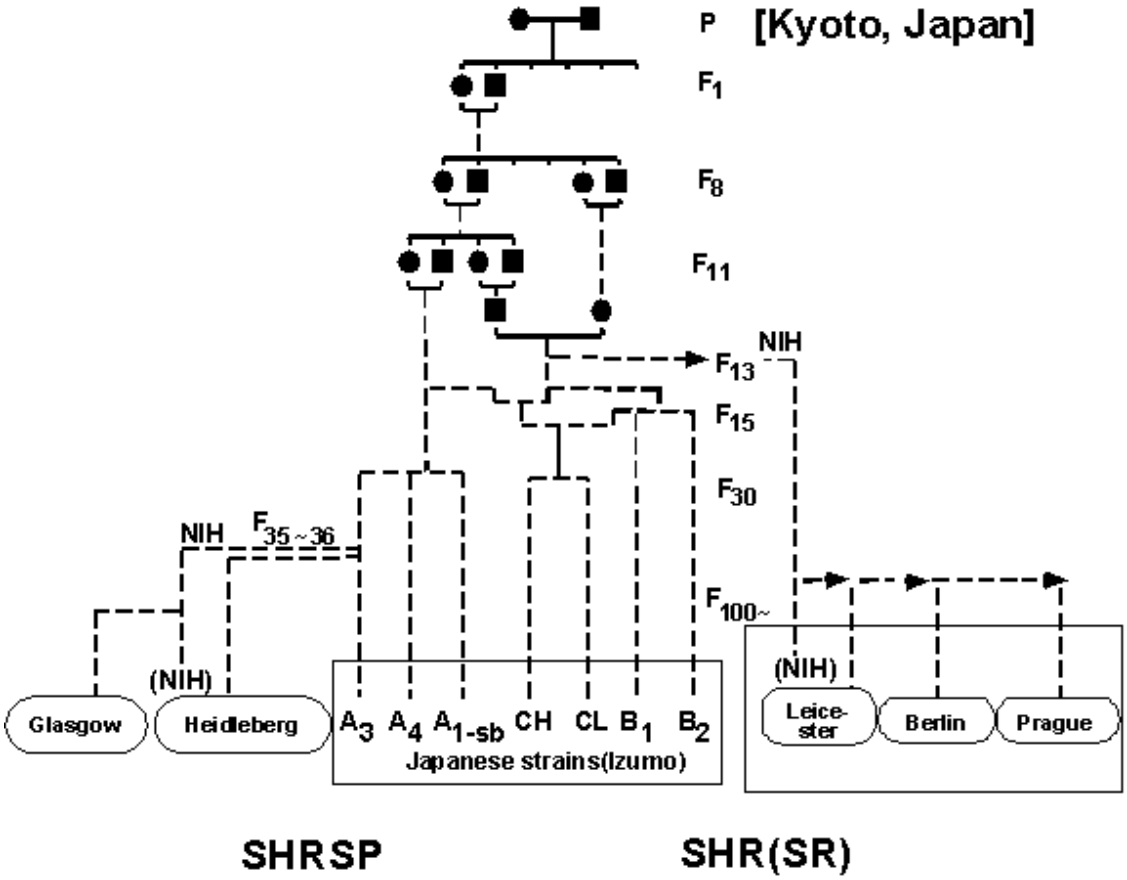

Figure 1-13: Genealogy of the Stroke Prone Spontaneously Hypertensive Rat. Image provided by Dr. Delyth Graham.

The SHRSP has an increased incidence of CV complications, specifically a higher tendency for stroke, as well as a more rapid onset of hypertension from 5 weeks of age rising to a SBP in male animals of approximately 230 – 250 mmHg (174) relative to the normotensive WKY in the original Kyoto strain. The SBP varies between sub-strain and in Glasgow the eventual SBP is approximately 190-200 mmHg (personal communication, Dr. Delyth Graham). Furthermore, SHRSP blood pressure is salt-sensitive, whereby replacing drinking water with a 1% NaCl solution produces a rise in blood pressure of approximately 30 mmHg and accelerates the occurrence of stroke (187). In contrast, the SHR and WKY are less salt sensitive (187). Male SHRSP have a shorter lifespan (52 – 64 weeks (188) or 14 – 20 weeks with salt loading (189)) relative to the SHR (approximately 2 years) and the WKY (approximately 3 years) (190). The pronounced CV phenotype and salt-sensitivity of the SHRSP makes it an ideal model to study human hypertension. The SHRSP displays a number of pathologies associated with human hypertension which make it a clinically relevant model (Fig 1-14).

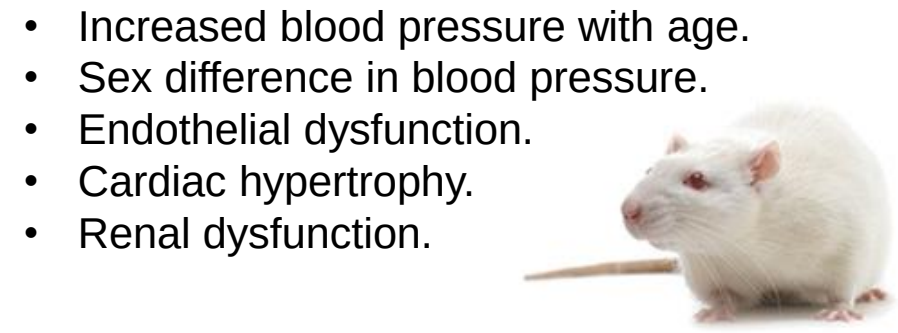

Figure 1-14: Characteristics of the Stroke Prone Spontaneously Hypertensive Rat.

1.4.1.4 Sex Differences in the Spontaneously Hypertensive Rat and the Stroke Prone Spontaneously Hypertensive Rat

Higher blood pressure in males is reflected in inbred models of hypertension such as the SHR, SHRSP, Dahl and (mREN-2)27 rats (191). Furthermore, there have been no studies to date which have shown a robust difference in blood pressure between male and female normotensive animals; suggesting that the observed gender dimorphism is specifically related to pathologies underlying the development and establishment of hypertension. The SHRSP and related SHR have been used to explore mechanistic differences in blood pressure regulation between male and female animals. As shown in Table 1-4, systolic blood pressure is greater in male SHR and SHRSP.

The Y chromosome in the SHRSP has been shown to carry a hypertension susceptibility locus (175). Furthermore, castration of male SHRSP before adulthood results in a reduction in blood pressure increase in these animals however anti-androgen treatment was not effective against established hypertension (192). This suggested an involvement for male sex hormones in the development but not maintenance of high blood pressure. Ovarectomized females show no difference in blood pressure in the SHR (193) but there is a significant increase in blood pressure when SHRSP are subject to the same procedure (194). The utilisation of animal models for studying the contribution of sex hormones to blood pressure regulation should be interpreted with caution as timing of surgery and dosage of hormone replacement therapy are often found to vary (191). Vascular biology also differs between male and female SHRSP. Aortic rings from SHRSP females have a greater endothelium-dependent nitric oxide mediated vasodilation (195) than males and have altered calcium handling machinery involved in vasoconstriction (196). In the SHR, vascular smooth muscle cells (VSMCs) from male animals have higher proliferative and migratory capacity (197). Female SHRSP are also relatively protected from hypertension related kidney damage (198) and have significantly reduced proteinuria when aged (199). Female SHRSP have been shown to have a significantly increased anti-inflammatory T regulatory cell (TReg) response induced by hypertension (200). Furthermore, female SHRSP were found to have a significantly lower mortality attributed to a more effective anti-inflammatory response (201).

1.5 Pregnancy & the Cardiovascular System

Pregnancy presents a major challenge to the maternal CV system; it requires rapid and extensive remodelling in order to provide for the developing fetus. The main driving forces for these changes are an increase in metabolic demand from the mother and fetus and maximising the uteroplacental blood flow. Changes in measurable CV parameters can be detected as early as 5 weeks of gestation in humans (202) and mostly return to normal two weeks post-partum in humans (203). CV changes are measured at gestational day 3.5 in rodents (204) and resolve slightly later with significantly elevated SV and CO detecTable up to three weeks after pregnancy (205). The occurrences of these changes in the CV system which occur very early in pregnancy, even before placentation, highlight the vital role that they play. Indeed, deficiency in the adaptation of the maternal CV system underlies a number of obstetric syndromes.

1.5.1 Cardiovascular System Adaptation to Pregnancy in Humans and Rodents

The dynamic process of systemic CV remodelling associated with pregnancy is most well-characterised in humans and in mice. Data from mice were used to expand upon changes seen in rats (Table 1-5) as adaptation in the two species is thought to be broadly similar. In humans and rodents, the blood flow to non-reproductive organs is unaltered by pregnancy whilst the uterine blood flow increases by around 20-fold (206). The key change during pregnancy affecting the CV system is a marked increase in blood volume due to activation of the RAAS early in pregnancy. This leads to an approximately 50% increase in CO which is seen in both humans and rodents (207, 208). In humans, the increase in CO early in pregnancy is primarily mediated by SV then later in pregnancy mediated by an increase in heart rate (209), whereas, it is thought to be predominantly due to an increase in SV in rodents (205). The vasculature accommodates this increase in CO by marked systemic vasodilatation. As a counter-balance, increased sympathetic drive to the heart, adrenal glands, kidney and skeletal muscle are vital to counteract hypotension. This combination of increased preload due to higher circulating blood volume and decreased afterload due to the global reduction in systemic vascular resistance results in eccentric remodelling of the heart and an increase in left ventricular mass, similar to that which is seen in elite athletes

(210, 211). Maladaptation of the maternal CV system is an underlying cause of CVD in pregnancy. For example, in pre-eclampsia there is a significantly reduced volume expansion and systemic vasodilatation but the sympathetic nervous system remains excessively activated relative to normotensive women (212).

Table 1-5 Physiological Adaptation of the Maternal Cardiovascular System in Humans and Rodents.

	Humans	Rodents
Cardiac Output	Increases up to 45% by the second trimester with an additional 15% for twin pregnancies (208) .	Increases up to 28% by gestational day 9.5 (205) and 40 - 60% by gestational day 17.5 (204, 207).
Heart Rate	Gradual increase throughout pregnancy to a maximum of 20-25% by the third trimester.	Gradual increase of 10-15% up to gestational day 17.5 (204, 205).
Stroke Volume	Increase early in pregnancy up to the second trimester.	Increases up to 30 - 40% by gestational day 17.5 (205, 207)
Blood Volume	Increases 20-100% with 45% being the most common (209). Plasma volume increases by 50% (213). Haematocrit decreases from normal value of 12-16 g/dl to minimum healthy levels of 11 g/dl in first trimester and 10.5 g/dl in second and third trimester (214).	Increase of 26% in plasma volume and haematocrit is decreased by 18% by gestational day 17.5 (204, 205).
Cardiac Remodelling	Left ventricular wall thickness increases by 28% and wall mass by 40-52% (203, 215, 216).	Left ventricular mass increases by 20-40% by gestational day 17.5 (205, 207).
Systemic Vascular Resistance	Decreases up to 35-40% in the first trimester followed by a plateau or slight increase in the third trimester (217).	Decreases up to 29% by gestational day 9.5 and up to 36% by gestational day 17.5 (205).
Renal Plasma Flow	Vasodilation of the kidneys causes a 50% increase in renal plasma flow and glomerular filtration rate (218).	Vasodilation of the kidneys reaches a maximum at mid-term which is accompanied by a 20% increase in glomerular filtration rate (219).
Renin-Angiotensin System	Renin-angiotensin system (RAS) is activated from gestational week 6-8 and rises until gestational week 28 – 30 (209). Every component of the RAS system is increased apart from angiotensin converting enzyme (ACE) (220).	RAS is activated in pregnancy. In humans where most of the increase in renin comes from the placenta; in rodents it may be a combination of both the placenta and kidneys (221).
Sympathetic Activity	Sympathetic nerve activity is increased from the first trimester (222). Increased maternal baroreceptor sensitivity and decreased responsiveness to α-adrenergic stimulation (223, 224). The pressor effect of infused angiotensin II is reduced (225). Vasoconstrictor response to sympathetic stimulation in the uterine arteries is reduced (226)	Sympathetic nerve activity is increased primarily through the activation of the hypothalamic paraventricular and arcuate nuclei (227). Pressor response to angiotensin II, noradrenaline and vasopressin is reduced in pregnant rats (228). Vasoconstrictor response to sympathetic stimulation is reduced (229).

All percentages quoted are representative as a change from pre-partum baseline.

In summary, the CV system of pregnant humans and rodents are broadly similar; characterised by a high volume, low pressure system with eccentric cardiac remodelling.

1.5.2 Mechanisms of Pregnancy-Dependent Cardiovascular Remodelling in Humans and Rodents

The pregnancy-related hormones – estrogen, progesterone and relaxin – play a central role in mediating CV adaptation to pregnancy. Estrogen and progesterone are principally produced by the corpus luteum formed by the ovary once an ovum has been released in early pregnancy; whilst the placenta is then the main production site for the second and third trimesters. Levels of estrogen and progesterone are related to increased vasodilation in humans (230). Both mice and rats show also a marked increase in estrogen and progesterone production during pregnancy. Progesterone and estrogen blunts the pressor response to angiotensin II in humans (225) and rats (231). Estrogen alone has been shown to have a protective effect on the CV system in SHRSP (232). Progesterone has been shown to have protective effects on the vasculature independent of estrogen in humans and rats (233). Progesterone administration lowers blood pressure in humans (234) and inhibits calcium mediated vasoconstriction (235) in rats. Relaxin is another hormone produced by the corpus luteum in humans and rodents. It increases to a peak by the end of the first trimester when it falls to a plateau for the remainder of pregnancy (236). Human recombinant relaxin administration in female, virgin rats and in mid-gestation rats results in approximately a 20% increase in CO (237, 238). Relaxin has also been shown to elicit a reduction in systemic vascular resistance (239) and an increase in renal blood flow (240) in pregnant rats. Placental growth factor (PlGF), another pregnancy-related factor produced in vast quantities by the placenta, has been shown to be involved in maternal CV adaptation to pregnancy. PlGF knockout mice had an altered blood pressure profile during pregnancy as well as reduced CO, increased left ventricular hypertrophy and renal pathology (207). The pattern of PlGF levels over pregnancy is similar in mice and in humans. PlGF levels are reduced in women who develop pre-eclampsia (241) therefore these findings may have some relevance in clinical situation. Treatment of an animal model of pre-eclampsia with human recombinant PlGF resulted in a decrease in blood pressure concurrent with a reduction in the circulating molecule soluble FLT-1 which acts as an endogenous

antagonist to VEGF signalling but had no beneficial effect on fetal weight or fetal loss. This suggests that PlGF plays a role specifically in the adaptation of the CV system perhaps through modulation of VEGF signalling (242).

1.5.3 Blood Pressure during Pregnancy in Humans and Rodents

The increase in CO during pregnancy must be accompanied by a reduction in systemic vascular resistance to stabilise maternal blood pressure. Typically during a healthy human pregnancy, systolic and diastolic blood pressure follows a similar U-shaped pattern (243, 244). Blood pressure decreases towards the middle of pregnancy (gestational week 20) followed by a steady increase toward delivery (Fig. 1-15A). In women who develop hypertensive disorders of pregnancy, this initial dip in blood pressure is absent followed by a rapid increase from mid-gestation (Fig. 1-15B). Women who are hypertensive before they become pregnant can fall into either of these categories. Some women experience the normal fall in blood pressure and may need their anti-hypertensive medication adjusted or even discontinued whilst others do not (39).

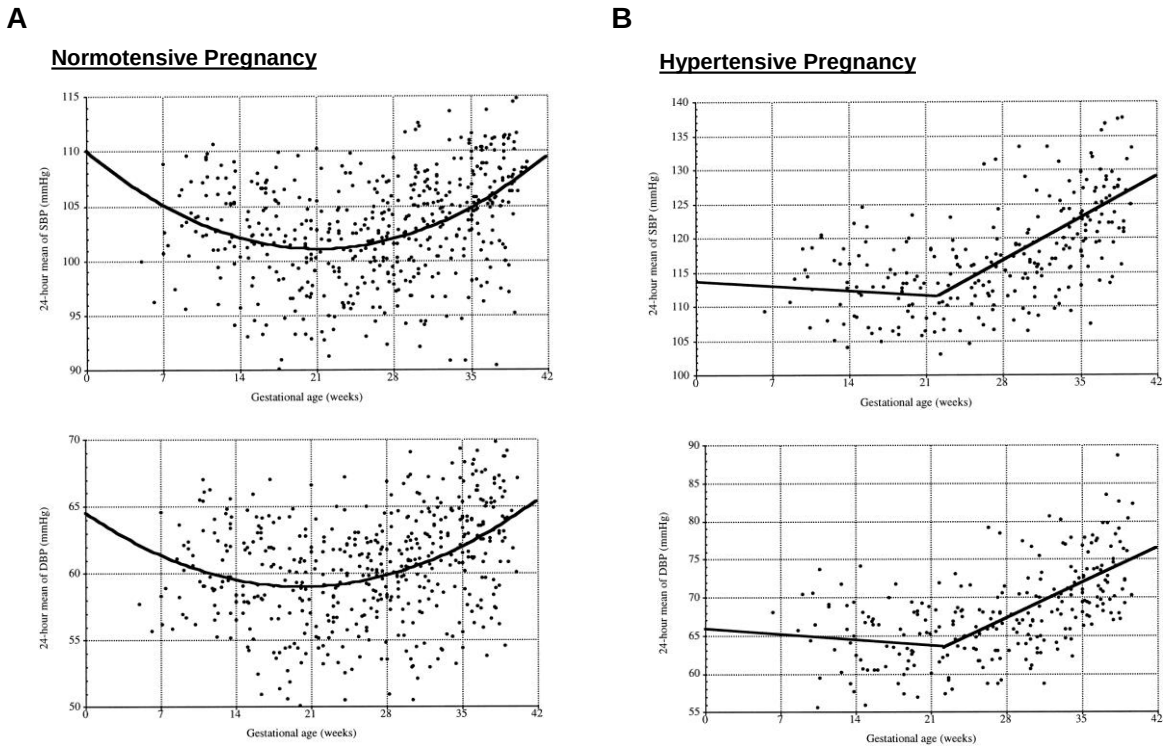

Figure 1-15: Blood Pressure Profile of Normotensive Pregnancy and Pregnancy Associated with Hypertensive Complications.

Women with normotensive pregnancy (A) experience a characteristic dip in blood pressure during the first half of pregnancy; this is absent in women who experience pregnancy-induced hypertension (B). Image adapted from Ayala et al. (1997)

The blood pressure profile of pregnant rats has both similarities and difference to humans (Fig. 1-16A-D). Normotensive WKY rats exhibit a decrease in systolic blood pressure until gestational day (GD) 7 when there is a plateau until GD 14 when systolic blood pressure decreases again towards parturition (Fig. 1-16C). The WKY rat is similar to the human in that it experiences an early decrease in systolic blood pressure but there is a contrast in that blood pressure decreases rather than increases towards parturition. it is hypothesised that there is a "hypotensive factor" which increases in the circulation to induce this fall in blood pressure (245). The early blood pressure profile of the SHRSP during pregnancy is similar to that of women who go on to develop hypertensive complications of pregnancy where there is limited blood pressure reduction during early gestation (Fig. 1-16C). In particular, the SHRSP exhibits the greatest blood pressure difference relative to the WKY from GD 10-14. This coincides with the critical period of development and maturation of the rodent placenta. The change in diastolic blood pressure over pregnancy is not as marked as SBP in rodents; in contrast to humans where reductions in the two are broadly similar (Fig. 1-16D).

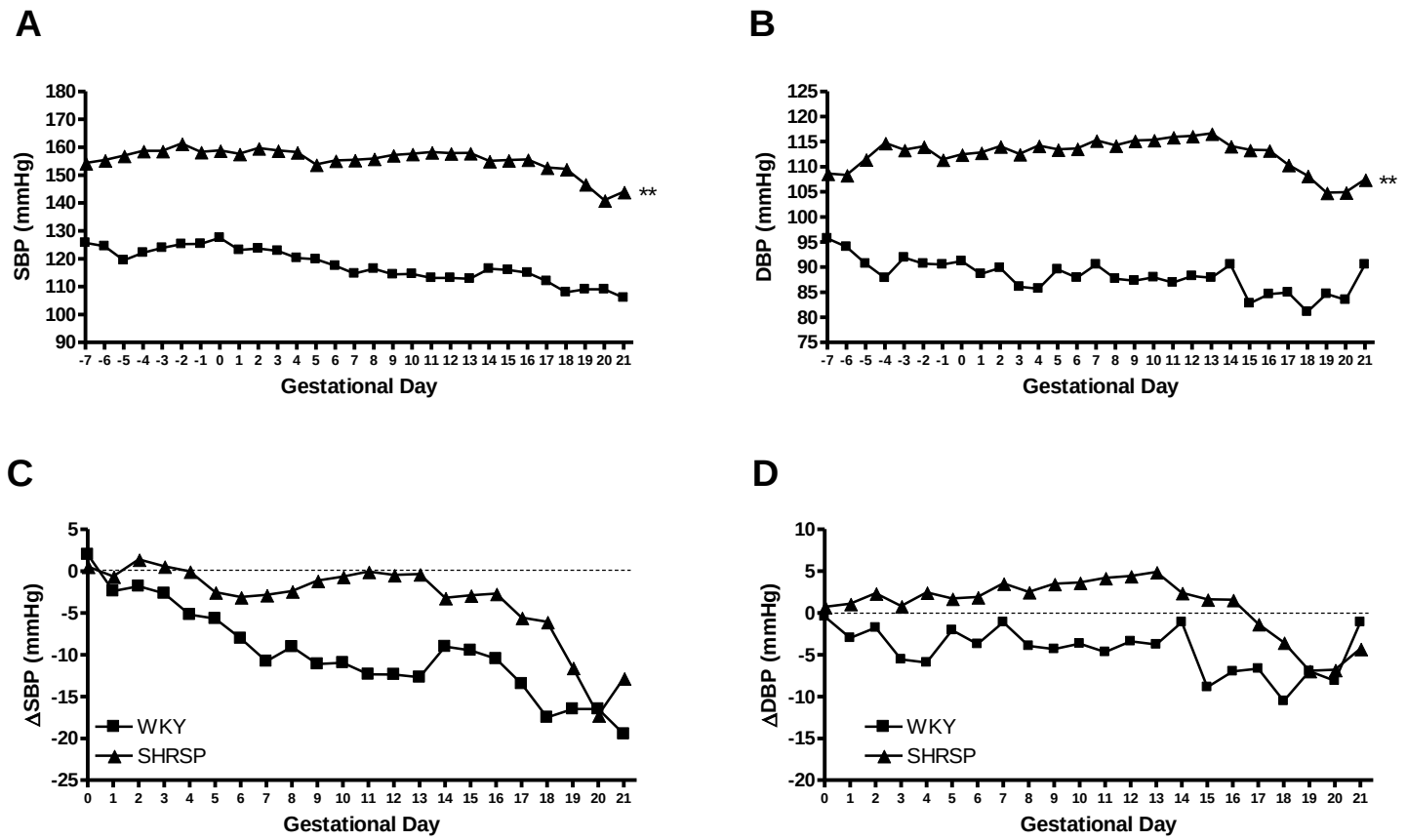

Figure 1-16: Blood Pressure Profile in the normotensive WKY rat and the Stroke prone Spontaneously Hypertensive Rat (SHRSP).

The SHRSP is hypertensive before and during pregnancy relative to the normotensive WKY (A-B). In a similar fashion to normotensive pregnant women, the WKY experiences an early reduction in blood pressure during gestation; this drop is not evident in the SHRSP (C-D). The decrease in systolic blood pressure (SBP) is not as pronounced as diastolic blood pressure (DBP). Unlike humans, rats experience a further drop in blood pressure towards parturition (C-D). Data are the author's own from previous work.

1.6 Animal Models of Human Pregnancy

For obvious ethical and practical reasons, research in pregnant women is particularly difficult therefore animal models of human pregnancy have been developed. Rodents, as discussed in section 1.4.1.1, are ideal for laboratory studies and various similarities exist between human and rodent pregnancy which are summarised in the following sections.

1.6.1 Placentation in Humans and Rats

The placenta of humans and rats are both chorioallantoic, derived from the chorion and allantois, and share a similar haemochorial structural organisation where the maternal blood is in direct contact with the chorion which encapsulates the fetal vasculature. The haemochorial placenta is an invasive structure characterised by extensive remodelling of the maternal spiral arteries discussed in section 1.6.3. Whilst the defined trimesters of pregnancy are not directly relaTable to particular time points in the rat; the major hallmarks of placental development occur in broadly the same temporal pattern (246). The outer cell layer of the blastocyst, termed the trophectoderm, gives rise to the chorionic ectoderm and ectoplacental cone (only present in rodents). The inner cell mass of the blastocyst will give rise to the embryo and the allantois (which will finally form the umbilical cord). The area of transfer between the maternal and fetal blood arises when the chorion, from the chorionic ectoderm, and allantoic mesoderm come into contact, termed chorioallantoic fusion. Folds appear in the chorion where the fetal vessels should begin to grow outwards from the allantois. This is followed by extensive branching to maximise surface area contact between the maternal and fetal circulation. In humans, this area becomes the villous tree and the analogous rat structure is the labyrinth (Fig. 1-17A) (247). The ectoplacental cone, present only in rodent placental development, forms the junctional zone of the rodent placenta. This borders the maternal decidua and is the site of rodent trophoblast progenitor cells.

In both humans and rat, the aforementioned development of the haemochorial placenta is principally actioned by the trophoblasts which also form the parenchyme of the tissue. Trophoblasts are organised down two pathways. They can fuse and develop a multi-nucleated structure known as the

syncytiotrophoblast which lines the floating villi and acts as the barrier to maternal blood. In humans, there is one syncytiotrophoblast layer which separates the maternal and fetal circulation whereas there are two in rats (Fig. 1-17B) (247). In humans, the others contribute to a cytotrophoblast shell which covers the decidua and forms cell columns anchoring the placenta to the uterus. Extra-villous trophoblasts migrate from the tips of these columns to remodel the maternal spiral arteries (section 1.6.3). In rodents, these invasive cells are derived from the junctional zone (Fig. 1-17C).

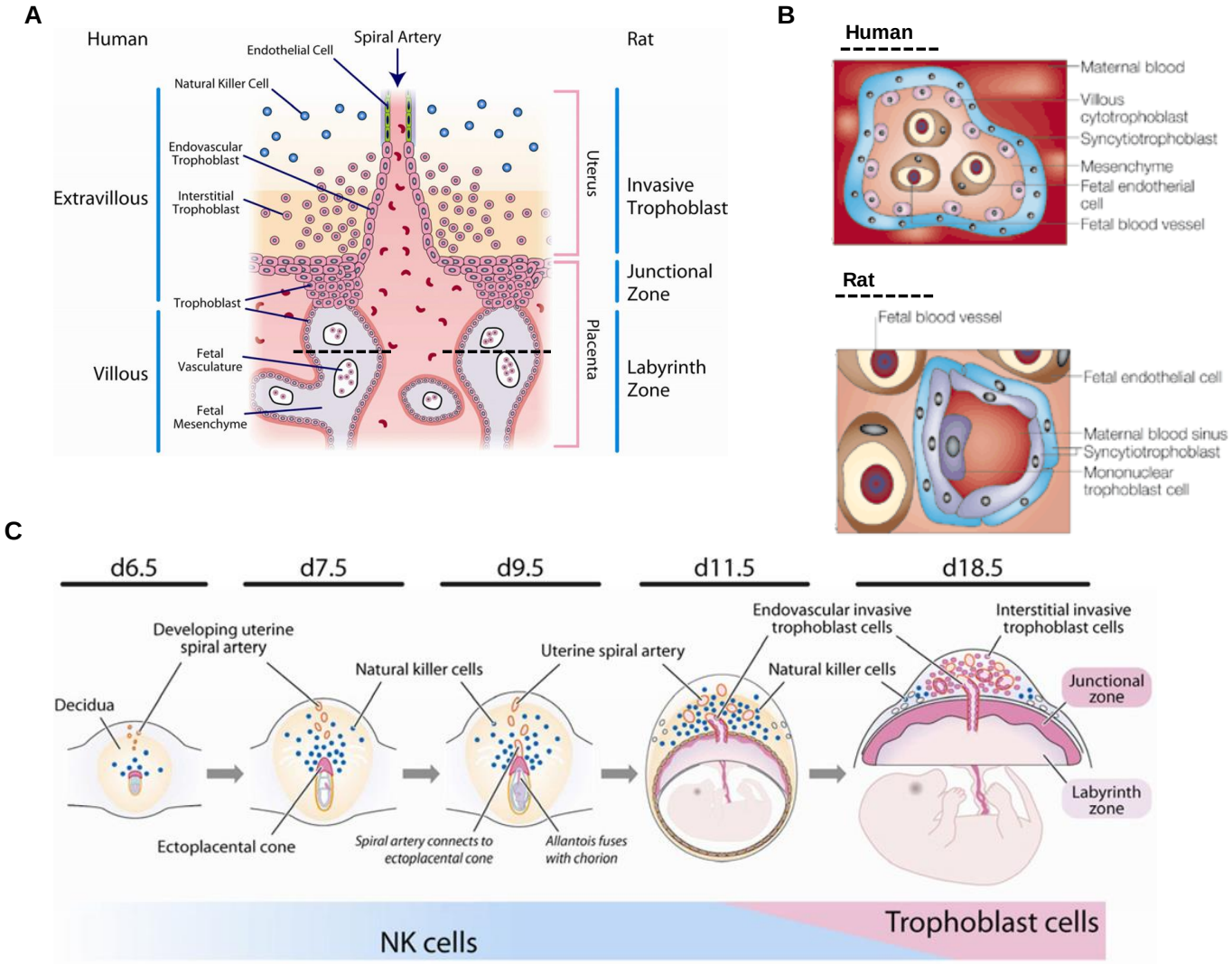

Figure 1-17: Comparative Placentation between Rodents and Humans.

(A) Humans and rats share a haemochorial placental type. In the human, the villous tree is analogous to the labyrinth zone in the rat. The extravillous area in humans is composed of a cytotrophoblast shell punctuated by columns where extravillous trophoblasts (EVTs) leave the tips of these columns and invade the uterine wall. This area is different in rats as it contains a junctional zone which borders the decidua and acts as a source of placental hormones and invasive extravillous trophoblasts (EVTs). Invasive EVTs in both humans and rats invade the maternal spiral arteries and uterus to a similar depth. (B) In humans, the fetal and maternal circulations are separated by one syncytiotrophoblast layer whereas there are two in the rat. (C) Humans and rats share a common chorioallantoic development of the placenta, a summary of rat placental development is shown in (C). Images adapted from Rossant & Cross (2001) & Soares et al. (2011).

1.6.2 Pregnancy-Dependent Uterine Artery Remodelling During Pregnancy in Humans and Rodents

In addition to the adaptations that occur in the systemic vasculature; the uterine arteries must also adapt in order to supply the developing fetus and a new organ – the placenta. The anatomy of the uterine arteries between human and rats is broadly similar (Fig. 1-18A-B). The uterus has a dual blood supply from both the ovarian and uterine arteries which arise from a common anastomotic loop. The uterine artery is subject to a series of branching which is important for reducing the pressure of blood reaching the placenta to around 8 – 15 mmHg (248) which would otherwise damage the delicate villous structure (249). Perpendicular vessels derived from the uterine artery enter into the body of the uterus giving rise to the arcuate arteries. In the myometrium, the radial arteries branch from the arcuate arteries. In rats, the arcuate and radial arteries are externally located (247). Further branching occurs at the interface between the myometrium and endometrium into the spiral arteries which penetrate inwards to the endometrium (Fig. 1-18C).

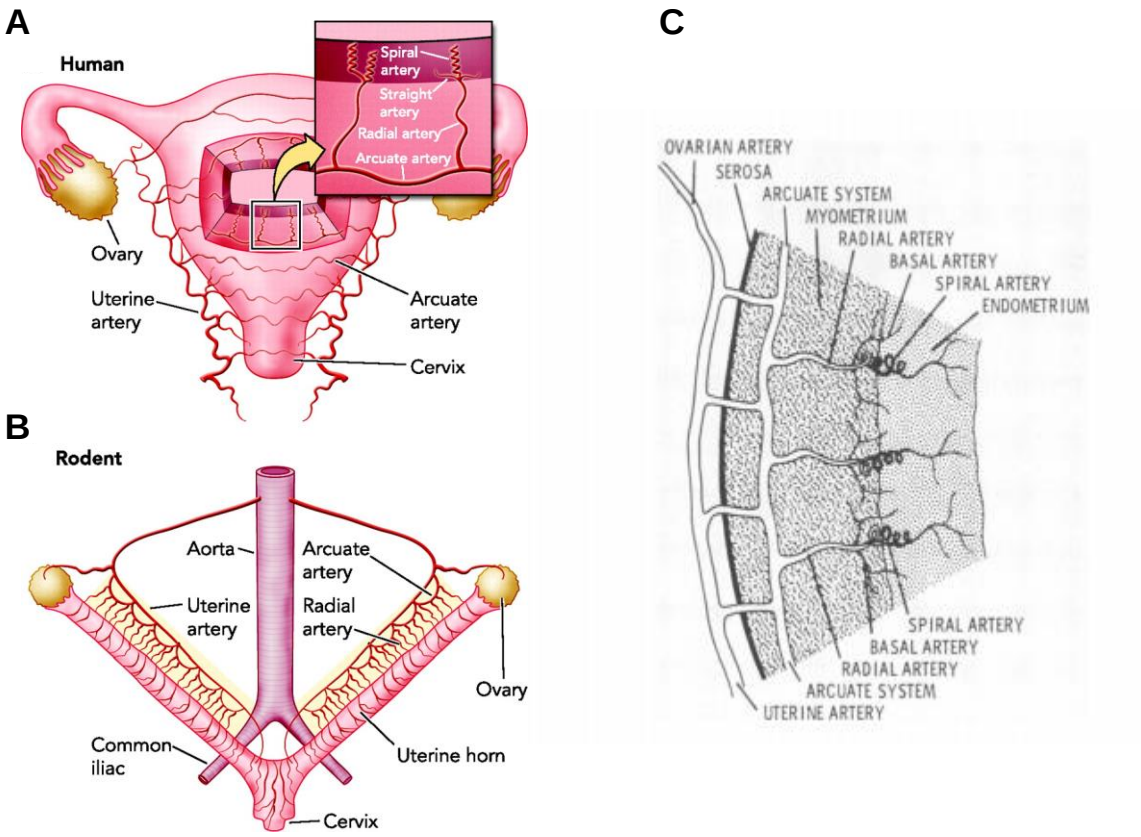

Figure 1-18: The Uterine Circulation in Humans and Rodents.

(A-B) The uterine arterial tree is similar in both humans and rodents. (C) In humans the arcuate and radial arteries are located internally; however in rats they are located externally. Image adapted from Osol & Moore (2013) and Robertson (1975).

1.6.2.1 Spiral Artery Remodelling During Pregnancy in Humans and Rodents

The inner-most branches of the uterine artery, the spiral arteries, are subject to extensive remodelling by cells from both maternal and fetal origin. The unique spiral structure of these arteries themselves is thought to play a role in dampening both the pressure and pulse of maternal blood but also act as a reserve length to accommodate pregnancy associated expansion (250). Decidualisation transforms the endometrium of the non-pregnant uterus into the pregnant decidua. This is stimulated by progesterone through cyclic AMP induction (251). In humans, this process begins spontaneously during the luteal phase of menstrual cycle but in rodents only occurs in response to implantation (252).

Decidualisation of the endometrium is characterised by changes in the secretory profile of endometrial stromal cells, an influx of specialised immune cells and maternal spiral artery remodelling (253). Upon decidualisation, endometrial stromal cells become characteristically round in appearance and express factors such as: prolactin, growth factors, pro-angiogenic factors and cytokines (IL-11 and IL-15) which stimulate the differentiation and proliferation of the specialised uterine population of natural killer (uNK) cells (254, 255). Decidualisation is associated with a marked increase in NK cell number; approximately 70% of infiltrating leukocytes within the decidua are NK cells (256). The other 25% are composed of macrophages, few T cells and very few B cells (257). The combination of decidualisation of the stromal cells and recruitment of NK cells primes the endometrium for the unique task of regulating the invasion of fetally-derived extravillous trophoblasts (EVT); these EVTs can take two pathways. Interstitial trophoblasts will invade the stroma and act to remodel the spiral arteries from the outside destroying the vascular media and replacing it with fibrinoid material (250, 256) (Fig 1-19A). The second pathway is for endovascular EVTs which will initially plug the maternal spiral arteries then travel in a retrograde fashion down the lumen of spiral arteries removing and replacing the vascular smooth muscle cells as they proceed then come to a halt somewhere around the inner third of the myometrium (250, 256) (Fig 1-19A). In this respect, rats are an excellent model of this process as they exhibit a similarly deep trophoblast invasion to humans; in mice this invasion is relatively shallow (258). The plug of the arteries is thought to prevent the untimely flow of maternal blood into the immature placental structure and to provide a low oxygen environment

which drives trophoblast proliferation (259); plugging however occurs more extensively in humans than in rats (252). In humans, interstitial invasion occurs prior to endovascular invasion (250) however in rodents it is the opposite (260). In addition to the role of the trophoblast, uNK cells play an important role in maternal spiral artery remodelling. Compelling evidence of this is seen when the smooth muscle layer of the uterine spiral arteries remains intact in an NK cell knockout mouse model (261). The uNK cells produce matrix metalloproteinases (MMPs) and pro-angiogenic factors that can directly promote vascular remodelling (262, 263). They also communicate with the invading trophoblast through the unique human leukocyte antigen (HLA) repertoire found on trophoblasts to indirectly mediate trophoblast-dependent spiral artery remodelling (256). Deficient remodelling of these spiral arteries is an underlying cause of pre-eclampsia, spontaneous pregnancy loss and fetal growth restriction (264) (Fig 1-19B). In this thesis, the focus will be on the remodelling of the uterine artery which is subject to a different mechanism.

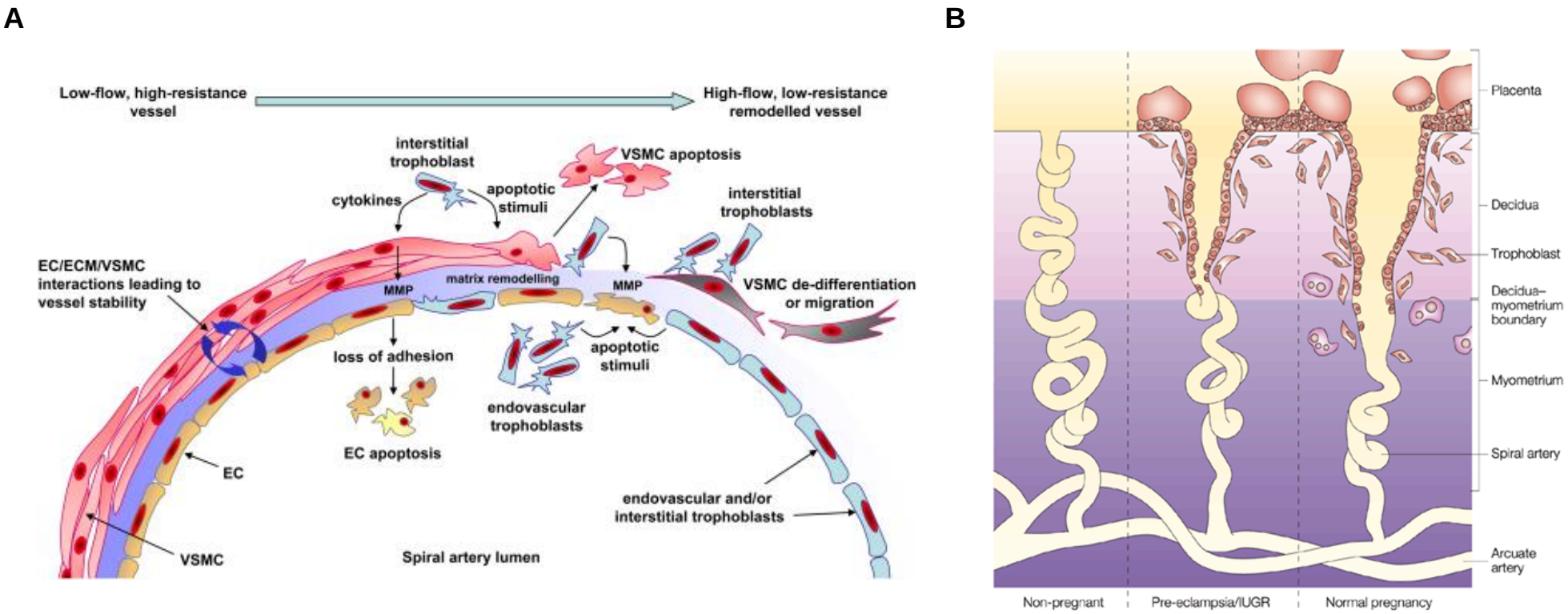

Figure 1-19: Mechanisms of Uterine Spiral Artery Remodelling.

(A) Fetally-derived invasive extravillous trophoblasts can act interstitially to remodel the maternal spiral arteries from the outside or intravascularly and enter the lumen of the vessel and remodel from the inside. The process of pregnancy-dependent spiral artery remodelling begins with decidualisation which causes endothelial cell (EC) vacuolation and smooth muscle cell swelling (VSMC); however the major effectors of change are the EVTs. EVTs or cells which they recruit such as macrophages and NK cells induce apoptosis and clearing of vascular cells, breakdown the existing extracellular matrix structure between cells and in the surrounding adventitia then lay down new fibrinoid material. (B) When spiral artery remodelling is deficient it results in a restriction of uteroplacental blood flow which underlies conditions such as pre-eclampsia and intra-uterine growth restriction (IUGR). Images from Whitely et al. (2010) & Moffet-King et al. (2002).

1.6.2.2 Uterine Artery Remodelling During Pregnancy in Humans and Rodents

Pregnancy-dependent uterine artery remodelling occurs through a combination of structural and functional changes. The diameter of the uterine artery approximately doubles in size in both humans (265, 266) and rats (266). The type of circumferential remodelling is designated as "outward hypertrophic" as there is an increase in lumen size and cross-sectional area but with no change in wall thickness (267). Uterine artery remodelling is slightly different in the mouse where medial thickening has been observed in pregnancy (268). In rodents which have multiple fetuses in one litter there is also significant lengthening, or axial remodelling, of the uterine artery where the pregnant vessel is 2-3 times the length of the non-pregnant vessel (248). This process is present but not as extensive in human pregnancy. At a cellular level, the increase in uterine artery size occurs through an increase in VSMC length of approximately 20% and proliferation of both the VSMC and endothelial cells (269). With respect to uterine artery function during pregnancy, the larger remodelled vessels exhibit a pattern of reduced contractility and increased relaxation in humans and rodents (248).

The alterations in uterine artery structure and function are predominantly to allow the vessel to accommodate a greatly increased blood flow. In humans, uteroplacental blood flow increases from a baseline of 20 – 50 ml/min to up to 1 l/min; a 20-fold increase (270). This is similar in rats where a 23-fold increase has been reported (271). Whereas the increase in uterine artery blood flow is linear in humans over time (272), changes in uterine artery blood flow are not detectable until gestational day 15 in the rat (273). Over the course of pregnancy an increasing proportion of uterine blood flow is directed to the placenta and by term 90% of the uterine artery blood flow is directed there (206). Increases in uterine blood flow in early pregnancy are principally due to the increase in diameter of the uterine artery whereas in late pregnancy it is a combination of both a marked increase in CO and uterine artery remodelling (267)

All vascular remodelling occurs through four key processes: growth, death, migration and alteration of the extracellular matrix. The mechanisms involved in simulating these processes in the uterine arteries during pregnancy are not well defined. The available evidence suggests that early remodelling relies on systemic mediators as uterine artery remodelling occurs before the placenta is established

(267) and pseudopregnant mice exhibit similar early changes in uterine artery structure to pregnant controls up to gestational day 5 (274). These early changes are small in comparison to the extensive remodelling that is seen in uterine arteries at late gestation. Therefore once the placenta is established, local signalling from the uteroplacental unit stimulates the largest changes in uterine artery structure. Evidence for this comes from unilateral horn ligation experiments in a number of animal models including rats which show that only the pregnant uterine horn exhibits extensive vascular remodelling (275-277). The main systemic factor that stimulates remodelling is thought to be estrogen (Fig. 1-20). Chronic estrogen treatment in ovarectomised guinea pigs stimulates a small increase in uterine artery diameter (278) and DNA synthesis in primary VSMC cultures (278). Work in estrogen receptor knockout mice have shown that the presence of estrogen receptor α is necessary for artery remodelling through the up-regulation of eNOS (279). However, no studies have yet been carried out in pregnant animals. The main local drivers of uterine artery remodelling are proposed to be shear stress and growth factors released from the placenta (267) (Fig. 1-20).

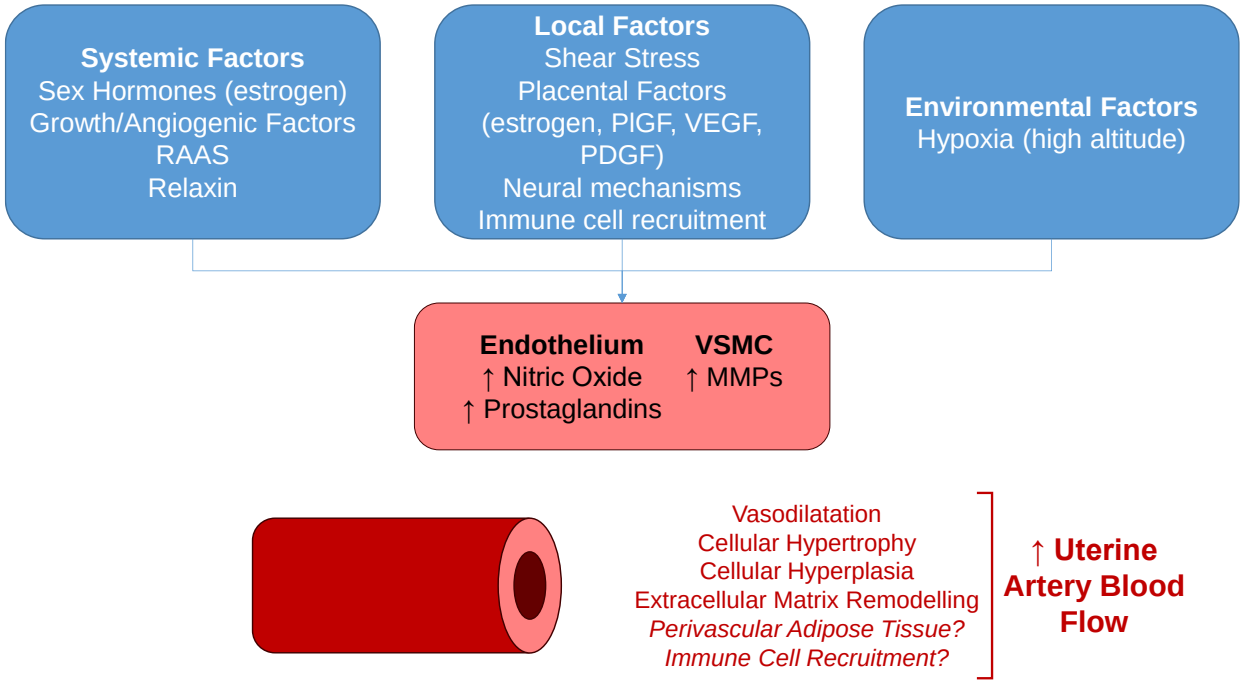

Figure 1-20: Known and Hypothetical Mechanisms of Pregnancy-Induced Uterine Artery Remodelling.

Uterine artery remodelling in response to pregnancy is dependent upon a number of systemic, local and environmental factors. The effect of estrogen on the uterine arteries during pregnancy is the best studied. However pregnancy-induced changes in other vasoactive molecules such as growth factors (VEGF, PDGF and PlGF), the renin angiotensin aldosterone system (RAAS) and relaxin produced from the placenta or elsewhere may also play a role in uterine artery remodelling. Locally, shear stress due to increased blood flow is thought to induce early changes in uterine artery structure whereas placentally derived factors play more of a role later in pregnancy. Immune cells which have been shown to actively remodel the spiral arteries may have a role in remodelling the uterine artery however this is yet to be defined. The perivascular adipose tissue may also potentially secrete vasoactive factors that promote remodelling as in other vascular beds. Women who live at high altitude (low PO_2) show altered uterine artery remodelling therefore maternal environment also plays a role. All of these pathways converge on stimulating the endothelium and vascular smooth muscle cells to promote structural and functional changes in the uterine artery.

1.7 Hypertensive Disorders of Pregnancy

Whilst women are normally protected from CVD compared to men, pregnancy is a specific point in time where women appear to be susceptible to CV complications. CVD is the leading cause of maternal mortality in the United Kingdom (280) and in the United States (281). Pregnant women can suffer orthostatic intolerance, heart failure, peripartum cardiomyopathy and arrhythmias. This thesis will focus on hypertensive disorders of pregnancy which are broadly classified into three groups: pre-eclampsia/eclampsia (PE), gestational hypertension and chronic hypertension. Gestational or chronic hypertension can present on their own but also confer increased risk to develop the more serious complication of pre-eclampsia. Uncontrolled hypertension during pregnancy has been identified as a major prevenTable cause of maternal mortality (282).

1.7.1 Pregnancy as a Cardiovascular Stress Test

How much either pre-existing CV risk, pregnancy associated changes or a combination of both contribute to maternal CVD during pregnancy is unknown. One hypothesis to describe this is that the significant adaptation of the CV system is a maternal "stress test" (283). The extensive CV remodelling required for a healthy pregnancy uncovers underlying cardiovascular risk factors. This abnormal vascular remodelling response pushes the woman over a clinical "threshold" detectable as some form of CVD during pregnancy such as pre-eclampsia or gestational hypertension (Fig 1-21). These women also have an increased incidence of CVD later in life due to these increased CV risk factors. However, another alternative explanation is that cardiovascular disease in pregnancy causes irreversible damage to the CV system manifesting as disease later in life (284). Realistically, it is probably a balance of both of these mechanisms.

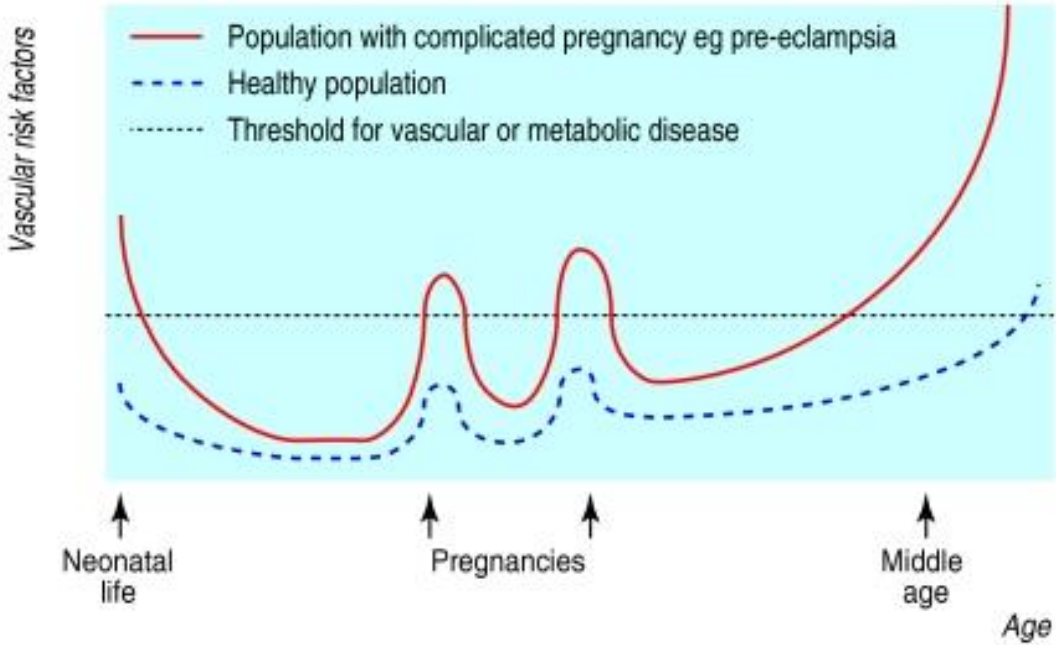

Figure 1-21: Pregnancy as a Cardiovascular Stress Test.
Image from Sattar and Greer (2002).

The link between CVD in pregnancy and an increase in future cardiovascular risk has been noted since the early 19th century (285). Recent studies including meta-analyses (286) have reported that women with severe forms of hypertension during pregnancy have a 3-4 fold increased risk of hypertension later in life (287-289) , 2 fold increased risk in developing ischemic heart disease (290) and stroke (291) and a 3-5 fold increase in renal disease (289, 292) but does not worsen pre-existing renal disease (293). Furthermore, there have also been links made with diabetes mellitus, venous thromboembolism, hypothyroidism and depression (294). In a wider sense, the Cardiovascular Health after Maternal Placental Syndromes study (CHAMPs) also reported that women who experienced placental complications had 2 times the incidence of cardiovascular disease later in life (295). This highlights that abnormal pregnancy can be related to CVD risk later in life. The evidence presented suggests that common risk factors and mechanisms may exist that underlie CVD in both non-pregnant and pregnant women.

1.7.2 Pregnancy-Specific Hypertensive Disorders

Pregnancy-specific hypertensive disorders, including pre-eclampsia (PE) and gestational hypertension, arise after 20 weeks of pregnancy. Gestational hypertension can be transient or develop into chronic hypertension which is unmasked by pregnancy and persists postpartum. Further, gestational hypertension can develop into the serious complication; PE. PE is defined using International Society for the Study of Hypertension in Pregnancy (ISSHP) criteria as the development of hypertension (SBP of 140 mmHg or greater and/or DBP of 90 mmHg or greater) and proteinuria (300 mg/24 h or greater or 2+ or greater on urine dipstick testing) after the 20th gestational week. PE affects between 5 and 8% of pregnancies worldwide (296) and can present with a number of serious complications for mother and baby such as preterm delivery, intrauterine growth restriction, hepatic or renal dysfunction, seizures, and coagulopathy. PE is responsible for up to 15% of maternal deaths worldwide (297). Currently, no effective cure for PE exists apart from delivery of the placenta highlighting a key role for the organ in this disease.

The current two step model of PE states that insufficient remodelling of the uterine spiral arteries by extravillous trophoblasts plays a critical role in the underlying development of pre-eclampsia (Section 1.6.2.1). This deficient remodelling and restricted blood flow underlies changes to the placenta which do not allow it to function normally resulting in the release of soluble factors which propagate the systemic effects of PE (298). Hypotheses surrounding the underlying drivers of the pathology in PE are abundant with dysregulation proposed in metabolism, immunology, angiogenesis and oxidative balance. It is well deserved that PE is referred to as the “disease of theories” as much of the multifactorial cause for this disease remains poorly understood (299) (Fig. 1-22).

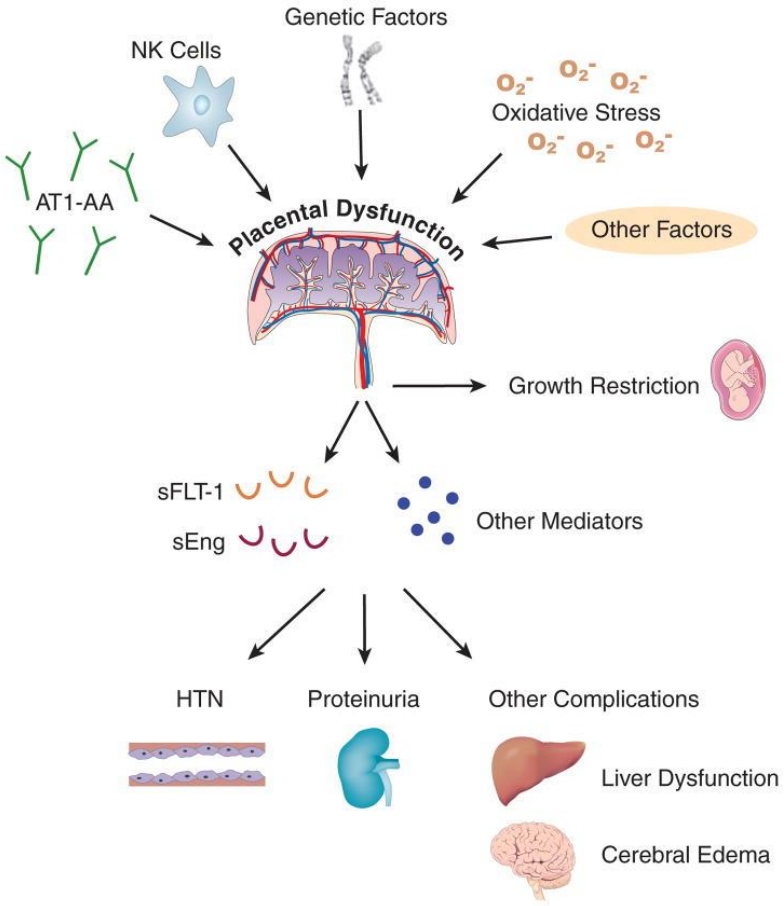

Figure 1-22 The Pathology of Pre-eclampsia.

Pre-eclampsia is a multi-systemic disorder with respect to its underlying cause and pathology. Excessive activation of the angiotensin II type 1 receptor through auto-antibodies (AT1-AA), abnormal immune activation of maternal NK cells by invading trophoblasts, genetic predisposition and oxidative stress may play a role in deficient spiral artery remodelling resulting in placental dysfunction. The placenta in pre-eclampsia releases anti-angiogenic mediators such as soluble FLT-1 and soluble endoglin (ENG) and other unknown mediators which have systemic effects on the vessels, kidney, liver and brain. The combined organ damage results in hypertension, proteinuria and can even develop into dangerous eclamptic seizures and HELLP syndrome. Image from Powe et al. (2011).

1.7.3 Chronic Hypertension during Pregnancy

Chronic hypertension in pregnancy is defined by the American College of Obstetricians and Gynaecologists (ACOG) as a blood pressure over 140 mmHg systolic and 90 mmHg diastolic which has presented pre-pregnancy or before gestational week 20 (300). Chronic hypertension has been stated to affect around 3% of pregnancies (301-304); additionally one longitudinal study reported an increase in prevalence over the study period (304). The occurrence of pregnancies complicated by chronic hypertension varies between populations (302) and ethnicities (305). The limitation of population-based studies of chronic hypertension in pregnancy is that the most recent cohort analysed was in 2008 (304). Pregnancies complicated by pre-existing hypertension are regarded by the literature to pose a clinical problem of increasing occurrence in developed countries (305, 306) as a number of key risk factors for hypertension are increasing in women, for example, maternal age at childbirth (307), obesity (308) and metabolic syndrome (309). CVD prevention in young women was recently identified as being a neglected area in a recent editorial (310) and as approximately 20% of pregnancies in the United Kingdom (311) and up to 50% of pregnancies in the United States (312) are unplanned there is a critical need for pre-natal counselling for women of childbearing age with hypertension.

Women with chronic hypertension are at an increased risk of pregnancy complications. A recent meta-analysis of the existing literature on this subject reported that women with chronic hypertension had higher incidences of superimposed pre-eclampsia (25.9%, 95% confidence interval 21.0% to 31.5%), caesarean section (41.4%, 35.5%- 47.7%), preterm delivery <37 weeks gestation (28.1%, 22.6% - 34.4%), birth weight <2500g (16.9%, 13.1% -21.5%), neonatal unit admission (20.5%, 15.7% - 26.4%) and perinatal death (4.0%, 2.9% - 5.4%) (306). An analysis of the Danish National Birth Cohort (81,008 pregnancies) found that women with chronic hypertension had 5.5 fold (95% confidence interval 3.2-9.4) increased risk of preterm delivery and a 50% increase in the risk of giving birth to an infant that is small for gestational age after adjustment for other risk factors (313). Women with chronic hypertension have also been reported to have an increased risk of placental abruption (relative risk 2.4, 2.3 – 2.5). Additionally, women with both chronic hypertension and superimposed pre-eclampsia have a further increased risk (7.7, 6.6 – 8.9) of placental abruption (314). Women with

chronic hypertension also have an increased risk of giving birth to infants with congenital malformations, specifically cardiac (1.6, 1.4-1.9) (315). In a more general sense, it has been reported that mothers with pre-existing cardiovascular disease, including hypertension but not specifically, have an increased maternal and perinatal morbidity (316). Taken together, this body of evidence indicates that a healthy maternal cardiovascular system is important for a healthy pregnancy. There is little evidence that assesses how the hypertensive mother adapts to pregnancy, however one small recent study has shown that women with chronic hypertension have increased left ventricular hypertrophy (left ventricle mass increased by approximately 20g and posterior wall thickness increased by 0.7mm) (317). However, scientific investigation of how the CV system of the hypertensive mother is affected by pregnancy is wanting.

Preconception counselling is highly recommended for women of childbearing age with chronic hypertension (318). At this point, it is useful for the clinician to complete a full biochemical screen in the blood and assess 24-hour protein in the urine. As pre-eclampsia is more prevalent in this population it makes later diagnosis easier. Baseline proteinuria is also an indicator of adverse pregnancy outcome (319). Almost all women presenting with chronic hypertension will have primary hypertension. Therefore, treating these women has the same caveats as treating any patient with essential hypertension with the added complication of the pregnancy. Pharmacological intervention remains a clinician-led decision; however, a number of drugs are recommended (Table 1-6). Angiotensin-converting enzyme (ACE) inhibitors and angiotensin-receptor blockers are contra-indicated in pregnancy due to the evidence of impaired neonatal kidney function and congenital abnormalities when used in the second half of pregnancy (320, 321).

Table 1-6 Drugs to treat chronic hypertension in pregnancy.

Drug	Mechanism of Action	Dosage	Comments
Methyldopa	Centrally-acting alpha agonist	0.5 – 3 g/d orally in 2 -3 doses	First line therapy Well tolerated. Established data which indicates no negative effects on offspring up to 7 years old (322). Limited use as an emergency hypertensive agent.
Labetalol	Alpha- and beta-blocker	200 – 2400 mg/d orally in 2 – 3 doses	First line therapy. Well tolerated. Bronchoconstrictive effects so may exacerbate asthma. Effective as an emergency hypertensive agent.
Metoprolol	Beta-blocker	50 – 400 mg/d orally in 2 - 3 doses	Possible association with fetal growth restriction when given in early pregnancy (323)
Nifedipine	L-type calcium channel blocker	30 – 120 mg/d slow release preparation in 1 dose	Less data on the use of nifedipine in pregnancy. No adverse effects when given in the second trimester (324)
Hydralazine	Vasodilator	100 – 600 mg/d orally in 2-4 doses	Effective as an emergency hypertensive agent. Largely unknown mechanism of action.
Hydrochlorothiazide	Diuretic	12.5 – 50 mg/d in 1 dose	Not normally recommended but may be necessary in salt-sensitive hypertension. May restrict maternal plasma volume expansion in pregnancy.

Table adapted from the American Congress of Obstetricians and Gynaecologists Task Force in Hypertension in Pregnancy and Seely *et al*. (2011).

Taking all of the available interventions into account, a recent meta-analysis concluded that anti-hypertensive treatment whilst halving the risk of severe hypertension in the mother does not reduce the risk of pre-eclampsia, perinatal death, preterm delivery and babies which are small for gestational age (325). However, a combination of calcium channel blocker and beta blockers were found to significantly reduce the incidence of pre-eclampsia compared to methyldopa. Further research is required to determine the most effective anti-hypertensive agent to treat chronic hypertension in pregnancy, if any. Whilst incidents at birth are well-documented, there is also a lack of evidence on whether controlling maternal blood pressure has any effect on the infant later in life. Another general limitation of most studies which assess the effectiveness of an anti-hypertensive agent on pregnancy outcome is the variance in what is used as a control group. For example, anti-hypertensive treatment has been compared against placebo-treated, untreated chronic hypertensive women, normotensive women or women taking another anti-hypertensive. Whilst meta-analysis is useful, caution must be taken in comparing different types of studies against one another when the control groups are not the same. The recent Control of Hypertension in Pregnancy Study (CHIPS) assessed the effect of tight (DBP 85 mmHg) or less tight (DBP 100 mmHg) control of blood pressure on pregnancy outcome. The study reported that there was no significant difference in adverse outcomes between the tight and less tight groups, however the occurrence of severe hypertension was reduced in the tight control group (326). Taking this study into account, there is still no defined target blood pressure that predicts an adverse outcome for mother and child.

This field of research would benefit greatly from a pre-clinical model that could be used to study the underlying mechanisms of pregnancy in the setting of maternal chronic hypertension. Understanding the mechanisms behind this increased risk for adverse outcome would help inform future work into which agents may be most useful for the treatment of hypertension and how the risk for mother and child could be reduced.

1.7.4 Rodent Models of Hypertensive Disorders of Pregnancy

There are a number of rodent models of hypertensive pregnancy present in the literature which have utilised surgical, genetic, pharmacological and dietary

interventions to increase blood pressure (327). The variety of animal models available is a strength reflecting the plethora of risk factors for the development of hypertension. However, drawing comparisons between these animal models can be problematic as the methodology underlying the production of the phenotype varies. A summary of the most important animal models of hypertension during pregnancy are given here.

Most animal models of hypertension during pregnancy are focussed on modelling the pathology associated with preeclampsia (section 1.7.2). A general limitation of these models is that they tend to mimic only the severe, early onset form of the disease. The rat reduced uterine perfusion pressure model (RUPP), developed by Granger *et al.* (328), involves the occlusion of the abdominal aorta and either one or both of the uterine arteries on gestational day (GD) 14 of pregnancy. The restriction of the abdominal aorta alone does not induce a preeclampsia like phenotype due to a compensated blood flow from the ovarian artery thus the clips are also needed at the ovarian end of the uterine artery. The RUPP rat displays pathology similar to that seen in women with PE from GD19 onwards (329-331). The underlying cause of the phenotype in this model is induced by the placental-ischemia that occurs as a result of the blood flow restriction. Therefore, this animal model is excellent for studying factors released by the ischemic placenta which underlie preeclampsia but this has its limitations. The intervention takes place after the critical period of placental development whereas the placental pathology associated with preeclampsia occurs early in pregnancy with the failure of the spiral arteries to remodel. It is also not possible to study vascular remodelling in the RUPP as the vessels have been artificially modified. Furthermore, it does not take into account any "risk factors" for preeclampsia as these animals are healthy before the procedure and would not have developed vascular complications during pregnancy otherwise. The selective RUPP model, recently published by Schenone *et al.* (332), clips only the uterine artery and not the abdominal aorta. This animal model develops a lower blood pressure increase and does not present with proteinuria such as in the Granger RUPP model (332). Genetically modified or pharmacologically induced rodent models have also been used to study mechanisms of preeclampsia. These models have the advantage that the vascular and placental pathology occurs spontaneously without surgical intervention. Mouse knockout models for eNOS

(333) and catechol-O-methyltransferase (COMT-/-) (334) (an estradiol metabolite that is normally increased in the final trimester of human pregnancy) have been shown to exhibit some features of preeclampsia; but these findings have not been robust in follow-up studies (335) or showed conflicting results in tissue from women with PE (336). A transgenic rat model which is produced from mating females expressing human angiotensinogen and males expressing human renin also exhibits a number of preeclampsia related pathologies (337). Paradoxically, the RAAS is not altered in the RUPP model of preeclampsia despite a similar rise in blood pressure in late gestation (327). This model also lacks clinical translation as inhibitors of the RAAS pathway are contraindicated in pregnancy (section 1.7.3). Furthermore, whilst the vascular remodelling is allowed to occur spontaneously in this model; the spiral artery remodelling is deeper and uterine artery resistance index is decreased relative to the normotensive animal suggesting a different underlying cause of the preeclampsia phenotype in contrast to human studies (338). Infusion of certain pharmacological agents during pregnancy, such as the eNOS inhibitor L-NAME, has been shown to produce a PE-like phenotype which is ameliorated by treatment with sildenafil (339). However, a recent clinical trial utilising sildenafil in women with PE did not show a therapeutic effect (340). Preeclampsia -like symptoms can also be induced by infusion of anti-angiogenic factors soluble FLT-1 (sFLT-1) (341) and soluble endoglin (sEng) (342) and pro-inflammatory cytokine TNFα (343).

Another group of animal models is centred on rodents who are borderline hypertensive pre-pregnancy then develop superimposed preeclampsia. This type of model has the unique benefit of taking into account predisposing maternal CV risk. The BPH/5 mouse model is characterised by mild blood pressure elevation (mean arterial pressure 128 mmHg vs. 106 mmHg) as a result of selective inbreeding. During pregnancy, the BPH/5 exhibits a 22mmHg increase in blood pressure in the second half of pregnancy relative to the wild type strain. This increase in blood pressure resolves postpartum. These mice also present with a reduced litter size, proteinuria and glomerulosclerosis at a late stage of pregnancy (344). Recently, the Dahl S rat (section 1.4.1.2) has also been characterised as a model of superimposed PE. The Dahl S exhibits a pregnancy-dependent increase in blood pressure, accompanied by deficient uterine remodelling and kidney pathology (345). Again sildenafil treatment, which has not shown promise in

clinical trials, reduced the severity of the maternal preeclampsia -like phenotype in the Dahl S (346). In spite of this variety of animal models, currently there is no rodent model of chronic hypertension in pregnancy that does not progress to manifestations of preeclampsia.

1.8 The SHRSP as a Model of Chronic Hypertension during Pregnancy

The central hypothesis of this thesis is that deficient vascular remodelling in response to pregnancy results from a combination of both maternal pre-disposition due to CV risk factors and pregnancy-specific changes. Thus, women with pre-existing maternal hypertension would exhibit deficient pregnancy-dependent uterine artery remodelling and this could explain the additional risk of adverse pregnancy outcome in this population. Our model of choice to test this hypothesis was the stroke prone spontaneously hypertensive rat (SHRSP). Some aspects of pregnancy in the SHRSP have already been briefly characterised (347, 348) however the vascular adaptation to pregnancy has not been studied systematically.

1.8.1 Deficient Uterine Artery Remodelling in the SHRSP

We previously examined uterine artery structure and function from virgin and pregnant (GD18) SHRSP and WKY rats using pressure and wire myography respectively. SHRSP showed a significantly impaired outward hypertrophic remodelling of the uterine artery relative to the WKY (Fig 1-23). In addition, where WKY uterine arteries showed a decrease in maximal noradrenaline response and increase in endothelium dependent relaxation this adaptation was all but absent in the SHRSP (Fig 1-23). Deficient uterine artery remodelling was associated with a significantly decreased pregnancy-dependent increase in uterine artery diastolic blood flow (349). We went on to show that significant blood pressure reduction using nifedipine from 6 weeks of age in the SHRSP did not have an effect on the abnormal uterine artery response (349). Therefore, the mechanisms behind this deficient vascular remodelling were not dependent on the presence of pre-existing maternal hypertension and we hypothesised that other CV risk factors must underlie this pathology.

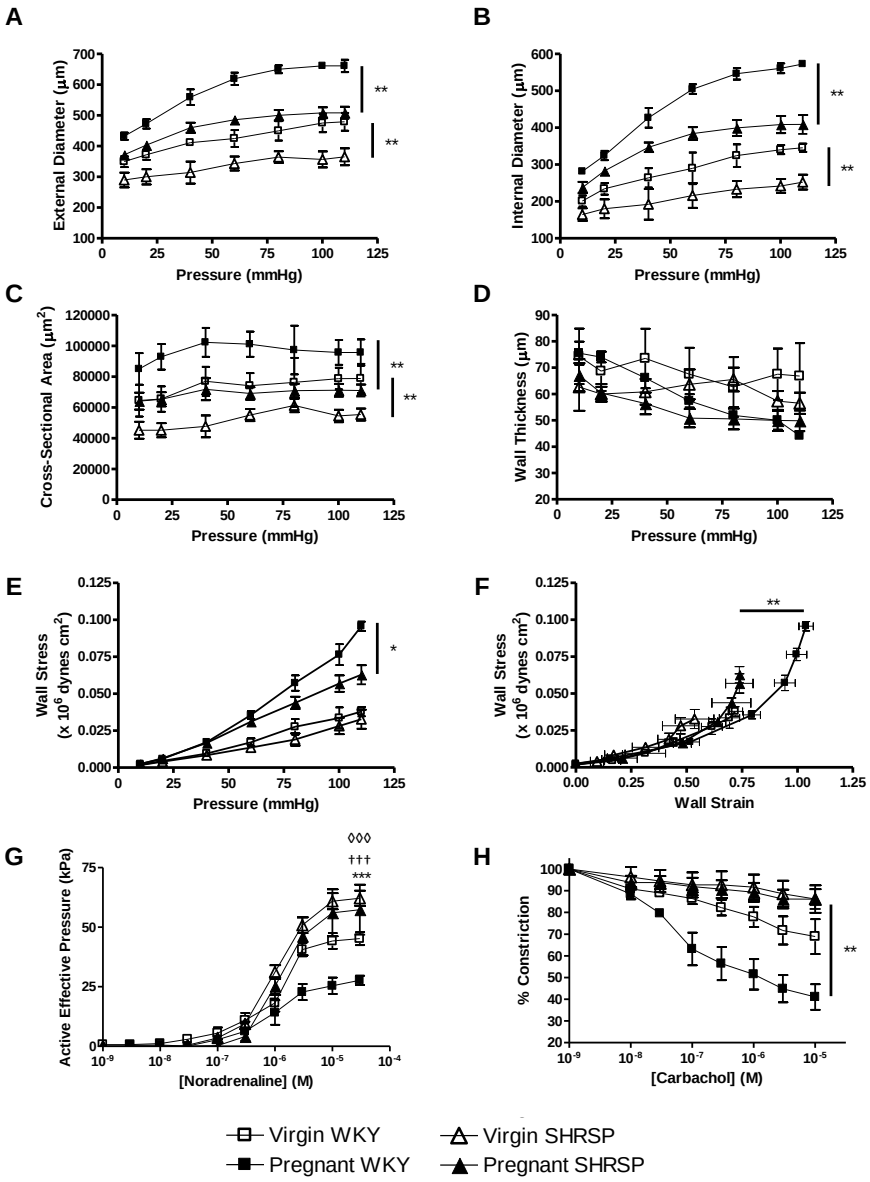

Figure 1-23 Abnormal Uterine Artery Remodelling in Response to Pregnancy in the Stroke Prone Spontaneously Hypertensive Rat (SHRSP)

Uterine arteries isolated in calcium free media were subject to pressure myography to measure external (A) and internal (B) diameter, cross-sectional area (C) and wall thickness (D) in female virgin WKY (n=4), pregnant WKY (gestational day 18) (n=6), virgin SHRSP (n=4) and pregnant SHRSP (gestational day 18) (n=6). External and internal diameter as well as cross-sectional area was significantly decreased in the pregnant SHRSP compared to the WKY (** p<0.01). Wall stress (E) was significantly decreased in pregnant SHRSP compared to the pregnant WKY. The stress/strain curve (F) was shifted to the right upon pregnancy in both strains but was significantly decreased in the pregnant SHRSP. Isolated uterine artery function was also measured using wire myography in the same animals. Maximum response to noradrenaline (G) was significantly decreased in virgin vs. pregnant WKY (††† p<0.001). Virgin SHRSP had a significantly increased maximum response to noradrenaline relative to virgin WKY (◊◊◊ p<0.001). Pregnant SHRSP vessels did not have a significantly decreased response to noradrenaline vs. virgin SHRSP. Pregnant SHRSP vessels had a significantly increased maximum response to pregnant WKY vessels (*** p<0.001). The EC50 values for noradrenaline were not significantly different between groups (data not shown). Furthermore, endothelium-dependent vasorelaxation to carbachol (H) was significantly impaired in both virgin and pregnant SHRSP (** p<0.01 vs. WKY). Data analysed by comparing area under the curve values using one-way ANOVA and Tukey's *post-hoc* test. Figure from Small *et al.* (2016).

1.9 Hypothesis & Aims

We hypothesised that deficient uterine artery remodelling seen in the SHRSP was dependent upon pre-existing maternal CV risk factors. Furthermore, we proposed that the SHRSP could act as a novel translational model of maternal chronic hypertension in pregnancy which would allow us to investigate novel therapeutic targets.

The aims which would allow us to address this hypothesis were as follows:

- Characterise and establish the SHRSP as a rat model of maternal chronic hypertension in pregnancy.

- Identify and therapeutically target a molecule involved in the pregnancy-associated pathology in the SHRSP.

- Utilise this model as a basis for proteomic analysis to discover novel targets involved in chronic hypertension during pregnancy.

Chapter 2 General Materials & Methods

This Chapter outlines laboratory practices and methods common to more than one Chapter. Each subsequent results Chapter has a specific materials & methods section.

2.1 General Laboratory Practice

Laboratory equipment and reagents used in this thesis were of the highest possible grade commercially available. Reagents deemed hazardous were dealt with appropriately as described in the relevant control of substances hazardous to health regulations. Appendix I gives details of the preparation of all laboratory-prepared reagents that were not obtained commercially. Reagents were weighed using an Ohaus Portable Advanced balance (sensitive to 0.01 g) or a Mettler HK160 balance (sensitive to 0.00001 g). Sterile disposable plastic ware or standard laboratory glass wear was used to prepare reagents. Glassware was washed using Decon 75 detergent, rinsed with distilled H_2O (dH_2O) and placed in a 37 ºC drying cabinet. RNase free disposable plastic ware (Thermo Fisher, Paisley, UK) was used when appropriate. Volumes from 1 µl to 1ml were measured using BioHit® pipettes (Sartorius, Surrey, UK) and disposable tips or RNase free filter tips (Thermo Fisher, Paisley, UK) when appropriate. dH_2O was used to prepare all aqueous solutions unless otherwise stated in appendix I. To dissolve solutions, a Jenway 1000 hotplate/stirrer was utilised. To mix solutions, a mini vortex 2800 rpm Lab Dancer (Fisher Scientific, Loughborough, UK) was utilised. Small samples <2 ml were centrifuged using a Heraeus™ Pico™ benchtop microcentrifuge (Thermo Fisher, Paisley, UK); larger samples were centrifuged in a Sorvall™ Legend™ Centrifuge (Thermo Fisher, Paisley, UK). A Julabo TW8 water bath and thermometer was used for experiments requiring incubations from 37 °C to 95 °C. For experiments requiring temperatures 95 – 100 °C, an Eppendorf ThermoMixer® was used. The pH of solutions was measured using a Metler Toledo pH meter calibrated with pH 4.0, 7.0 and 10.0 standards (Sigma -Aldrich, Dorset, UK).

2.2 Animals

2.2.1 Animal Strains

The strains of animals used in this thesis are the stroke prone spontaneously hypertensive rat (SHRSP) and the control strain Wistar Kyoto (WKY) rat. These inbred strains have been maintained at the University of Glasgow since 1991 when 6 males and 7 females of each strain were gifted to Prof. A.F. Dominiczak from Dr. D.F. Bohr from the University of Michigan, USA. These animals were previously sourced from the National Institutes of Health, Bethesda, USA (Genealogy shown in Fig. 1-13). The Glasgow strain of SHRSP have slightly lower blood pressures than the original strain (16 week old males: Glasgow 190-200 mmHg, original strain 230-250 mmHg) also detailed in section 1.8.

2.2.2 Animal Housing

All animals were housed under controlled lighting (from 0700 to 1900 hours) and temperature (21 ± 3 °C) and received a normal diet (rat and mouse No.1 maintenance diet, Special Diet Services) provided *ad libitum*. All animal procedures were approved by the Home Office according to regulations regarding experiments with animals in the United Kingdom (Project License Number 60/4286 held by Dr. Delyth Graham).

2.3 Animal Procedures

2.3.1 Time Mating

Females were time mated at 12 weeks of age (± 4 days). Non-pregnant animals were age-matched at 15 weeks (i.e. 12 weeks of age + 21 days of pregnancy) ± 4 days. For mating, females and stud males of the relevant strain were housed together in a mesh bottomed breeding cage. Day 0 of pregnancy was defined as the day that a coital plug was observed indicative of successful mating having taken place. For animals that were subject of radiotelemetry, the breeding cage was placed on the receiver panel to avoid any loss of data.

2.3.2 Metabolic Cage

The metabolic cage allows individual housing of an animal to collect information on water intake and urine output over 24 hours. The metabolic cage has a gridded bottom which allows urine and faeces to pass through which are then separated by a funnel so that they can be collected separately. A fixed amount of water (200 ml) was given and food was available *ad libitum* over the 24-hour period. Animals were acclimatised for 4 hours, 3 days prior to measurement. Urine samples were collected from virgin animals that were housed in the metabolic cage 1 day prior to mating then at GD 6, GD 12 and 18. Urine samples were aliquoted on ice and stored at -80 ºC until use.

2.3.3 Radiotelemetry Probe Implantation

Radiotelemetry probes were implanted in anaesthetised animals under 2.5 – 3.5 % isoflurane/O_2 using sterile conditions. Within the abdominal cavity, the intestines were temporarily externalised and kept moist using sterile gauze soaked in sterile PBS (Thermo Fisher, Paisley, UK). Three Mersilk sloops were placed around the main aorta and both iliac arteries to occlude the flow of blood. The catheter of the probe was then implanted into a small hole made in the abdominal aorta using a 21 G needle and secured with a small cellulose patch and VetBond™ biological glue (Data Sciences International, Sheffield, UK). Following the implantation, the intestines were replaced and the probe was sutured into the muscle wall of the abdominal cavity. Each animal was placed in an individual cage upon a receiver which relayed the information to an attached computer collected by the probe every 5 minutes for 10 seconds. Animals were allowed to recover for 10 days after surgery before they were time mated.

2.3.3.1 Radiotelemetry Data Handling

Data was analysed using Microsoft Excel and the daytime and night time average was used to calculate a daily average which is plotted in the graphs for clarity.

2.3.4 Tissue Collection Protocols

2.3.4.1 Tissue Collection at GD 14.5 – 20.5

Animals were sacrificed under terminal general anaesthesia. The thoracic cavity was opened and maternal blood was collected via cardiac puncture of the left ventricle using a disposable 5 ml syringe and 23 G needle. Blood was then transferred into heparinised VACUETTE® tubes and kept on ice before centrifugation at 1300 rpm for 10 minutes to obtain plasma. Plasma was aliquoted on ice and stored at -80 ºC until use. Maternal tissues were harvested and weighed then either fixed in 10% formalin or snap frozen in liquid nitrogen. The uterine horn was excised and animals with <4 fetuses were excluded from any further study at this point. Individual uteroplacental units were dissected then fetuses and placenta (without the attached uterine tissue) were weighed. At GD 20 only, fetal tissues – head, heart, liver and kidneys - were also dissected and weighed. Placenta were either taken intact including the uterus (mesometrial triangle and decidua) for fixation in 10% formalin or dissected into four layers: maternal uterine tissue (mesometrial triangle and decidua), junctional zone, labyrinth and chorionic plate then snap frozen in liquid nitrogen. Accurate dissection of the placenta was ensured by utilising qPCR markers for the various layers (Figure 1-6). In order to establish continuity and good record keeping, a tissue collection protocol worksheet was developed (Appendix II).

2.3.4.2 Uterine and Mesenteric Artery Collection for Myography

Uterine artery segments were harvested from a consistent place in the area of the uterine artery closer to the vagina than the ovary from the uterine horn with the most fetuses and the mesentery was collected in laboratory-prepared calcium free physiological salt solution (PSS) (0.25 M NaCl, 0.001 M KCl, 2 mM $MgSO_4$, 50 mM $NaHCO_3$, 2 mM KH_2PO_4, 1 mM glucose, 0.5 ml of 23 mM EDTA) (Appendix I) in a 50 ml disposable plastic tube and dissected using a microscope within 1 hour of sacrifice. The uterine artery and third order mesenteric arteries were dissected and used for further experiments (Fig. 2-1). The average diameter of the uterine artery rings was 400 µm and the mesenteric artery rings was 270 µm. The dissected vessels were stored in calcium free PSS (Appendix I) overnight at 4 ºC and used for myography within 24 hours. Vessels were stored in calcium free PSS as they were used for both wire and pressure myography; pressure

myography requires that calcium is absent from the PSS to ensure vessels are tonic. Vessels used for myography were as clean as possible with all visible surrounding adipose tissue removed.

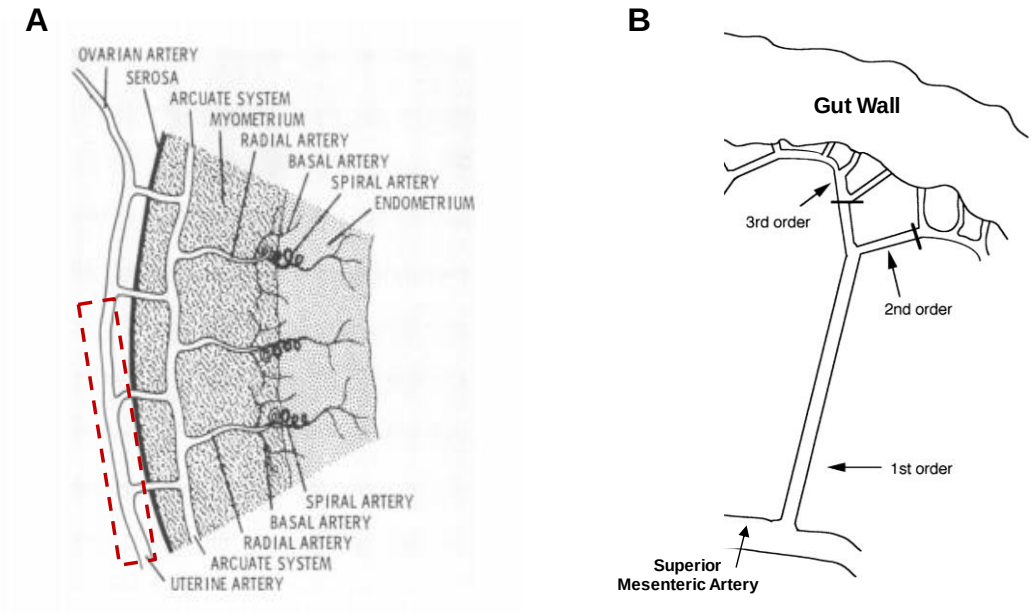

Figure 2-1 Arteries used for myography studies:

The uterine artery is highlighted in a red box (A). The third order mesenteric is indicated by an arrow in (B). Images are adapted from Robertson (1975) and Pourageaud *et al.* 1997 (350, 351).

2.4 Gene expression

2.4.1 Ribonucleic Acid (RNA) Extraction

Tissue was homogenised using a polytron 2100 rotor homogenizer in 700 µl QIAzol® (Qiagen, Manchester, UK). QIAzol® contains phenol to disrupt cell membranes and guanidinium salt which acts to block nucleases. RNA was extracted using the miRNeasy® mini kit (Qiagen, Manchester, UK) according to manufacturer's instructions. Briefly, 140 µl of chloroform was added to the 700 µl of QIAzol® then shaken vigorously by hand. This was followed by incubation at room temperature for 2 minutes then centrifugation for 15 minutes at 12,000 x g at 4 ºC. Polar nucleic acid remains in the clear aqueous phase which is then collected into a new tube and nucleic acids are precipitated with the addition of 1.5 volumes of ethanol. The solution is then applied to the RNeasy® mini column and is subject to a number of washing and concentrating steps using ethanol based wash buffers: RWT and RPE. RNA was eluted in 30 µl of nuclease free H_2O (NFW)

and the eluate was run through the column twice to maximise RNA extraction. A DNase step was not completed for samples as there were also needed to detect microRNAs (miRNAs). RNA was kept on ice and stored at -80 ºC until use.

2.4.1.1 Ribonucleic Acid Quantification and Quality Control

Total RNA concentration (ng/µl) was determined using a Nanodrop® ND1000 (Thermo Fisher, Paisley, UK) where a 260/280 ratio of 2.0 and a 260/230 ratio of 2.0-2.2 was used to indicate purity. RNA is detected at 260nm; whereas absorbance at 280 and 230nm indicates contamination by phenols and thiocyanate (found in QIAzol® lysis reagent) respectively. To validate RNA quality, a sample amount of placental tissue from SHRSP (n=3) and WKY (n=3) was subject to Agilent quality control testing (Fig. 2-2) (352) where RNA integrity number (RIN) were all >9.0. RNA was stored at -80 ˚C until use.

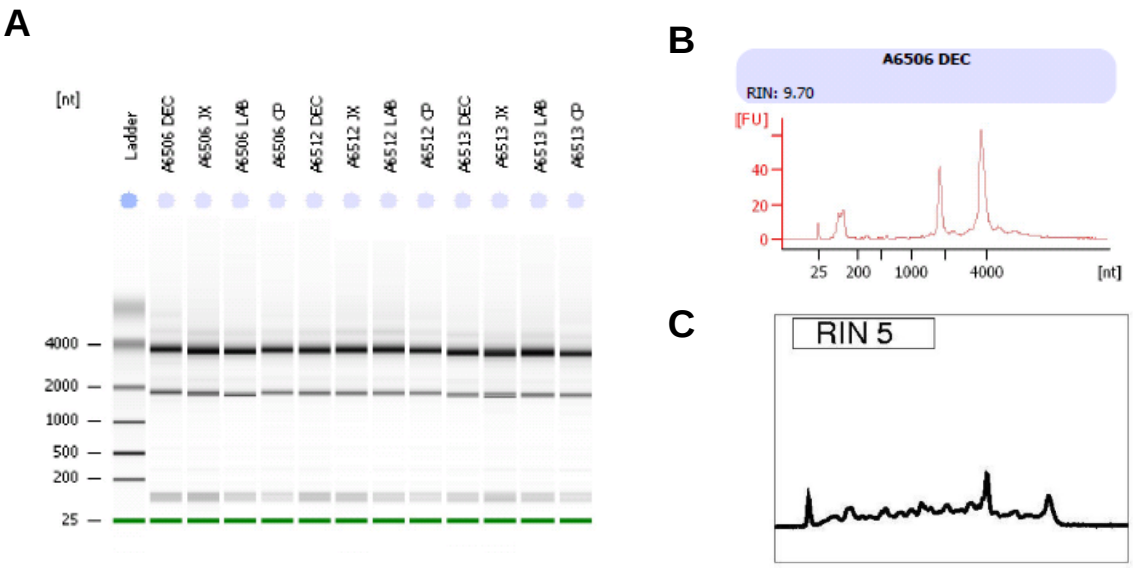

Figure 2-2 Example results from Agilent RNA quality control for WKY placenta.

Agilent testing takes into account the full electrophoretic spectrum of RNA (A). Good quality RNA shows clear bands at 28s and 18s ribosomal RNA and little presence of small degradation products (A-B). The example shown in (C) shows a poorer quality RNA sample where 28s and 18s peaks are reduced and there is an increased presence of shorter fragments. Image (C) is adapted from Schroeder *et al.* (2006).

2.4.2 Reverse Transcription Polymerase Chain Reaction (RT-PCR)

RT-PCR was used to prepare complimentary DNA (cDNA). RT-PCR was performed using the Taqman® Reverse Transcription Kit (Applied Biosystems,

Thermo Fisher, Paisley, UK) according to manufacturer's instructions. 1 µg RNA input diluted in NFW was used. In summary, 20 µl reactions were set up as:

10 x RT buffer	2 µl
25mM $MgCl_2$	4.4 µl
10 mM dNTPs	4 µl
Oligo dTs	1 µl
RNase Inhibitor	0.4 µl
Multiscribe	0.5 µl
TOTAL	**12.3 µl**
RNA (1 µg) + NFW	**7.7 µl**

Reactions were set up in a 96 well skirted plate (Thermo Fisher, Paisley, UK) and sealed with an adhesive sealing sheet to prevent evaporation (Thermo Fisher, Paisley, UK). The reaction was run on a Multi Block System Satellite 0.2 Thermo Cooler (Thermo Fisher, Paisley, UK)) on the following settings: 25 °C 10 min, 48 °C 30 min, 95 °C 5 min. cDNA was then stored at -20 °C until use.

2.4.3 Quantitative Polymerase Chain Reaction (qPCR)

Fluorescence based quantitative PCR is carried out on a thermal cycler which incorporates a fluorescence detector. By using a fluorescent reporter in the PCR reaction it is possible to quantify the production of DNA. In the log linear phase of the PCR reaction, fluorescence from the generated DNA is higher than the background; when this is measurable it is known as the threshold cycle (Ct) (353). There are two detection chemistries with respect to qPCR which have both been utilised in this thesis. SYBR® green is a dye which will intercalate in double stranded DNA; therefore this technique is only appropriate for measuring one amplicon at a time and specificity must be added by the addition of primers. Taqman® is one example of the technology where a fluorophore is directly conjugated to a probe specific for the gene of interest. Using Taqman® gives the ability to multiplex reactions by employing different probe-fluorophore complexes.

2.4.3.1 SYBR® Green qPCR

Sybr based qPCR was used to quantify gene expression using cDNA prepared in section 1.4.2. 5 µl reactions were set up using the following reagents:

Power SYBR® PCR Mastermix	6.35 µl
10µM Forward Primer	0.5 µl
10µM Reverse Primer	0.5 µl
NFW	2.65 µl
TOTAL	**10 µl**
+cDNA	**2.5 µl**

Reactions were set up in a 384 well plate (Thermo Fisher, Paisley, UK) and sealed with an optical adhesive sealing sheet (Thermo Fisher, Paisley, UK). Relevant primer details are given in Chapter 1. Gene expression protocol was run on an ABI PRISM 7900HT PCR system at the following settings: 95 °C, 15 min; followed by 40 cycles of 95 °C, 15 s; 60 °C, 1 min followed by a 30 minute dissociation step to check for primer specificity. Ct values were analysed using the 2(-delta delta Ct) method (354), with dCt indicating normalisation to the housekeeper, Glyceraldehyde-3-Phosphate Dehydrogenase (*Gapdh*).

2.4.3.2 Taqman® qPCR

Taqman® qPCR was used to quantify gene expression using cDNA prepared in section 1.4.2. Reactions were run in duplex where the gene of interest was run using a FAM labelled probe and the housekeeper using a VIC labelled probe. 10 µl duplex reactions were set up using the following reagents:

2x Taqman® mastermix	5 µl
Probe-FAM labelled	0.5 µl
Probe-VIC labelled	0.5 µl
NFW	2.5 µl
TOTAL	**8.5 µl**
+cDNA	**1.5 µl**

Reactions were set up in a 384 well plate (Thermo Fisher, Paisley, UK) and sealed with an optical adhesive sealing sheet (Thermo Fisher, Paisley, UK). Gene expression experiments in Chapter 3 were run on an ABI PRISM 7900HT PCR system at the following settings: 95 °C, 15 min; followed by 40 cycles of 95 °C, 15 s; 60 °C, 1 min. Gene expression in Chapters 4 - 6 were run on a QuantiStudio® 12K Flex at the following settings: 95 °C, 15 min; followed by 40 cycles of 95 °C, 15 s; 60 °C, 1 min. Ct values were analysed using the 2(-delta delta Ct) method (354), with dCt indicating normalisation to the housekeeper. The housekeeper for placental gene expression was ß-actin (*Actb*) and Glyceraldehyde-3-Phosphate Dehydrogenase (*Gapdh*) in heart samples.

2.5 Western blot

2.5.1 Protein Extraction for Western Blot

Protease inhibitor (Roche, West Sussex, UK) and phosphate inhibitor (Roche, West Sussex, UK) were added to laboratory prepared RIPA buffer pH 8.8 (50 mM Tris-HCl pH 7.4, 150 mM NaCl, 1mM EDTA, 1% NP-40, 0.1% SDS, 0.5% Na Deoxycholate) (Appendix I) on day of use. Tissue was homogenised using a polytron 2100 rotor homogenizer in 1ml of RIPA buffer. Homogenates were centrifuged at 8000 rpm for 10 minutes when supernatant was collected and aliquoted. Homogenates were aliquoted and stored at -80 °C until use.

2.5.2 Western Blot

Protein concentration was determined using bicinchoninic acid (BCA) assay (BioRad, Hemel Hempstead, UK). Protein samples were diluted to 20 µg in dH_2O to a final volume of 15 µl then 5 µl of NuPAGE® LDS Sample Buffer was added to each sample. Samples were incubated at 95 °C for 5 minutes then allowed to cool to room temperature. Samples were loaded on to a pre-cast Novex® 4-12% polyacrylamide gel (Thermo Fisher, Paisley, UK) for separation by electrophoresis in 1x NuPAGE® MES SDS/dH_2O running buffer (Thermo Fisher, Paisley, UK) at 200 v for 1 hour using a Mini-PROTEAN® Tetra Vertical Electrophoresis Cell (BioRad, Hertfordshire, UK). 10 µl of Amersham rainbow ladder RPN800E (Sigma-Aldrich, Dorset, UK) was loaded on the furthest left lane to determine protein size. Following separation, in Chapter 3 and 4 proteins were transferred using wet transfer at 40 v for 1 hour in a Mini Trans-Blot® cell (BioRad, Hertfordshire, UK) in 1x NuPAGE® transfer buffer/160ml methanol and 600 ml dH_2O (Thermo Fisher, Paisley, UK). Western blots in Chapter 6 were transferred using the semi-dry Thermo Scientific™ Pierce™ Power Blotter system (Thermo Fisher, Paisley, UK) in Pierce™ 1-step transfer buffer for 7 minutes. Proteins were transferred to Amersham™ Hybond™ P 0.45 PVDF membrane which had been activated in methanol (GE Life Sciences, Buckinghamshire).

2.5.3 Membrane Blocking & Antibody Incubation

Membranes were blocked with 5 % fat free milk powder in tris-buffered saline solution with Tween (TBS-T) for 2 hours at room temperature. Following blocking, membranes were incubated with the respective primary antibody overnight at 4 °C. Following overnight incubation in primary antibody, membranes were washed 4 x 5 minutes in TBS-T. Membranes were then incubated in the relevant horseradish peroxidase conjugated secondary antibody in 5 % fat free milk powder in TBS-T for one hour at room temperature. Specific details for membrane blocking and antibody incubation are given in the materials & methods section of the Chapter with the associated western blot.

2.5.4 Western Blot Development & Analysis

Proteins were visualised using Amersham enhanced chemiluminescence (ECL) western blotting detection reagents GE Life Sciences, Buckinghamshire) in a 1:1 ratio. ECL acts a chemiluminescent reagent which is produced by interaction with the horse radish peroxidase conjugated secondary antibody. Carestream medical X-ray film (Carestream, Hemel Hempstead, UK) was used to visualise protein bands. A Kodak X-Omat 1000 was used to develop the X-ray films.

2.6 Histology

2.6.1 Tissue Preparation for Histology

Tissues were fixed for 24 hours in 10% formalin at room temperature. After 24 hours, tissues were rinsed and formalin replaced with PBS. Tissues were then placed in histology cassettes (Thermo Fisher, Paisley, UK) and placed in a Citadel 1000 processor (Fisher Scientific, Loughborough, UK) at the following settings: 70 % ethanol 30 minutes, 95 % ethanol 30 minutes, 100% ethanol 30 minutes, 100% ethanol 30 minutes, 100% ethanol 45 minutes, 100% ethanol 45 minutes, 100% ethanol 60 minutes, 100% ethanol/xylene 30 minutes, xylene 30 minutes, xylene 30 minutes, wax 30 minutes, wax 30 minutes, wax 45 minutes, wax 45 minutes. The total running time was 8 hours and 30 minutes. Tissues were embedded using Shandon Histocentre 3 embedding centre (Fisher Scientific, Loughborough, UK) and Histoplast paraffin (Thermo Fisher, Paisley, UK). Placenta was cut through the centre with the cut side face down. Kidneys were cut transversely through the ureter and the cut side was placed face down. Paraffin sections of 5 µm were cut using a Leica Finese 325 Microtome (Fisher Scientific, Loughborough, UK) and baked on to silanised slides at 60 °C overnight. Slides were then stored at room temperature until use. Paraffin blocks were stored at 4 °C. Immediately prior to staining, slides were deparaffinised in histoclear 2 x 7 minutes then rehydrated through an ethanol gradient (100%, 90% and 75%; 5 minutes each) into distilled H_2O for 5 minutes.

2.6.2 Haematoxylin and Eosin Stain

Haematoxylin and eosin (H&E) stain was used to assess cellular structure of tissues. Slides were cleared and rehydrated as described in section 2.6.1. Slides

were stained in VFM Harris' haematoxylin stain (CellPath, Powys, UK) for 2 minutes followed by 5 minute wash in running tap water. Slides were then stained in eosin Y solution (CellPath, Powys, UK) for one minute. Negatively charged haematoxylin principally stains the negative nucleic acids of the nucleus dark purple. Positively charged eosin stains the negatively charged proteins and cytoplasmic contents. Slides were dipped in tap water then dehydrated through an ethanol gradient (70%, 90%, 100%; 5 minutes each). Slides were cleared in histoclear 2 x 5 minutes and mounted using DPX (Sigma-Aldrich, Dorset, UK). Slides were viewed using light microscopy.

2.6.3 Threshold Quantification of Staining Using Image J

8-10 images were taken at 4x objective and laced together using Microsoft Image Composite Editor 2.0. This was to ensure a high quality image when using the zoom tool on Image J. Positive staining for histology was determined using a threshold quantification method using Image J. Slides were analysed by an operator who was blinded to the identity of the slides; details of the operators are given in the author's declaration. The area of interest was selected and transformed into a RGB stack. The stack which made the positive staining most apparent was chosen by the operator. A threshold was then chosen so that only true positive staining was detected. This threshold was set for all of the images analysed. The % positive staining was determined as the amount of pixels over the given threshold ratio/the total number of pixels x 100.

2.7 Statistical Analysis

For the animal studies reported in this thesis, every effort was made to adhere to the Animal Research: Reporting of *in vivo* Experiments (ARRIVE) guidelines (355). Animal groups were randomised and, where possible, blinded before data analysis was carried out. In this instance, no power calculations were carried out prior to the beginning of experiments. Data were analysed and presented using GraphPad version 4.0 (San Diego, California, USA) where values stated are indicative of the mean ± standard error of the mean (SEM). A p value of less than 0.05 was considered to be significant for all experiments conducted. The relevant statistical analysis carried out for each data set is given in the associated Figure legend. In brief, for comparisons of a continuous variable between two

experimental groups (e.g. WKY vs. SHRSP) an unpaired Student's t test was employed. For data sets with more than two experimental groups (e.g. WKY, SHRSP and etanercept treated SHRSP) one-way analysis of variance followed by a post-hoc Tukey's test was used.

Chapter 3 Characterisation of the SHRSP as a Rat Model of Chronic Hypertension in Pregnancy

3.1 Introduction

Chronic hypertension in pregnant women confers a significant health risk for both the mother and fetus as discussed in section 1.7.3 (306). However, research on the impact of chronic hypertension during pregnancy is relatively limited. This led to the aim of developing the stroke prone spontaneously hypertensive rat (SHRSP) as a pre-clinical model of chronic hypertension during pregnancy. Previous work (section 1.8.1) showed that the SHRSP present at gestational day (GD) 18 with a significant reduction in uteroplacental blood flow and litter size relative to the normotensive WKY (349). Concurrently, the SHRSP exhibited abnormal pregnancy-dependent uterine artery remodelling in response to pregnancy which was characterised by a decrease in the diameter of the uterine artery and a blunted response to endothelium dependent vasorelaxation in comparison to vessels from WKY at GD18 (349).

As the SHRSP are hypertensive before and during pregnancy, we have previously used nifedipine in an intervention study in this model to assess the contribution of elevated blood pressure to the pathology associated with pregnancy (349). Nifedipine (25 mg/kg/day) was used from 6 weeks of age so that treated SHRSP never became hypertensive before or during pregnancy. Despite this significant blood pressure lowering, nifedipine treatment did not improve uterine artery structure and function or litter size in the SHRSP (Fig. 3-1) (349). Therefore, we concluded that the pregnancy pathology that was seen in the SHRSP was independent of high blood pressure. Since pregnancy has been characterised only briefly in the SHRSP (348) and variation exists between the inbred colonies (356), a thorough characterisation study was required before proceeding with follow-up mechanistic studies in this model. Additionally, as a model of maternal chronic hypertension it was unknown to what degree the SHRSP would share similarities with rodent models of pre-eclampsia.

We hypothesised that the SHRSP would exhibit maternal biomarkers, placental damage and fetal growth restriction consistent with hypertension during pregnancy seen in humans and other rat models. To address this hypothesis, a

characterisation study was conducted in pregnant (GD18) SHRSP and WKY to measure a number of maternal, placental and fetal factors known to be associated with hypertensive pregnancy.

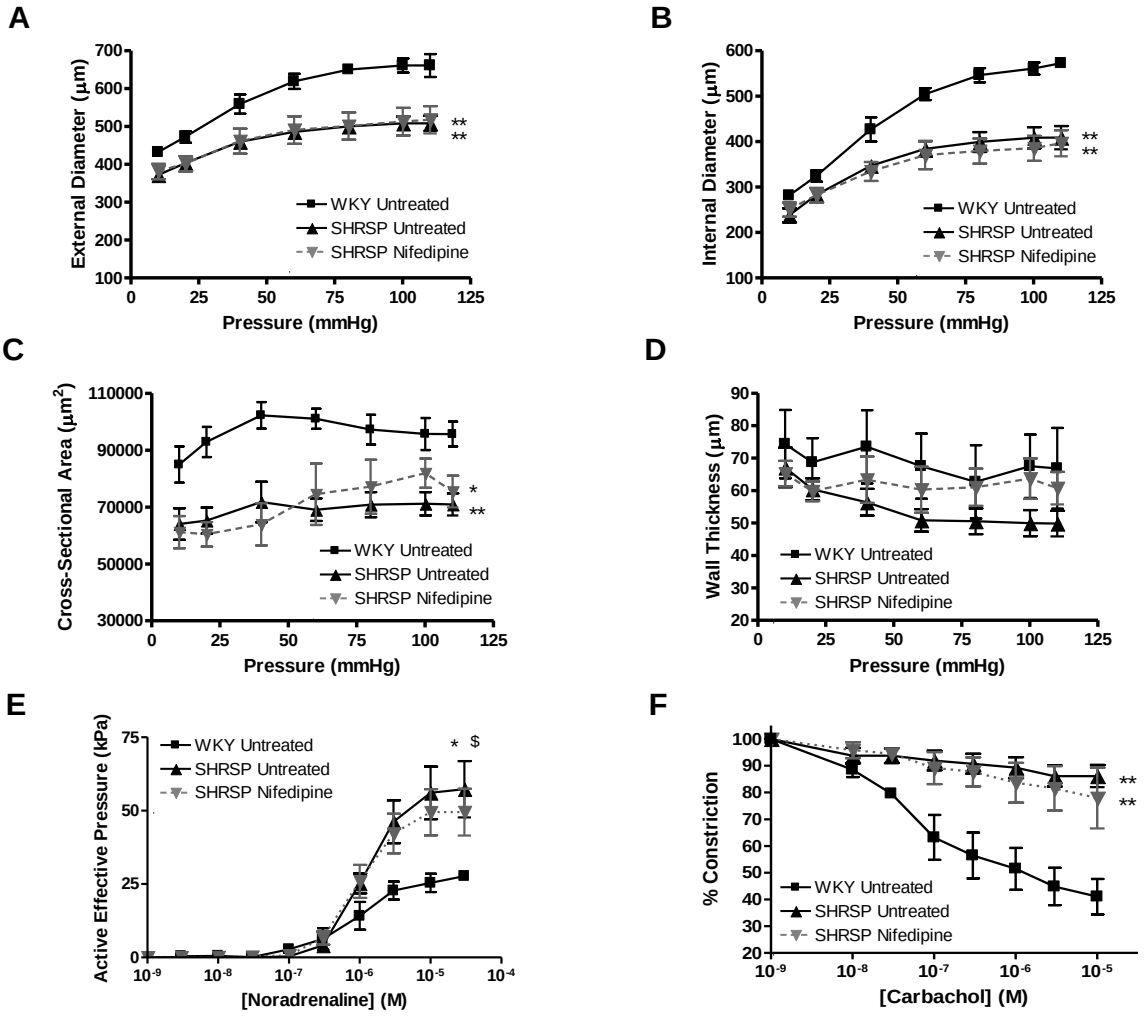

Figure 3-1 Nifedipine treatment does not improve uterine artery structure or function in the SHRSP.

Isolated uterine artery structure was assessed using pressure myography to measure external (A) and internal (B) diameter, cross-sectional area (C) and wall thickness (D) in pregnant (gestational day 18) untreated WKY (n=6), untreated SHRSP (n=6) and nifedipine treated SHRSP (n=6). External and internal diameter as well as cross-sectional area was significantly decreased in both untreated and nifedipine treated SHRSP (* $p<0.05$ vs. WKY; ** $p<0.01$ vs. WKY analysed by area under the curve followed by one-way ANOVA and post-hoc Tukey test). Isolated uterine artery function was also measured using wire myography in the same animals. Maximum response to noradrenaline (E) was significantly increased in both virgin and pregnant SHRSP (* $p<0.05$ SHRSP vs. WKY, $ $p<0.05$ Nifedipine vs. WKY analysed by area under the curve followed by one-way ANOVA and post-hoc Tukey test). Furthermore, endothelium-dependent vasorelaxation to carbachol (F) was significantly impaired in both untreated and nifedipine treated SHRSP (** $p<0.01$ vs. WKY analysed by area under the curve followed by one-way ANOVA and post-hoc Tukey test).

3.2 Materials & Methods

General materials & methods can be found in Chapter 2.

3.2.1 Animals

The work presented in this Chapter has used pregnant WKY and SHRSP that were untreated. This was an independent group of animals from the previous nifedipine study. Females were time mated at 12 weeks of age (± 4 days). Non-pregnant animals were age-matched at 15 weeks ± 4 days (i.e. 12 weeks of age + 21 days of pregnancy). The number of animals and particular gestational day (GD) is given in the associated Figure legend.

3.2.1.1 Baseline Characteristics at Sacrifice

Dams were weighed throughout pregnancy at GD0, 6, 12 and 18 and bodyweight was recorded. At the point of sacrifice (GD18), the uterine horn was excised and weighed separately. Pregnancy independent weight gain was calculated as (*GD18 bodyweight – uterine horn weight*). Maternal organs (heart, lungs, liver, spleen and kidneys) were excised, cleaned and weighed immediately following sacrifice. Post-mortem organ weight was normalised to tibia length as bodyweight changes over the course of pregnancy. In the uterine horn, the number of fetuses and resorptions was recorded. Resorption rate was expressed as (*[the number of resorptions/total number in litter] x 100*).

3.2.2 Identification of Implantation Sites using Evans' Blue

Rats were anaesthetized (2.5% isoflurane) and maintained under deep terminal anaesthesia throughout the procedure. 250 µl of 1% Evans' blue dye (Sigma-Aldrich, Dorset, UK) in PBS was injected into the exposed femoral vein. After 10 minutes, the animal was sacrificed under terminal anaesthesia and the uterine horn was excised. Implantation sites were counted as clear bands of positive blue staining.

3.2.3 Enzyme Linked Immunosorbent Assay (ELISA)

Maternal plasma sFLT-1 (DVR100B), PlGF (DPG00) and ET-1 (QET00B) were measured using commercially available kits (R&D Systems, Abingdon, UK) according to manufacturer's instructions. Kits were controlled using a positive control provided by the manufacturer and a negative control where dH_2O was used instead of sample. The method used a 7-point standard curve consisting of 1-in-2 serial dilution steps from the top standard: sFLT-1 concentration of 20,000 pg/ml down to a bottom standard with concentration of 31.3 pg/mL, PlGF concentration of 1000 pg/ml down to a bottom standard with concentration of 15.6 pg/mL and ET-1 concentration of 2500 pg/ml down to a bottom standard with concentration of 0.343 pg/mL. The limits of detection for the kits were as follows: sFLT-1 13.3 pg/ml, PlGF 7 pg/ml, ET-1 0.102 pg/ml. All samples presented were above the limit of sensitivity with the exception of the measurement of PlGF in 2 SHRSP plasma samples. All results shown in this Chapter were from one plate therefore there it was not necessary to calculate inter-assay variation.

3.2.4 Polymerase Chain Reaction (PCR)

RNA extraction and gene expression studies were carried out and analysed as described in section 2.4.

3.2.4.1 Uteroplacental Layer Dissection Sybr qPCR

Primers were designed using Primer3 software (357) then synthesised by Eurofins, Abingdon, UK. Primer sequences for *Des* (F: GGGACATCCGGCTCAGTAT R: AGAGCATCAATCTCGCAGGT), *Prl8a4* (F: GCATGTATGGTGGAAGAGGGT R: GCAATCTTTTCCAGTTATGAGACA), *Vegfr2* (F: AAGCAAATGCTCAGCAGGAT R: GAGGTAGGCAGGGAGAGTCC) and *Gapdh* (F: GACATGCCGCCTGGAGAAAC R: AGCCCAGGATGCCCTTTAGT).

3.2.4.2 Genes of Interest Taqman® qPCR

Gene expression was carried out using the following probes from Thermo Fisher, Paisley, UK: *Nppa* (Rn00664637_g1), *Nppb* (Rn00580641_m1), *Vegfa* (Rn01511602_m1), *Hif1a* (Rn01472831_m1), *Sod1* (Rn00566938_m1), *Gapdh* (4352338E) and *Actb* (4352340E).

3.2.5 Western Blot for Cleaved Capsase-3

Western blot was carried out as described in section 2.5. Membranes were incubated in the following primary antibody diluted in 5% Marvel skimmed milk powder in TBS-T overnight at 4 ºC: caspase-3 #9662 1:500 (Cell Signalling Technology, Leiden, Netherlands). Caspase-3 was detected using horse radish peroxidase (HRP) conjugated swine-α-rabbit secondary antibody (Dako, Ely, UK) diluted 1:1000 in 5% Marvel skimmed milk powder/TBS-T.

3.2.6 Histology

Preparation of paraffin blocks and sections were carried out as described in section 2.6.1.

3.2.6.1 Haematoxylin and Eosin (H&E) stain

Haematoxylin and eosin (H&E) stain was used to assess cellular structure of the placenta. Slides were cleared and rehydrated as described in section 2.6.1. Slides were stained in VFM Harris' haematoxylin (acidified) (CellPath, Newtown, UK) for 2 minutes followed by 5 minute wash in running tap water. Slides were then stained in eosin Y solution for one minute. Slides were dipped in tap water then dehydrated through an ethanol gradient (70%, 90%, 100%; 5 minutes each). Slides were cleared in histoclear 2 x 5 minutes and mounted using DPX (Sigma-Aldrich, Dorset, UK). Slides were viewed using light microscopy. In order to quantify the size of the placental layers a mid-sagittal section was used; indicated by the presence of the maternal channel. The respective layers were drawn around using the polygon tool on ImageJ (National Institutes of Health, Bethesda, USA) and the area was expressed as a percentage of the total area.

3.2.6.2 Perl's Prussian Blue Stain

Perl's Prussian blue stain was used to assess free blood in the placenta; specifically, this stain detects iron (20). Slides were cleared and rehydrated as described in section 2.6.1. Briefly, 4% ferrocyanide solution and 4% acidified water (HCl) were mixed immediately before incubating slides for 45 minutes then counter-stained with 1% neutral red. Slides were dipped in tap water then dehydrated through an ethanol gradient (95%, 100%; 5 minutes each). Slides were

cleared in histoclear 2 x 5 minutes and mounted using DPX (Sigma-Aldrich, Dorset, UK). Slides were viewed using light microscopy and analysed using threshold quantification in ImageJ (National Institutes of Health, Bethesda, USA) as described in section 2.6.4.

3.2.6.3 Periodic acid-Schiff Stain

Periodic acid – Schiff stain was used to quantify glycogen cell content in the placenta. Slides were cleared and rehydrated as described in section 2.6.1. Slides were incubated in 1% periodic acid (Sigma-Aldrich, Dorset, UK) in dH_2O for 10 minutes to oxidise aldehyde groups followed by 1 minute wash under running tap water. Slides were then stained with Schiff's reagent (Sigma-Aldrich, Dorset, UK) for 10 minutes which reacts with the oxidised aldehyde groups to form a magenta dye. This was followed by a 1 minute wash under running tap water and dehydration through an ethanol gradient (70%, 90%, 100%; 5 minutes each). Slides were cleared in histoclear 2 x 5 minutes and mounted using DPX (Sigma-Aldrich, Dorset, UK). Slides were viewed using light microscopy and analysed using threshold quantification in ImageJ (National Institutes of Health, Bethesda, USA) as described in section 2.6.4.

3.3 Results

3.3.1 Maternal Adaptation to Pregnancy in the SHRSP and WKY

Over gestation, maternal weight gain is significantly reduced in the SHRSP relative to the WKY (Fig. 3-2A). Additionally, raw maternal weights are given in Table 3-1. Animals were also weighed at GD18 once the uterine horn was excised which we termed "pregnancy independent weight gain"; this was also significantly decreased in SHRSP relative to WKY (Fig. 3-2B).

Post-mortem tissue weights were recorded from non-pregnant and pregnant (GD18) WKY and SHRSP and normalised to tibia length. Whilst there was no significant strain difference in heart weight between non-pregnant animals; there was a significant increase in heart weight in pregnant SHRSP relative to WKY (Fig. 3-3A). There was no pregnancy or strain-dependent difference in the weight of the lungs or spleen (Fig. 3-3B-C). There was a similar pregnancy-dependent increase in liver weight in both WKY and SHRSP (Fig. 3-3D). With respect to kidney

weight, this was increased in both non-pregnant and pregnant SHRSP relative to WKY (Fig. 3-3E). Additionally, there was no pregnancy dependent change in kidney weight in either strain (Fig. 3-3E).

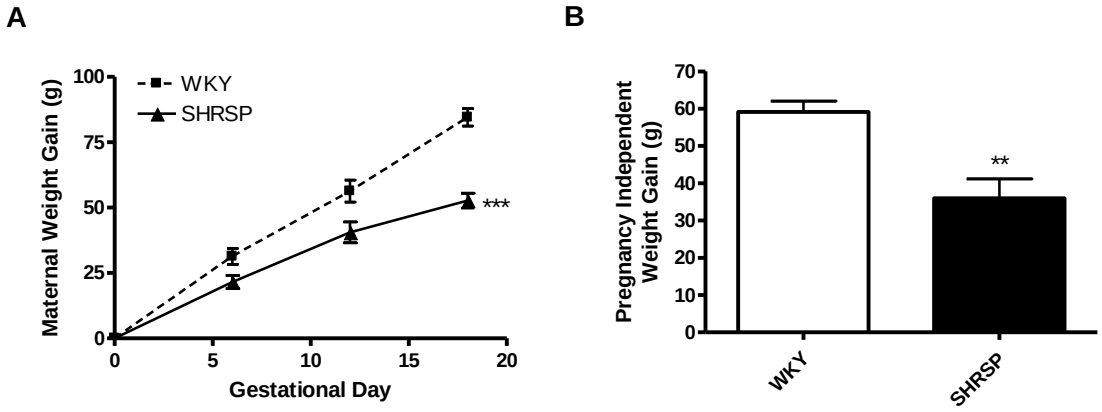

Figure 3-2 Maternal weight gain over pregnancy is reduced in the SHRSP relative to the WKY.

Bodyweight was recorded in untreated WKY and SHRSP (n=6). Maternal weight gain over the course of pregnancy (A) was significantly decreased in SHRSP relative to WKY (*** $p<0.005$ vs. WKY GD18 analysed by comparing area under the curve values using Student's t-test). Since this reduction in weight gain could be a result of a reduction in litter size in these animals, the animals were weighed at GD18 without the uteroplacental unit which we have referred to as "pregnancy independent" weight gain. Pregnancy independent weight gain (B) was significantly reduced in the SHRSP (** $p<0.01$ vs. WKY GD18 analysed by Student's t-test).

Table 3-1 Raw maternal weights recorded over gestation in the WKY and SHRSP

Gestational Day	WKY	SHRSP	P value
0	172.43 ± 5.25 g	159.33 ± 2.76 g	0.06
6	203.79 ± 3.04 g	178.19 ± 3.74 g	<0.01
12	228.74 ± 2.95 g	197.89 ± 3.80 g	<0.01
18	254.41 ± 5.20 g	212.61 ± 4.82 g	<0.01

WKY (n=6); SHRSP (n=6)

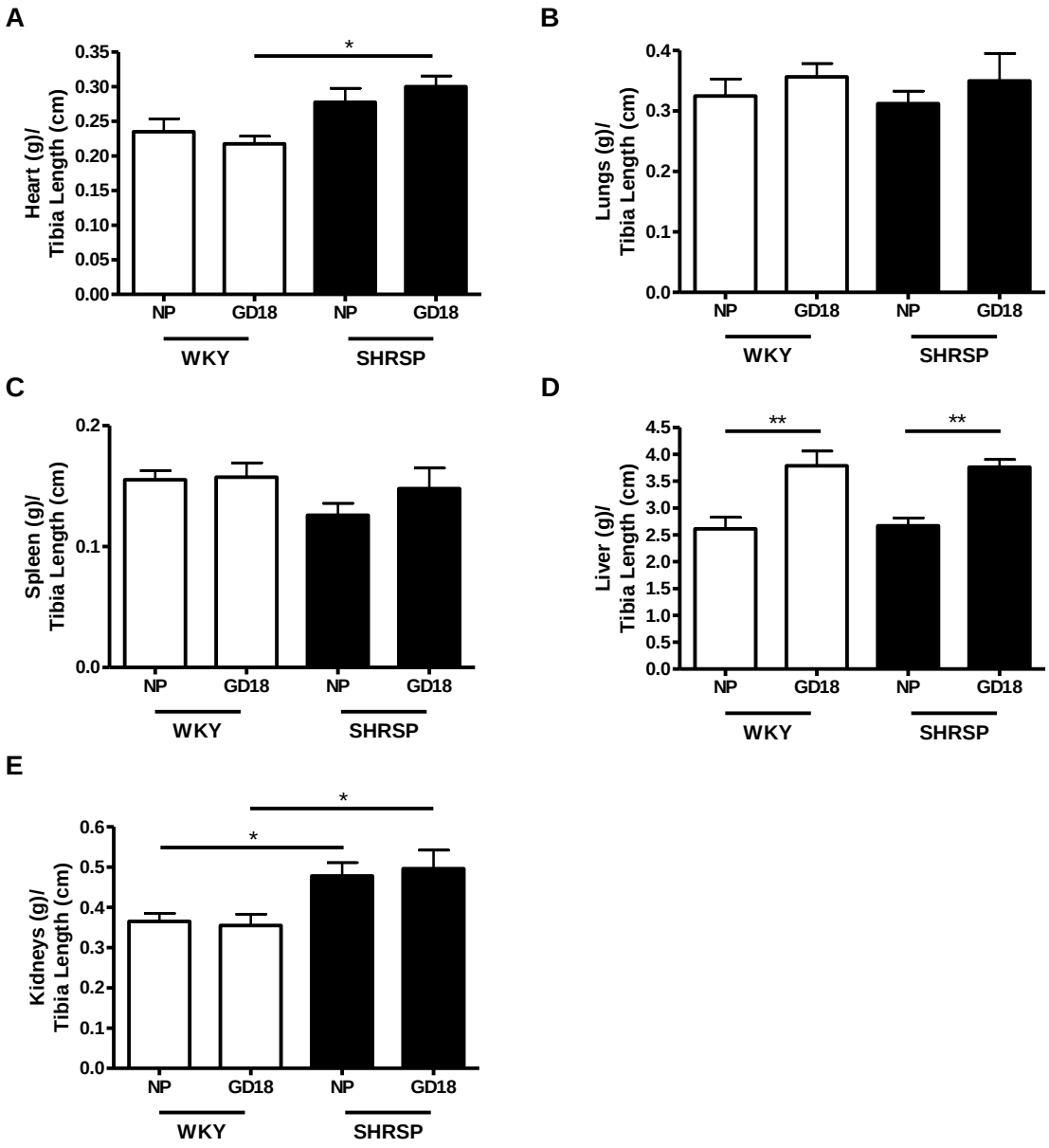

Figure 3-3 Heart and kidney weight are increased in SHRSP relative to the WKY.

Post-mortem organ weight was measured in non-pregnant (n=5) and pregnant (GD18) (n=5) WKY and non-pregnant (n=5) and pregnant (n=5) SHRSP. Organ weights were normalised to tibia length as bodyweight changes over gestation. Heart weight (A) was not significantly different between non-pregnant animals but was greater in pregnant SHRSP relative to pregnant WKY (* $p<0.05$ vs. WKY GD18 analysed by one-way ANOVA followed by a post-hoc Tukey's test). There were no significant differences in the lungs or spleen between non-pregnant and pregnant animals or between WKY and SHRSP (B-C). Liver weight (D) was significantly increased in a pregnancy-dependent manner in both WKY and SHRSP (** $p<0.01$ vs. NP analysed by one-way ANOVA followed by a post-hoc Tukey's test). Kidney weight (E) was greater in SHRSP at both non-pregnant and pregnant time-points relative to the WKY (* $p<0.05$ vs. WKY analysed by one-way ANOVA followed by a post-hoc Tukey's test).

3.3.1.1 SHRSP Exhibit Features of Pregnancy-dependent Left Ventricular Hypertrophy

Left ventricle weight was increased in a pregnancy and strain dependent manner similar to that of heart weight (Fig. 3-4A) in SHRSP relative to WKY (Fig. 3-4B). Gene expression of natriuretic peptides, ANP and BNP, were altered in the left ventricle of SHRSP relative to WKY. ANP (*Nppa*) expression was increased in left ventricle taken from both non-pregnant and pregnant SHRSP relative to the WKY (Fig. 3-4C). BNP (*Nppb*) expression in the left ventricle tissue was not significantly different between strains in non-pregnant animals but was significantly increased in left ventricle tissue from pregnant SHRSP relative to WKY (Fig. 3-4D).

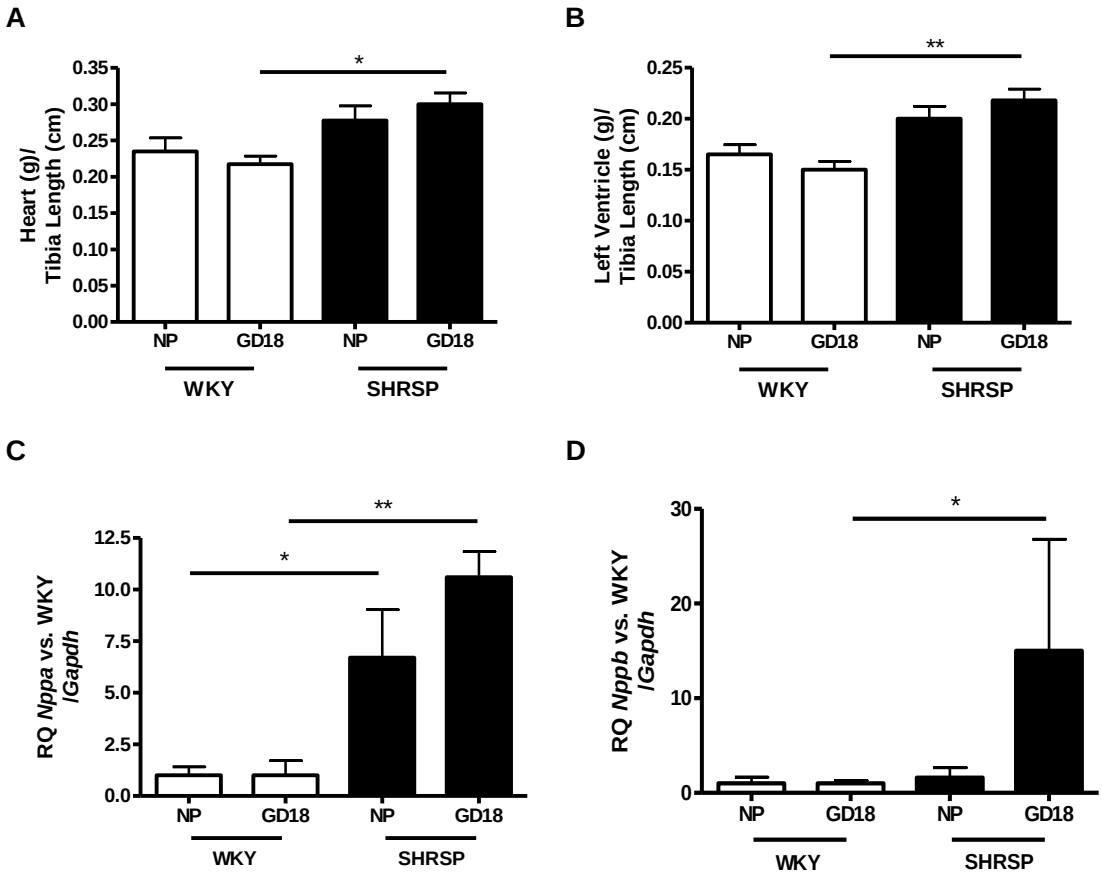

Figure 3-4 SHRSP exhibit features of left ventricular hypertrophy during pregnancy.

Heart (A) and left ventricle (B) weight was increased in pregnant (GD18) SHRSP (n=5) relative to WKY (n=5) (* p<0.05, **p<0.01 vs. GD18 WKY analysed by one-way ANOVA followed by a post-hoc Tukey's test) but not between non-pregnant WKY (n=5) and non-pregnant SHRSP (n=5). Gene expression of ANP (*Nppa*) in left ventricle (n=5) tissue (C) was increased in both non-pregnant and pregnant (GD18) SHRSP relative to WKY (* p<0.05, **p<0.01 vs. GD18 WKY analysed by one-way ANOVA followed by a post-hoc Tukey's test). Gene expression of BNP (*Nppb*) in left ventricle tissue (n=5) (D) was increased only in pregnant (GD18) SHRSP relative to WKY (* p<0.05, **p<0.01 vs. GD18 WKY analysed by one-way ANOVA followed by a post-hoc Tukey's test).

3.3.1.2 Maternal biomarkers associated with hypertensive pregnancy are altered in pregnant SHRSP

Biomarkers which have been previously shown to be associated with the incidence of hypertension during pregnancy were measured in maternal plasma from pregnant (GD18) WKY and SHRSP. The potent vasoconstrictor molecule endothelin-1 (ET-1) was significantly increased in plasma from pregnant SHRSP relative to WKY (Fig. 3-5A). Anti-angiogenic soluble receptor, soluble Flt-1 (sFLT-1) was also significantly increased in plasma from pregnant SHRSP (Fig. 3-5B). There was a trend for a decrease in placental growth factor (PlGF) in plasma from SHRSP relative to WKY (Fig. 3-5C). Accordingly, the sFLT-1:PlGF ratio was significantly increased in SHRSP relative to WKY (Fig. 3-5D). As sFLT-1 can also act as a receptor for VEGF; VEGF was measured in the plasma. However, the levels were absent or below the limit of detection of the assay at GD18. Using plasma samples from earlier gestational time points showed that plasma VEGF decreased over the course of pregnancy in both WKY and SHRSP (Fig. 3-5E).

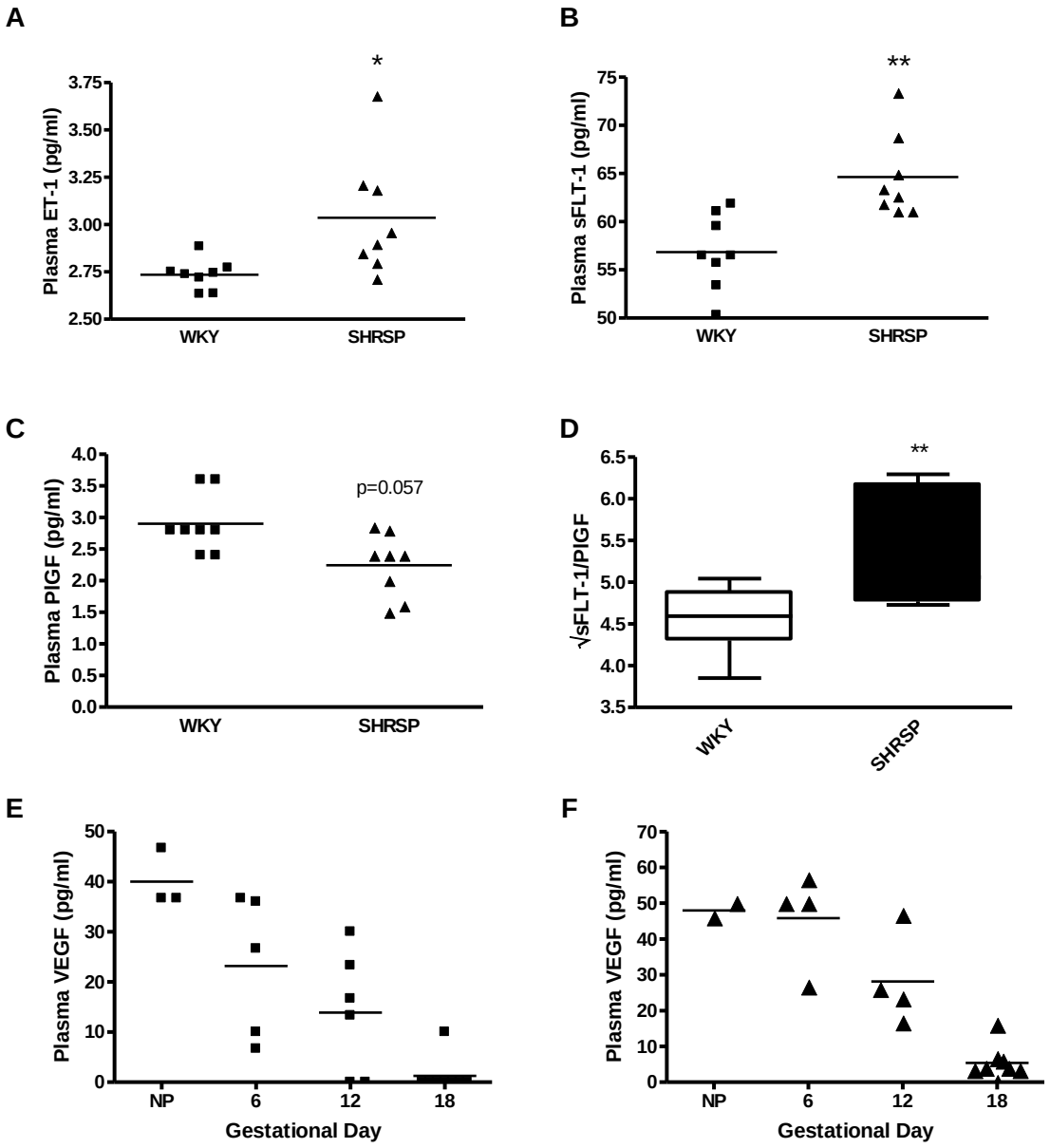

Figure 3-5 Maternal plasma biomarkers associated with hypertensive pregnancy are altered in the SHRSP.

Biomarkers were measured using ELISA in maternal plasma taken from pregnant (GD18) WKY (n=8) and SHRSP (n=8). Endothelin-1 (ET-1) (A) and soluble FLT-1 (sFLT-1) (B) were increased in plasma from SHRSP relative to WKY (* $p<0.05$, ** $p<0.01$ vs. GD18 WKY analysed by Student's t-test). Placental growth factor (PlGF) showed a trend for a decrease in SHRSP ($p = 0.057$ vs. GD18 WKY analysed by Student's t-test) (C). The sFLT-1/PlGF ratio was increased in SHRSP relative to WKY (** $p<0.01$ vs. GD18 WKY analysed by Student's t-test) (D). The detection of free vascular endothelial factor (VEGF) in the plasma (E) showed a trend to decrease over the course of gestation in both WKY (NP n=3, GD6 n=5, GD12 n=6, GD18 n=8) and SHRSP (F) (NP n=2, GD6 n=4, GD12 n=4, GD18 n=8) and as a result was undetectable in most samples at GD18.

3.3.2 Placental Biology is Altered in Pregnant SHRSP

The rat placenta is composed of distinct layers with characteristic cellular composition and function (discussed in section 1.6.1). A protocol was developed for dissecting the tissue into four constituent layers: the mesometrial triangle and decidua, junctional zone, labyrinth and chorionic plate. To verify accurate dissection, qPCR markers were used (Fig. 3-6). Desmin (*Des*) was highest in the uterine tissue (mesometrial triangle and decidua) (Fig. 3-6A), prolactin (*Prl8a4*) was highest in the junctional zone (Fig. 3-6B) and VEGF receptor 2 (*Vegfr2*) was highest in the vascularised mesometrial triangle and labyrinth zone (Fig. 3-6C). The chorionic plate had the lowest expression for all of these markers (Fig. 3-6A-C).

Gene expression markers associated with oxidative stress were tested in dissected placental tissue from pregnant (GD18) WKY and SHRSP. Expression of hypoxia inducible factor 1 α (*Hif1a*) (Fig. 3-7A) and superoxide dismutase 1 (*Sod1*) (Fig. 3-7B) were increased in SHRSP in the vascular compartments of the placenta; the uterine tissue and labyrinth. Vascular endothelial growth factor (*Vegf*) (Fig. 3-7C) was increased in the main placental unit (junctional zone and labyrinth) of the SHRSP relative to the WKY.

Upon visual inspection of the placental tissue on dissection, a darkened area of potential haemorrhage or necrosis was identified within the outer - region of the junctional zone in the majority (>50%) of SHRSP placenta which was not evident in the WKY (Fig 3-8A). Perl's Prussian blue staining revealed a significant increase in free blood principally localised in the junctional zone of the placenta in the SHRSP compared to the WKY (Fig 3-8B-C). Cell death in the placental tissue was evaluated using western blot for caspase-3 cleavage. A greater amount of caspase-3 cleavage was observed in GD18 placental tissue from SHRSP relative to WKY (Fig 3-8D-E).

Haematoxylin and eosin staining for cellular structure showed that there was no difference in the size of the layers of the uteroplacental unit at GD18 between WKY and SHRSP (Fig 3-9A-B). However, periodic acid-Schiff (PAS) stain revealed that the SHRSP had a significantly reduced proportion of PAS positive glycogen cells in the junctional zone of the GD18 placenta compared to WKY (Fig

3-9C-D). There was no significance difference in PAS positive staining in the decidua and mesometrial triangle between strains (Fig. 3-9E).

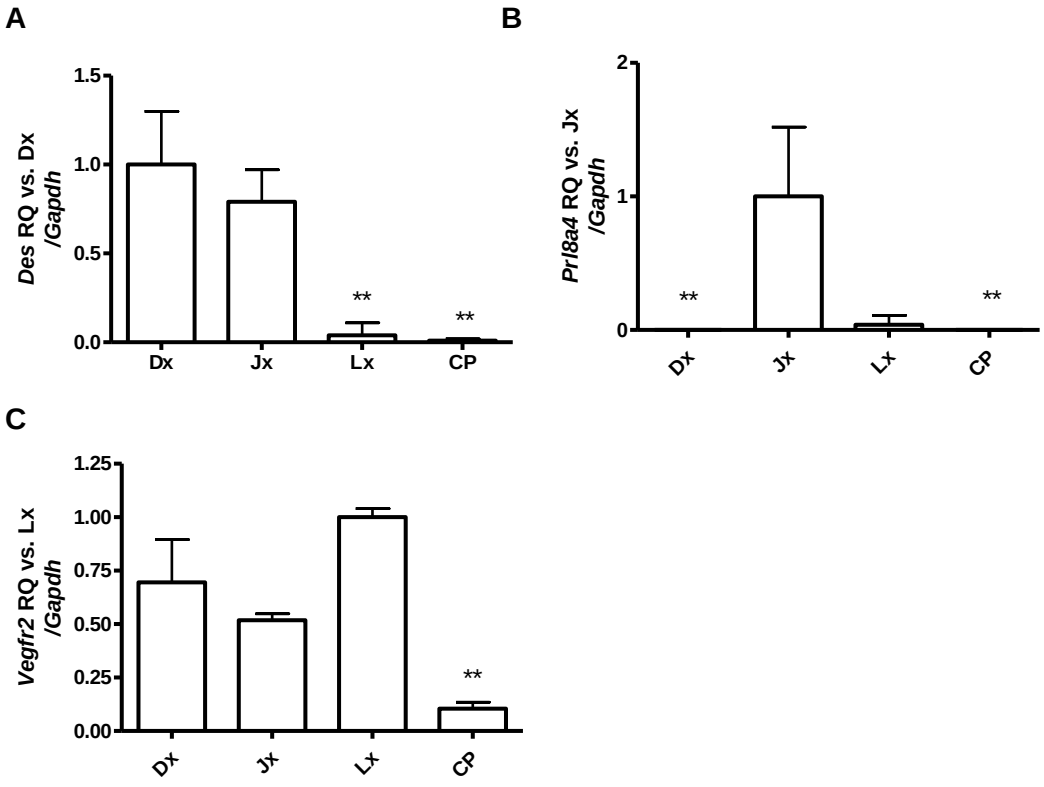

Figure 3-6 qPCR markers for placental layers.

The placenta was dissected into four layers: maternal tissue (the mesometrial triangle and decidua) (Dx), junctional zone (Jx), labyrinth (Lx) and chorionic plate (CP) in pregnant (GD18) WKY (n=6). Desmin (*Des*) (A) was most highly expressed in the maternal tissue (Dx) (** $p<0.01$ vs. Dx analysed by one-way ANOVA followed by post-hoc Tukey's test). *Prl8a4* (B) was most highly expressed in the junctional zone (Jx) (** $p<0.01$ vs. Jx analysed by one-way ANOVA followed by post-hoc Tukey's test). *Vegfr2* (C) had highest expression in the vascularised areas of the placenta; the Dx and the Lx (** $p<0.01$ vs. Lx analysed by one-way ANOVA followed by post-hoc Tukey's test).

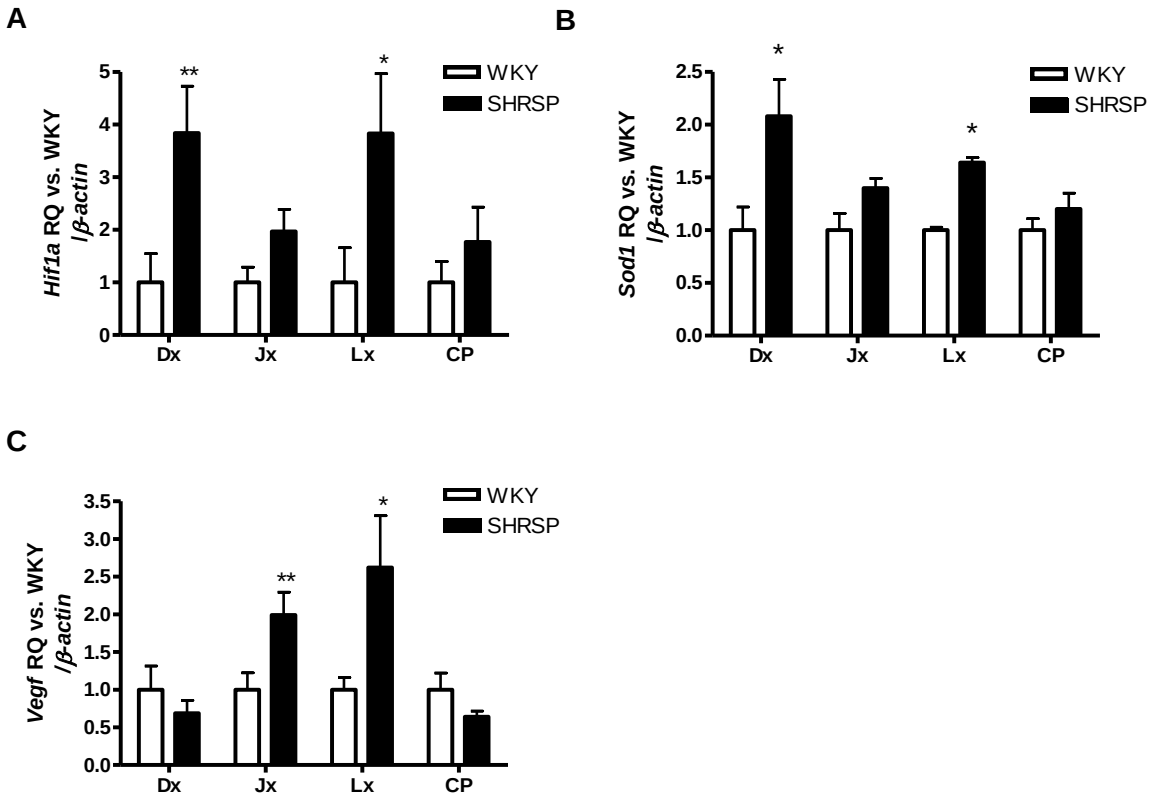

Figure 3-7 Placental markers of hypoxia are increased in placenta from pregnant SHRSP.

Placentae from pregnant (GD18) SHRSP (n=8) and WKY (n=8) were dissected into the main layers of the placental unit: decidua (Dx), junctional zone (Jx), labyrinth zone (Lx) and chorionic plate (CP). Genes of interest were assessed in these zones separately; the SHRSP showed an increase in *Hif1a* (A) and *Sod1* (B) expression in both the decidua and labyrinth whilst *Vegf* (C) expression was upregulated in the junctional zone and labyrinth (* $p<0.05$, ** $p<0.01$ vs. GD18 WKY analysed by Student's t-test).

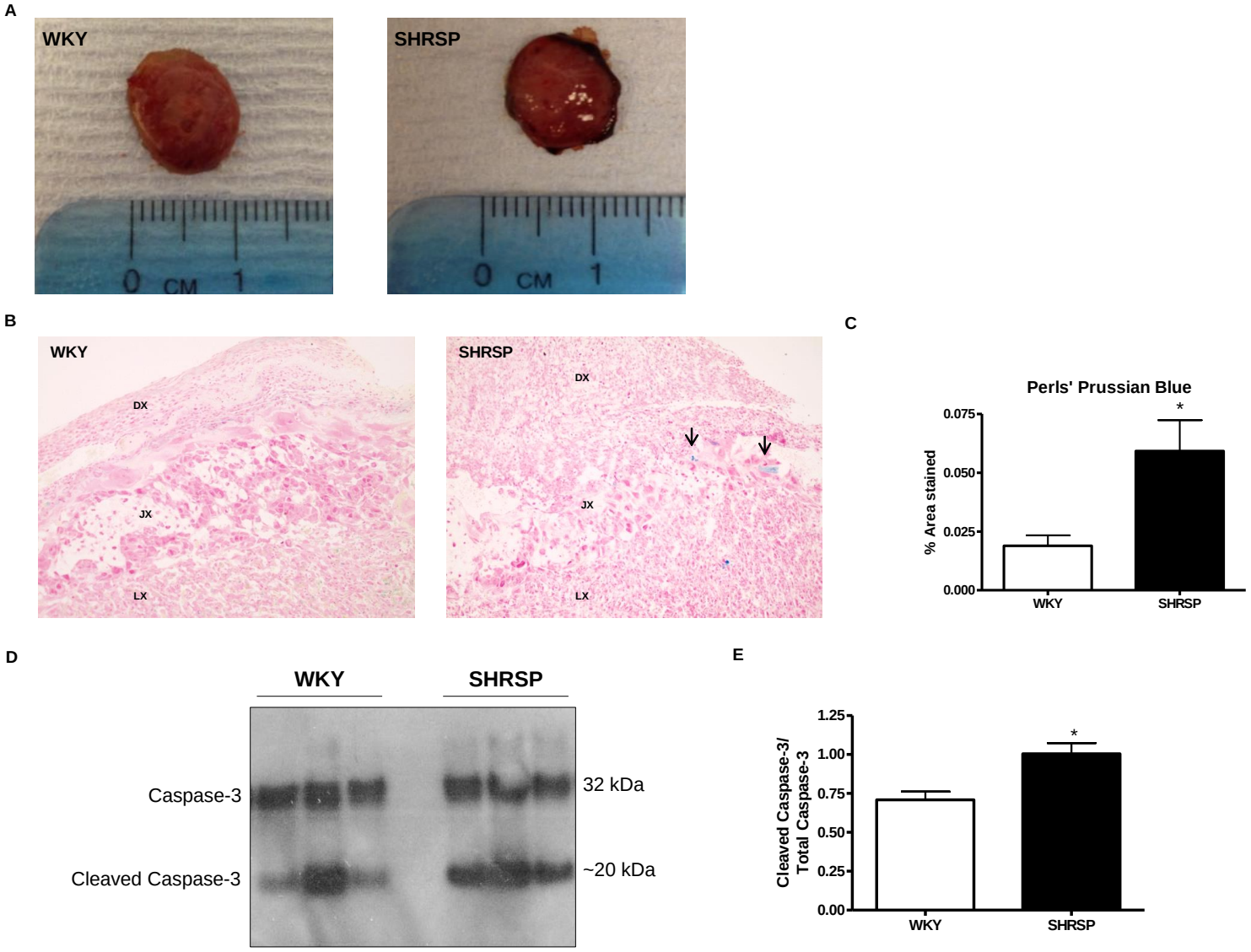

Figure 3-8 The SHRSP placenta at GD18 exhibits increased free blood and cell death.

Visual inspection of the placental tissue from SHRSP exhibited blackened areas that were localised to the edges of the junctional zone (Jx) (A). Perl's Prussian blue staining (B) in sections of placenta from WKY (n=8) and SHRSP (n=8) showed that SHRSP had an increase in free blood localised to the Jx of the SHRSP placenta relative to the WKY (C) (* $p<0.05$ vs. GD18 WKY analysed by Student's t-test). Western blotting for caspase-3 showed that placenta from GD18 SHRSP showed an increased proportion of cleaved: full length caspase-3 relative to WKY (2 technical replicates; n=3 SHRSP and WKY) (D-E) (* $p<0.05$ vs. GD18 WKY analysed by Student's t-test). Dx: decidua, Jx: junctional zone, Lx: labyrinth.

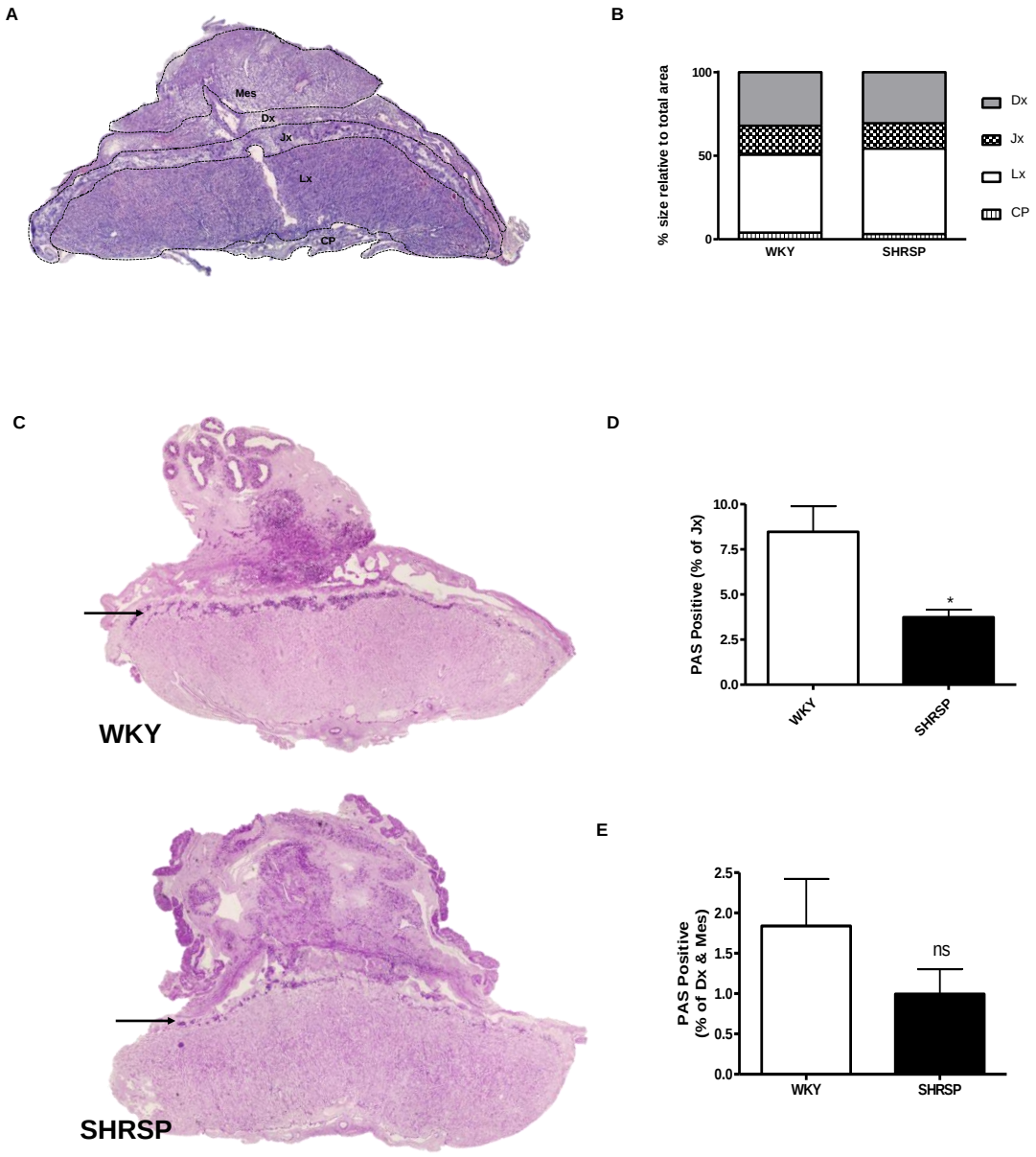

Figure 3-9 The SHRSP placenta exhibits premature glycogen cell loss from the junctional zone.

Haematoxylin & eosin stain was used to assess cellular structure of the placenta in WKY (n=8) and SHRSP (n=8) (A). Analysis of haematoxylin & eosin stained sections of placenta showed that there was no significant difference in the size of the layers of the uteroplacental unit (B). Mes: mesometrial triangle, Dx: decidua, Jx: junctional zone, Lx: labyrinth, CP: chorionic plate. Periodic acid Schiff stain in sections of placenta from WKY (n=8) and SHRSP (n=8) showed that SHRSP had less glycogen cells present in the Jx relative to the WKY (C-D). This did not appear to be due to migration into the uterine tissue as there was no significant difference in PAS positive cells in this area (E).

3.3.3 Blastocyst Implantation is Not Impaired in the SHRSP

Using a dye injection technique at GD6 (Fig. 3-10A), the number of implantation sites was not found to be different between WKY and SHRSP (Fig. 3-10B).

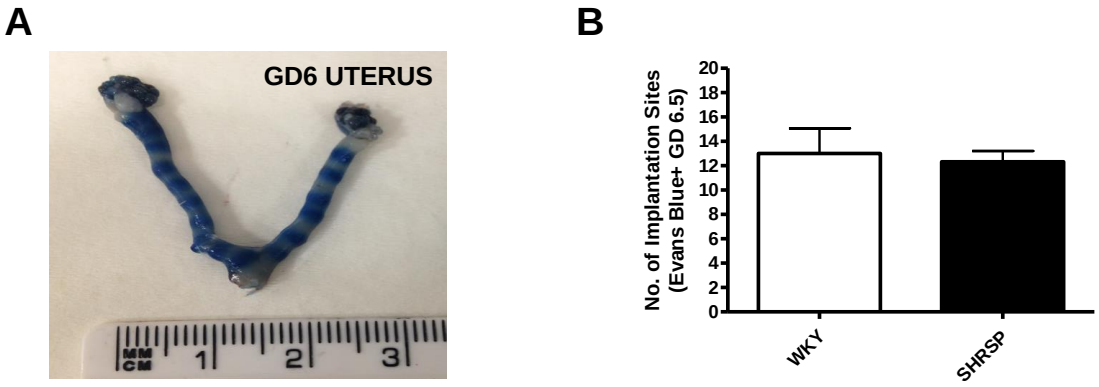

Figure 3-10 Blastocyst implantation is not altered in the SHRSP relative to the WKY.

Blastocyst implantation was determined at GD6 in untreated SHRSP (n=3) and WKY (n=4) using Evans' blue dye infusion (A) under terminal anaesthesia. There were no significant difference between WKY and SHRSP in the number of implantation sites detected (B).

3.3.4 Resorption frequency is increased in SHRSP

Sites of late spontaneous pregnancy loss, termed resorptions, were counted at GD18 in WKY and SHRSP (Fig. 3-11). The number of dams that presented with 1 or more resorptions was greater in the SHRSP (66.7 %) relative to WKY (36%). Of those dams which had resorptions, the percentage of the litter that were lost was also increased in SHRSP relative to WKY at GD14 and GD18 (Table 3-2).

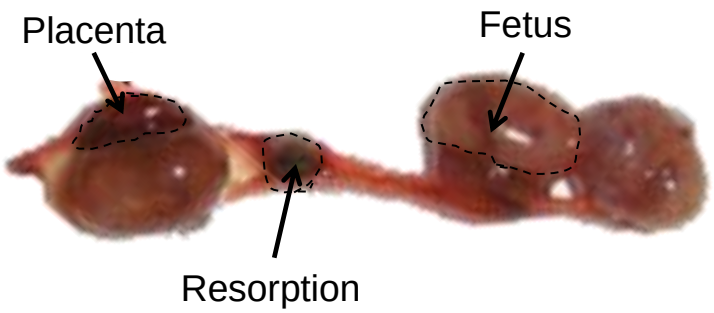

Figure 3-11 Example of a fetal resorption.

Table 3-2 Resorption frequency is increased in SHRSP at GD14 and GD18.

% Resorption Frequency	WKY	SHRSP
GD14	11.67 ± 0.72 %	30.63 ± 0.79 %
GD18	14.82 ± 0.58 %	28.45 ± 0.69 %

GD14 WKY n=5; SHRSP n=5. GD18 WKY n=8; SHRSP n=8. Figures are presented as mean of each strain of the percentage of the litter affected by resorption ± SEM.

3.3.5 Fetal and Placental Growth is Not Restricted in the SHRSP

Post-mortem placental and fetal weights were recorded from WKY and SHRSP at GD 14, 18 and 20. There was no significant difference in placental or fetal weight at any time point between strains (Fig 3-12A-B). More detailed fetal measurements were taken at GD20 from WKY and SHRSP. There was no difference in fetal head: weight ratio (Fig 3-12C) or fetal heart: liver ratio (Fig. 3-12D) between strains.

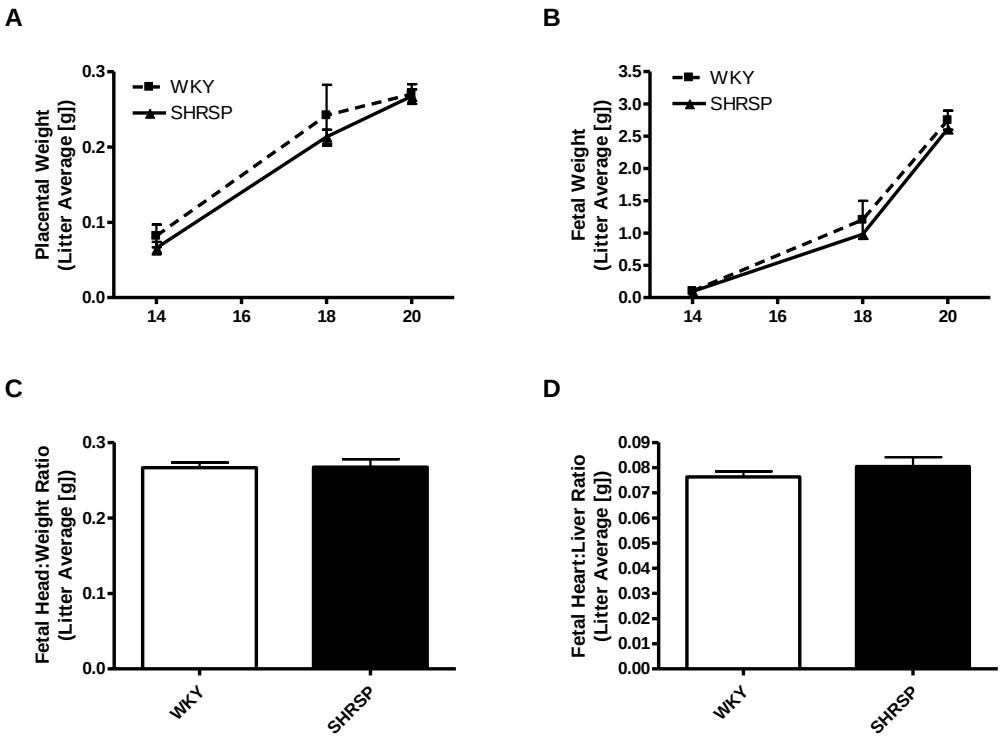

Figure 3-12 Fetal and placental weight is not altered in the SHRSP relative to the WKY.

Post-mortem placental and fetal weight was measured **in** GD14 (n=5), (GD18) (n=8) and GD20 (n=5) WKY and GD14 (n=5), (GD18) (n=8) and GD20 (n=5) SHRSP (A-B) where there were no strain-dependent differences. Detailed fetal measurements were taken at GD20 only (n=5 in both WKY and SHRSP) (C-D). There was no significant difference in fetal head: weight ratio (C) or heart: liver ratio (D). Data are expressed as an average weight from each litter.

3.4 Discussion

The work presented in this Chapter shows that the SHRSP exhibits altered maternal adaptation to pregnancy relative to the WKY. Furthermore, the SHRSP exhibits placental pathology characterised by an increase in oxidative stress-related genes, increased cell death and a loss of glycogen cells at GD18. There are no strain dependent differences in placental and fetal weight or blastocyst implantation.

Normal pregnancy in humans and rodents is associated with physiological eccentric cardiac hypertrophy in response to a prolonged increase in cardiac load secondary to an increase in blood volume (discussed in section 1.5.1) (358). In this study, the WKY shows no significant pregnancy-dependent increase in heart or left ventricular weight however, there was a significant increase in both of these parameters in the SHRSP. The expression of ANP is increased from non-pregnant to pregnant animals from both strains; this may be in response to increased cardiac load due to volume expansion. In normal human pregnancy, serum ANP is increased early in pregnancy; however it is not known how directly related this is to cardiac ANP secretion (359). Increased ANP has been detected in cardiac tissue from rat models of hypertensive pregnancy but these were not compared to non-pregnant controls (360). In contrast to ANP, BNP is only increased during pregnancy in SHRSP. Levels of serum BNP in healthy women has been reported to be not changed (361) or slightly increased (362) during pregnancy. Further echocardiogram and histology could be used to assess features of left ventricular hypertrophy that are not detectable in post-mortem analysis such as cardiomyocyte structure.

The potent vasoconstrictor molecule, endothelin-1 (ET-1), was modestly but significantly increased in maternal plasma from SHRSP at GD18 relative to normotensive WKY. ET-1 has been shown to be instrumental in the vascular dysfunction that is seen in hypertension which occurs independently of pregnancy (363) and during pre-eclampsia (364). One limitation of the measurements in this study are the lack of a non-pregnant comparison as SHRSP are hypertensive before and during pregnancy. The ratio of maternal plasma biomarkers sFLT-1: PlGF has been shown to have predictive ability in women who went on to develop pre-eclampsia in the recent PROSPECTIVE study (365). In addition, lower maternal

PlGF measured in the plasma has been shown to be predictive of the development of superimposed preeclampsia in women with chronic hypertension (366). An increase in sFLT-1: PlGF ratio is also seen in the SHRSP; but these changes are much smaller (approximate sFLT-1: PlGF increase of 1) than those seen in models of pre-eclampsia such as the RUPP (approximate sFLT-1: PlGF increase of 30) (329). Similarly to the RUPP rat, an sFLT-1: PlGF of above 38 has been shown to have some predictive value for women who may be at risk of developing pre-eclampsia in the PROSPECTIVE cohort (365). Plasma (free) VEGF was not detectable at late pregnancy (GD18) in either strain in this study in contrast to other work in pregnant rats (367). Similarly to this study, free VEGF is not detectable in most women during late gestation (368). A recent study by Weissgerber *et al*. identified that utilising different commercially available ELISA kits for VEGF led to inconsistent results in rodent models (369). The Weissgerber study showed that plasma VEGF was below the limit of detection of the R&D Systems rat VEGF ELISA assay, such as the one used in this study, at GD18.

Placental weight or the size of the uteroplacental layers are not altered between WKY and SHRSP. However, a darkened area was identified in the majority of the SHRSP placentas upon visual inspection which we hypothesised could be haemorrhage or necrosis. There was a small but significant increase in free blood in the SHRSP relative to the WKY evaluated by Perl's Prussian blue staining but this was not marked enough to suggest haemorrhage. There was a significant increase in caspase-3 cleavage, which is indicative of an increase in cell death. These findings suggest that these black areas are most likely to be necrotic tissue. Placental tissue from women with pre-eclampsia also shows an increase in cell death and caspase-3 activation (370). Further investigations should employ other markers for upstream mediators of apoptosis such as Bcl-2 and Bax. Hypoxia-reoxygenation has been shown to induce placental cell death (371). In-keeping with these findings, an increase in oxidative stress related genes was detected in placenta from the SHRSP. Further work should measure reactive oxygen species such as superoxide and hydrogen peroxide as well as assess oxidative stress induced DNA damage in the placenta of the SHRSP.

The SHRSP placenta exhibited a premature loss of glycogen cells from the placenta relative to the WKY at GD18. This can be attributed to a loss rather than

a migration as there was no significant difference in the number of PAS positive cells in the mesometrial triangle or decidua. Firstly, this could be explained by increased cell death in the placenta as assessed by caspase-3 western blotting. Notably, caspase-3 protein was measured in whole placenta homogenate (junctional zone and labyrinth) so no localisation was possible. Alternatively, the glycogen cells have been proposed to be an energy store for the placenta (372). The reduction in uteroplacental perfusion in the SHRSP may cause the placenta to utilise glycogen stores prematurely relative to the WKY. Future studies should assess strain-dependent differences in glucose metabolism in the placenta which have thus far not been reported in whether this model or in women with chronic hypertension. In addition, placental samples from earlier time points should be tested for glycogen cell content to determine when in gestation these stores are lost. A technique such as TUNEL-labelling of the sections of placenta would be able to localise whether cell death is taking place in these glycogen cells. In addition to these hypotheses, the SHRSP has been shown to have abnormal glucose metabolism relative to WKY (373); therefore the SHRSP could also be metabolising placental glycogen stores in a strain-specific way. Glycogen cells are not present in the human placenta therefore the clinical translation of these findings is not clear.

As a reduction in litter size had previously been identified at GD18 in the SHRSP relative to the WKY, the number of implantation sites was examined. There was no difference in the number of blastocyst implantation sites between strains there was, however, an increase in resorption frequency with respect to the number of dams presenting with resorptions and the percentage of the litter affected. This suggests that whilst the same number of implantations takes place in both WKY and SHRSP; more fetuses are lost sometime between GD6 and 14 in the SHRSP. An increase in resorption rate is a similar trait observed in other rodent models of hypertensive pregnancy (374, 375). In the absence of fetal growth restriction, an increase in resorption rate alone is not directly translatable to the human condition. SHRSP dams exhibit reduced weight gain during pregnancy relative to the WKY. This will be, in part, attributed to the smaller litter size in the SHRSP. In order to remove this variable, the SHRSP dam was weighed once the uterine horn had been removed at the point of sacrifice; this was also significantly reduced in the SHRSP. To explore these findings further, individual fat pads could be

excised and weighed. In disagreement with our hypothesis, there was no evidence of fetal growth restriction in the SHRSP. This is in contrast to work in the related SHR strain which showed evidence of fetal growth restriction at GD20 (376).

The findings presented in this chapter provided a better understanding of pregnancy in the SHRSP. Further work went on to identify a molecule that could be targeted for the therapeutic benefit of the deficient uterine artery remodelling and adverse pregnancy outcome in this model.

Chapter 4 Excess TNFα Signalling Plays a Central Role in Deficient Uterine Artery Function in the SHRSP

4.1 Introduction

Recent work has redefined the role of immunology in pregnancy, such that normal gestation is characterised by a dynamic regulation of the immune system. This is relative to the classical hypothesis that pregnancy was characterised by a universal shift to an anti-inflammatory state (377, 378). In this new model, the initial and final "immunological stages" of gestation refer to the first trimester and parturition respectively. During these stages, there is tightly regulated sterile inflammation (379, 380). In contrast, during the middle stage, characterised by rapid fetal development, there is an anti-inflammatory environment (378). The pro-inflammatory cytokine TNFα has vital roles in the physiology of normal pregnancy. In particular, it promotes blastocyst implantation and the remodelling of the maternal spiral arteries through stimulation of invasive extravillous trophoblasts (381). In humans, placental TNFα is increased in the second trimester in comparison to the first and third trimesters (382). The balance between normal and pathological levels of TNFα is fine and, paradoxically, excess amounts have prohibitive effects on the physiological role of TNFα (383, 384).

Activation of the immune system is linked to adverse maternal and fetal outcome in humans (377). This observation has been recapitulated in rat models using lipopolysaccharide injection to induce low-grade systemic inflammation which results in the manifestation of PE-like symptoms (385), preterm labour (386), fetal growth restriction and/or fetal loss (387, 388). In these studies, TNFα was shown to play a central role. TNFα infusion into pregnant rats results in a dose-dependent increase in blood pressure associated with an increase in vasoconstriction (389). This is similar to what is observed in non-pregnant human subjects (discussed in section 1.3.3.1) suggesting that the mechanisms by which TNF induces vascular dysfunction are broadly conserved. Increased circulating TNFα levels have been reported in women with severe hypertension during pregnancy (390-392), however, TNFα expression in the placenta is more controversial (393, 394). A single nucleotide polymorphism in the TNFα gene (G308A) in humans has also been associated with a significantly increased risk of

pre-eclampsia (395) but not in all studies (396). Furthermore, whether an increase in pro-inflammatory TNFα is a cause or effect of an abnormal vascular response to pregnancy is unknown.

A chronic increase in TNFα is a common observation in hypertension and adverse pregnancy outcome (138, 139) (discussed in section 1.3.3.1). From our earlier characterisation study (Chapter 3), we identified TNFα as a candidate molecule for abnormal pregnancy response in the SHRSP. We hypothesised that pro-inflammatory TNFα provides a link between vascular dysfunction and adverse pregnancy outcome and plays a causative role in the abnormal uterine vascular remodelling observed in our model. To investigate this hypothesis we carried out an intervention study using etanercept, a monoclonal antibody which binds and sequesters TNFα, in SHRSP.

4.2 Materials & Methods

General materials & methods can be found in Chapter 2.

4.2.1 Etanercept Treatment

Etanercept (Wyeth Pharmaceuticals, Maidenhead, UK) was prepared fresh on the day of use using sterile phosphate buffered saline (PBS) (Thermo Fisher Scientific, Paisley, UK). SHRSP were treated with 0.8 mg/kg dose or vehicle (PBS) via subcutaneous injection at gestational day 0, 6, 12 and 18. This treatment regimen was chosen as etanercept is given weekly to treat inflammatory conditions such as rheumatoid arthritis in humans. Etanercept was always given by 10am with no more than 100 µl total injected using a disposable 1ml syringe and 26 G x ½" needle (BD Bioscience, Oxford, UK) given to the back of the neck. Animals were either subject to radiotelemetry implantation and allowed to progress to parturition or sacrificed at gestational day (GD) 18 for myography.

4.2.2 Radiotelemetry Probe Implantation

Systolic (SBP) and diastolic blood pressure (DBP), heart rate and activity were directly monitored using the Dataquest V telemetry system (Data Sciences International). Prior to implantation, the radiotelemetry transmitter was calibrated to be accurate within ± 6 mmHg. For reuse, radiotelemetry probes were

sterilised in Terg-A-Zyme (Alconox Inc) for 24 hours. Radiotelemetry implantation was performed at 10 weeks of age when the animals were of a sufficient bodyweight to undergo the surgery. Radiotelemetry implantation was carried out as described previously by our group (397) and detailed in section 2.3.3. The data represented has been analysed to show a daily average from the daytime and nighttime values.

4.2.3 Doppler Ultrasound

Doppler waveform recordings were used to assess uterine artery blood flow. Rats were lightly anaesthetized throughout the procedure at approximately 1.5 % isoflurane in oxygen. Hair on the abdomen was removed by shaving. Ultrasound gel was applied to exposed skin as an ultrasound coupling medium. Rats were imaged trans-abdominally using an Acuson Sequoia c256 imager fitted with a 15 MHz linear array transducer (Siemens). An example of where measurements were taken from the uterine artery is shown in Figure 4-1. Peak systolic velocity (PSV) and end diastolic velocity (EDV) was measured from 6 consecutive cardiac cycles. Resistance index (RI) was calculated as *(RI = [PSV- EDV]/PSV)*.

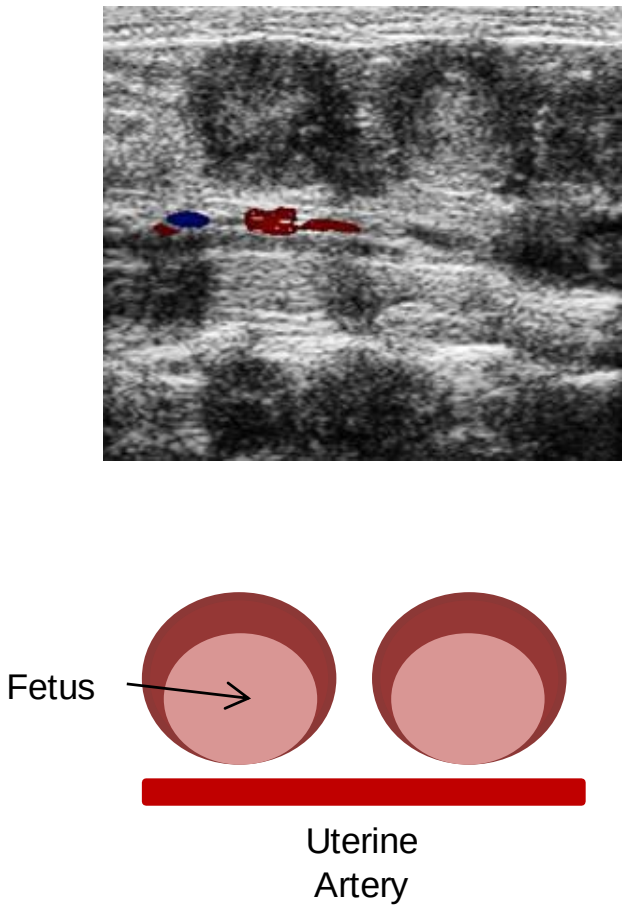

Figure 4-1: Representative ultrasound image of the uterine artery used for Doppler measurements.

4.2.4 Placental Tissue Explants

Placental tissue was harvested in ice cold PBS from WKY and SHRSP. Under sterile conditions, the tissue was dissected into pieces <5mm in ice cold DMEM F-12 Media +0.5% FBS +1% penicillin/streptomycin (Thermo Fisher Scientific, Paisley, UK). The tissue pieces were split evenly between 2 wells of a 24 well plate (Thermo Fisher Scientific, Paisley, UK) in 1ml of media. After 1 hour, the explants were washed in PBS and replaced with 1ml of fresh media. Explants were incubated for 20 hours at 37 °C, after which the media was collected, aliquoted and stored at -80 °C until use.

4.2.5 TNFα Measurement in Plasma, Urine and Explant Media using Enzyme Linked Immunosorbent Assay (ELISA)

TNFα in plasma, urine and explant was measured using a commercially available kit (RTA00) (R&D Systems, Abingdon, UK) according to manufacturer's instructions. Kits were controlled using a positive control provided by the manufacturer and a negative control where dH_2O was used instead of sample. The method used a 7-point standard curve consisting of 1-in-2 serial dilution steps from the top standard where TNFα concentration was 800 pg/ml down to a bottom standard with concentration of 12.5 pg/ml. The limits of detection for this kit are < 5pg/ml and plasma samples are expected to fall below the lowest standard of 12.5 pg/ml. All results shown in this Chapter were from one plate therefore there it was not necessary to calculate inter-assay variation.

4.2.6 Pressure Myography

Pressure myography was used to construct pressure-diameter relationships to assess uterine artery structure under isobaric conditions. Vessels for pressure myography were mounted in calcium free PSS (0.25 M NaCl, 0.001 M KCl, 2 mM $MgSO_4$, 50 mM $NaHCO_3$, 2 mM KH_2PO_4, 1 mM glucose). The pressure myograph system (Danish Myo Technology, Aarhus, Denmark) was set up and equilibrated according to manufacturer's instructions. Arteries were tied to two glass cannulas using nylon thread. Any side branches of the artery were also tied closed with nylon thread. The myography had two in-line pressure transducers which continually measured inflow and outflow pressure which was altered by adjusting the height of reservoirs of calcium free PSS. Vessels were maintained at 37 ºC and

95 % O_2 and 5 % CO_2 throughout the experiment. After equilibration at 70 mmHg for one hour, the vessels were subject to increasing intraluminal pressure: 10, 20, 40, 60, 80, 100 and 110 mmHg. Measurements of internal and external diameter were taken after five minutes at each pressure. Wall thickness was calculated as *[(external diameter - internal diameter) / 2]*. Cross sectional area was calculated as *[(π/4) x (external diameter² - internal diameter²)]*.

4.2.7 Wire Myography

Wire myography was used to assess mesenteric and uterine artery function under isometric conditions. Uterine artery rings were mounted in PSS (0.25 M NaCl, 0.001 M KCl, 2 mM $MgSO_4$, 50 mM $NaHCO_3$, 2 mM KH_2PO_4, 1 mM glucose, 2.5 mM $CaCl_2$). Uterine artery rings (4.8 – 5.2 μm in length) were mounted on two stainless steel wires on a four channel small vessel myograph (AD Instruments, Oxford, UK). Changes in contraction and relaxation were detected by a force-sensitive transducer connected to a laptop running LabChart 8 (AD Instruments, Oxford, UK). Vessels were maintained at 37 ºC and 95 % O_2 and 5 % CO_2 throughout the experiment. Vessels were normalized and subject to a wake up procedure as previously described (398). To establish the vessel's contractile response curve, noradrenaline (Sigma-Aldrich, Dorset, UK) was added at the following increasing concentrations: $1x10^{-9}$, $1x10^{-8}$, $1x10^{-7}$, $1x10^{-6}$, $1x10^{-5}$ and $3x10^{-5}$ M. To determine the vessel's endothelium-dependent relaxation response, vessels were pre-constricted with $1x10^{-5}$ M noradrenaline followed by the addition of carbachol (Sigma-Aldrich, Dorset, UK) at the following increasing concentrations: $1x10^{-8}$, $1x10^{-7}$, $1x10^{-6}$, $1x10^{-5}$ and $1x10^{-5}$ M. Active effective pressure (P) in kPa was calculated by *P = (active wall tension/[normalised lumen diameter/2])*. Percentage relaxation was calculated *[(active effective pressure at relevant carbachol dose / noradrenaline $1x10^{-5}$ response) x 100]*.

4.2.8 Periodic acid-Schiff Stain

Periodic acid – Schiff stain was used to quantify glycogen cell content in the placenta. Slides were cleared and rehydrated as described in section 2.6.1. Slides were incubated in 1% periodic acid (Sigma-Aldrich, Dorset, UK) in dH_2O for 10 minutes to oxidise aldehyde groups followed by 1 minute wash under running tap water. Slides were then stained with Schiff's reagent (Sigma-Aldrich, Dorset, UK)

for 10 minutes which reacts with the oxidised aldehyde groups to form a magenta dye. This was followed by a 1 minute wash under running tap water and dehydration through an ethanol gradient (70%, 90%, 100%; 5 minutes each). Slides were cleared in histoclear 2 x 5 minutes and mounted using DPX (Sigma-Aldrich, Dorset, UK). Slides were viewed using light microscopy and analysed using threshold quantification in ImageJ (National Institutes of Health, Bethesda, USA) as described in section 2.6.4.

4.2.9 Quantitative PCR (qPCR) for *Tnfr1* Expression

Gene expression for Tnfr1 was carried out using the following probes from Thermo Fisher, Paisley, UK: *Tnfr1* (Rn01511602_m1) and *Actb* (4352340E).

4.2.10 Western Blot for Phosphorylated NFκB

Western blot was carried out as described in section 2.5. Membranes were incubated in the following primary antibodies diluted in 5% bovine serum albumin (BSA) (Sigma-Aldrich, Dorset, UK) in TBS-T overnight at 4 ºC: phospho-NFκB (Ser536) #3033 1:1000 (Cell Signalling Technology, Leiden, Netherlands), total NFκB #8242 1:1000 (Cell Signalling Technology, Leiden, Netherlands) and GAPDH #ab8245 1:5000 (Abcam, Cambridge, UK). Phospho-NFκB and total NFκB were detected using horse radish peroxidase (HRP) conjugated swine-α-rabbit secondary antibody (Dako, Ely, UK) diluted 1:10000 in 5% BSA/TBS-T. GAPDH was detected using HRP conjugated rabbit-α-mouse secondary antibody (Dako, Ely, UK).

4.3 Results

4.3.1 Tumor Necrosis Factor α (TNFα) is a Promising Target Molecule in Pregnant SHRSP

TNFα was increased in pregnant (GD18) SHRSP plasma and urine relative to the pregnant WKY (Fig. 4-2A-B). In addition, increased secretion of TNFα was detected in media taken from placental tissue explants from GD18 SHRSP (Fig. 4-2C). Gene expression of the main pro-inflammatory TNFα receptor-1 (Tnfr1), was also significantly increased in the GD18 uteroplacental unit from SHRSP relative to WKY (Fig. 4-2D).

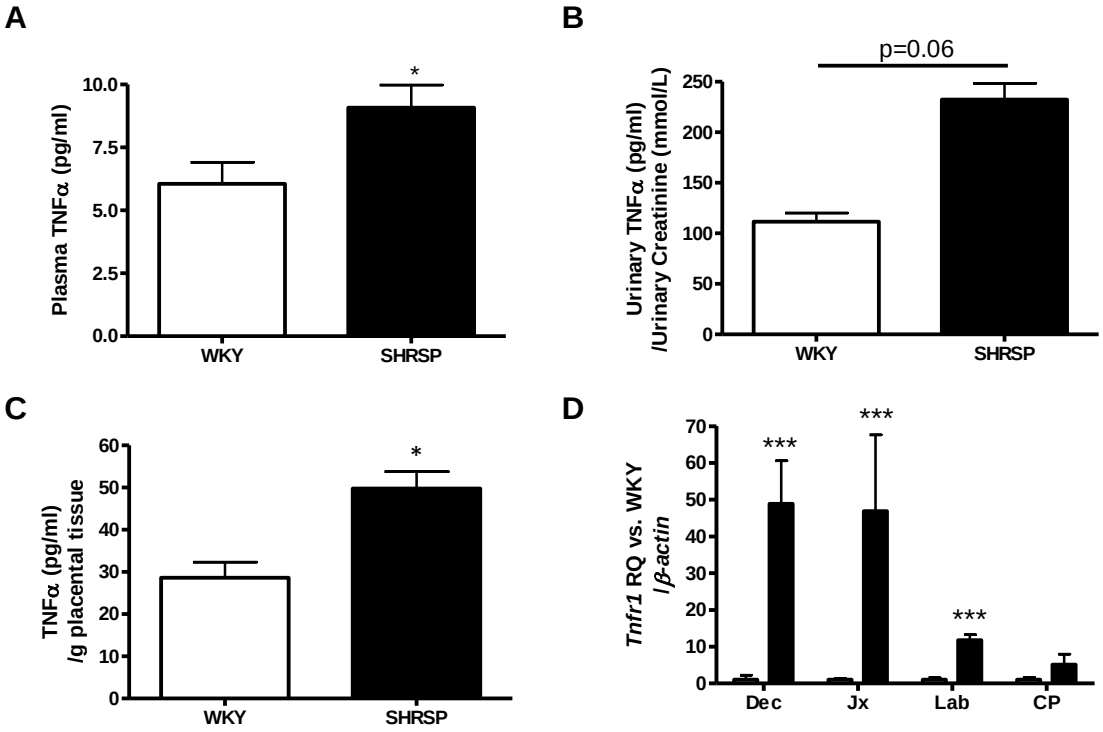

Figure 4-2 TNFα is increased in the SHRSP relative to the WKY.

TNFα was measured in plasma (A) and urine (B) using ELISA where pregnant (GD18) SHRSP (n=6) showed elevated levels relative to the GD18 WKY (n=6) (* $p<0.05$ vs. GD18 WKY analysed by Student's t-test). Secretion of TNFα (C) was increased from placental explants taken from GD18 SHRSP (n=5) relative to WKY (n=5) (* $p<0.05$ vs. GD18 WKY analysed by Student's t-test). Placentae from pregnant (GD18) SHRSP and WKY (n=8) were dissected into the main layers of the placental unit: decidua (Dx), junctional zone (Jx), labyrinth zone (Lx) and chorionic plate (CP). Gene expression of TNFα receptor-1 (Tnfr1) (D) was significantly increased in the SHRSP (n=6) relative to the WKY (n=6) uteroplacental unit at GD18 (** $p<0.01$, *** $p<0.005$ vs. WKY GD18 WKY analysed by Student's t-test).

4.3.2 Etanercept Reduces Systolic Blood Pressure in the SHRSP

Treatment with etanercept (0.8 mg/kg s.c.) was given at gestational day (GD) 0 of pregnancy and repeated at GD6, 12 and 18. The effect of etanercept treatment on blood pressure in the SHRSP relative to vehicle treated controls was monitored using radiotelemetry. SHRSP are hypertensive before and during pregnancy in contrast to the normotensive WKY strain (Fig. 4-3A-B). Etanercept treatment had no effect on SHRSP blood pressure in early pregnancy (GD0-12). After the dose administered at GD12, there was a significant ($p<0.05$) average decrease of 11.5 ± 2.1 mmHg in systolic blood pressure (SBP) from GD12-21 in SHRSP treated with etanercept relative to vehicle treated SHRSP (Fig. 4-3A). No significant difference in diastolic blood pressure (DBP) was observed between SHRSP and etanercept treated SHRSP (112.4 ± 1.2 mmHg vs. 108.5 ± 2.6 mmHg; $p=0.13$) (Fig. 4-3B). Relative to their pre-pregnancy blood pressure, etanercept treated SHRSP exhibited broadly the same pattern as vehicle treated SHRSP, notably there was no early decrease in systolic or diastolic blood pressure which is observed in the WKY (Fig. 4-3C-D). Activity was significantly decreased in both SHRSP and SHRSP treated with etanercept relative to the WKY over the course of pregnancy (Fig. 4-3E). Heart rate was not significantly different between groups (Fig. 4-3F).

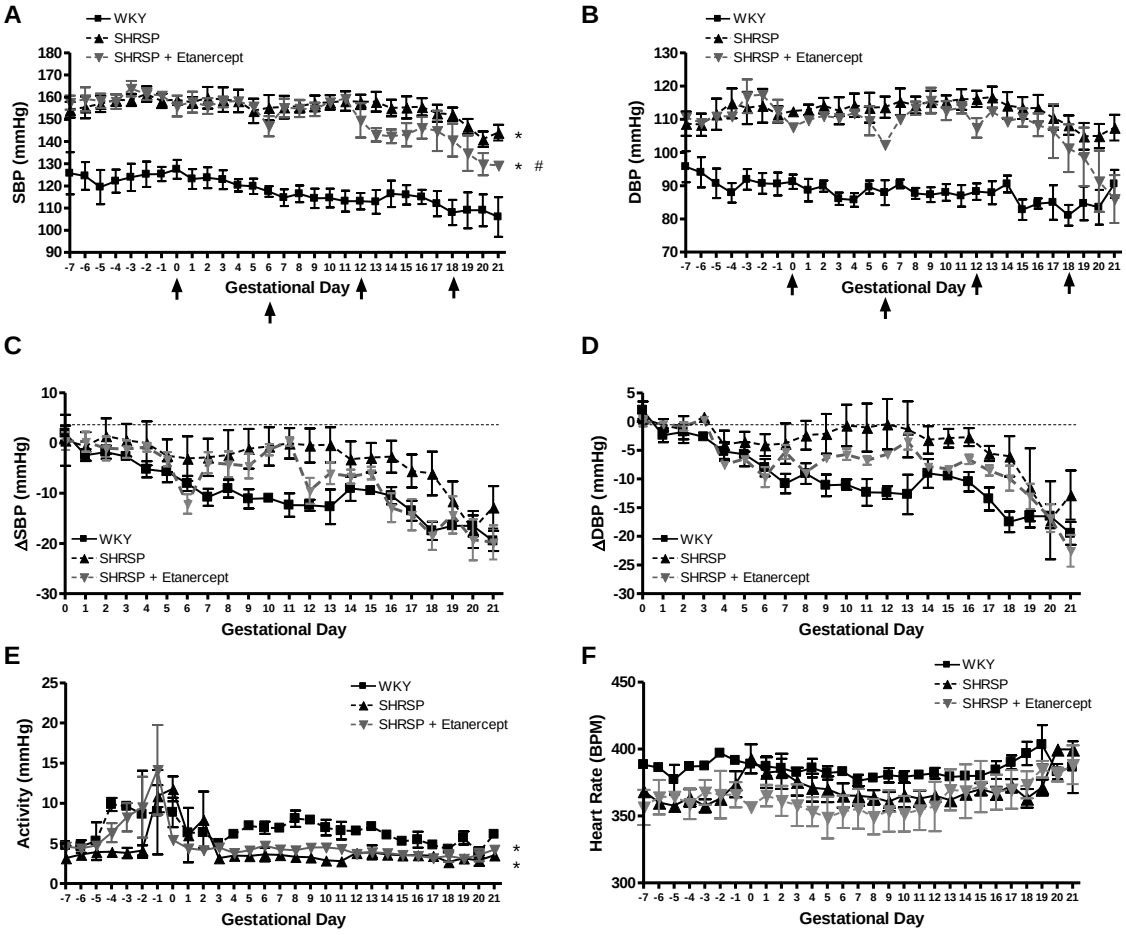

Figure 4-3: Etanercept treatment significantly reduces systolic blood pressure from GD 12-21 of pregnancy in the SHRSP.

Systolic blood pressure (SBP) (A) and diastolic blood pressure (DBP) (B) were monitored using radiotelemetry in untreated WKY (n=6), vehicle treated SHRSP (n=4) and etanercept treated SHRSP (n=6) from 7 days before pregnancy (GD-7 to -1) and during pregnancy (GD0 – 21). SHRSP were treated with etanercept (0.8 mg/kg s.c.) at GD 0, 6, 12 and 18. SHRSP and SHRSP treated with etanercept had significantly increased SBP and DBP relative to the WKY from GD-7 to GD21 (A-B) (* $p<0.05$ vs. WKY analysed by two-way ANOVA). Etanercept treated SHRSP had a significant decrease in SBP (A) from GD12-21 relative to vehicle treated SHRSP (# $p<0.05$ vs. SHRSP analysed by ΔSBP [SHRSP-ETN SHRSP] GD12-21 followed by a Student's t-test). The difference in blood pressure relative to non-pregnant values shows that etanercept treatment does not restore the early decrease in SBP (C) and DBP (D) seen in WKY. Activity (E) was significantly decreased in both SHRSP and SHRSP treated with etanercept relative to the WKY (* $p<0.05$ vs. WKY analysed by two-way ANOVA). Heart rate (F) was not significantly changed between the groups. Data points represent daily averages. Arrows in panels A and B represent days of treatment with etanercept.

4.3.3 Etanercept Improves Placenta and Litter Size in the SHRSP

Placental glycogen cell content was assessed using PAS stain at GD18. Glycogen storage in the placenta of SHRSP was reduced relative to the WKY (Fig. 4-4A-B). Etanercept treatment in the SHRSP restored PAS positive glycogen cells within the junctional zone of the placenta (Fig. 4-4A-B). Furthermore, litter size was significantly increased by etanercept treatment in SHRSP (Fig. 4-4C). There was no difference in fetal or placental weight between any of the groups (Fig 4-5). Concurrently, the number of dams which presented with 1 or more resorptions was decreased in SHRSP treated with etanercept (Table 4-1).

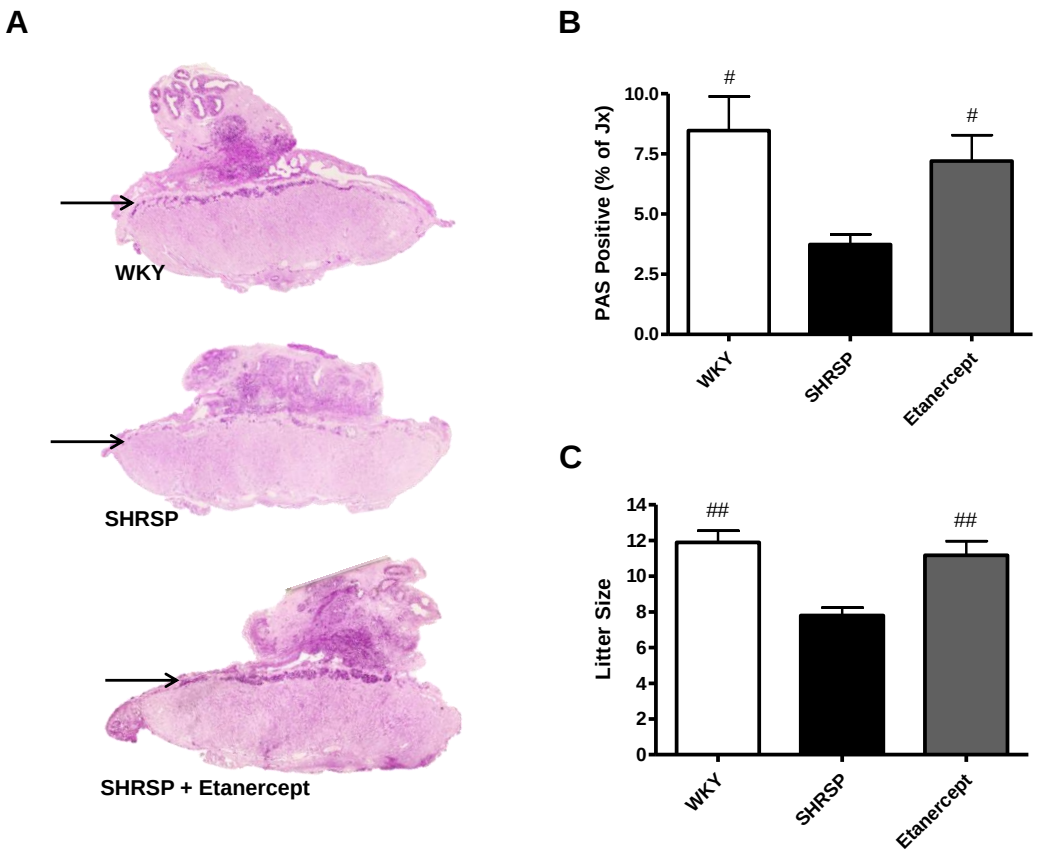

Figure 4-4: Etanercept treatment significantly improves glycogen cell loss from the placenta and litter size in the SHRSP.

Glycogen cell content in the junctional zone (Jx) of the placenta was assessed by counting the number of PAS positive cells in untreated WKY (n=6), vehicle treated SHRSP (n=6) and etanercept treated SHRSP (n=6). A representative uteroplacental unit for each group is shown in (A) and quantified in (B) (## $p<0.01$ vs. SHRSP analysed by one-way ANOVA followed by a post-hoc Tukey's test). Litter size was counted at GD18 in untreated WKY (n=12), vehicle treated SHRSP (n=6) and etanercept treated SHRSP (n=6) where etanercept treated SHRSP and WKY had a significantly increased litter size relative to the SHRSP (C) (## $p<0.01$vs.SHRSP analysed by one-way ANOVA followed by a post-hoc Tukey's test).

Table 4-1 Etanercept reduces the frequency of SHRSP with spontaneous pregnancy loss.

	% Animals with Spontaneous Resorption
WKY	30
SHRSP	66.7
SHRSP + Etanercept	25

The percentage of animals with spontaneous pregnancy loss was calculated as (number of animals with 1 or more resorption/total number of animals) x 100 in untreated WKY (n=12), vehicle treated SHRSP (n=6) and etanercept treated SHRSP (n=6).

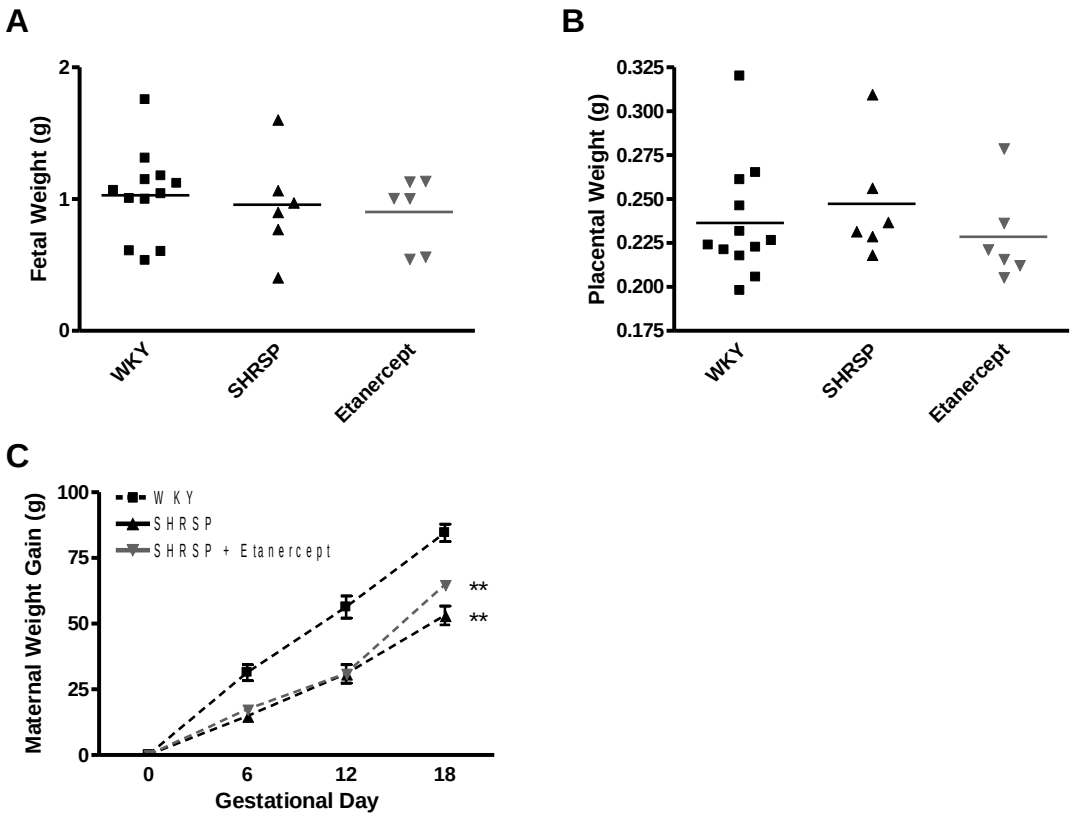

Figure 4-5: Maternal, fetal and placental weight are unaffected by etanercept treatment in the SHRSP.

Fetal (A) and placental (B) weight did not show any significant differences between untreated WKY (n=12), vehicle treated SHRSP (n=6) and etanercept treated SHRSP at GD18 (n= 6). Maternal weight gain (B) during pregnancy was significantly decreased in both SHRSP and SHRSP treated with etanercept relative to WKY (** $p<0.01$ vs. WKY analysed by area under the curve followed by one-way ANOVA).

4.3.4 Etanercept Improves Uterine Artery Function in Pregnant SHRSP

Pressure myography was used to assess uterine artery (average diameter approximately 400 μm) properties from pregnant (GD18) WKY, SHRSP and SHRSP treated with etanercept. Etanercept treatment did not significantly alter the diameter or wall thickness of the uterine arteries from pregnant SHRSP (Fig. 4-6A-D). Investigation of uterine artery vasomotor function using wire myography showed that uterine arteries from pregnant SHRSP had a significantly increased contractile response to noradrenaline (Fig. 4-6E) and a blunted endothelium-dependent vasorelaxation (Fig. 4-6F) relative to the WKY (28). In contrast, uterine arteries from pregnant SHRSP treated with etanercept exhibited a marked reduction in contractile response which was not significantly different from the normotensive WKY (Fig. 4-6E) and a significant increase in the vasorelaxation response to carbachol (Fig. 4-6E). In contrast to the uterine arteries, etanercept did not improve the function of SHRSP third-order mesenteric arteries (average diameter approximately 270 μm) (Fig. 4-7A-B).

These improvements in uterine artery vasomotor function translated into an increase in uterine artery blood flow assessed by Doppler ultrasound. Etanercept treatment partially restored the physiological increase in diastolic volume over the course of pregnancy which is present in the WKY but absent in the SHRSP (Fig. 4-8A). This resulted in a significantly reduced uterine artery resistance index in etanercept treated SHRSP relative to control SHRSP (Fig. 4-8B).

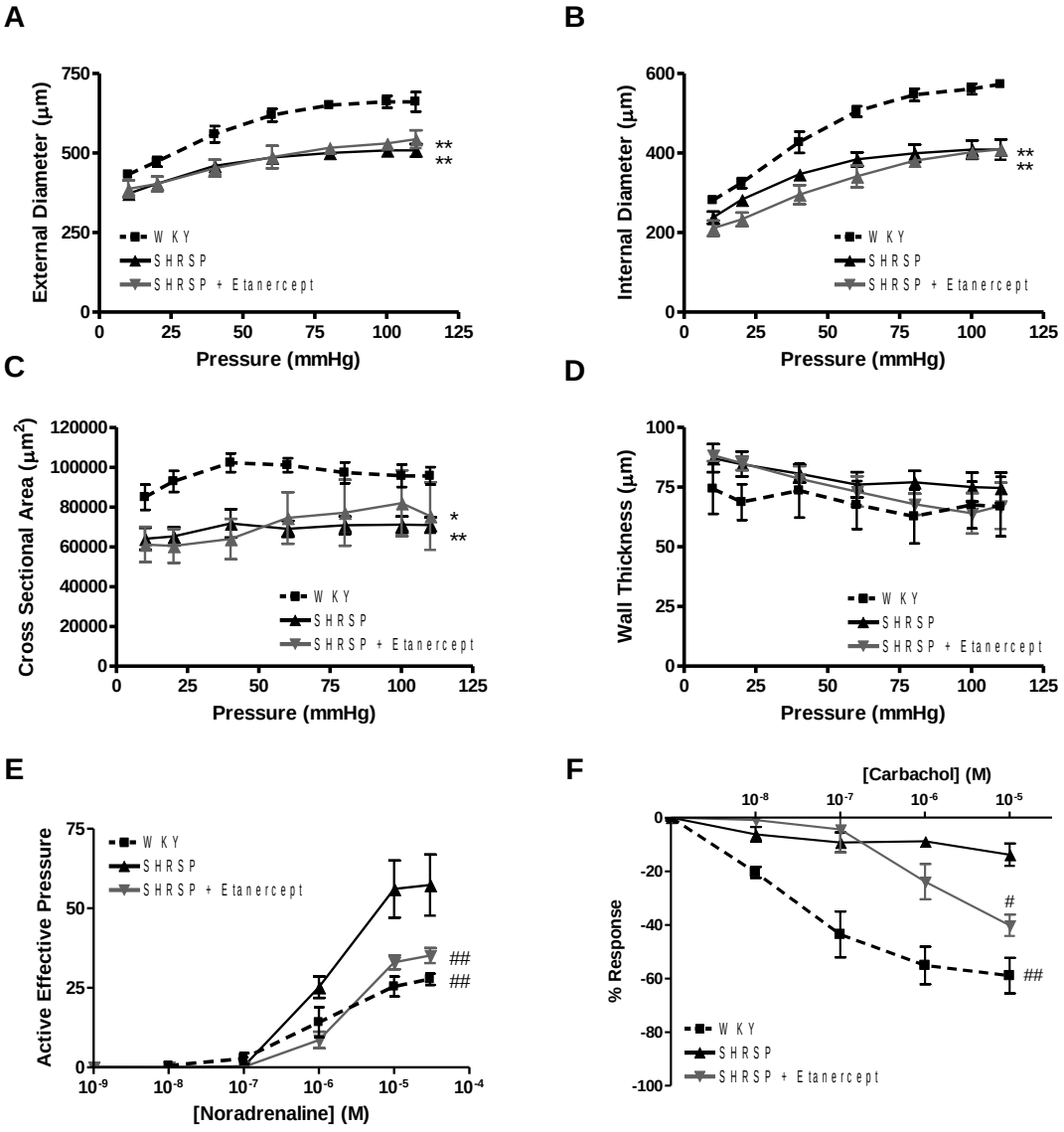

Figure 4-6 Etanercept treatment improves uterine artery function in pregnant SHRSP but not structure.

Isolated uterine artery structure was assessed using pressure myography to measure external (A) and internal (B) diameter, cross-sectional area (C) and wall thickness (D) in untreated WKY (n=6), vehicle treated SHRSP (n=6) and etanercept treated SHRSP (n=6) at GD18 of pregnancy. External and internal diameter as well as cross-sectional area was significantly decreased in both vehicle treated and etanercept treated SHRSP (* $p<0.05$ vs. WKY; ** $p<0.01$ vs. WKY analysed by area under the curve followed by one-way ANOVA and post-hoc Tukey's test). Isolated uterine artery function was assessed using wire myography in untreated WKY (n=6), vehicle treated SHRSP (n=6) and etanercept treated SHRSP (n=6) at GD18 of pregnancy. Uterine arteries from vehicle treated SHRSP (GD18) had a significantly increased contractile response to noradrenaline (NA) (E) and significantly decreased relaxation response to carbachol (F) relative to uterine arteries from GD18 WKY (## $p<0.01$ vs. SHRSP analysed by calculating area under the curve followed by one-way ANOVA). Uterine arteries from etanercept treated SHRSP had a significantly reduced contractile response to NA (E) relative to SHRSP (## $p<0.01$ vs. SHRSP analysed by calculating area under the curve followed by one-way ANOVA) and a significantly increased relaxation response to carbachol (F) at 1×10^{-5} M (# $p<0.05$ vs. SHRSP analysed by a Student's t-test).

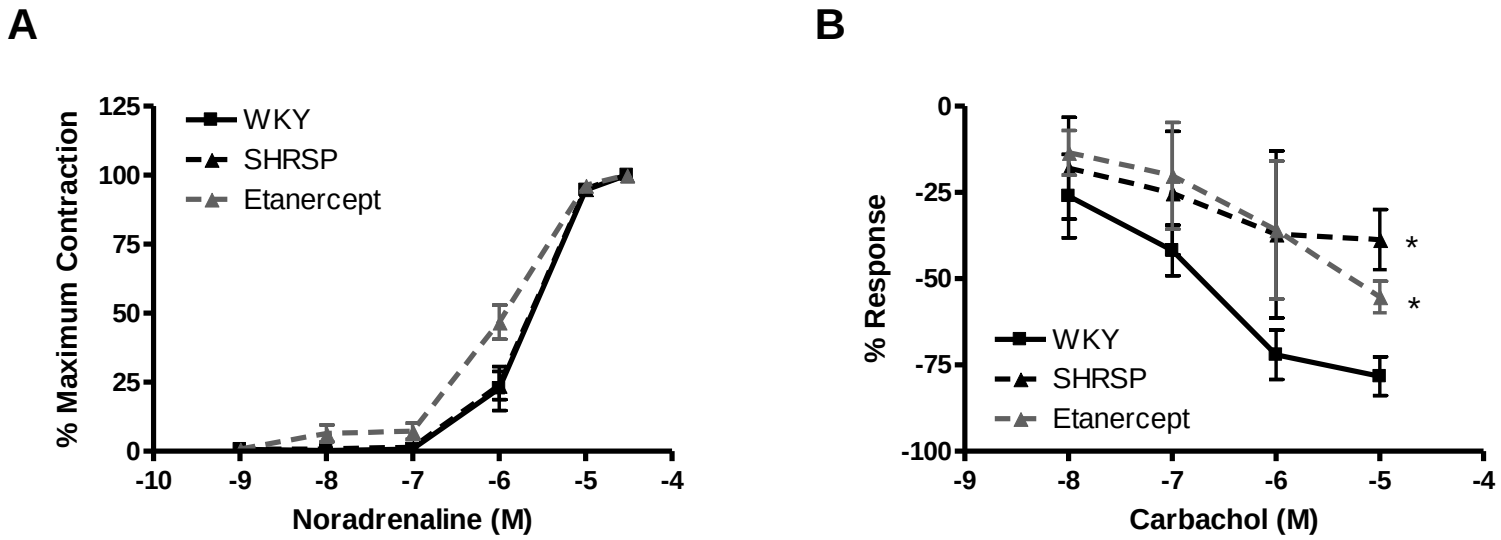

Figure 4-7 Etanercept treatment does not alter third-order mesenteric artery function in the SHRSP.

Isolated third-order mesenteric artery function was assessed using wire myography in WKY (n=4), SHRSP (n=6) and SHRSP treated with etanercept (n=6) at GD18 of pregnancy. There was a trend for etanercept to shift the contractile response to noradrenaline (A). Etanercept treatment did not significantly improve endothelium dependent vasorelaxation to carbachol (* $p<0.05$ vs. GD18 WKY analysed by calculating area under the curve followed by one-way ANOVA and post-hoc Tukey test) (B).

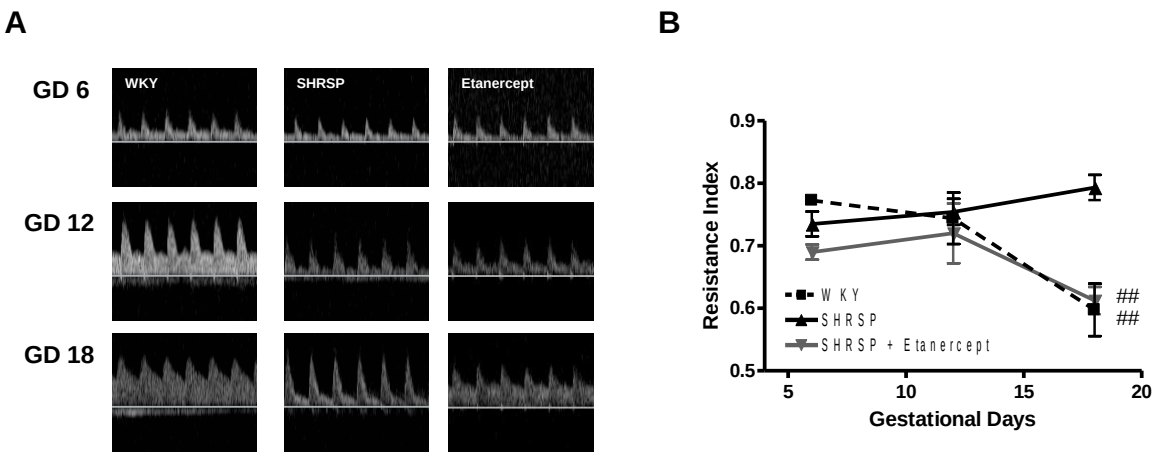

Figure 4-8 Etanercept treatment improves uterine artery blood flow in pregnant SHRSP.

Uterine artery blood flow was assessed using Doppler ultrasound in untreated WKY (n=6), vehicle treated SHRSP (n=6) and etanercept treated SHRSP (n=6) at GD6, 12 and 18. Representative Doppler traces are shown in (A). The pregnancy-induced increase in diastolic blood flow which is present in the WKY but not in SHRSP is partially restored in SHRSP treated with etanercept (A) resulting in a significant reduction in resistance index at GD18 (B) (## $p<0.01$ vs. SHRSP analysed by one-way ANOVA followed by a post-hoc Tukey's test).

4.3.5 Etanercept Affects the TNFα Pathway in the Placenta

In order to determine whether etanercept treatment had an effect on the TNFα signalling pathway in the placenta, we studied a subset of TNFα signalling components (Fig. 4-9A). The transcription factor NFκB which is phosphorylated as a result of TNFR1 activation was down-regulated in the placenta of SHRSP treated with etanercept relative to both the WKY and SHRSP (Fig. 4-9B). The expression of the protease, ADAM17, which produces soluble TNFα from the transmembrane form was also significantly decreased in the uteroplacental unit from etanercept treated SHRSP relative to both the WKY and SHRSP (Fig. 4-9C). The release of soluble TNFα from placental explants cultured for 20 hours was significantly increased in both the SHRSP and SHRSP treated with etanercept relative to the WKY (Fig. 4-9D).

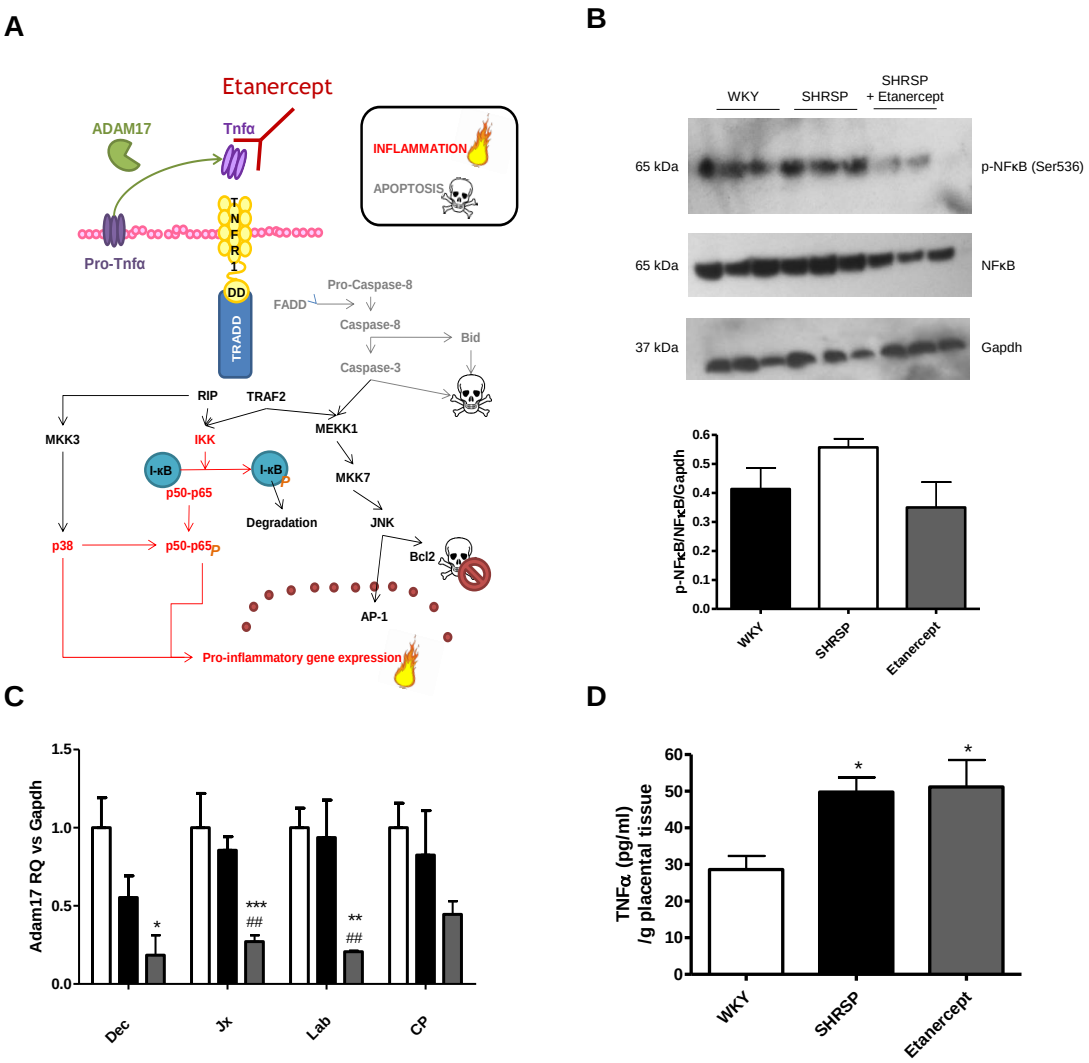

Figure 4-9 Etanercept Treatment Alters the TNFα signalling pathway in the Placenta.

(A) Etanercept inhibits TNFα signalling by binding and sequestering the molecule. The activation of downstream NFκB shows a trend to be decreased in SHRSP treated with etanercept (n=3) relative to WKY (n=3) and vehicle-treated SHRSP (n=3) (B). Gene expression of *Adam17* was significantly decreased in SHRSP treated with etanercept relative to SHRSP and WKY (n=6) (C) (* p<0.05, ** p<0.01, *** p<0.005 vs. WKY GD18, ## p<0.01 vs. SHRSP GD18 analysed by one-way ANOVA followed by a post-hoc Tukey's test) Dec = decidua, JX = junctional zone, Lab = labyrinth, CP = chorionic plate. TNFα release from placental explants was measured using ELISA after 20 hours where it was significantly increased in both the SHRSP and SHRSP treated with etanercept relative to the WKY (n=4-6) (D) (* p<0.05 vs. WKY GD18 analysed by one-way ANOVA followed by a post-hoc Tukey's test).

4.4 Discussion

The work presented in this Chapter demonstrates that etanercept treatment has beneficial effects on the placenta and litter size of the SHRSP, which was associated with an improvement in uterine artery function and uteroplacental blood flow.

Etanercept has been shown to reduce blood pressure in a rat model of pre-eclampsia (343, 399), insulin resistance (400) and lupus (401). In contrast, it had no effect on blood pressure in non-pregnant hypertensive rats (402). These differing results suggest that etanercept has context-dependent effects on blood pressure; this may be related to the extent or localisation of inflammation present in each condition. Etanercept treatment reduced SBP but not DBP; this suggests that there should be a decrease in peripheral resistance in etanercept treated SHRSP. However, the wire myography data from the third order mesenteric arteries shows that etanercept treatment does not improve the function of these vessels. Further functional investigations should be carried out in resistance vessels, as well as determination of the collagen content of these vessels. The average SBP reduction of 11.5 mmHg in the pregnant SHRSP in this study is comparable to the reduction seen in other work using pregnant hypertensive rats (343, 399). Notably, the decrease in SBP is not present in the SHRSP until after GD12. This coincides with the development of the rat placenta from GD10-12 where the five distinctive layers which define the mature uteroplacental unit are present (246). This suggests that the placenta may be the source of excess TNF-α which contributes specifically to blood pressure regulation in late pregnancy. This significant reduction in SBP in late pregnancy has no negative impact on fetal growth as no significant difference in fetal weight was observed between vehicle and etanercept treated SHRSP. In fact, pregnancy outcome is improved in SHRSP treated with etanercept where there is a significant increase in litter size and a decrease in dams presenting with resorptions at GD18. Etanercept treatment has been previously shown to reduce spontaneous pregnancy loss in a model of abnormal maternal inflammation during pregnancy (388).

Etanercept does not have an effect on the structure of the uterine arteries from pregnant SHRSP. Therefore, from these findings, we propose that TNFα does not play a central role in activating the mechanisms involved in the outward

hypertrophic remodelling of the uterine arteries that is associated with pregnancy. However, etanercept treatment does improve the endothelium-dependent vasorelaxation in uterine arteries from pregnant SHRSP. TNFα has a well-defined role in endothelial dysfunction by diminishing the bioavailability of vasodilator nitric oxide through down-regulation of the expression of the eNOS pathway (35, 36) and through increased superoxide production (37). In this study, L-NAME was not used to investigate the specific contribution of nitric oxide to the carbachol-mediated relaxation in these vessels. Therefore, the impaired vasorelaxation could be due to a lack of bioavailable nitric oxide or differences in the muscarinic receptor itself. Etanercept also significantly reduces the uterine artery vasocontractile response to noradrenaline in our model. The role of TNFα as an active mediator of contractile ability of vascular smooth muscle cells is less well defined. TNFα can induce the production of vasoconstrictor endothelin-1 (38) and can alter calcium handling (39). In the context of the myography experiment presented here, etanercept may have a role in down-regulation or desensitisation of contractile adrenoreceptors in order to blunt response to noradrenaline. In another vascular function study using resistance vessels from ovarectomized female rats where systemic TNFα is elevated; etanercept treatment reduces contractility and improves endothelium dependent vasorelaxation (40). In keeping with the improvement in uterine artery function in the SHRSP, uteroplacental blood flow is partially restored with etanercept treatment. In this study, intra- and inter-observer variability for uterine artery doppler was not calculated; this should be taken into account in future studies to ensure that the changes observed in blood flow are solely attributed to treatment. Correction of deficient uteroplacental blood flow during pregnancy using a TNFα antagonist has not previously been shown in the literature. However, plasma TNFα has been shown to have a positive correlation with abnormal uterine artery resistance index and the presence of notching in humans (35). We have previously hypothesised that deficient uteroplacental perfusion in SHRSP leads to the premature utilization of glycogen stores in the placenta. In agreement, improvement of uteroplacental blood flow in etanercept treated SHRSP restores the presence of placental glycogen cells at GD18.

Small amounts of etanercept have been shown to cross the placental barrier in humans; a ratio of between 14:1 and 30:1 (maternal serum: cord blood) has been

reported in the literature (403, 404). Therefore, etanercept may reach the rat placenta and have effects on the TNFα signalling pathway. In the placenta of SHRSP, etanercept treatment did have an effect on the TNFα pathway. Etanercept treatment inhibited phosphorylation of downstream NFκB in the placenta of SHRSP. ADAM17 has been shown to be the major producer of soluble TNFα in human placental trophoblasts (405). In placental tissue from etanercept treated SHRSP, *Adam17* was significantly down-regulated relative to vehicle treated SHRSP and WKY. However, soluble TNFα released from the placenta was still increased in SHRSP treated with etanercept and vehicle treated SHRSP. It could be that the increase in soluble TNFα in etanercept treated SHRSP may act as a negative feedback mechanism which turns off ADAM17 expression. However, why this system is not present in the vehicle treated SHRSP where an increase in soluble TNFα from the placenta is similar to etanercept treated animals cannot be explained by this data. With respect to strain-specific differences between the SHRSP and WKY, there is a trend for an increase in the phosphorylation of NFκB which could be indicative of an increase in TNFR1 signalling in the placenta. Whilst there is an increase in soluble TNFα in the SHRSP relative to the WKY, there is no significant difference in ADAM17 expression. This suggests that it could be that ADAM17 is more active in SHRSP than WKY despite similar levels in the placenta.

Currently, etanercept has not been utilised in a clinical study for the treatment of hypertensive pregnancy. Evidence of a therapeutic effect comes predominantly from studies in the RUPP rat model of pre-eclampsia where it has been shown to: reduce mean arterial blood pressure by approximately 16 mmHg (343), reduce cardiac hypertrophy and improve NO bioavailability (399), reduce cerebral oedema (406) and reduce the release of anti-angiogenic sFLT-1 from the placenta (407). Etanercept also improved abnormal placentation in a mouse model of hypertensive pregnancy (408). Etanercept has been used during pregnancy in women with inflammatory bowel disease and rheumatoid arthritis where small studies have reported no adverse pregnancy outcomes; reviewed in (409). It has also been used in pilot studies as a treatment for women with recurrent spontaneous miscarriage where it has been shown to have a promising therapeutic benefit and reduce the number of peripheral pro-inflammatory NK cells (410, 411). Therefore, etanercept has been classified FDA class B for use in pregnancy. More convincing evidence of the safety of anti-TNFα therapy in pregnancy will

come from the ongoing OTIS (Organisation of Teratology Information Specialists) Autoimmune Diseases in Pregnancy Project (NCT01086059) expected to report in early 2017. This is a large prospective study enrolling women with autoimmune diseases who have been treated with anti-TNFα therapy, encompassing separate arms for a number of TNFα antagonists including etanercept, during the first trimester of pregnancy and followed up to 1 year postpartum. These women will be matched to a non-treated control population with a similar autoimmune disease (412).

These findings shown in this Chapter indicated that excess TNFα from an unidentified source in the SHRSP plays a central role in abnormal uterine artery function and pregnancy outcome in this model. Following on from this, the next set of experiments set out to identify the source of excess TNFα in the SHRSP.

Chapter 5 The Role of Natural Killer Cells in SHRSP Pregnancy

5.1 Introduction

The immune system is dynamic over the course of gestation (413) and whilst the maternal-fetal interface is a major area of maternal immune cell regulation during pregnancy; changes also occur in the circulating leukocytes. Pregnancy is associated with a modest leukocytosis (414). This is likely to be influenced by placenta derived factors such as growth factors, cytokines or hormones or particles derived from placental shedding such as syncytiotrophoblast vesicles or fetal and placental cell-free DNA which are detecTable in the maternal circulation (415). Changes in the immune system during pregnancy principally occur in cells of the innate immune system whereas the adaptive immune system is relatively suppressed (416). The hypothesised up-regulation of cells with immunosuppressive function such as regulatory T cells (Tregs) during pregnancy has produced a number of conflicting results with some studies showing an increase (417), no change (418) or even a decrease (419). Pregnancy is associated with an increase in number and activation of circulating monocytes and granulocytes (420). However, not all cellular components of the innate immune system are activated. Notably, the activity of dendritic cells (421) and NK cells (422) are suppressed during pregnancy.

The study of NK cells in pregnancy has principally focussed on the uterine specific population of these cells (uNK) which play an important role in remodelling the uterine spiral arteries (discussed in section 1.6.2.1) (423). Changes in peripheral NK cells do not directly mirror the status of uNK cells; therefore the two populations should be considered separately (424). For the purposes of this work, the focus will be on circulating (peripheral) NK cells in pregnancy. In humans, circulating NK cell numbers are increased relative to non-pregnant women in the first trimester followed by a decline in late pregnancy. The cytotoxicity of NK cells follows this pattern (425). A similar temporal study of NK cell number over pregnancy has not yet been reported in rats. Alterations in peripheral NK cells have mostly been associated with recurrent pregnancy loss and infertility however these findings are based on relatively small, observational

studies (424). Other small studies have also explored a pro-inflammatory shift of NK cells in pre-eclampsia (PE) (426).

It was identified that excess TNFα played a causative role in abnormal uterine artery function and adverse pregnancy outcome in the SHRSP from the intervention study using etanercept (Chapter 4). It was hypothesised that the excess TNFα was due to an activation of the maternal immune system in the pregnant (GD18) SHRSP relative to the WKY. To investigate this hypothesis, a flow cytometry based approach was employed to measure maternal immune cell subtypes in the circulation and placenta.

5.2 Materials & Methods

General materials & methods can be found in Chapter 2.

5.2.1 Etanercept Treatment

Etanercept (Wyeth Pharmaceuticals, Maidenhead, UK) was prepared fresh on the day of use using sterile phosphate buffered saline (PBS) (Thermo Fisher Scientific, Paisley, UK). SHRSP were treated with 0.8 mg/kg dose or vehicle (PBS) via subcutaneous injection at gestational days 0, 6, 12 and 18. This treatment regimen was chosen as etanercept is given weekly to treat inflammatory conditions such as rheumatoid arthritis in humans. Etanercept was always given by 10am with no more than 100 µl total injected using a disposable 1ml syringe and 26 G x ½" needle (BD Bioscience, Oxford, UK) given to the back of the neck.

5.2.2 Flow Cytometry

Leukocytes were isolated on the day of collection. Tissue from three uteroplacental units from pregnant (GD18) WKY, SHRSP and SHRSP treated with etanercept were dissected, perfused with PBS (Thermo Fisher Scientific, Paisley, UK) then harvested in ice-cold PBS (Thermo Fisher Scientific, Paisley, UK). The placental tissue was disrupted using scissors to produce a single cell suspension which was passed through a 70 µm cell strainer (BD Bioscience, Oxford, UK). Leukocytes were isolated from blood collected in heparinized tubes (BD Bioscience, Oxford, UK) from non-pregnant and pregnant (GD18) rats by density gradient centrifugation with Histopaque® (Sigma-Aldrich, Dorset, UK). Cells were

washed once (1300 rpm for 6 minutes) and resuspended in 3ml of 2% FBS/PBS (FACS buffer) and placed on ice. Cells were counted using a haemocytometer and 1 x 10^6 leukocytes were subject to staining procedure. Cells were used for staining on the day of tissue collection.

5.2.2.1 Extracellular Flow Cytometry Panel

Isolated leukocytes from WKY (NP: n=4, GD18: n=5), SHRSP (NP: n=4, GD18: n=5) and SHRSP treated with etanercept were stained using Zombie® live/dead dye (Biolegend, London, UK) for 15 minutes at room temperature in the dark followed by staining for extracellular markers using fluorochrome conjugated primary antibodies for 20 minutes on ice in the dark. Two panels of antibodies were used. Panel 1: anti-CD45-PerCP/Cy5.5, anti-CD3-APC, anti-CD4-PE/Cy7, anti-CD8-FITC and anti-CD161-PE, (Biolegend, London, UK). Panel 2: anti-CD45-PerCP/Cy5.5, anti-CD103-AlexaFluor®647, anti-CD4-PE/Cy7, anti-RT1B-FITC (Biolegend, London, UK) and anti-HIS36-PE (BD Bioscience, Oxford, UK). Cells were washed and resuspended in FACS buffer for immediate analysis using a BD FACSCanto II machine (BD Bioscience, Oxford, UK) with BD FACSDIVA™ software where 10,000 CD45+ events was used as a cut-off in each sample. Exported data was analysed using FlowJo (FlowJo, LLC) where leukocytes in blood were expressed as a percentage of total and in tissue were expressed as an absolute number.

5.2.2.2 Intracellular Staining

Cells from pregnant (GD18) WKY, SHRSP and SHRSP treated with etanercept were cultured in RPMI 1640 media +10% FBS +1% penicillin/streptomycin (Thermo Fisher Scientific, Paisley, UK) then stimulated using a cell stimulation cocktail at 2 µl/ml media and incubated at 37 °C for 4 hours. The cell stimulation cocktail contained polycolonal activators: concanavalin A, lipopolysaccharide, phorbol esters plus ionomycin, phytohaemaglutinin and staphylococcus enterotoxin B (BD Bioscience, Oxford, UK). Cells were harvested after this time and stained using Zombie® live/dead dye (Biolegend, London, UK) for 15 minutes at room temperature in the dark followed by staining for extracellular markers using fluorochrome conjugated primary antibodies for 20 minutes on ice in the dark (anti-CD45-PerCP/Cy5.5, anti-CD3-APC and anti-CD161-PE; Biolegend, London,

UK). Cells were then fixed in intracellular fixation buffer (eBioscience, Hatfield, UK) for 45 minutes and washed in 1% permeabilisation buffer (eBioscience, Hatfield, UK) at 1100rpm for 6 minutes at 4 °C. Cells were then stained according to manufacturer's instructions for intracellular TNFα (anti-TNFα-PE-Cy7; eBioscience, Hatfield, UK) and Granzyme-B (anti-granzyme-B-FITC antibody, Biolegend, London, UK) at room temperature for 30 minutes in the dark. Cells were washed and resuspended in FACS buffer for immediate analysis using a BD FACSCanto II machine (BD Bioscience, Oxford, UK) with BD FACSDIVA™ software where 10,000 CD45+ events was used as a cut-off in each sample. Exported data was analysed FlowJo (FlowJo, LLC) where cells expressing positive intracellular staining were given as a percentage of the total cell of interest population.

5.2.3 Immunohistochemistry for Granzyme B

Slides were cleared and rehydrated as described in section 2.6.1. To quench endogenous peroxidase, sections were incubated in 3% hydrogen peroxide/methanol for 30 minutes at room temperature followed by 2 x 10 minute washes in dH_2O. Antigen retrieval was achieved using laboratory-prepared 0.01M sodium citrate buffer (pH 6) (Appendix I) heated to 95 °C in a water bath for 15 minutes followed by 2 x 10 minute washes in dH_2O. Sections were blocked in a humidified chamber at room temperature with approximately 100 µl of 15% swine serum/PBS (Vector Laboratories, Peterborough, UK)).Briefly, sections from GD18 placenta from WKY, SHRSP and SHRSP treated with etanercept were blocked in 15 % swine serum (Vector Laboratories, Peterborough, UK) in PBS then incubated in a primary antibody for granzyme B (#ab53097; Abcam, Cambridge, UK) diluted in 5% swine serum (Sigma-Aldrich, Dorset, UK) in PBS overnight at 4 ºC. Granzyme B was detected using horse radish peroxidase (HRP) conjugated swine-α-rabbit secondary antibody (Dako, Ely, UK) diluted 1:100 in 2% BSA/TBS-T. Slides were cleared and visualised using light microscopy as described in section 2.6.4.

5.2.4 Cytokine Array

Cytokine array (R&D Systems, Abingdon, UK) was performed according to manufacturer's instructions with 250 µg protein input. Mean pixel density was analysed using ImageJ software. Mean pixel density was normalised to the mean

of the reference spots present on the array. Data are presented as both normalised mean pixel density and as a percentage of WKY.

5.2.5 Cell Free DNA (cfDNA) Isolation from Placental Explant Media

Placental tissue was harvested in ice cold PBS from WKY and SHRSP. Under sterile conditions, the tissue was dissected into pieces <5mm in ice cold DMEM F-12 Media +0.5% FBS +1% penicillin/streptomycin (Thermo Fisher Scientific, Paisley, UK). The tissue pieces were split evenly between 2 wells of a 24 well plate (Thermo Fisher Scientific, Paisley, UK) in 1ml of media. After 1 hour, the explants were washed in PBS and replaced with a fresh 1ml of media. Explants were incubated for 20 hours at 37 °C after which the media was collected, and stored at -80 °C. Explant media (approximately 1ml) was centrifuged for 10 minutes at 12000 x g to remove debris. The supernatant (800 µl) was subject to DNA isolation using the QIAamp DNA blood & tissue kit (QIAgen, Manchester, UK) according manufacturer's instructions. The amount of proteinase K, lysis buffer AL and ethanol was modified in proportion to the larger amount of starting material. Immediately following extraction, DNA was quantified using a NanoDrop 2000 (section 2.4.1.1) (Thermo Fisher, Paisley, UK).

5.3 Results

5.3.1 CD3- CD161+ NK Cells are increased in the Maternal Circulation and Placenta in Pregnant SHRSP

From the beneficial effects we observed in pregnancy outcome and uterine artery function in SHRSP treated with etanercept; we deduced that excess TNFα signalling played a causal role in the pathology observed during pregnancy in this model. Whilst TNFα can be produced in some quantity from almost all cell types, we focussed on one of the major producers, the immune cells, in order to identify the source(s) of excess TNFα in the SHRSP. A flow cytometry panel was designed to quantify immune cell populations in pregnant WKY and SHRSP in the maternal blood and placenta (gating strategy example Fig. 5-1A). Of the populations analysed, NK cells (CD3- CD161+) were the most markedly increased in the SHRSP relative to WKY in both the maternal circulation (Fig. 5-1B) and placenta (Fig. 5-1C-D). Further, pregnancy specific changes were detected in peripheral CD3- CD161+ cells in maternal blood (Fig. 5-1E). In WKY, these cells were significantly

decreased from non-pregnant (NP) to pregnant (GD18) (Fig. 5-1E). In contrast, there was a significant increase in peripheral NK cells in SHRSP from NP to GD18 (Fig. 5-1E).

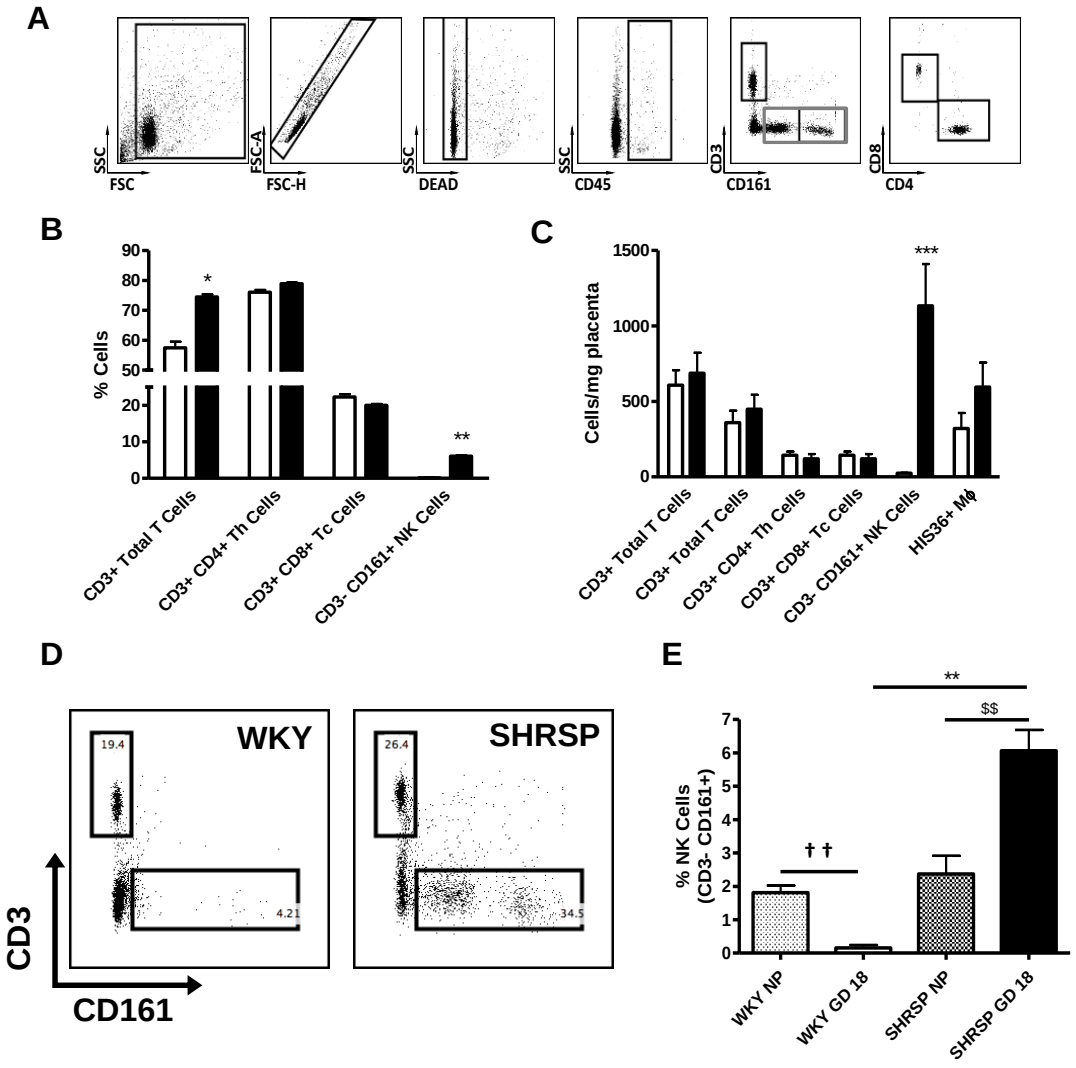

Figure 5-1 CD3- CD161+ natural killer cells are significantly increased in pregnant SHRSP.

Flow cytometry was used to measure immune cell populations (gating strategy example (A) in maternal blood (B) and placenta (C) from pregnant (GD18) WKY (n=5) and SHRSP (n=6). A bimodal population of CD3-CD161+ was observed in (A), this analysis incorporated all CD161+ cells as indicated by the grey box (A) and the black box in (D). CD3+ T cells and CD3- CD161+ NK cells were elevated in maternal blood from SHRSP relative to WKY (B) (* $p<0.05$ vs. WKY, ** $P<0.01$ vs. WKY analysed by Student's t test). CD3- CD161+ NK cells were also significantly increased in placenta from SHRSP relative to WKY (C). A representative dot plot showing the increase in CD3- CD161+ cells in placenta from SHRSP relative to WKY is shown in (D). Natural killer (NK) cell numbers were assessed using flow cytometry in virgin (NP) (n=4) and GD18 (n=5-6) SHRSP and WKY (E). WKY exhibited a significant decrease in the percentage of NK cells in the maternal blood from NP to GD18 (†† $p<0.01$ vs. WKY NP analysed by one-way ANOVA followed by post-hoc Tukey test). In contrast, SHRSP exhibited a significant increase in the percentage of NK cells in the maternal blood from NP to GD18 ($$ $p<0.01$ vs. SHRSP NP analysed by one-way ANOVA followed by post-hoc Tukey test). Th: T helper cell, Tc: cytotoxic T cell.

5.3.2 CD3- CD161+ NK Cells are a Source of Excess TNFα in the Maternal Circulation and Placenta in Pregnant SHRSP

The significant increase in NK cell number in the maternal circulation and placenta of the SHRSP made this cell type a promising candidate for a source of

excess TNFα. Therefore, this population was investigated further using intracellular staining. Intracellular staining of CD161+ cells in both the maternal circulation (Fig. 5-2A-B) and placenta (Fig. 5-2C-D) showed that TNFα production is significantly increased in the SHRSP relative to the WKY at GD18. TNFα production from CD161+ cells is not different between strains pre-pregnancy (Fig. 5-3). Furthermore, TNFα production from CD3+ T cells or other CD45+ cells was not significantly different between the strains (Fig. 5-4).

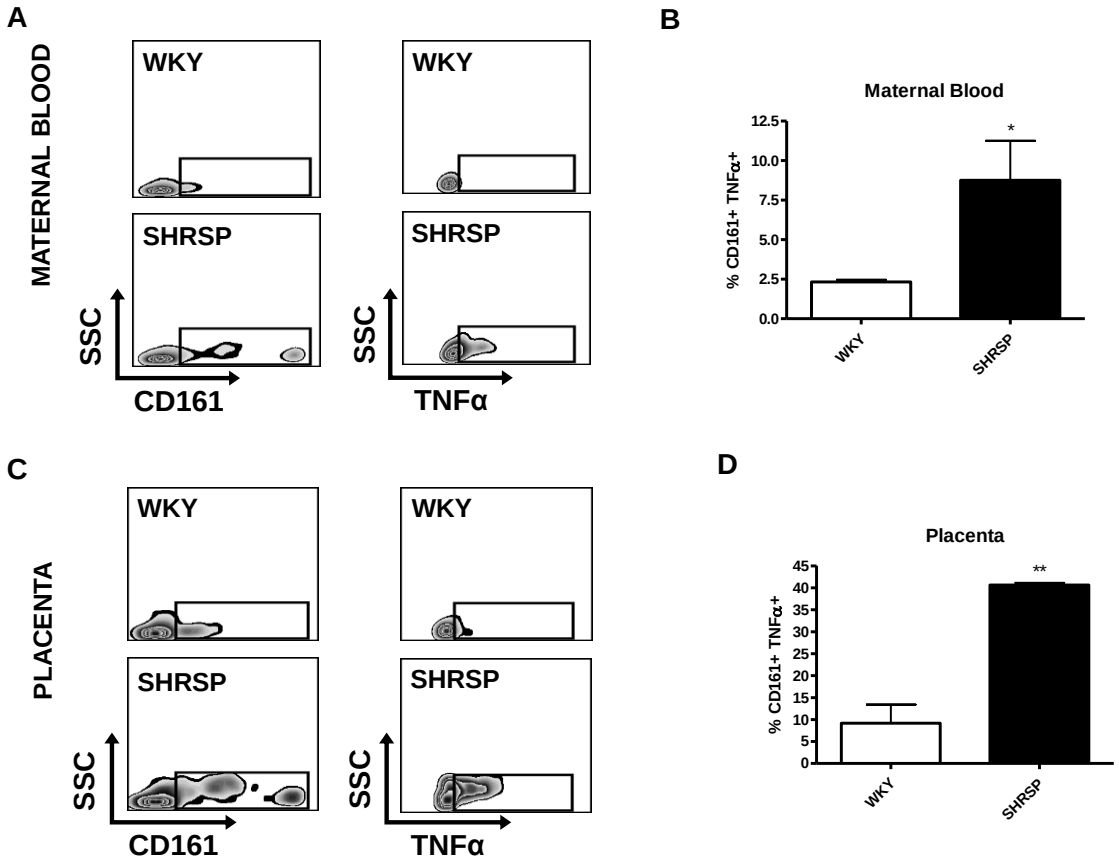

Figure 5-2 CD161+ cells are a source of excess TNFα in pregnant SHRSP maternal circulation and placenta.

Intracellular flow cytometry was used to measure TNFα production in CD161+ natural killer cells in maternal blood (A-B) and placenta (C-D) from pregnant (GD18) WKY (n=4) and SHRSP (n=4). CD161+ cells from the maternal circulation (A-B) and placenta (C-D) showed an increased production of TNFα from pregnant SHRSP relative to WKY (* $p<0.05$, ** $p<0.01$ vs. WKY GD18 analysed by Student's t test).

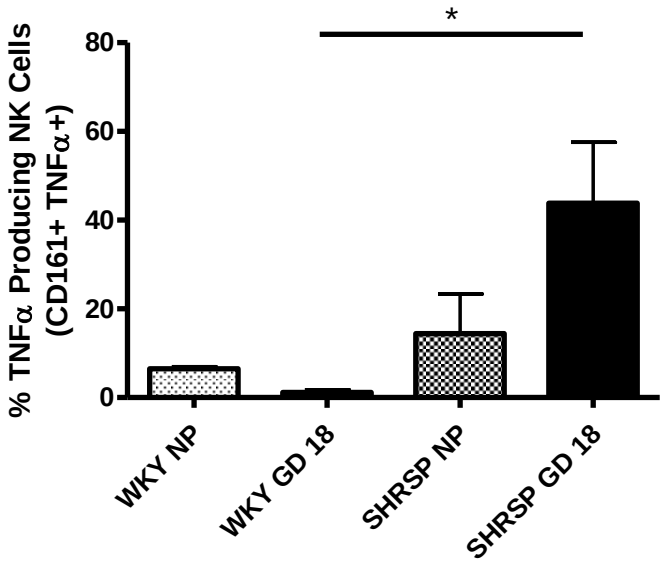

Figure 5-3 TNFα producing CD161+ cells are increased in a pregnancy dependent manner in SHRSP.

Intracellular flow cytometry was used to measure TNFα production in CD161+ natural killer cells from non-pregnant (NP) WKY (n=4), NP SHRSP (n=4), pregnant (GD18) (n=4) WKY and GD18 SHRSP (n=4). TNFα staining in CD161+ cells exhibited a trend for a decrease from NP to pregnant WKY; however there was the opposite trend in the SHRSP. CD161+ cells positive for TNFα were significantly increased in pregnant SHRSP relative to WKY (* $p < 0.05$ vs. WKY GD18 analysed by one-way ANOVA followed by post-hoc Tukey test).

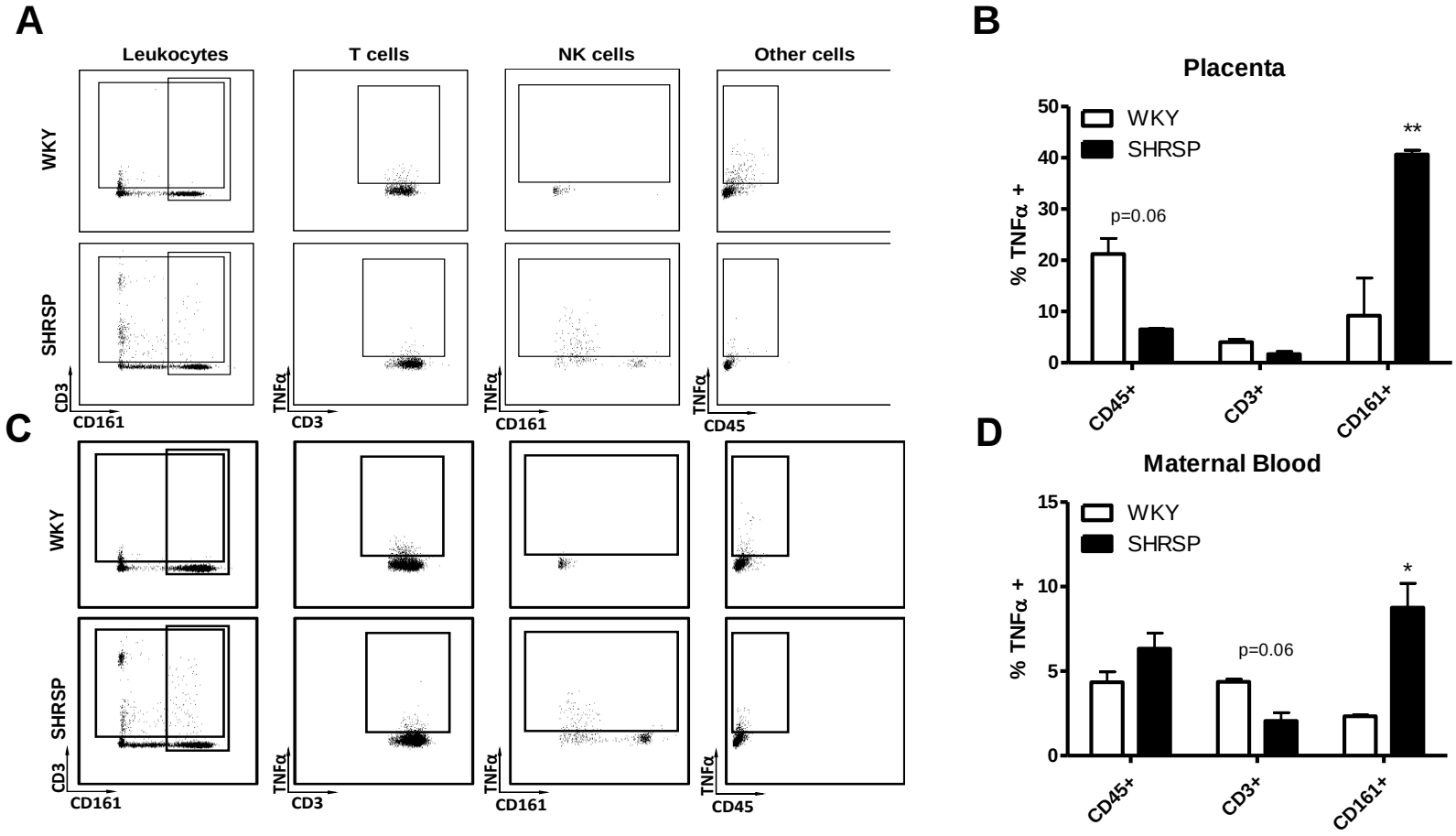

Figure 5-4 TNFα production from CD3+ cells and other CD45+ cells is not significantly different between WKY and SHRSP.

Intracellular staining was used to quantify TNFα production from immune cells in the maternal blood and placenta from WKY (n=4) and SHRSP (n=4). In placenta (A-B) and maternal blood (C-D) there was no significant difference in TNFα production from CD3+ or other CD45+ cells, only in CD161+ cells (* $p<0.05$, ** $p<0.01$ vs. WKY GD18 analysed by one-way ANOVA followed by post-hoc Tukey test). CD45+: Leukocytes, CD3+ T Cells, CD161+ NK Cells.

5.3.3 Etanercept Reduces the Population of CD3- CD161+ NK Cells in the Placenta of Pregnant SHRSP

As etanercept had previously been shown to have beneficial effects on both pregnancy outcome and uterine artery function in the SHRSP (Chapter 4), the effect of etanercept treatment in SHRSP on maternal blood and placental immune cell populations was investigated. In maternal blood samples, the number of CD3+ T cells was increased in both SHRSP and SHRSP treated with etanercept relative to the WKY; however no difference was observed in the balance of CD4+ or CD8+ T cells (Fig. 5-5A-C). Etanercept treatment also did not affect the percentage of CD3- CD161+ NK cells or CD3+ CD161+ NK-T cells in the maternal circulation (Fig. 5-5D-E). There were no differences in the percentage of dendritic cells in the maternal blood between strains or with etanercept treatment (Fig. 5-5F).

Etanercept treatment had independent effects on the immune cell populations of the placenta that differed from its effects on the maternal circulation (Fig. 5-6). Placental tissue from etanercept treated SHRSP had a greater number of CD3+ T cells, specifically CD4+ T helper cells relative to SHRSP and WKY (Fig. 5-6A-C). Etanercept treatment reduced the number of CD3- CD161+ NK cells present in the SHRSP placenta (Fig. 5-6D) but not the CD3+ CD161+ NK-T cells (Fig. 5-6E). Dendritic cells were not robustly detected in placental samples from all strains (Fig. 5-6F). There was a trend for etanercept treatment to reduce the number of macrophages in placenta from SHRSP; however this was not significant ($p=0.069$) (Fig. 5-6G).

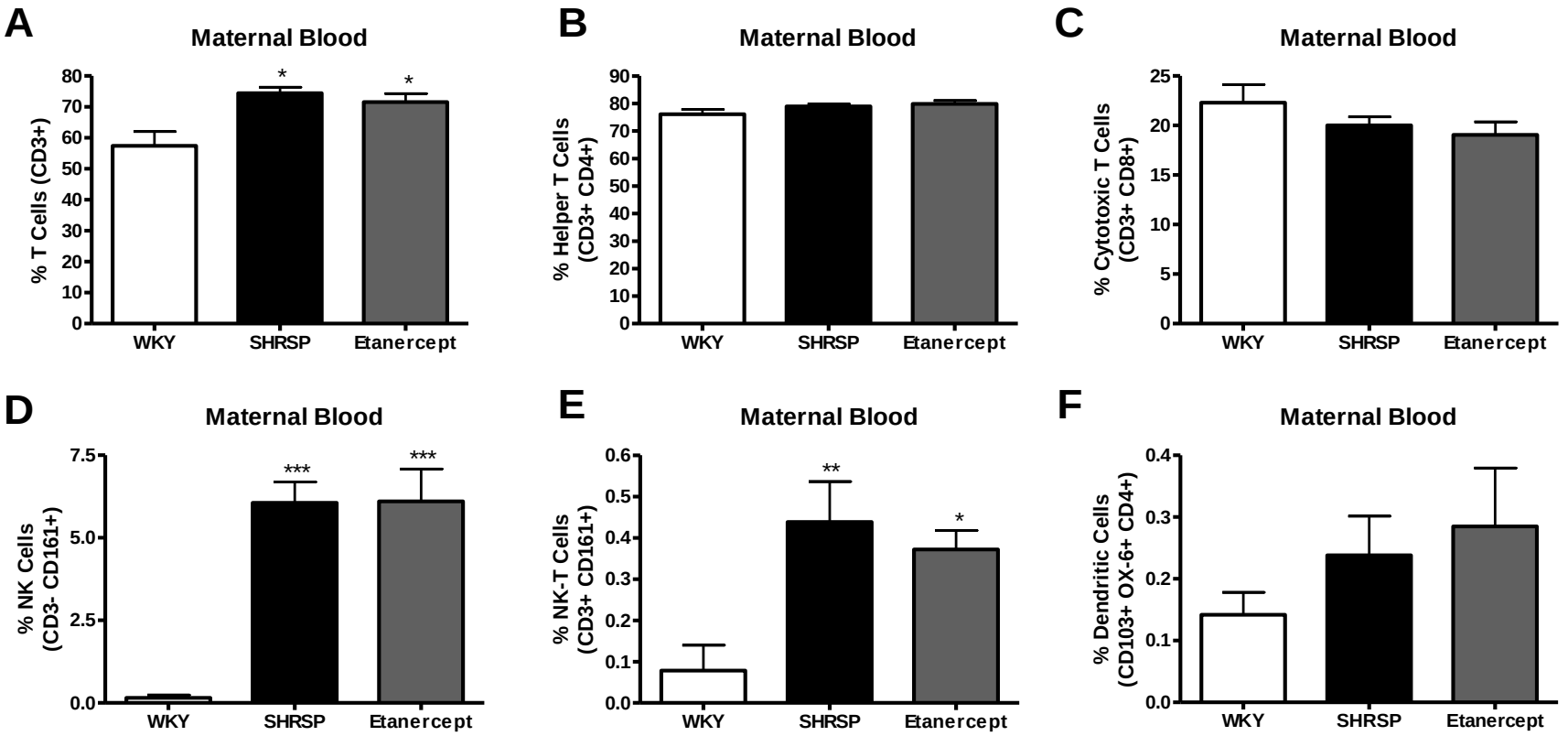

Figure 5-5 Flow cytometry panel in maternal blood from pregnant WKY, SHRSP and SHRSP treated with etanercept.

A flow cytometry panel was used to quantify immune cell sub-types in the maternal blood from pregnant (GD18) WKY (n=5), SHRSP (n=6) and SHRSP treated with etanercept (n=6). The percentage of T cells (A) in the maternal blood significantly increased in SHRSP and SHRSP treated with etanercept relative to the WKY (* p< 0.05 vs. WKY GD18 analysed by one-way ANOVA followed by post-hoc Tukey test), however there were no significant differences between the balance of helper (B) and cytotoxic T cells (C). Both NK cells (D) and NK-T cells (E) were significantly increased in SHRSP and SHRSP treated with etanercept relative to the WKY (* p< 0.05, ** p< 0.01 vs. WKY GD18 analysed by one-way ANOVA followed by post-hoc Tukey test). There were no significant alterations in the presence of dendritic cells (G).

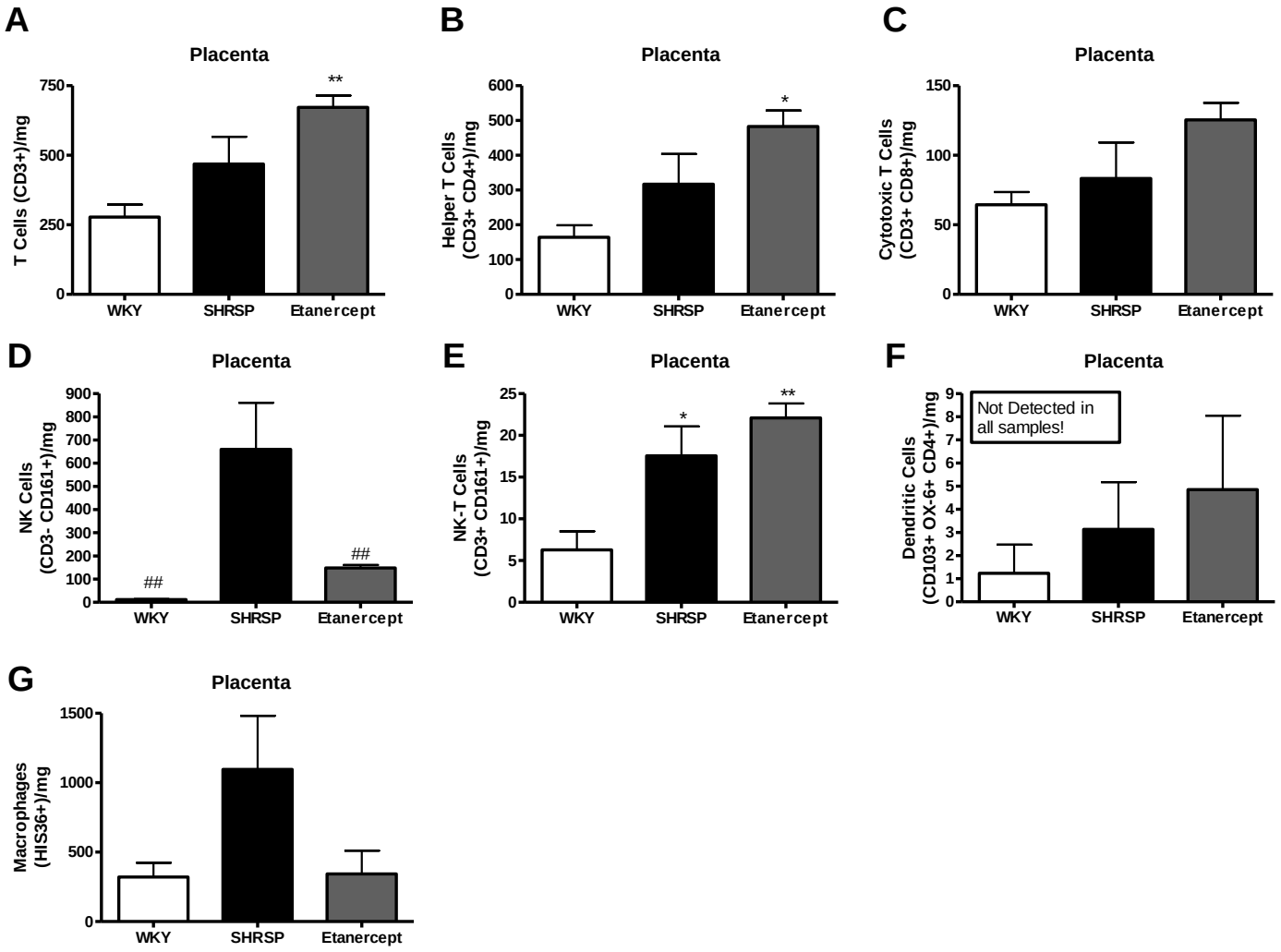

Figure 5-6 Flow cytometry panel in placenta from pregnant WKY, SHRSP and SHRSP treated with etanercept.

A flow cytometry panel was used to quantify immune cell sub-types in placenta from pregnant (GD18) WKY (n=5), SHRSP (n=6) and SHRSP treated with etanercept (n=6). T cells (A) were significantly (** $p< 0.01$ vs. GD18 WKY analysed by one-way ANOVA followed by post-hoc Tukey test) and Th cells (B) were significantly increased in SHRSP treated with etanercept relative to WKY. NK cells (D) were significantly increased in the SHRSP relative to the WKY and SHRSP treated with etanercept (## $p< 0.01$ vs. GD18 SHRSP analysed by one-way ANOVA followed by post-hoc Tukey test). NK-T cells were significantly increased in SHRSP and SHRSP treated with etanercept (* $p < 0.05$, ** $p< 0.01$ vs. WKY analysed by one-way ANOVA followed by post-hoc Tukey test) (E). The detection of dendritic cells was variable and not measurable in all samples (F). There was a trend for macrophages to be increased in SHRSP relative to WKY and SHRSP treated with etanercept (G).

5.3.4 Etanercept Treatment Reduces CD161 Expression and Granzyme B Production in NK cells from the Placenta of Pregnant SHRSP.

Etanercept treatment in the SHRSP significantly reduced the number of CD161+ NK cells present in the SHRSP placenta (Fig. 5-7A) but not the maternal circulation (Fig. 5-7B). From the dot plot derived from flow cytometry analysis, the CD161+ population of cells from SHRSP but not WKY placental tissue could be divided into a CD161 low ($CD161_{Low}$) population and a CD161 positive (CD161+) population (Fig. 5-7C). Reduction of CD161+ cells in the placenta from SHRSP treated with etanercept was associated with a significant increase in the $CD161_{Low}$ population (Fig. 5-7D). These two sub-populations were investigated further using intracellular staining for granzyme B as a marker of cytotoxicity. The CD161+ population had a characteristically cytotoxic phenotype where the majority of these cells (~70%) stained positively for intracellular granzyme B from placenta in both SHRSP and SHRSP treated with etanercept (Fig. 5-7E-F). In contrast, the $CD161_{Low}$ population had a significantly decreased proportion of granzyme B expression (~12%) from placenta in both SHRSP and SHRSP treated with etanercept (Fig. 5-7E-F).

In order to investigate whether the increase in NK cells was localised to a particular area in the placenta, immunohistochemistry for granzyme B was carried out in sections of placenta from WKY, SHRSP and SHRSP treated with etanercept at GD18. Concurrent with the flow cytometry data, granzyme B positive cells were increased in the SHRSP placenta relative to the WKY (Fig. 5-8). The granzyme B positive cells were low in number and appeared to be randomly distributed throughout the labyrinth zone (Fig. 5-8B-C).

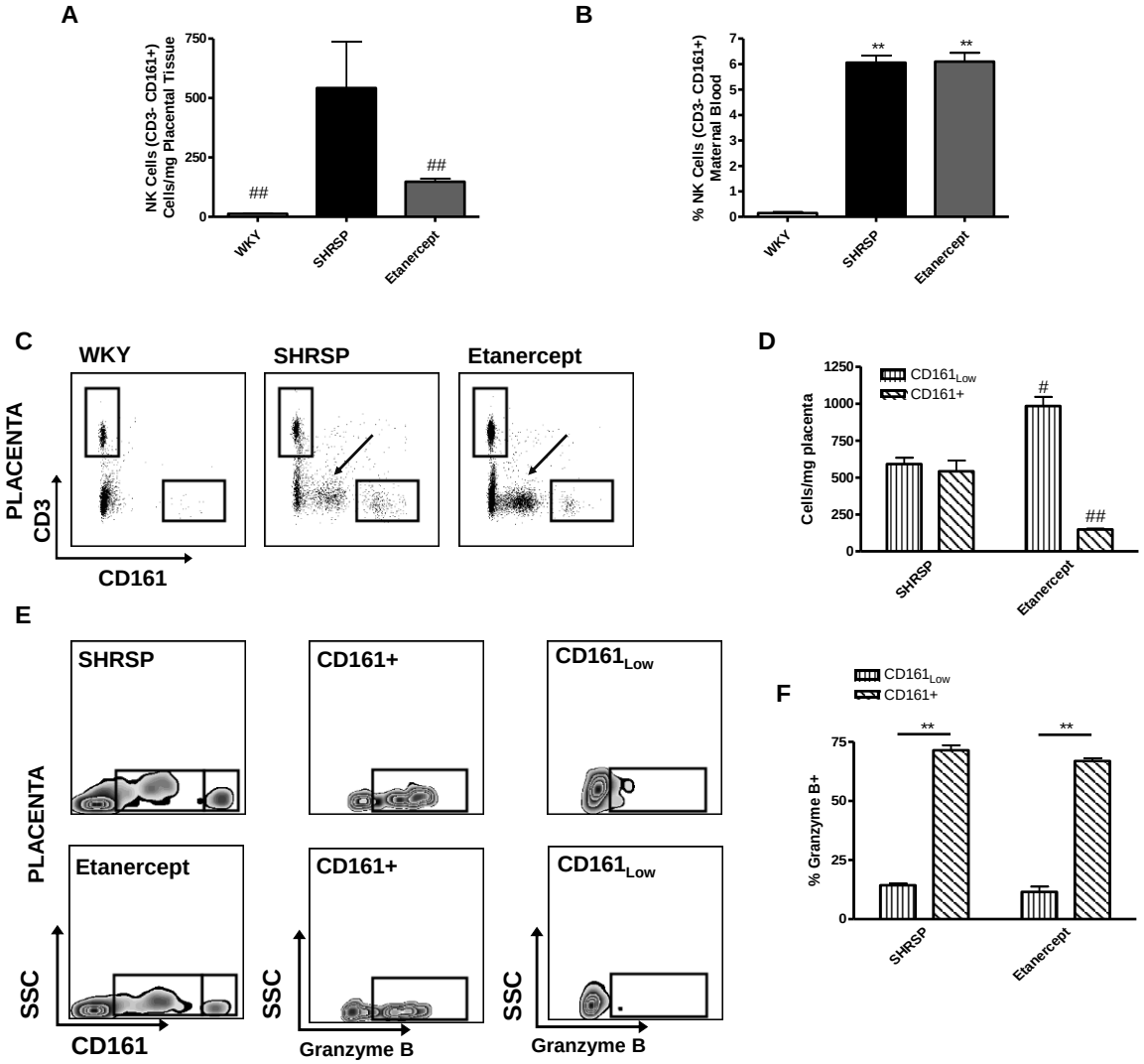

Figure 5-7 Etanercept reduces granzyme B-producing CD161+ cells in the SHRSP placenta.

Flow cytometry was used to quantify CD3- CD161+ NK cells in SHRSP (n=6) and SHRSP treated with etanercept (n=5). Etanercept treatment significantly decreased CD3- CD161+ cells in the SHRSP GD18 placenta (A) (## $p<0.01$ vs. SHRSP GD18 analysed by one-way ANOVA followed by post-hoc Tukey test) but not maternal blood (B) (graphs are repeated from Fig. 5-5 & 5-6). Etanercept treatment caused a shift in CD161+ expression from a high to low phenotype; arrows indicate $CD161_{Low}$ population and boxes indicate CD161+ population (# $p<0.05$, ## $p<0.01$ vs. SHRSP GD18 analysed by one-way ANOVA followed by post-hoc Tukey test) (C-D). CD161+ cell populations were characterised using intracellular staining where CD161+ populations exhibited high expression of cytotoxic granzyme B and $CD161_{Low}$ population exhibited significantly lower expression of granzyme B (E-F) (** $p<0.01$ vs. $CD161_{Low}$ analysed by Student's t test).

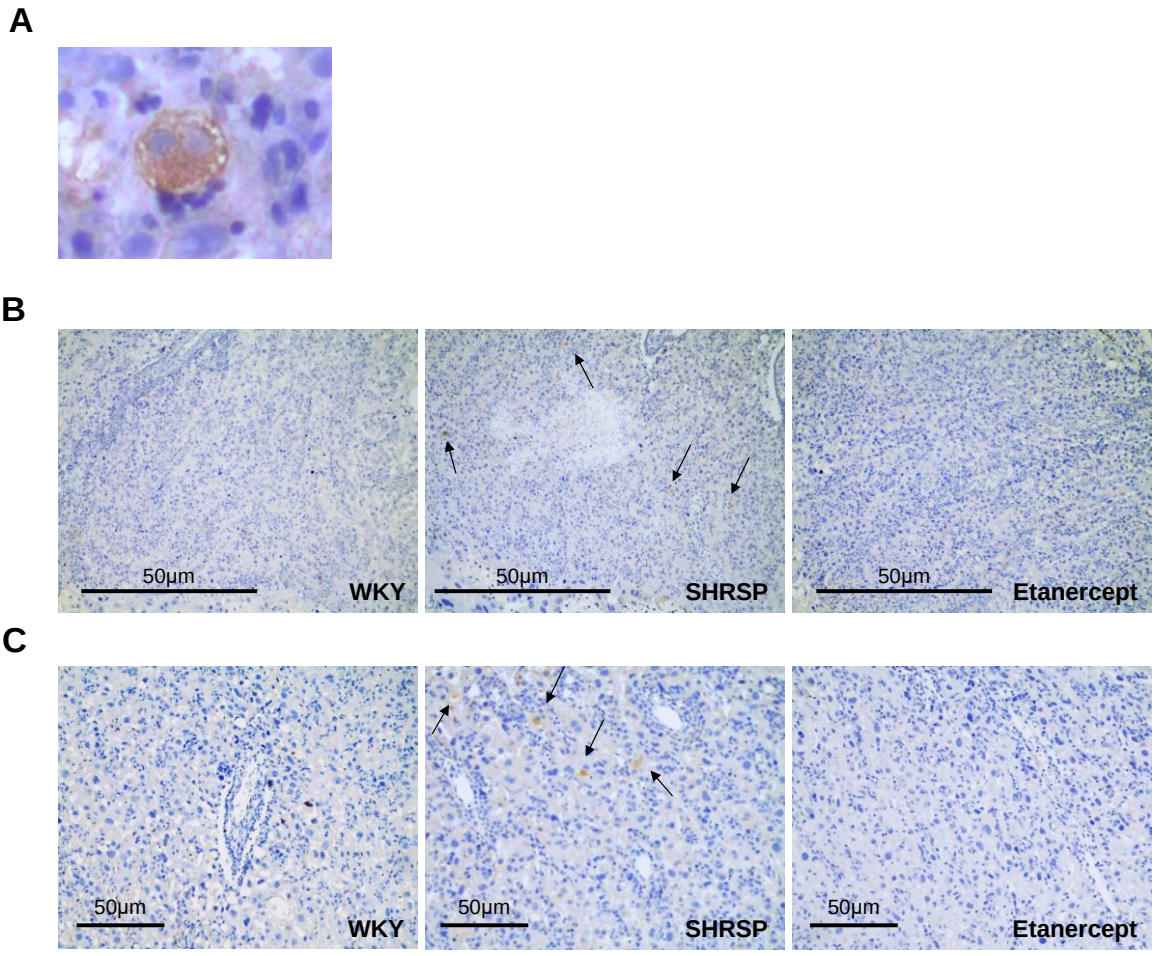

Figure 5-8 Granzyme B positive cells are increased in placenta from SHRSP.

Immunohistochemistry for granzyme B was used to detect cytotoxic cells in the placenta of WKY (n=6), SHRSP (n=6) and SHRSP treated with etanercept (n=6). A 100x magnification image of a granzyme B positive immune cell is shown in (A). Granzyme B positive cells were detecTable in the labyrinth zone of SHRSP but not WKY or etanercept treated SHRSP (B-C).

5.3.5 Peptide Array Demonstrates that Placenta from SHRSP is a Site of Global Inflammation

Differences in immune cells were detected in SHRSP relative to WKY, which were also altered by etanercept treatment. In order to explore other cytokines which could be playing a role in this process, a cytokine array was performed in placental tissue from GD18 WKY, SHRSP and SHRSP treated with etanercept (Fig. 5-9 & 5-10). Of the 29 cytokines that were spotted on the array; 19 were detectable in of placenta from SHRSP and 10 were detectable in placenta from WKY and SHRSP. The 9 cytokines that were detected in all samples from SHRSP but not from all WKY or etanercept treated SHRSP were: interleukin (IL) -1a, IL-

1b, IL-1ra, IL-2, IL-3, IL-13, IP-10, ciliary neurotrophic factor (CNTF), CXCL31/fractalkine and CXCL9/monocyte induced by gamma interferon (MIG).

From visual inspection of the cytokine arrays from WKY, SHRSP and SHRSP treated with etanercept there is a striking increase in the number and intensity of positive spots in SHRSP relative to both the placenta samples from WKY and etanercept treated SHRSP (Fig. 5-10A). Analysis of the pixel density of the positive spots showed that IL-17, CXCL7, intracellular adhesion molecule 1 (ICAM-1), L-selectin and VEGF were highest expressed cytokines across all groups (Fig. 5-10B). All of the cytokines measured demonstrated consistent significant up-regulation in placenta from SHRSP relative to lower levels in WKY and SHRSP treated with etanercept (Fig. 5-10C). With respect to fold change, the highest cytokine in the SHRSP relative to the WKY was CXCL31/fractalkine expressed approximately 10-fold greater (Fig. 5-10C).

A

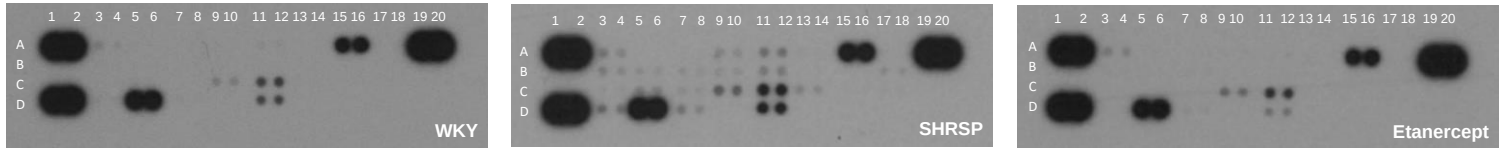

B

	1	2	3	4	5	6	7	8	9	10	11	12	13	14	15	16	17	18	19	20
A	REF	REF	CINC-1	CINC-1	CINC-2a	CINC-2a	CINC-3	CINC-3	CNTF	CNTF	Fractal-kine	Fractal-kine	GM-CSF	GM-CSF	ICAM-1	ICAM-1	IFNγ	IFNγ	REF	REF
B		IL-1a	IL-1a	IL-1b	IL-1b	IL-1ra	IL-1ra	IL-2	IL-2	IL-3	IL-3	IL-4	IL-4	IL-6	IL-6	IL-10	IL-10			
C		IL-13	IL-13	IL-17	IL-17	IP-10	IP-10	LIX	LIX	L-selectin	L-selectin	MIG	MIG	MIP-1α	MIP-1α	MIP-3α	MIP-3α			
D	REF	REF	RANTES	RANTES	CXCL7	CXCL7	TIMP-1	TIMP-1	TNFα	TNFα	VEGF-A	VEGF-A				Neg. Con.	Neg. Con.			

Figure 5-9 Representative array for WKY, SHRSP and SHRSP treated with etanercept.

Representative cytokine array for WKY (n=4), SHRSP (n=4) and SHRSP treated with etanercept (n=4) is shown in (A) with an accompanying map in (B). Red text indicates cytokines that were not detected in this experiment; bold black text indicates cytokines that were detected. IL: interleukin, IP-10: interferon gamma induced protein 10, CINC-1: cytokine induced neutrophil chemoattractant 1, CNTF: ciliary neurotrophic factor, CXCL: chemokine ligand, ICAM-1: intracellular adhesion molecule-1, RANTES: regulated on activation, normal T cell expressed and secreted, TIMP-1: tissue inhibitor of metalloproteinases 1, VEGF: vascular endothelial growth factor.

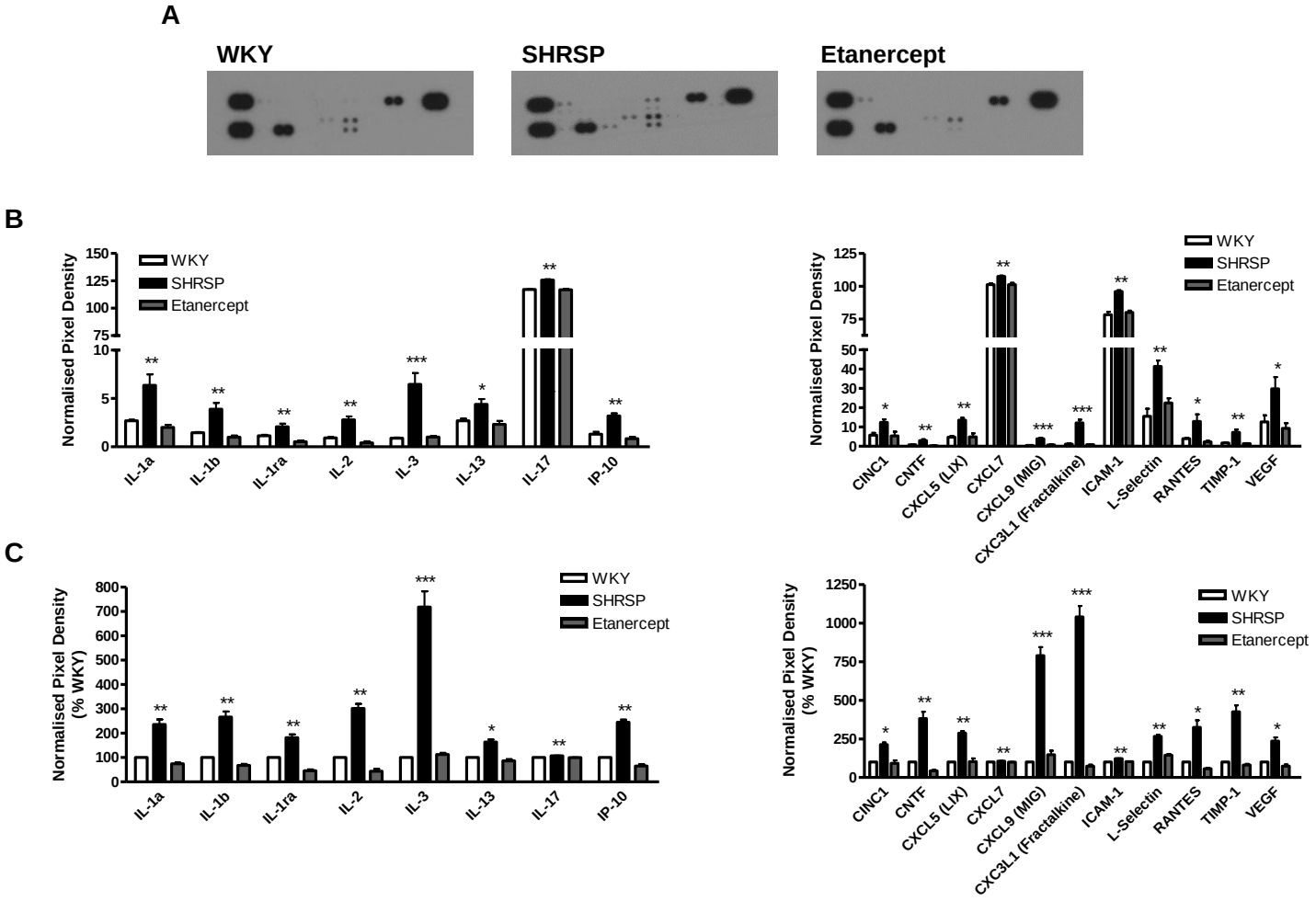

Figure 5-10 The array profile is altered in GD18 placenta from SHRSP relative to WKY and SHRSP treated with etanercept.

An array was used to profile cytokine expression in placenta taken at GD18 in WKY (n=4), SHRSP (n=4) and SHRSP treated with etanercept (n=4). A representative result for each group is shown in (A); more positive spots were present in the SHRSP (19/29 cytokines detected) than the WKY and etanercept treated SHRSP (10/29 cytokines detected). Mean pixel density was normalised to the mean of the reference spots on the array and across all samples IL-17, CXCL7, intracellular adhesion molecule 1 (ICAM-1), L-selectin and VEGF were the most highly expressed (B). Normalised pixel density was compared to WKY (C) where all cytokines showed a similar pattern of up-regulation in the SHRSP relative to the WKY and etanercept treated SHRSP (* p<0.05, **p<0.01 *** p<0.005 vs. GD18 WKY analysed by one-way ANOVA followed by post-hoc Tukey test) (C). Graphs in (B) and (C) are split due to the large number of hits. IL: interleukin, IP-10: interferon gamma induced protein 10, CINC-1: cytokine induced neutrophil chemoattractant 1, CNTF: ciliary neurotrophic factor, CXCL: chemokine ligand, ICAM-1: intracellular adhesion molecule-1, RANTES: regulated on activation, normal T cell expressed and secreted, TIMP-1: tissue inhibitor of metalloproteinases 1, VEGF: vascular endothelial growth factor.

5.3.6 The Placenta from SHRSP Reveals Increased Shedding of DNA

In addition to the measurement of cytokine profiles from the placenta, DNA detected in placental explant media from GD18 WKT and SHRSP was quantified using a NanoDrop spectrophotometer. Explant media from placenta of SHRSP displayed a trend for increased total DNA relative to the WKY (Fig. 5-11). As a negative control, fresh media only was subject to the same DNA extraction and quantification procedure. DNA was not detected by NanoDrop in this negative control sample.

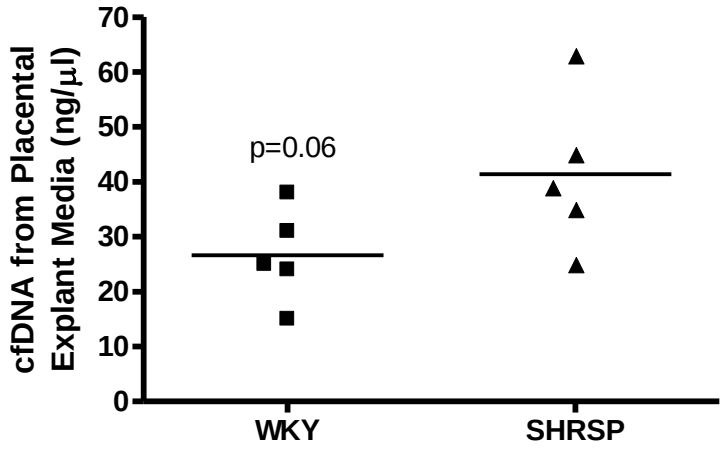

Figure 5-11 Cell free DNA is increased in media of placental explants from SHRSP relative to WKY.

Placental tissue explants from WKY (n=5) and SHRSP (n=5) were cultured from 20 hours then the media was collected. Quantification of DNA using the nanodrop spectrophotometer showed that total DNA was increased relative to the WKY (p=0.06 vs. GD18 SHRSP analysed by Student's t test).

5.4 Discussion

The work presented in this Chapter reveals that there are alterations in both immune cells and cytokines between pregnant (GD18) WKY and SHRSP. Specifically, a population of CD3- CD161+ NK cells have been identified to be increased in a pregnancy-dependent manner in the SHRSP maternal circulation and placenta. These NK cells were a source of excess TNFα at GD18 in SHRSP pregnancy. Etanercept treatment reduced the number of NK cells in the placenta, but not the maternal circulation, by down-regulating the expression of CD161 which was associated with a decrease in cytotoxic granzyme B production. Additionally, the placenta from SHRSP expressed an altered cytokine profile

indicating a pro-inflammatory environment which is not present in WKY and was reduced by treatment with etanercept.

In order to identify the source of excess TNFα in pregnant SHRSP, a flow cytometry panel was designed for TNFα-producing immune cells. The number of CD3- CD161+ NK cells was increased in a pregnancy-dependent manner in the SHRSP but not in the control WKY. Investigations of circulating NK cells in other rodent models of hypertensive pregnancy are limited. A study in NOD.SCID mice (90% depletion in peripheral NK cells but a 57% increase in uNK proliferation) has reported that there is a significant increase in blood pressure during pregnancy relative to the background NOD strain (427). These results indicate that NK cells appear to play a role in blood pressure regulation during pregnancy. Notably, these results may be affected by the fact that NK cell biology differs between mouse strains as discussed in section 1.3.2. Some small clinical studies which have focussed on pre-eclampsia have reported an increase in circulating NK cells which express a greater amount of IFNγ relative to samples from normotensive women (428). However, this paper did not define which cell-surface markers were used for NK cell detection nor did it investigate the expression of TNFα. Another study showed that CD56+ NK cells derived from maternal blood express VEGF and that this population was reduced by 45% in women with preeclampsia (429). Whilst it is well established that the uNK cell population express VEGF which is thought to be important for their role in spiral artery remodelling (430); these findings indicate that perhaps circulating NK cells are not all potentially damaging.

CD161+ cells from SHRSP produced excess TNFα relative to control WKY. Whilst the data presented cannot conclusively prove that excess TNFα is not being produced by other cell types; intracellular staining for TNFα was not significantly different in CD3+ or other CD45+ cells. TNFα is also produced by invasive extravillous trophoblasts, however, at GD18 of pregnancy trophoblasts do not exhibit potent invasive behaviour in rats (431). Recent work has proposed an interaction between TNFα and the activation of peripheral NK cells in women with preeclampsia. In this study by Fukui *et al.*, NKp46+ (an activating NK receptor) NK cells show a sustained reduction from 3 months prior to delivery in women with preeclampsia (422). The number of NKp46+ cells was found to be negatively correlated with numbers of TNFα producing NK cells and the authors hypothesised

that excess TNFα production was driving the NK cells to a pro-inflammatory phenotype which lacked NKp46 expression.

The numbers of total CD161+ cells were increased in placenta from SHRSP and SHRSP treated with etanercept whereas numbers were small in the WKY placenta. Therefore, a currently unknown TNFα-independent mechanism exists which recruits NK cells to the placenta of SHRSP. Within this placental CD161+ cell population, etanercept induces a significant reduction in CD161 expression which is associated with a reduction in granzyme B production. Conversely, this infers that TNFα signalling is a critical step involved in CD161 up-regulation and granzyme B production in NK cells. Previously, TNFα has been shown to work in concert with IFN-γ to promote the cytotoxic activity of NK cells (122). The CD161 antibody used in this study detects the NKRP1A and NKRP1B cell surface receptors selective for NK cells. As discussed in section 1.3.2.1, the killer ability of NK cells is protected by a sophisticated mechanism of activating and inhibitory receptors whereby the resulting action is determined by the balance of these signals. NKRP1A (112) is an activating receptor and NKPR1B an inhibitory receptor in the rat (115). CD161 is conserved in mice where it is also selective for NK cells (106) and in humans where it is only expressed on a subset of NK cells (108). Whilst this study has shown that CD161+ NK cells are associated with a cytotoxic phenotype, future work should examine the balance of activating and inhibiting receptors on the NK cell surface in hypertensive pregnancy in order to further define their role in pathology. Definitive causality could be investigated by using NK cell depleting antibodies during pregnancy in SHRSP or using adoptive transfer of NK cells from pregnant SHRSP into pregnant WKY.

From the findings regarding the effect of etanercept treatment on the CD161+ NK cells in the placenta of the SHRSP; it was hypothesised that there were two independent, sequential mechanisms. The first was a TNFα independent recruitment of NK cells to the placenta which only occurred in the SHRSP but not WKY. The second was a TNFα dependent expression of CD161 and granzyme B which led to a classically cytotoxic NK cell which was down-regulated by etanercept treatment in the SHRSP. In order to test this hypothesis, a cytokine array was performed in GD18 placental tissue from WKY, SHRSP and SHRSP treated with etanercept. The aim was to identify an SHRSP-specific cytokine that was not

affected by etanercept treatment which would be a candidate for promoting NK cell recruitment to the placenta. The results of the array revealed that the placenta at GD18 in the SHRSP was a site of active inflammation with an increase in number of cytokines detected by the array. Analysis of the array did not show the hypothesised SHRSP-specific cytokine; in fact every cytokine displayed a similar pattern of down-regulation in placenta from both the WKY and etanercept treated SHRSP relative to untreated SHRSP. Therefore, etanercept normalised the global inflammatory response seen in the SHRSP. Whether this has to do with changes in cytokine profile resulting from the etanercept induced shift from CD161+ to $CD161_{Low}$ cell remains to be investigated. One limitation of this assay is that the main cytokines produced from NK cells; TNFα and IFNγ, were not detectable in any samples. This could be due to technical issues, such as, these are soluble factors or were below the limit of detection of the assay. However, the assay did detect an increase in molecules which play a critical role in the activation and proliferation of NK cells such as IL-2 (432), upstream molecules which stimulate TNFα and IFNγ production and signalling such as IL-1 (433, 434) and downstream messengers whose transcription is turned on specifically in response to an increase in IFNγ such as IP-10/CXCL10 (435) and MIG/CXCL9 (436).

The promising findings from this work should be confirmed in blood and tissue samples from women with chronic hypertension in pregnancy to define their clinical relevance. One advantage of studying the peripheral population of NK cells rather than the uNK cells is that they can be collected by standard phlebotomy. Furthermore, changes in peripheral immune cells can be detected from 12 weeks of gestation (437) giving rise to their potential as early biomarkers of future pregnancy complications. The increase in NK cells could be a maternal immune response against debris shed from the placenta. As there was no "SHRSP-specific cytokine" found in the previously discussed array; this could be an alternative mechanism for NK cell recruitment to the placenta in the SHRSP. This debris which encompasses apoptotic bodies, deported syncytiotrophoblast and extracellular vesicles as well as sub-cellular fragments including DNA has been shown to be increased in women with preeclampsia (415, 438). This debris could act as a danger-associated molecular pattern (DAMP) which triggers pattern recognition receptors on cells of the innate immune system; including NK cells (discussed in section 1.3.2.3). Total DNA quantified from placental tissue explants shows that

SHRSP have a greater total concentration relative to the WKY. This spectrophotometer data should be confirmed using quantitative PCR for a placental specific genre. Placental debris may also communicate messages from the placenta to the mother in a more specific way as exosomes derived from syncytiotrophoblast have been shown to express an array of receptors and molecules involved in mechanisms of angiogenesis (439), thrombin generation (440), gene expression by miRNAs (441) and immunomodulation (442) including of circulating NK cells (443).

The findings presented in this Chapter provide an explanation for the source of excess TNFα observed in the SHRSP and defines a novel action of etanercept on NK cells in the placenta. The pathway, which leads to an increase in NK cell number and/or activation in this model, may have clinical relevance for women with hypertension.

Chapter 6 Kidney Dysfunction and Urinary Peptidomics in Pregnant SHRSP

6.1 Introduction

The kidney plays a central role in healthy pregnancy. This is highlighted by the fact that women with chronic kidney disease have an increased risk of developing pregnancy complications; where up to 70% experience preterm delivery and up to 40% will develop preeclampsia (444, 445). Significant structural and functional changes occur in the kidney during pregnancy including a 1 - 1.5cm increase in size, a 50% increase in glomerular filtration rate (GFR), and up to an 80% increase in renal plasma flow (RPF) (446, 447) (Fig. 6-1). These alterations are broadly conserved in rats (discussed in section 1.5.1) (448). In addition, the kidney is the site of water and electrolyte balance which ultimately contributes to the regulation of maternal blood pressure (449). Kidney pathology is commonly observed in hypertensive individuals and women with preeclampsia. Chronic hypertension can result in arteriosclerosis, altered filtration of electrolytes and perturbed renin production (450). With respect to preeclampsia, the presence of proteinuria is a key diagnostic criteria which differentiates the condition from pregnancy-induced hypertension (451). Preeclampsia is associated with an impaired glomerular filtration (452) which is thought to be due to a characteristic swelling of the endothelial cells in the glomeruli, known as glomerular endotheliosis, detecTable in histological examination of kidneys from women with pre-eclampsia (452) and in rodent models (341, 453).

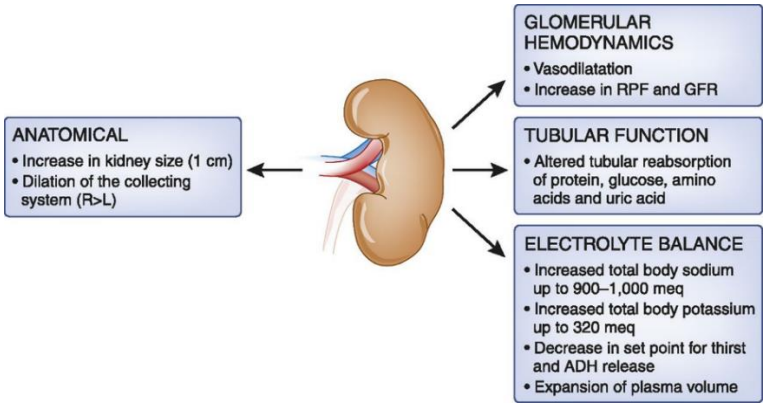

Figure 6-1 Normal renal structural and functional changes in response to pregnancy. RPF: renal plasma flow, GFR: glomerular filtration rate. Image from Odutayo *et al.* (2012).

Urine is produced as the filtrate passes through the nephron in three stages: filtration, absorption and secretion. Blood cells and large proteins cannot pass as plasma is filtered through the glomeruli. This filtrate passes through the tubules where ions, water and other small molecules are absorbed back into the body and waste products are secreted into the filtrate from the capillaries. The remaining fluid forms the urine which is passed through the collecting duct into the bladder then excreted. Due to this process, the urinary peptidome can give information about proteins that may be currently involved in local processes in the kidneys and some that are reflective of more distant organs obtained through filtration of the dynamic plasma peptidome giving a "snapshot" of what is currently happening in the body (454) (Fig. 6-2). Peptides derived from processes in the kidney and urogenital tract form the majority of those detected in the urinary peptidome (70%) whilst peptides from the circulation constitute the remainder (455). In humans, urine is a useful biological fluid for analysis as it is an easily accessible and plentiful resource, it is relatively stable at room temperature for a short period of time and at -20^{o}C for several years (456). The small peptides present are generally soluble and due to their size do not require protein digestion before analysis (455). Urinary peptidomics has been investigated in the field of cardiovascular research two-fold: to develop biomarker panels for prediction and risk stratification and as a screening tool for novel peptides involved in disease pathology (457). In particular, a number of studies have shown that there are alterations in the urinary peptidome in people with hypertension (458) and in healthy pregnant women compared to those who develop pre-eclampsia (459). Despite this, research characterising the urinary peptidome in women with chronic hypertension are limited.

The kidney is centrally involved in both blood pressure regulation and undergoes extensive changes in response to pregnancy. Whilst chronic hypertension and preeclampsia have been associated with an altered urinary peptidome; a similar study has not been conducted in chronic hypertension during pregnancy. We hypothesised that the urinary peptidome would be altered in both a pregnancy-dependent and strain-dependent manner in the WKY and SHRSP. We aimed to investigate this hypothesis by conducting a non-biased peptidome screen of urine collected pre-pregnancy, at gestational day (GD) 12 and 18.

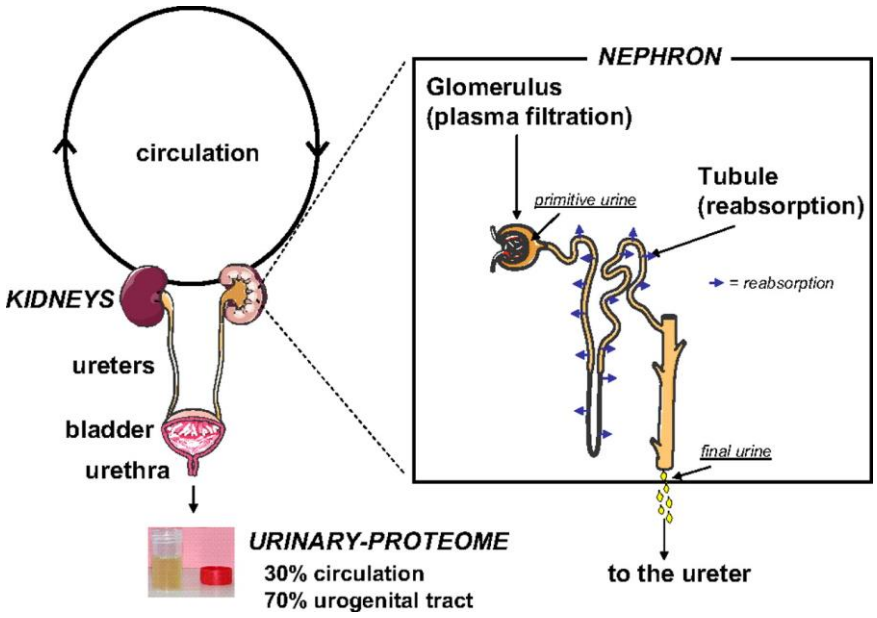

Figure 6-2 The urinary peptidome.

The kidney filters plasma from the circulation which then passes through the tubules where water and small molecules are reabsorbed and waste products are passed from the capillaries into the filtrate. The resulting urine is then representative of both the circulation and of local action at the kidney. Image from Decramer *et al.* (2008).

6.2 Materials & Methods

General materials & methods can be found in Chapter 2.

6.2.1 Animals

The work presented in this Chapter has used pregnant WKY and SHRSP that were untreated. Females were time mated at 12 weeks of age (± 4 days). Non-pregnant animals were age-matched at 15 weeks ± 4 days (i.e. 12 weeks of age + 21 days of pregnancy). The number of animals and particular gestational day (GD) is given in the associated Figure legend.

6.2.2 Histology

Preparation of paraffin blocks and sections were carried out as described in section 2.6.1.

6.2.2.1 Periodic acid-Schiff Stain

Sections of 2 µm where used for periodic acid – Schiff stain to stain the basement membrane of the kidney for morphological scoring. Slides were cleared and rehydrated as described in section 2.6.1. Slides were incubated in 0.5 % periodic acid (Sigma-Aldrich, Dorset, UK) in dH_2O for 15 minutes to oxidise aldehyde groups followed by 3 changes of dH_2O. Slides were then stained with Schiff's reagent (Sigma-Aldrich, Dorset, UK) for 15 minutes which reacts with the oxidised aldehyde groups to form a magenta dye followed by a wash in warm running tap water for 1 minute and two changes of dH_2O. Sections were counter-stained using Gill's haematoxylin (Sigma-Aldrich, Dorset, UK). This was followed by a 1 minute wash under running tap water and dehydration through an ethanol gradient (95%, 2 x 100%; 5 minutes each). Slides were cleared in histoclear 2 x 5 minutes and mounted using DPX (Sigma-Aldrich, Dorset, UK).

6.2.2.2 Histological analysis of the kidneys

Slides were visualised using an Aperio Slide Scanner (Leica Biosystems, Milton Keynes, UK) at 20x magnification by Clare Orange at the Queen Elizabeth University Hospital pathology unit. Images were downloaded from Leica Digital Image Hub then analysed using Image J by two independent operators who were blinded to the identity of the sections. Measurement of the cortex and medulla area was carried out by drawing around the relevant area and calculating the number of pixels. Glomerular density was counted as the number of glomeruli/ 10x field of view in 25 fields of view/section. Glomerular diameter was measured using 4 lines/glomerulus in 25 glomeruli/section. Glomerular lobule count was conducted manually in 25 glomeruli/section.

6.2.3 Urinary Peptidomics

6.2.3.1 Urinary Peptidome Extraction

700 µl aliquot of urine was diluted with 700 µl of 2 M urea and 0.1 M NH_4OH containing 0.02% SDS. A size cut-off for peptides <20 kDa was carried out using Centrisart ultracentrifugation filter devices (Sartorius, Gottingen, Germany) at 3000 x g for 1 hour at 4 ^oC. To remove urea, electrolytes, and salts the filtrate was then ran through a PD-10 desalting column (Amersham Bioscience,

Buckinghamshire, UK) and peptide elution was done using 0.01 % aqueous NH_4OH. Finally, all samples were lyophilized, stored at 4 °C, and resuspended in high-performance liquid chromatography grade H_2O to a final concentration of 2 µg/µl before analysis.

6.2.3.2 Capillary Electrophoresis-Mass Spectrometry (CE-MS) for Peptide Detection

CE-TOF-MS analysis was performed using a P/ACE MDQ CE sytem (Beckman Coulter, Fullerton, USA) online coupled to a microTOF MS (Bruker Daltonic, Bremen, Germany) as described in (460). Samples were injected with 2 psi for 99 seconds (250 nl) and separation of peptides in the cartridge maintained at 25 ºC was attained at 25 kV for 30 minutes and increasing pressure (0.5 psi) for another 35 minutes. The sheath liquid consisted of 30% isopropanol, 0.4% formic acid in HPLC grade water, and running buffer consisted of 79:20:1 (v/v) water, acetonitrile and formic acid. The ESI sprayer (Agilent Technologies, California, USA) was grounded and the ion spray inference potential was set at -4,5 kV. Spectra were accumulated over a mass-to-charge ratio of 350-3000 for every 3 seconds.

Peak picking, deconvolution, deisotoping of mass spectral ion peaks were processed using MosaiquesVisu software (461). The CE-migration time and ion signal intensity were normalized based on reference signal from internal peptide standards/calibrants (peptides from housekeeping proteins) in rats (462). For calibration, a local regression algorithm was applied with calibrants. The peak list generated for each peptide consisted of molecular weight (kDa) and normalized CE migration time (minutes) and normalized signal intensity. The peptide list from all the samples that passed the quality control criteria were compared and annotated in a Microsoft SQL database. The criteria for clustering peptides in different samples were: (i) mass deviation less than ± 50 ppm for small peptide (<800 Da) and gradually increasing to ±75 ppm for larger peptides (20 kDa) (ii) CE-migration time deviation with linear increase from ±0.4 to ±2.5 min in the range from 19-50 minutes. Each peptide was given a unique identification number (Peptide ID). Peptides detected with the frequency of ≥70 % in at least one group were considered for further analysis. Peptides were considered significant

according to Wilcoxon rank-sum test ($p < 0.05$) followed by adjustment for multiple testing (Benjamini and Hochberg).

6.2.3.3 Liquid Chromatography- Tandem Mass Spectrometry (LC-MS/MS) for Peptide Sequencing

The peptide mixture extracted for CE-MS were also used for sequencing of the peptides in LC-MS/MS. Sequencing was performed on an Ulitmate 3000 nano-flow system (Dionex/LC Packings, USA) connected to an LTQ Orbitrap hybrid mass spectrometer (Thermo Fisher Scientific, Germany) equipped with a nano-electrospray ion source. After loading (5 µl) onto a Dionex 0.1 × 20 mm 5 µm C18 nano trap column at a flowrate of 5 µl/min in 98 % 0.1 % formic acid and 2 % acetonitrile, sample was eluted onto an Acclaim PepMap C18 nano column 75 µm × 15 cm, 2 µm 100 Å at a flow rate of 0.3 µl/min. The trap and nano flow column were maintained at 35 °C. The samples were eluted with a gradient of solvent A: 98 % 0.1 % formic acid, 2 % acetonitrile verses solvent B: 80 % acetonitrile, 20% 0.1 % formic acid starting at 1 % B for 5 minutes rising to 20 % B after 90 minutes and finally to 40 %B after 120 minutes. The column was then washed and re-equilibrated prior to the next injection.

The eluant was ionized using a Proxeon nano spray ESI source operating in positive ion mode into an Orbitrap Velos FTMS (Thermo Finnigan, Bremen, Germany). Ionization voltage was 2.6 kV and the capillary temperature was 200°C. The mass spectrometer was operated in MS/MS mode scanning from 380 to 2000 amu. The top 20 multiply charged ions were selected from each scan for MS/MS analysis using CID at 35% collision energy. The resolution of ions in MS1 was 60,000 and 7,500 for CID MS2.

MS and MS/MS data files were searched, in this case, against the Uniprot mouse non-redundant database using SEQUEST (Thermo Proteome Discoverer) with non-specific enzyme as enzyme specificity. Peptide data were extracted using high peptide confidence and top one peptide rank filters. A peptide mass tolerance of ± 10 ppm and a fragment mass tolerance of ± 0.8 Da. Determine the false discovery rates by reverse database searches and empirical analyses of the distributions of mass deviation, whereby Ion Scores can be used to establish score and mass accuracy filters.

6.2.4 Quantitative PCR (qPCR) for *Umod* Expression

Gene expression for Umod was carried out using the following probes from Thermo Fisher, Paisley, UK: *Umod* (Rn01507237_m1) and *Actb* (4352340E).

6.3 Results

6.3.1 The SHRSP Kidney is increased in Size Relative to the WKY but does not Exhibit Histological Abnormalities

Post-mortem kidney weight was increased in both NP and GD18 SHRSP relative to WKY (Fig. 6-6A). PAS staining was then used to examine the kidneys histologically (Fig. 6-6B). There was a trend towards an increase in the size of the medulla region in NP SHRSP relative to NP WKY ($p = 0.059$); however there was no significant strain difference between pregnant animals (Fig. 6-6C). In contrast, cortex size was significantly increased in pregnant SHRSP relative to pregnant WKY but with no difference in NP animals (Fig. 6-6D).

Further histological analysis was implemented to examine the glomeruli and for evidence of hypertension-associated pathology. Firstly, the anatomical distribution and structure of the glomeruli was analysed (Fig. 6-7A). Glomerular density in the cortex was increased in the SHRSP relative to WKY at both NP and GD18 time points (Fig. 6-7B). The number of glomerular lobules was decreased from NP to GD18 WKY but was not significantly different between NP and GD18 SHRSP or between strains (Fig. 6-7C). There were no significant strain-dependent or pregnancy-dependent differences in glomerular diameter (Fig. 6-7D).

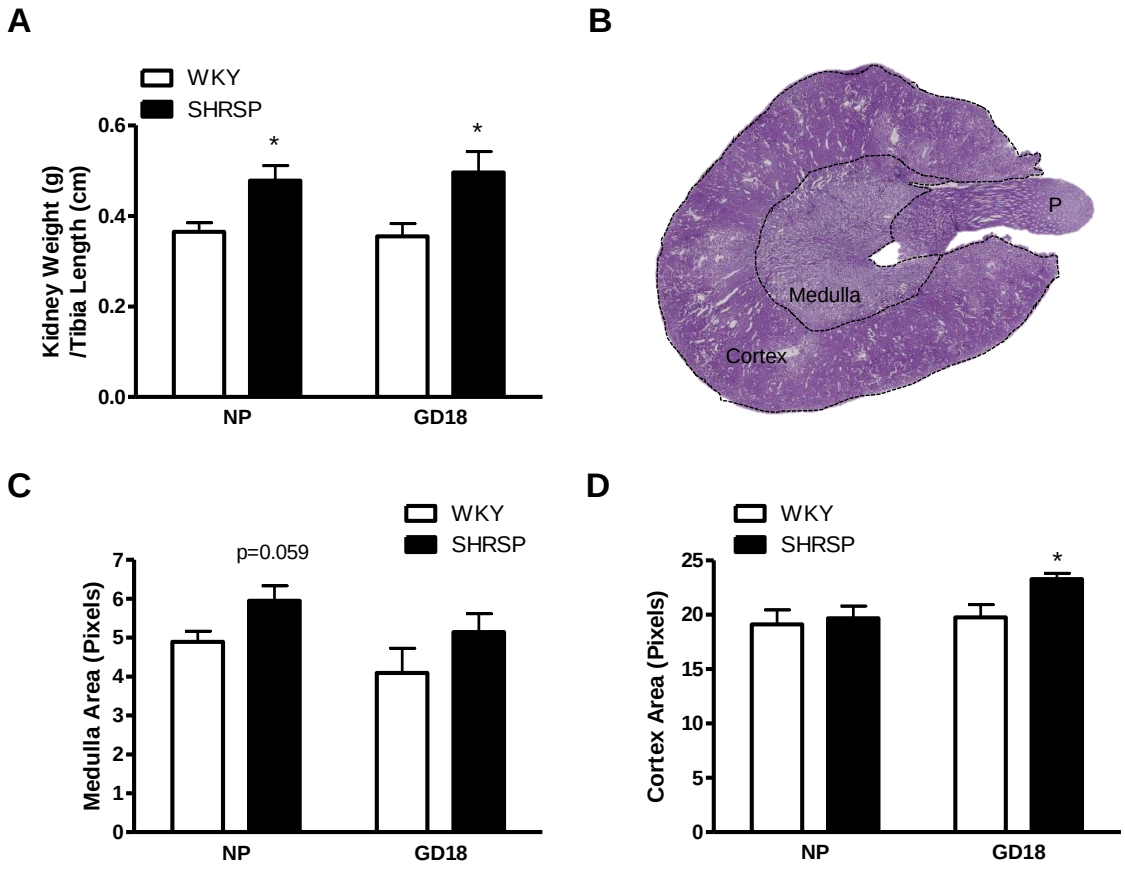

Figure 6-3 Kidney size is increased in non-pregnant and pregnant (GD18) SHRSP relative to WKY.

Post-mortem kidney weight was found to be increased in both non-pregnant (NP) and pregnant (GD18) SHRSP relative to WKY (* $p<0.05$ vs. WKY analysed by Student's t test) (A). Kidneys were then analysed histologically using periodic acid-Schiff stain (representative image B) in NP and GD18 WKY and SHRSP (n=4-6). Medulla area showed a trend to be increased in NP SHRSP ($p=0.059$ analysed by Student's t test) but not in pregnant animals (C). Cortex area did not show strain-dependent differences in NP animals but was increased in GD18 SHRSP relative to WKY (* $p<0.05$ vs. GD18 WKY analysed by Student's t-test). P: papilla.

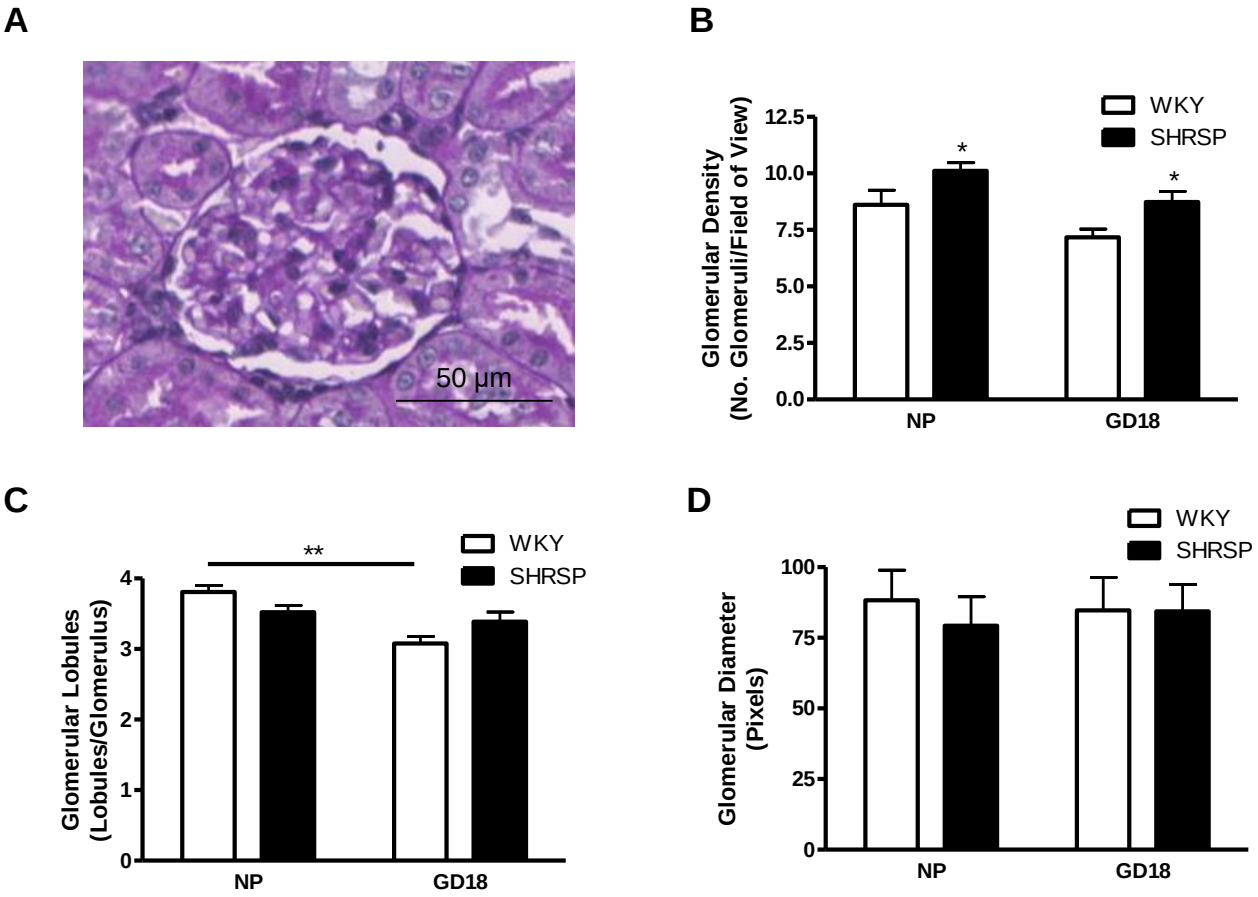

Figure 6-4 Glomeruli distribution is altered in non-pregnant and pregnant (GD18) SHRSP relative to WKY.

The distribution and anatomical structure of the glomeruli (A) was quantified in kidney sections from non-pregnant (NP) and GD18 WKY and SHRSP (n=4-6). Glomerular density was increased in a strain dependent manner in the SHRSP and was not affected by pregnancy (* $p<0.05$ vs. WKY analysed by Student's t-test) (B). Glomerular lobules were decreased from NP to GD18 WKY (** $p<0.01$ vs. GD18 WKY analysed by Student's t-test) but this change was not significant in the SHRSP (C). There were no strain-dependent or pregnancy-dependent changes in glomerular diameter (D).

Detailed inspection of the slides was performed to examine pathologies associated with systemic hypertension and hypertensive pregnancy: namely capillary occlusion, protein resorption droplets and vasculopathy. There were no major pathologies detecTable in the kidney sections in a strain-dependent or pregnancy-dependent manner (Fig. 6-8A-B). There was a trend for the diameter of the vessels supplying the kidney to be increased between NP and pregnant animals in both strains but this could not be formally quantified as these samples were not collected by perfusion-fixation (Fig. 6-8B).

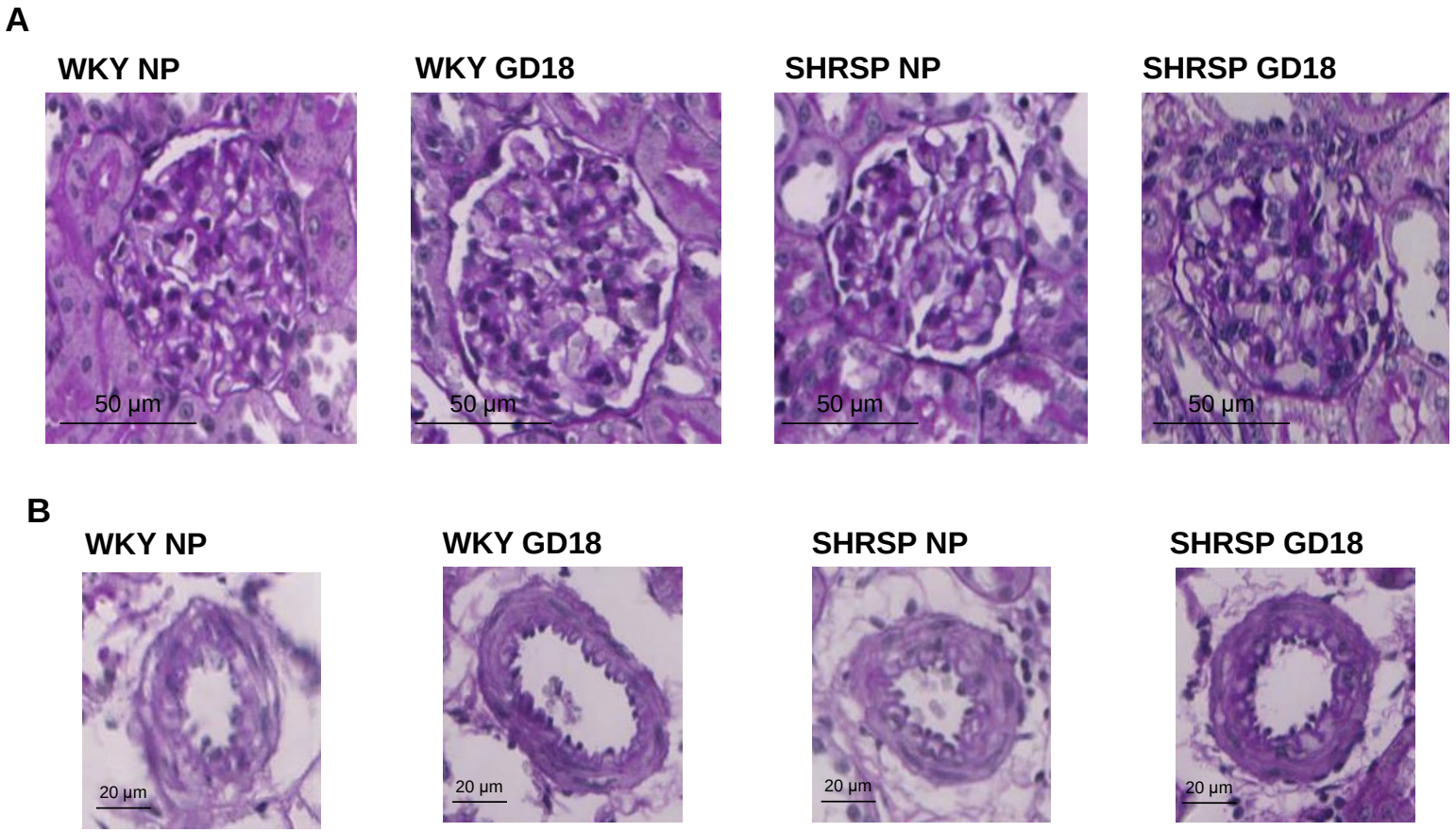

Figure 6-5 The SHRSP does not show histological abnormalities in the glomeruli or vessels of the kidney

Kidney sections from non-pregnant (NP) and GD18 WKY and SHRSP were stained with periodic acid-Schiff stain and inspected for pathology (n=4-6). No noTable changes in glomerular structure were detected in a strain or pregnancy dependent manner (A). There was no evidence of vasculopathy; however there was a trend for vessel size to increase during pregnancy in both strains (C).

6.3.2 The Urinary Peptidome is altered during Pregnancy and between WKY and SHRSP

A peptidome screen was performed in WKY and SHRSP urine at pre-pregnancy, GD12 and GD18 to identify strain, pregnancy and disease-dependent alterations (Fig. 6-9). The various comparisons were: (i) WKY against various gestational days, (ii) SHRSP against various gestational days and (iii) comparison between WKY and SHRSP at a given gestational day (Fig. 6-10). The longitudinal comparison (i and ii) within the WKY and SHRSP) resulted in identification of 630 and 739 peptides respectively, which were considered to be strain- and pregnancy-dependent alterations (Fig. 6-10). While the comparison between WKY and SHSRP resulted in 788 peptides which were differentially expressed in a disease-specific manner and were taken forward for further study (Fig. 6-10).

The 788 disease-specific peptide markers (Appendix III) were further evaluated using repeated measure ANOVA. Peptides were grouped by their pattern of gestation-dependent regulation where some were significantly altered at all time points, a single time point or at two different time points (Table 6-1).

The peptides which showed significantly different expression at all gestational days or at GD12 and GD18 only (marked in bold on Table 1-1) were considered for further analysis. These 123 peptides were investigated for their gestation-dependent regulation pattern between strains with cut-off criteria of ≥1.5 fold change and $p \leq 0.05$ (Appendix IV). Principal component analysis (PCA) on the peptide intensities for the 123 differential peptides was performed (Fig. 6-11) which was able to differentiate between samples. The heat map was also plotted for these 123 differentially expressed peptides to observe peptide clusters with common patterns of regulation (Fig. 6-12). Compared to WKY, SHRSP consisted of 7 and 39 peptides up- and down-regulated, respectively, at pre-pregnancy, GD12 and 18. Also, 36 peptides were up-regulated and 41 peptides were down-regulated in SHRSP at GD12 and GD18. Of the 123 peptides, 35 were able to be sequenced using LC-MS/MS (Appendix V).

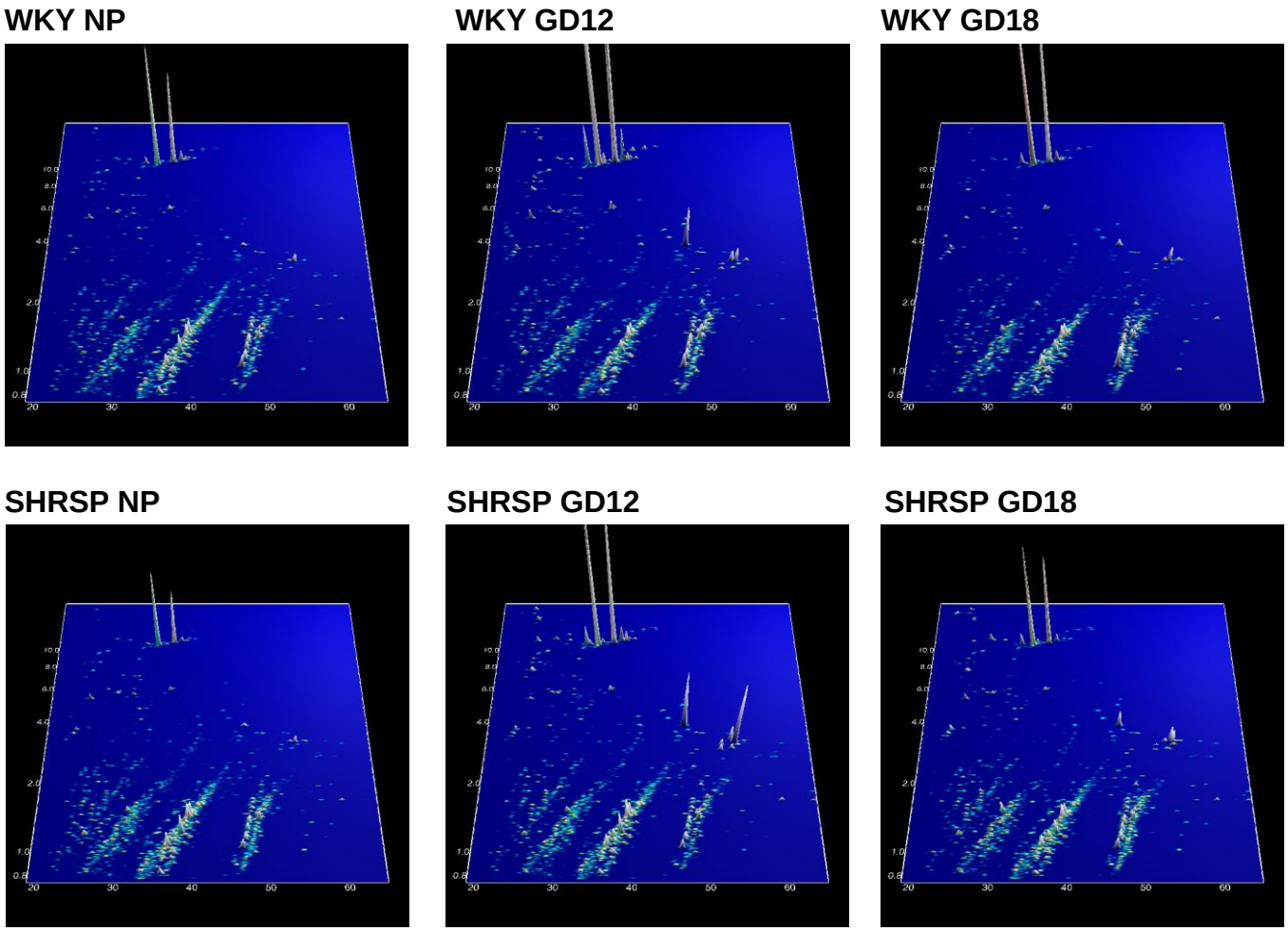

Figure 6-6 Contour plots for peptide mass fingerprint in WKY and SHRSP at pre-pregnancy (NP), gestational day (GD) 12 and 18. The x-, y- and z-axis represents CE-migration time, mass-to-charge ratio and peptide peak intensities, respectively.

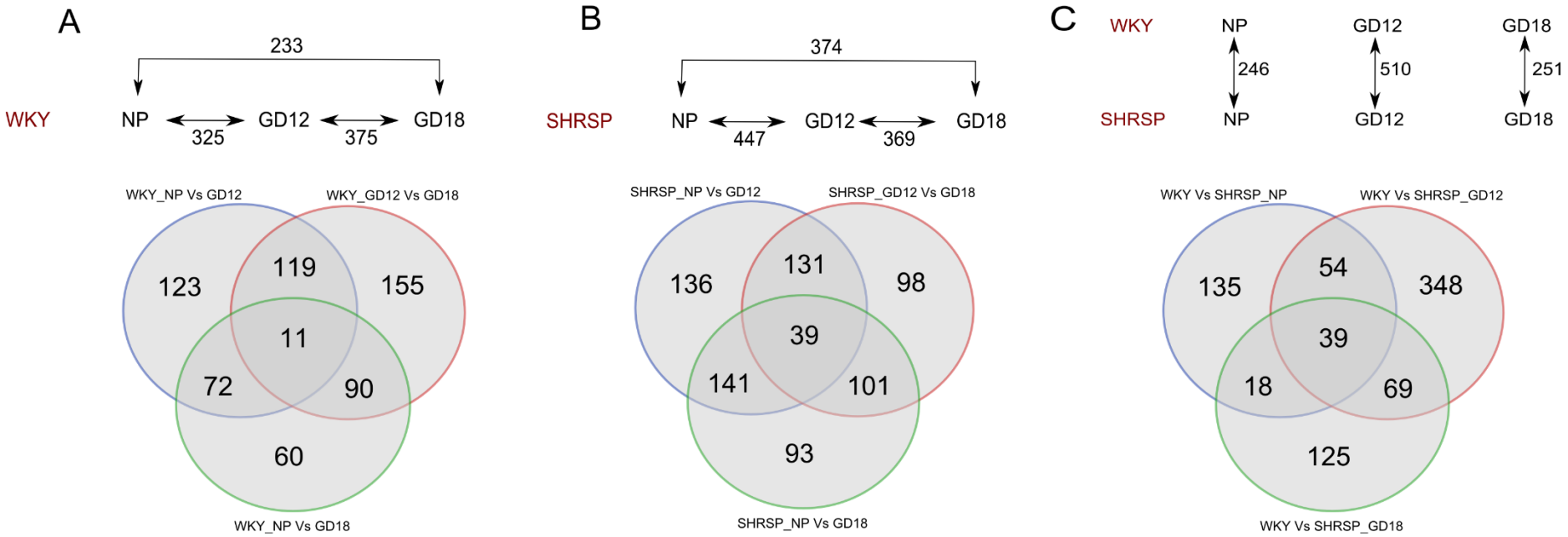

Figure 6-7 Venn diagram for various comparisons.

Figures show Venn diagram comparison for (A) comparison within WKY strain against various gestational days, (B) comparison within SHRSP strain against various gestational days and (C) comparison between WKY and SHRSP at a given gestational day. The numbers represent the number of significant differential peptides.

Table 6-1 Number of differentially expressed peptides between WKY and SHRSP at different gestational time point comparisons

Regulation Pattern	Number of peptides
NP, GD12 and GD18	**46**
NP and GD12	63
GD12 and GD18	**77**
NP and GD18	23
NP	104
GD12	285
GD18	99

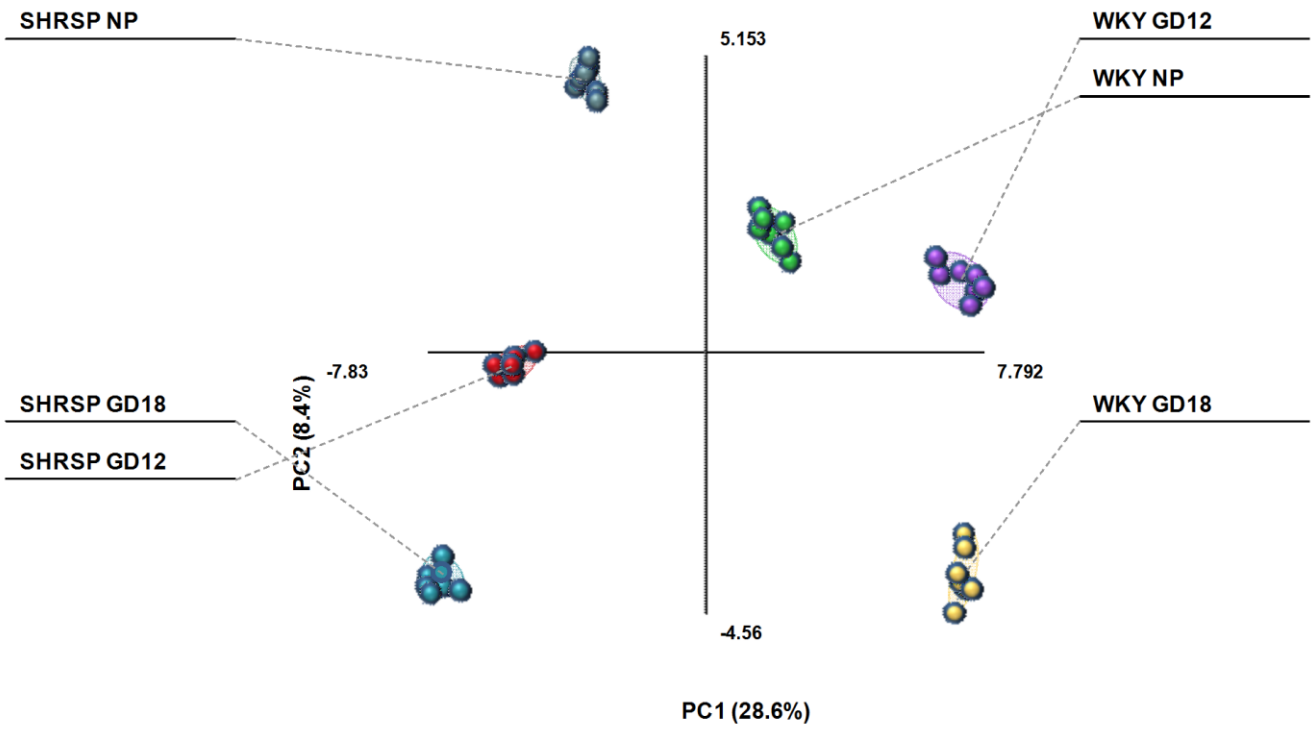

Figure 6-8 Principal component analysis of 123 differentially expressed peptides in WKY and SHRSP at pre-pregnancy (NP), gestational day (GD) 12 and 18.

The first principal component (PC1: strain) accounted for 28.6 % of total variance. The second principal component (PC2: gestation) accounted for 8.4 % of total variance. The cumulative variance of components was 43 %. Samples included in analysis were n=7 for each group represented by the labelled, coloured circles. Loading variables were the 123 differentially expressed peptides.

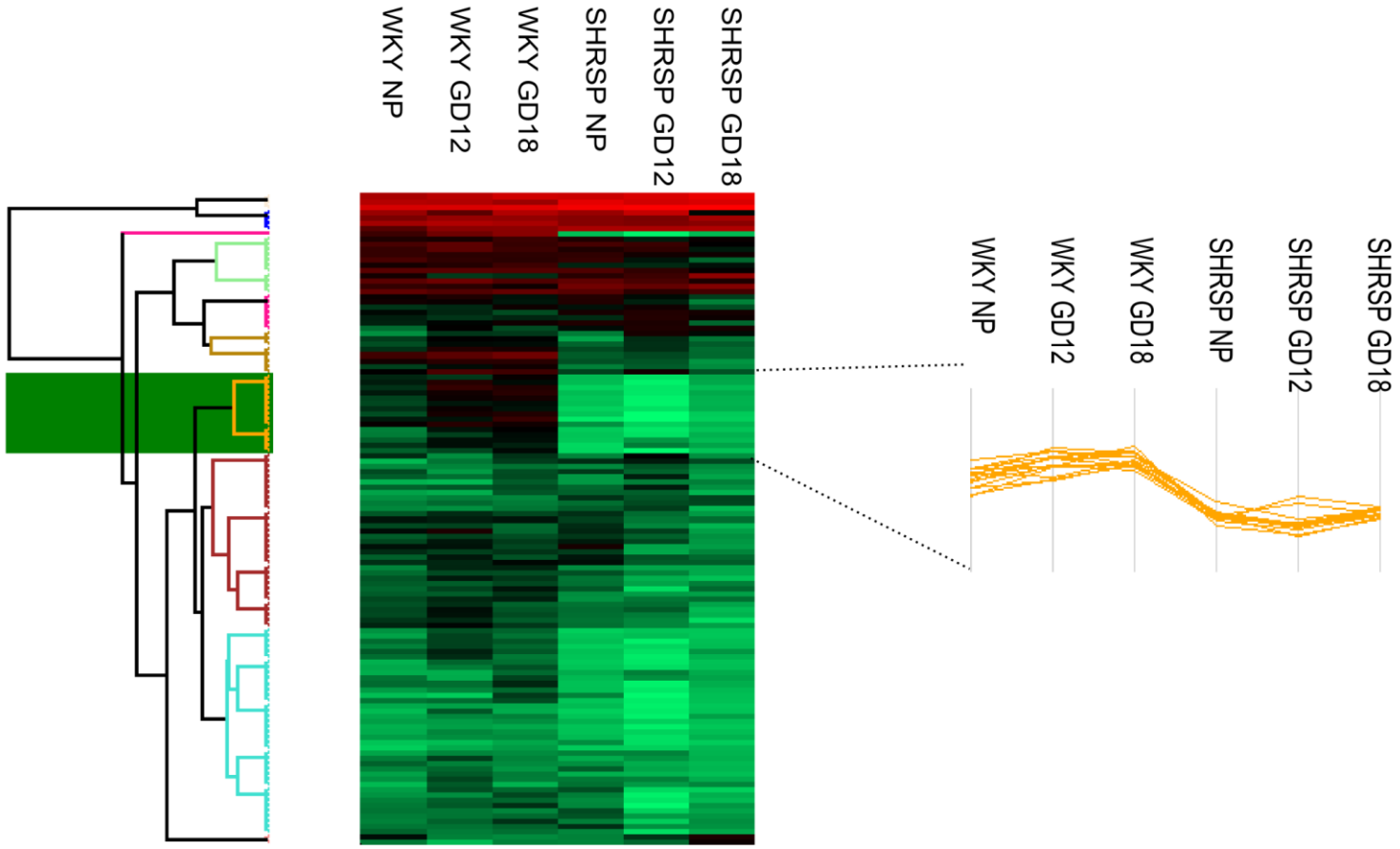

Figure 6-9 Heat map analysis of 123 differentially expressed peptides in WKY and SHRSP at pre-pregnancy (NP), gestational day (GD) 12 and 18.

Peptides were clustered in the heat map according to their gestation-dependent pattern of regulation. Intensities were converted to a logarithmic scale (Log_2) and the colour code represents the peptide intensity green (3) through black to red (14).

6.3.3 Uromodulin is increased in the Urine and Kidney of Pregnant SHRSP relative to WKY

Sequencing by LC-MS/MS was carried out on the 123 differentially expressed peptides where 35 were successfully sequenced and aligned to the rat protein database using UniProt (Appendix V). From these sequenced peptides, those derived from the protein uromdulin were found to be significantly increased in the SHRSP relative to the WKY in a pregnancy-dependent manner (Fig. 6-13). As uromodulin has previously been identified as a candidate molecule involved in renal dysfunction and hypertension, this was chosen to be investigated further.

Gene expression of *Umod* was measured in the kidney to investigate whether the increase in urinary uromodulin in the SHRSP could be derived from this tissue. *Umod* gene expression was increased in kidney tissue from SHRSP at pre-pregnancy (NP) and GD18 (Fig. 6-14).

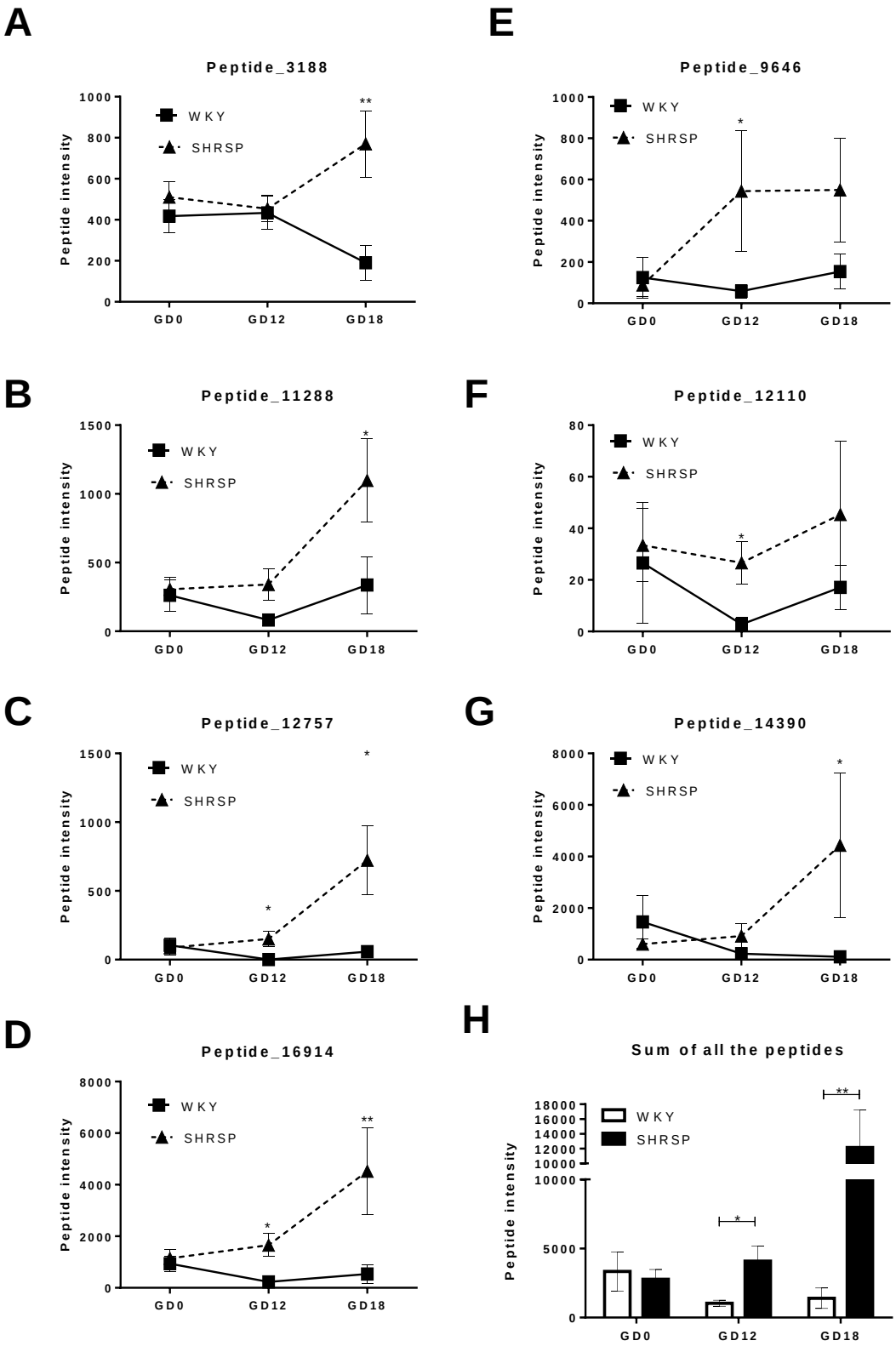

Figure 6-10 Urinary uromodulin peptides are increased in the SHRSP relative to WKY in a pregnancy-dependent manner.

Seven peptides (3188, 9646, 11288, 12110, 12757, 14390 and 16914) detected in the urinary peptidome were derived from uromodulin protein (A-G). Of these peptides, they were all increased in a pregnancy-specific manner in SHRSP (n=7) relative to WKY (n=7) at GD12, GD18 or GD12 and 18.Taking into account the sum of all of the seven peptides (H) showed that uromodulin peptides were increased in a pregnancy-specific manner at GD12 and GD18 in SHRSP relative to WKY (* $p<0.05$, ** $p<0.01$ vs. WKY analysed by Student's t test).

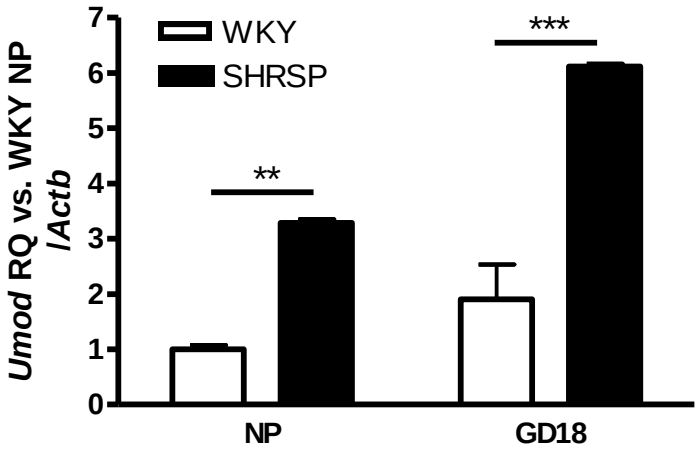

Figure 6-11 Gene expression of *Umod* in kidney tissue from WKY and SHRSP pre-pregnancy (NP) and gestational day (GD) 18.

Gene expression of *Umod* was measured in kidney tissue from non-pregnant and pregnant (GD18) WKY and SHRSP (n=5). *Umod* expression was increased in kidney tissue from SHRSP at both NP and GD18 time points (** $p<0.01$, *** $p<0.005$ vs. WKY analysed by one-way ANOVA).

6.4 Discussion

The work presented in this chapter shows that SHRSP exhibit strain-dependent and pregnancy-dependent alterations in the urinary pepidome. Uromodulin was identified to be increased in SHRSP in a pregnancy specific manner from this screen which was then validated at mRNA level in the kidney.

histological analysis was carried out to interrogate kidney structure. The SHRSP kidney weight was increased relative to the WKY in both non-pregnant and pregnant animals suggesting this was a strain-dependent difference; this has also been documented in this model previously (463). In-keeping with the increased post-mortem tissue weight; the cortex and medulla size was increased in SHRSP relative to WKY. However, cortex size was only increased in GD18 SHRSP compared to WKY and not in non-pregnant animals. Glomerular density was also significantly increased in both NP and pregnant SHRSP relative to WKY but there was no change in glomerular diameter between strains or during pregnancy. These measurements could have been improved by carrying out stereology on serial sections to determine glomerular volume. Close inspection of the kidney sections did not reveal any major pathology of the kidney vasculature or glomeruli in the SHRSP relative to the WKY. There was a trend for an increase in vessel size from NP to

pregnant animals in both strains however this could to be formally quantified as these tissues were not collected under perfusion fixation. This could be a worthwhile future study to investigate vascular remodelling in the kidney given the abnormal vascular function that has already been characterised in this model (349). It was perhaps not unexpected that there was no detectable glomerular damage by histological evaluation as it has been shown previously that male SHRSP do not develop kidney pathology until 1 year of age or this can be accelerated with salt treatment (464). Chronic hypertension during pregnancy in humans is not normally associated with renal damage unless these women go on to develop super-imposed preeclampsia. Therefore, the functional changes that have been detected in the SHRSP urine may be suggestive of a mild, pre-structural dysfunction of the kidney. Whether this itself is pathological and contributes to the reduction in plasma volume expansion in SHRSP or has a lasting effect on kidney function remains to be seen. A similar study looking at changes in urinary metabolites has not been conducted in women with chronic hypertension.

This study then went on to characterise the urinary peptidome in SHRSP and WKY at three time points: pre-pregnancy, mid-pregnancy (GD12) and late pregnancy (GD18). To identify relevant peptides, there was a focus on 123 peptides which were found to be differentially expressed between WKY and SHRSP at all time points (NP, GD12 and GD18) or at GD12 and 18 only. The 123 peptides were principally composed of collagen alpha chains, serum albumin, pro-thrombin, actin, serpin A3K, pro-epidermal growth factor and uromodulin. In comparison, in urinary peptidomic screens of women with preeclampsia the most common constituents are: albumin and tubular proteins which is thought to reflect renal tubule damage. However, a characteristic signature is yet to be determined despite a number of studies (451). As uromodulin has been previously highlighted to play a role in renal dysfunction and systemic arterial hypertension (465) this led us to investigate this molecule in the WKY and SHRSP.

Uromodulin was first isolated from the urine of pregnant women (466) and it's excretion is increased in a time-dependent manner over gestation in humans (467). All of the urinary uromodulin peptides detected in the screen were increased in a pregnancy-dependent manner in the SHRSP relative to the WKY. In a recent study which took an untargeted approach to study the urinary peptidome

in women with and without preeclampsia; the authors identified the exact same seven peptides as we have identified in our study to be increased in the preeclampsia group (468). The SHRSP pregnancy-dependent increase in uromodulin was validated by increased *Umod* gene expression in kidney tissue. However in contrast to the urinary peptide levels, there was also a significant increase in *Umod* gene expression from kidney tissue between WKY and SHRSP at a non-pregnant time point. Total levels of uromodulin peptides were significantly correlated with both urinary sodium and urinary albumin levels. Uromodulin acts at the thick ascending limb of the kidney to promote sodium retention through NKCC2 (465, 469). Therefore, the results in our study of a negative correlation between uromodulin peptides and urinary sodium are in-keeping with these findings. Future work should measure NKCC2 expression in non-pregnant and pregnant WKY and SHRSP.

In conclusion, SHRSP exhibit strain-dependent and pregnancy-dependent functional and structural alterations in the kidney relative to the WKY. This was associated with an altered urinary peptidome. The protein uromodulin, which has already been shown to have a role in systemic hypertension, has been highlighted in this pilot study as a potential protein of interest. These findings represent pre-clinical work which can be used as a starting point for similar studies specifically in pregnant women with chronic hypertension which remains an under-researched area.

Chapter 7 General Discussion

It is well established that chronic hypertension during pregnancy confers an increased risk for maternal and fetal morbidity and mortality (301, 305, 306). However, studies which solely focus on this growing clinical problem (303) are wanting. This work sought to establish a rat model of chronic hypertension in pregnancy utilising the SHRSP in order to investigate the pathological mechanisms involved in the vascular response to pregnancy. Previous work showed that the SHRSP exhibited deficient uterine artery remodelling in response to pregnancy which was associated with adverse pregnancy outcome at GD18 (349). The significant reduction of blood pressure using nifedipine from 6 weeks of age in the SHRSP did not improve these factors (349). Therefore, we hypothesised that the abnormal adaption to pregnancy in the SHRSP was due to other maternal cardiovascular risk factors.

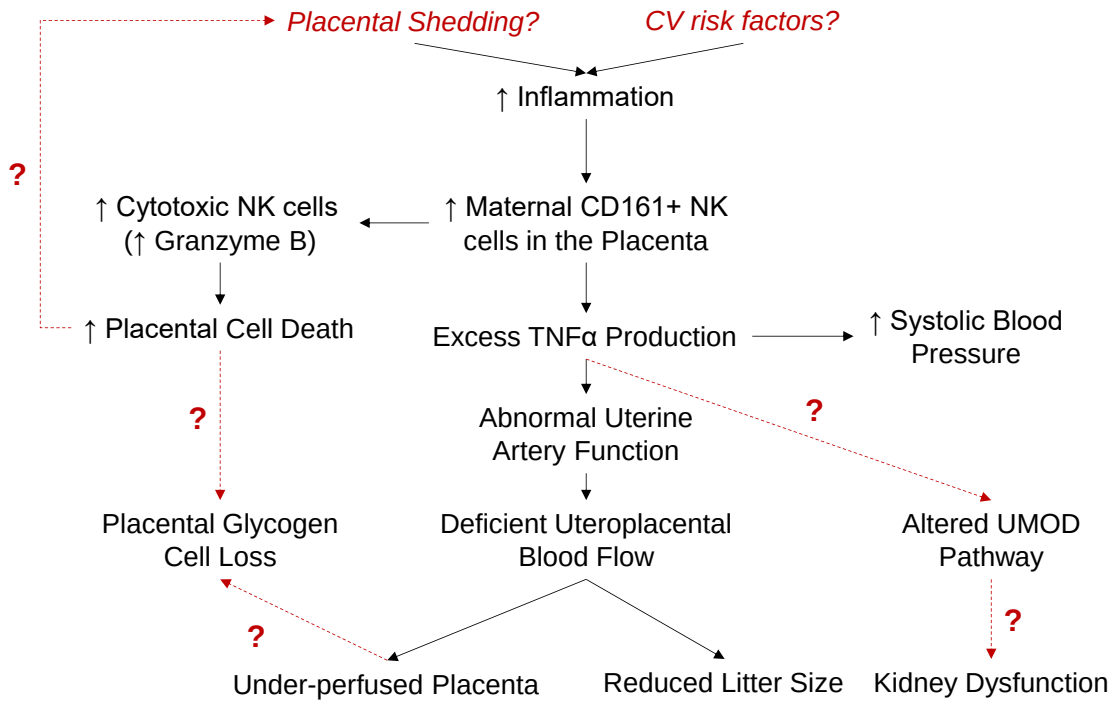

Figure 7-1 Excess TNFα in pregnant SHRSP is central to the pathology in this model.

The flow chart summarises the TNFα – dependent mechanism proposed in this thesis. Black arrows indicate conclusions that have been made from evidence presented in this thesis whereas red dashed arrows indicate that further work is required.

Inflammation is a central component of the phenotype in pregnant SHRSP; however the underlying cause remains to be elucidated (Fig. 8-1) Genetic mutations can lead to activation of the immune system in the context of human autoimmune diseases (470). Linkage analysis has also uncovered quantitative trait loci which contribute to circulating inflammatory biomarkers in clinical studies (471). Whilst linkage analysis has been carried out in the SHRSP and WKY to explore a genetic component for heart rate (472), left ventricular mass (473), hypertension (474) and renal injury (475) among other traits; components of inflammation have not been explored. Linkage analysis studies such as those discussed have generated a number of congenic strains. To date, pregnancy has not been studied in existing strains of congenic SHRSP or WKY. Linkage analysis for inflammation-associated phenotype may yield new loci involved in the regulation of the immune system in the SHRSP. The genome sequence is also available for the WKY and SHRSP which could be utilised to identify variants in, for example, the gene for TNFα which exist between the two strains. Such investigations may highlight a genetic contribution to adverse pregnancy outcome or inflammatory response in the SHRSP. Secondly, there could also be a physiological stimulus which leads to inflammation in the pregnant SHRSP. An increase in sub-cellular fragments or debris shed from the placenta can activate the maternal immune system (415). A preliminary investigation into shed placental cfDNA suggested that this could be a promising area of further study in this model. Placental DNA is hypomethylated at CpG islands (476) which differentiates it from maternal circulating DNA fragments. Hypomethylated DNA is recognised by TLR9 in humans (477) and this mechanism is conserved in rats (478). TLR9 is expressed on NK cells, among other immune cells, and could be measured in a future extracellular flow cytometry experiment in circulating maternal leukocytes from WKY and SHRSP.

Increased maternal inflammation in the SHRSP manifests itself as an increase in CD3- CD161+ NK cells. Etanercept treatment decreased the expression of CD161 and granzyme B in placental CD3- CD161+ NK cells thus limiting their cytotoxic ability. It has also been shown in this thesis that placenta from GD18 SHRSP have an increase in caspase 3 cleavage which indicates the induction of programmed cell death. NK cell mediated apoptosis results in up-regulation of caspase 3 cleavage (479) therefore it is reasonable to propose that the effectors

of increased cell death in the placenta are the CD3- CD161+ Granzyme B + NK cells which are increased in number in the SHRSP relative to WKY. Despite the appearance of significant necrosis by gross examination; there was no difference in placental weight between WKY and SHRSP at GD18. On histological analysis the glycogen cells in particular were depleted in the SHRSP. Why these cells in particular would be targeted for apoptosis or if they indeed were lost to increased cell death in the placenta of the SHRSP is unknown. There exists a technical difficulty in staining the glycogen cells with immunohistochemistry in that the thick matrix of glycogen stored within the cytoplasm of these cells traps the antibody and leads to false positive staining. With further optimisation, it would be beneficial to be able to stain the placenta for activated caspases using immunohistochemistry to localise this increase in cell death in the SHRSP placenta. Another mechanism for glycogen cell loss could be premature utilisation of the energy stores in SHRSP placenta to compensate for the reduced nourishment from deficient uteroplacental blood flow. Indeed, it could be a combination of both of these mechanisms whereby the glycogen cells are utilised and then the cells are targeted for apoptosis.

Excess TNFα is central to the pathology in pregnant SHRSP; etanercept treatment improved uterine artery function and blood flow as well as pregnancy outcome. UMOD was identified from the peptidomics screen to be increased in a pregnancy-specific manner in SHRSP. In clinical studies, urinary UMOD is increased in people with essential hypertension and correlated significantly with increased plasma biomarkers of inflammation including TNFα (480). Additionally, UMOD has the ability to bind cytokines, including TNFα (481). The expression of TNFα was not measured in kidneys from pregnant WKY and SHRSP nor was sodium assessed in etanercept treated animals. In answering these two questions, it may be possible that there is an interaction between UMOD, TNFα and sodium balance in the kidney during pregnancy in the SHRSP. An alternative mechanism of interest which links inflammation and UMOD is the sub-cellular localisation of the protein. UMOD plays a key role in the activation of the innate immune system at the kidney and has been shown to induce both monocytes and granulocytes to produce pro-inflammatory cytokines (482). UMOD, which is normally localised to the thick ascending limb of the kidney, can be found within immune complexes in the renal interstitial space in humans (483) and a rat model (484) of nephritis. When in the

interstitium, UMOD can interact with dendritic cells via TLR4 to mount a humoral immune response (485). Immunohistochemistry for UMOD in the kidney of WKY and SHRSP would be necessary to determine whether UMOD itself is involved in inflammation at the kidney.

The vascular work in this thesis has focussed predominantly on the uterine artery. As the SHRSP exhibits spontaneously deficient uterine artery remodelling it would be interesting to study the smaller, downstream vessels such as the radial and spiral arteries. Deficient remodelling of the radial arteries is a characteristic of human preeclampsia but not fetal growth restriction (486). Notably, the decrease in lumen size has been shown to be due to inward eutrophic remodelling (486). There was no change in wall thickness between uterine arteries from WKY and SHRSP; however this may not be the case for the smaller radial arteries as seen in this human study. Radial artery remodelling occurs in healthy pregnant rats with a 4.8 fold change in length and 60% change in lumen diameter reported (487). Radial arteries from pregnant rats either supply the myometrium or placenta; these two lineages have different vascular reactivity and relaxation response to NO (488) thus care must be taken with which vessel is isolated. Studies of the radial arteries in rat models of hypertensive pregnancy are limited. Using anti – peroxisome proliferator-activated receptor γ (PPARγ) treatment it is possible to induce a preeclampsia like syndrome in rats (489). Utilising anti- PPARγ from GD15 - 21 has been shown to significantly reduce endothelium dependent vasorelaxation of rat radial arteries (490). In addition, a recent study showed that testosterone treatment between GD15 - 19 in rats impairs radial artery remodelling (63).

Failure of the spiral arteries to remodel is a pathological hallmark of preeclampsia. Whilst women with chronic hypertension have an increased risk of developing preeclampsia; trophoblast invasion has never been explored in women with chronic hypertension. At the maternal-fetal interface, TNFα is expressed by decidual uNK cells, decidual macrophages, invading extravillous trophoblast (491) and intervillous cytotrophoblast (492). TNFα production from decidual leukocytes plays a key role in the regulation of trophoblast migration and programmed cell death as they invade into the uterine wall (491). However, increased levels of TNFα have been shown to reduce the migration of first trimester villous explant

cultures through up-regulation of plasminogen activator inhibitor 1 (PAI-1) (492-494). PAI-1 acts to inhibit the activation of plasminogen into plasmin which in turn prevents pro-MMPs being turned into MMPs; MMPs play a critical role in trophoblast invasion (495). In combination with IFNγ, the effects of TNFα were augmented such that trophoblast apoptosis was increased and proliferation and MMP secretion were also inhibited (492). This suggests that the balance of cytokines is important and that TNFα and IFNγ, both produced from NK cells, have synergistic effects. In addition, TNFα treatment also inhibited the integration of a trophoblast cell line (JEG-3) into an *in vitro* model of endothelial cell tube formation. In this case the mechanism was proposed to be through a failure of correct integrin expression (496). TNFα treatment has also been shown to promote trophoblast shedding from first trimester villous explants which induce endothelial cell activation in an *in vitro* model potentially linking placental inflammation and vascular dysfunction (497). As there is evidence of global inflammation in the SHRSP placenta a next step would be to treat VSMCs and endothelial cells with explant culture medium to assess molecular changes in these cell types.

Uterine uNK cells play a key role in remodelling the spiral arteries in humans and rodents. However, the CD3- CD161+ cells in this thesis are more representative of peripheral NK cells and not the uterine specific population of uNK cells. As there have been changes identified in the peripheral NK cell population it would be logical to explore uNK cells in the WKY and SHRSP. At present, there is no specific marker for rat uNK cells however these do exist in humans and mice. Immunohistochemistry for perforin has been used to identify uNK cells in rats (498). It has also been shown that the migration of uNK cells into the uterus precedes trophoblast invasion in the rat; indicating they may have a priming role to play for trophoblast invasion (499). Whilst the vascular remodelling capacity of uNK cells is subject of intense study; the role of peripheral NK cells in systemic vascular remodelling has not yet been reported in the literature. Leukocytes found in the perivascular adipose tissue have been shown to alter vascular function in obesity and cardiovascular disease (500). Recent work has also shown that perivascular adipose tissue surrounding mesenteric arteries from late pregnant (GD20) rats had a blunted (44%) contractile effect to phenylephrine. Leukocyte populations in perivascular adipose tissue during pregnancy have currently not been reported in the literature. Given the perturbation of peripheral

NK cells in the SHRSP and the role of TNFα in uterine artery dysfunction; investigation of NK cells in the perivascular adipose tissue of the uterine arteries may provide a closer link to inflammation and vascular dysfunction observed in this model.

NK cells were once thought to be a unique example of an innate lymphoid cell (ILC) however recent work has identified that, in fact, the NK cell belongs to a much larger family of ILCs which encompasses a number of smaller sub-sets. The ILC family are defined by their ability to produce T_h like cytokines but lack lineage-specific markers of other immune cell subtypes and a T cell receptor therefore do not respond in an antigen-dependent manner (501). Whilst work on ILC families in rats is currently non-existent within the literature; a number of studies have defined extracellular markers which differentiate between ILC subtypes in humans and mice (501). In particular, group 3 innate lymphoid cells (ILC3s) express the NK cell activating receptor NKp46 but do not express cytotoxic molecules such as perforin or granzymes or IFNγ and TNFα; instead they predominantly produce IL-22 (502). In the placenta of the SHRSP, a CD3- $CD161_{Low}$ Granzyme B- population was identified that was increased when SHRSP were treated with etanercept. This population of cells share a similarity with the ILC3 discussed. NKp46 expression is conserved on rat NK cells and serves as an activating receptor (503) however it could not be measured in this study as it is not a commercially available antibody. Further classification of this CD3- $CD161_{Low}$ Granzyme B- population of cells may show that these are not NK cells where CD161 expression has been reduced but the related ILC3.

The SHRSP is not a model of superimposed preeclampsia as it does not exhibit a pregnancy-specific rise in blood pressure or proteinuria. In another hypertensive rat strain, the Dahl S, the introduction of salt treatment (1.9 % NaCl in drinking water) from GD 15 onwards induced characteristics of preeclampsia (504). In addition, follow-up studies from this model have shown abnormal uterine artery function (505) and an increase in placental cell death (506). The SHRSP blood pressure is salt sensitive whereby treatment with 1 % NaCl in drinking water results in approximately a 30 mmHg increase (187). Female and male SHRSP respond to salt loading (1 % NaCl) differently. Male SHRSP show a significant increase in blood pressure after 2 months of salt treatment but no change after a further 5 months

of treatment. In female SHRSP, there was a rise in SBP after 1 month of treatment and a further gradual increase over the next 6 months of treatment (507). 4 % NaCl in drinking water of female SHRSP resulted in a 60 mmHg increase in SBP relative to the control group; however these rats started to exhibit stroke from 12 weeks and mortality rate was 100 % at 20 weeks of age (508). However, the salt sensitivity of blood pressure is subject to sub-strain dependent differences. The Glasgow sub-strain of SHRSP males exhibit almost 100% lethality after three weeks of treatment with 1% NaCl. Glasgow female SHRSP are less salt sensitive and tend to survive longer than 3 weeks on 1% NaCl (Dr. Delyth Graham, Personal Communication). Therefore, for future studies using salt loading in pregnant SHRSP both the sub-strain used and the dose of NaCl should be carefully considered. From the findings of this thesis, inflammation has been shown to be a causative factor for pathology in the pregnant SHRSP. A recent editorial highlighted a potential role of salt and activation of the immune system in hypertensive pregnancy (509). A mechanism involving macrophages has recently been shown to be able to regulate intradermal storage of sodium (510). Increased salt has also been shown to activate T_h17 cells, a pro-inflammatory cell type, in a rat model of autoimmune disease (511). T_h17 cells in the placenta have been shown to play a role in preeclampsia and adverse pregnancy outcome as well as interacting with NK cells at the maternal-fetal interface (512). Therefore, a reasonable hypothesis is that salt treatment may worsen the inflammatory phenotype seen in pregnant SHRSP. IL-17 production in the SHRSP placenta was not measured and this should be taken into account in a future salt study in light of this this evidence.

Chronic hypertension during pregnancy has been a relatively neglected area of research. In Figure, 7-2, PubMed was used to search for the terms “chronic hypertension pregnancy” and “pre-eclampsia/preeclampsia” from 2004 to 2014 as a crude marker to quantify research output in each area. PubMed hits for preeclampsia were of a 7-10 magnitude higher than those hits for chronic hypertension (Fig. 7-2). In addition, whilst research output in pre-eclampsia underwent a steep increase between 2010 and 2014; chronic hypertension research has stayed relatively sTable (Fig. 7-2). There are a few reasons to explain this trend. From the available literature, poorer outcomes for maternal and fetal morbidity and mortality occur in mothers with pre-eclampsia than in mothers with

chronic hypertension alone (306) which has driven the need to prioritise preeclampsia research. However, women with maternal chronic hypertension are a growing population (302) whereas total cases of preeclampsia have been shown to have a relatively sTable incidence over the last 30 years in the developed world (513). Women with chronic hypertension are also more commonly included as a sub-group in part of a bigger preeclampsia study. Indeed, women with chronic hypertension also have a higher risk of developing superimposed preeclampsia where the risk is that they are inappropriately included in a preeclampsia cohort. As recent meta-analysis and editorials indicate there is an acute need to develop clinical and pre-clinical work which focusses on pre-existing maternal cardiovascular disease and how this affects pregnancy outcome (305, 306, 310). Additionally, no large patient cohort currently exists which specifically examines women with maternal chronic hypertension.

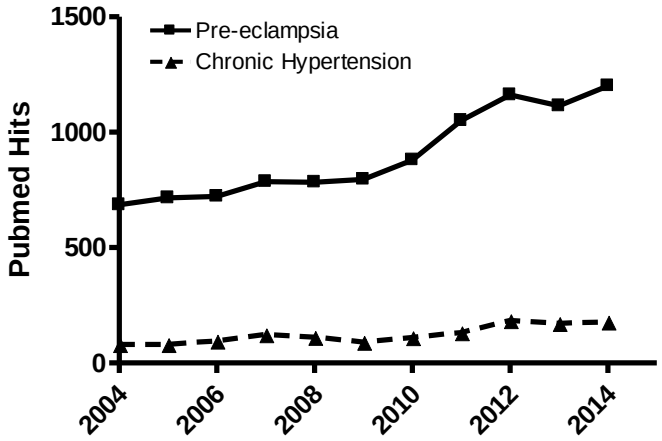

Figure 7-2 PubMed hits comparing search terms for “pre-eclampsia/preeclampsia” and “chronic hypertension pregnancy”.
Data accessed and compiled by the author using PubMed (http://www.ncbi.nlm.nih.gov/pubmed) on the 2/12/15.

Whilst there is no immediate novel clinical treatment which can be derived directly from the findings presented in this thesis; the translational value lies in elucidating a novel TNFα-dependent mechanism in the first pre-clinical rat model of maternal chronic hypertension which can act as a stimulus for future clinical studies. In addition, observations from such human studies can now be tested in a well-characterised model yielding the elucidation of novel clinically-relevant mechanisms in this previously under-researched area.

Appendix I: Laboratory-Prepared Solutions

Acidified Ferrocyanide Reagent

Prepare reagent A and B separately.

To make 200 ml:

- Reagent A 4 % potassium ferrocyanide in dH_2O (w/v): 4g potassium ferrocyanide (K4Fe(CN)6 · 3H2O; Sigma-Aldrich, Dorset, UK) dissolved in 100 ml dH_2O.
- Reagent B 4 % hydrochloric acid in dH_2O (v/v): 4 ml concentrated HCl (36.5 – 38.0 %; Sigma-Aldrich, Dorset, UK) diluted in 100 ml dH_2O.

Mix reagents A and B immediately before adding to slides.

Must be made fresh each experiment.

Flow Cytometry Wash Buffer

To make 500 ml:

Dilute 10 ml fetal bovine serum (FBS) in 490 ml dH_2O.

Must be made fresh each experiment.

Phosphate Buffered Saline 10x

To make 1 l:

Dissolve

NaCl (Sigma-Aldrich, Dorset, UK) 80 g

KCl (Sigma-Aldrich, Dorset, UK) 2.0 g

Na_2HPO_4 (Sigma-Aldrich, Dorset, UK) 14.4 g

KH_2PO_4 (Sigma-Aldrich, Dorset, UK) 2.4 g

in 800 ml dH_2O.

Adjust pH to 7.4.

Top up to 1 l with dH_2O.

Can be kept at room temperature up to 24 months.

Phosphate Buffered Saline 1x

To make 1 l:

Dilute 100 ml of Phosphate buffered saline 10 x in 900 ml of dH_2O.

Can be kept at room temperature up to 24 months.

Physiological Salt Solution

Prepare stock solution A and B which can be kept at 4ºC for up to 3 months.

- To make 1 l PSS Stock Solution A: Dissolve 139.1 g NaCl, 7.0 g KCl and 5.92 g $MgSO_4$ (all Sigma-Aldrich, Dorset, UK) in 1 l dH_2O.

- To make 1 l PSS Stock Solution B: Dissolve 42 g NaHCO3 and 3.2 g KH2PO4 (all Sigma-Aldrich, Dorset, UK) in 1 l dH2O.

To make 2 l physiological salt solution:

Dilute 100 ml Stock Solution A

100 ml Stock Solution B

in 500 ml dH_2O.

Dissolve 4 g glucose (Fisher Scientific, Loughborough, UK).

Bubble in 95 % O_2 5% CO_2 for 5 minutes.

Add 5 ml $CaCl_2$ (Fisher Scientific, Loughborough, UK).

Can be kept 4°C for up to 3 days.

Physiological Salt Solution: Calcium Free

To make 1 l physiological salt solution calcium free:

Dilute 50 ml PSS Stock Solution A

50 ml PSS Stock Solution B

in 500 ml dH_2O.

Dissolve 2 g glucose (Fisher Scientific, Loughborough, UK).

Bubble in 95 % O_2 5% CO_2 for 5 minutes.

Add 0.5 ml 23 mM EDTA (Sigma-Aldrich, Dorset, UK).

Can be kept 4°C for up to 3 days.

Physiological Salt Solution: High Potassium

- Prepare 500 ml Special PSS Stock Solution A: Dissolve 92.23 g KCl and 100 ml $MgSO_4$ (all Sigma-Aldrich, Dorset, UK) in 500 ml dH_2O.

To make 500 ml physiological salt solution high potassium:

Dilute 25 ml Special PSS Stock Solution A

25 ml PSS Stock Solution B

in 300 ml dH_2O.

Dissolve 1 g glucose (Fisher Scientific, Loughborough, UK).

Bubble in 95 % O_2 5% CO_2 for 5 minutes.

Add 1.25 ml $CaCl_2$ (Fisher Scientific, Loughborough, UK).

Can be kept 4°C for up to 2 months.

RIPA Buffer

Prepare 10ml stock solutions of:

- 1 M Tris-HCl: Dissolve 1.21 g Tris-HCl (Fisher Scientific, Loughborough, UK) in 10 ml dH_2O.
- 5 M NaCl: Dissolve 2.9 g NaCl (Sigma-Aldrich, Dorset, UK) in 10ml dH_2O.
- 0.5 M EDTA: Dissolve 1.86 g EDTA (Sigma-Aldrich, Dorset, UK) in 10 ml dH_2O.

To make 100 ml of RIPA buffer, add:

Sodium deoxycholate (Fisher Scientific, Loughborough, UK) 0.5g

1 M Tris-HCl 5 ml

5 M NaCl 3 ml

0.5 M EDTA 0.2 ml

to 75 ml of dH_2O.

Adjust pH to 8.8.

Add: SDS 0.1 g

NP-40 1ml

Top up to 100ml.

Sodium Citrate Buffer

Prepare two stock solutions which can be kept at 4ºC for up to 6 months.

- To make 500 ml 0.1 M citric acid: Dissolve 10.5 g citric acid (Sigma-Aldrich, Dorset, UK) in 500 ml dH_2O.
- To make 500 ml 0.1 M trisodium citrate: Dissolve 14.7 g trisodium citrate (Sigma-Aldrich, Dorset, UK) in 500 ml dH_2O.

Make 0.01 M citrate buffer fresh on the day of experiment. To make 500ml:

Dilute 9 ml 0.1 M citric acid

41 ml of 0.1M trisodium citrate

in 400 ml dH_2O.

Adjust pH to 6.0.

Top up to 500 ml dH_2O.

Must be made fresh each experiment.

Tris Buffered Saline 10x

To make 1 l:

Dissolve

24.23 g Tris-HCl (Fisher Scientific, Loughborough, UK)

80.06 g NaCl (Sigma-Aldrich, Dorset, UK)

in 800 ml dH_2O.

Adjust pH to 7.6.

Top up to 1 l dH_2O

Can be kept at room temperature up to 12 months.

Tris Buffered Saline 1x

To make 1 l:

Dilute 100 ml of Tris buffered saline 10 x into 900 ml of dH_2O.

Appendix II: Sacrifice Protocol Sheet

Date:
Strain:
Maternal ID:
Maternal weight:

GD .....

Fetal Location

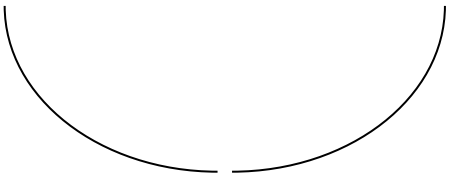

Heart	W LV
Lungs	
Liver	
Spleen	
Kidney	L R
Tibia	

Fetal ID	Fetal whole weight	Placental weight	Fetal weights					Notes
			Head	Heart	Liver	Kidney	Spleen	

Appendix III: 788 urinary peptides altered between WKY and SHRSP

Pre-pregnancy WKY Vs SHRSP		Gestational day 12 WKY Vs SHRSP				Gestational day 18 WKY Vs SHRSP	
PeptideID	p value	PeptideID	p value	PeptideID	p value	PeptideID	p value
2545	0.001	421	0.001	11725	0.010	519	0.001
10647	0.001	1304	0.001	18543	0.010	880	0.001
11171	0.001	1338	0.001	24940	0.010	4119	0.001
13543	0.001	1699	0.001	101782	0.010	22329	0.001
100383	0.001	2090	0.001	3791	0.011	4586	0.001
8591	0.001	2684	0.001	5823	0.011	8591	0.001
15819	0.001	2803	0.001	929	0.011	8661	0.001
100359	0.001	3734	0.001	1054	0.011	13580	0.001
101391	0.001	3930	0.001	3258	0.011	14788	0.001
101695	0.001	4042	0.001	4379	0.011	14896	0.001
106356	0.001	4170	0.001	6395	0.011	15819	0.001
4119	0.001	4218	0.001	6531	0.011	100964	0.001
6352	0.001	4586	0.001	8230	0.011	101154	0.001
8230	0.001	5098	0.001	9006	0.011	101201	0.001
12237	0.001	5147	0.001	9871	0.011	101695	0.001
15972	0.001	5254	0.001	10732	0.011	102001	0.001
14896	0.002	5661	0.001	10825	0.011	10647	0.001
10625	0.002	6044	0.001	11875	0.011	11171	0.001
22329	0.002	6304	0.001	12049	0.011	24031	0.001
4197	0.002	6596	0.001	14090	0.011	36219	0.001
9589	0.002	6975	0.001	14472	0.011	101391	0.001
35922	0.002	7006	0.001	16054	0.011	101392	0.001
100033	0.002	7441	0.001	100322	0.011	12407	0.002
103080	0.002	8592	0.001	102908	0.011	35684	0.002
5748	0.002	10615	0.001	3672	0.011	5661	0.002
13928	0.002	10647	0.001	4446	0.011	13543	0.002
11655	0.002	10835	0.001	4451	0.011	17594	0.002
4864	0.002	11171	0.001	4836	0.011	5497	0.002
6975	0.002	12407	0.001	6546	0.011	105750	0.002
10311	0.002	12426	0.001	6565	0.011	100383	0.002
12417	0.002	12582	0.001	7590	0.011	7574	0.002
6333	0.003	12628	0.001	7979	0.011	10165	0.002
5661	0.003	13543	0.001	8560	0.011	100572	0.002
11852	0.003	13670	0.001	9286	0.011	5474	0.002
7502	0.004	17939	0.001	9447	0.011	8590	0.003
11488	0.004	18503	0.001	9571	0.011	9325	0.003
13270	0.004	35922	0.001	13236	0.011	20566	0.003
13578	0.004	100383	0.001	13570	0.011	11430	0.003
19853	0.004	100773	0.001	15252	0.011	13851	0.003

100217	0.004	101176	0.001	15577	0.011	100773	0.003
100433	0.004	101193	0.001	15972	0.011	6395	0.003
100954	0.004	101420	0.001	18196	0.011	10197	0.003
100964	0.004	2985	0.001	20303	0.011	9833	0.003
101001	0.004	9647	0.001	25101	0.011	8128	0.004
102001	0.004	11488	0.001	33216	0.011	8894	0.004
102056	0.004	11744	0.001	100761	0.011	9820	0.004
18164	0.004	14788	0.001	101145	0.011	10192	0.004
19881	0.004	15819	0.001	101274	0.011	11488	0.004
35466	0.004	31459	0.001	101730	0.011	17410	0.004
35994	0.004	100359	0.001	102322	0.011	17742	0.004
100495	0.004	100433	0.001	107303	0.011	100744	0.004
100864	0.004	100806	0.001	107543	0.011	100806	0.004
103088	0.004	100954	0.001	193	0.011	100954	0.004
103092	0.004	100964	0.001	6367	0.011	101001	0.004
109190	0.004	101001	0.001	8019	0.011	101219	0.004
100218	0.004	101154	0.001	8661	0.011	101224	0.004
5254	0.004	101201	0.001	9301	0.011	101403	0.004
11841	0.004	101219	0.001	10081	0.011	101782	0.004
20119	0.004	101403	0.001	11467	0.011	102908	0.004
9729	0.005	101695	0.001	11550	0.011	106650	0.004
15071	0.005	101850	0.001	13079	0.011	12729	0.004
16262	0.005	102000	0.001	13819	0.011	13985	0.004
13742	0.005	102001	0.001	13977	0.011	1512	0.004
3813	0.005	102056	0.001	14697	0.011	4362	0.004
13901	0.006	108357	0.001	15787	0.011	5254	0.004
4933	0.006	109289	0.001	17163	0.011	4864	0.004
8156	0.006	880	0.001	19102	0.011	34236	0.004
11737	0.006	1512	0.001	100217	0.011	27020	0.005
103116	0.006	1615	0.001	100537	0.011	14020	0.006
193	0.006	1891	0.001	100545	0.011	21602	0.006
101201	0.006	4119	0.001	101174	0.011	4692	0.006
13580	0.007	4320	0.001	101275	0.011	5244	0.006
24519	0.007	5952	0.001	101946	0.011	6367	0.006
4218	0.007	6084	0.001	102804	0.011	10772	0.006
7588	0.007	7578	0.001	102868	0.011	11573	0.006
10884	0.007	8056	0.001	108122	0.011	16631	0.006
17798	0.007	10311	0.001	109525	0.011	27487	0.006
15724	0.008	10377	0.001	109530	0.011	36280	0.006
1949	0.009	11841	0.001	12259	0.012	3784	0.007
18591	0.009	13290	0.001	100343	0.012	10695	0.007
7982	0.010	16047	0.001	7035	0.013	3135	0.007
10197	0.010	16746	0.001	13742	0.013	13591	0.007
35447	0.010	17843	0.001	100374	0.013	16914	0.007
101392	0.010	100000	0.001	100572	0.013	10270	0.007
107880	0.010	100173	0.001	3472	0.013	5596	0.007
8709	0.010	2712	0.001	6647	0.013	20556	0.009

14788	0.010	4468	0.001	35161	0.013	5114	0.010
4680	0.010	12124	0.001	9432	0.014	15395	0.010
9113	0.010	13580	0.001	100226	0.014	15428	0.010
17522	0.010	16333	0.001	9113	0.014	1756	0.010
12583	0.010	19131	0.001	12110	0.014	3258	0.010
1054	0.011	100139	0.002	100864	0.014	12958	0.010
2186	0.011	101208	0.002	100977	0.014	20731	0.010
5098	0.011	106579	0.002	105334	0.014	100063	0.010
7006	0.011	108649	0.002	9131	0.014	102567	0.010
11216	0.011	29610	0.002	21178	0.014	102712	0.010
11667	0.011	13928	0.002	102119	0.015	102902	0.010
12049	0.011	2637	0.002	7442	0.015	15228	0.010
21160	0.011	7161	0.002	13152	0.015	3188	0.010
35127	0.011	7982	0.002	35713	0.017	16054	0.010
35169	0.011	102902	0.002	856	0.017	1406	0.011
35490	0.011	106602	0.002	100360	0.017	9705	0.011
101635	0.011	1107	0.002	1755	0.017	12605	0.011
11837	0.011	3493	0.002	2619	0.017	2910	0.011
17480	0.011	4706	0.002	2981	0.017	3668	0.011
20506	0.011	8344	0.002	3668	0.017	7534	0.011
21295	0.011	8184	0.002	4864	0.017	9863	0.011
21651	0.011	13458	0.002	5198	0.017	10013	0.011
100471	0.011	14896	0.002	5215	0.017	12628	0.011
100585	0.011	106074	0.002	7083	0.017	13740	0.011
108057	0.011	4828	0.002	8295	0.017	3943	0.011
2102	0.011	13476	0.002	9144	0.017	6546	0.011
2433	0.011	102911	0.002	10707	0.017	7560	0.011
3265	0.011	109223	0.002	11099	0.017	8681	0.011
4717	0.011	1140	0.002	11866	0.017	9199	0.011
6367	0.011	1146	0.002	13159	0.017	11101	0.011
6857	0.011	3114	0.002	13923	0.017	11141	0.011
8600	0.011	5460	0.002	17077	0.017	13079	0.011
11261	0.011	5635	0.002	31029	0.017	14066	0.011
100333	0.011	6397	0.002	100658	0.017	14162	0.011
100627	0.011	6441	0.002	100916	0.017	33248	0.011
100744	0.011	9863	0.002	11250	0.019	34855	0.011
101219	0.011	12289	0.002	107005	0.019	34882	0.011
9178	0.013	13456	0.002	18031	0.020	100018	0.011
2844	0.013	14426	0.002	5789	0.020	100095	0.011
9571	0.013	15933	0.002	27418	0.020	100730	0.011
14221	0.013	20939	0.002	29455	0.020	101024	0.011
15118	0.013	100026	0.002	35234	0.020	101148	0.011
35384	0.013	101092	0.002	101520	0.020	101216	0.011
9042	0.014	7866	0.003	9251	0.020	101292	0.011
102610	0.014	10322	0.003	11644	0.020	102056	0.011
102676	0.014	11179	0.003	17878	0.020	102918	0.011
109175	0.014	18217	0.003	2102	0.020	3628	0.012

6115	0.014	12742	0.003	102700	0.020	101186	0.012
35539	0.014	102559	0.003	23262	0.020	16685	0.013
6436	0.017	19332	0.003	7289	0.021	7588	0.013
14030	0.017	101392	0.003	16914	0.021	14404	0.014
100110	0.017	100887	0.003	106551	0.021	6545	0.014
101985	0.017	100989	0.003	4457	0.021	3930	0.014
100773	0.017	4692	0.003	13336	0.021	16262	0.014
106579	0.017	4986	0.004	13711	0.021	101550	0.014
2182	0.017	5014	0.004	14340	0.021	2981	0.015
4362	0.017	8404	0.004	7181	0.021	11253	0.015
9033	0.017	13615	0.004	6693	0.024	12439	0.015
11492	0.017	25688	0.004	29323	0.024	3355	0.015
35325	0.017	34349	0.004	31267	0.024	12582	0.015
35348	0.017	100394	0.004	101528	0.024	5098	0.017
35412	0.017	100885	0.004	5114	0.024	12185	0.017
6084	0.019	101391	0.004	8688	0.024	16851	0.017
13498	0.019	102091	0.004	14253	0.024	12757	0.019
7119	0.020	106650	0.004	15563	0.024	5033	0.020
8899	0.020	107308	0.004	100114	0.024	5119	0.020
22263	0.020	286	0.004	101918	0.024	9006	0.020
35678	0.020	431	0.004	103105	0.024	100468	0.020
101733	0.020	1063	0.004	7741	0.024	16489	0.020
8410	0.020	5083	0.004	8561	0.024	274	0.021
103107	0.020	5870	0.004	100150	0.024	9226	0.021
5546	0.020	6058	0.004	9325	0.025	20153	0.021
7095	0.020	6624	0.004	32956	0.025	5065	0.021
11671	0.021	7570	0.004	1251	0.026	7740	0.021
10778	0.021	8621	0.004	1850	0.026	12561	0.021
13970	0.021	12786	0.004	2749	0.026	7866	0.021
12818	0.021	13794	0.004	3135	0.026	5215	0.024
25712	0.021	15154	0.004	3392	0.026	1615	0.024
3672	0.024	17570	0.004	4454	0.026	4673	0.024
8464	0.024	34358	0.004	4922	0.026	6232	0.024
10718	0.024	101325	0.004	5425	0.026	8862	0.024
12786	0.024	101713	0.004	5497	0.026	12256	0.024
100096	0.024	103116	0.004	7471	0.026	13270	0.024
101332	0.024	103178	0.004	7653	0.026	13742	0.024
102131	0.024	106000	0.004	9090	0.026	15071	0.024
103131	0.024	106903	0.004	10030	0.026	15355	0.024
2488	0.024	16870	0.004	10106	0.026	17998	0.024
4364	0.024	12278	0.004	10197	0.026	29610	0.024
4492	0.024	35907	0.004	11671	0.026	100111	0.024
5067	0.024	3620	0.004	12640	0.026	100646	0.024
7035	0.024	4824	0.004	12826	0.026	102160	0.024
13060	0.024	6189	0.004	13740	0.026	106356	0.024
13154	0.024	7302	0.004	14273	0.026	12579	0.024
35714	0.024	8834	0.004	16851	0.026	6676	0.024

102918	0.024	11216	0.004	17688	0.026	929	0.025
6380	0.025	12574	0.004	21602	0.026	10098	0.025
12582	0.025	14404	0.004	24236	0.026	1850	0.026
5699	0.026	15228	0.004	33722	0.026	4230	0.026
6441	0.026	33289	0.004	35169	0.026	4824	0.026
7051	0.026	33712	0.004	35204	0.026	7716	0.026
7471	0.026	16000	0.004	101204	0.026	8418	0.026
7740	0.026	19659	0.004	4134	0.026	11622	0.026
9219	0.026	100218	0.004	5900	0.026	6647	0.026
12574	0.026	100599	0.004	8316	0.026	12711	0.026
13451	0.026	12958	0.004	19881	0.026	14169	0.026
20566	0.026	6511	0.005	100050	0.026	18543	0.026
35515	0.026	103080	0.005	102595	0.028	5402	0.028
31459	0.026	9742	0.005	12969	0.028	100026	0.028
13960	0.026	9744	0.005	29574	0.028	2269	0.028
101166	0.026	8006	0.005	100973	0.029	6510	0.029
8170	0.028	9589	0.005	102151	0.029	9720	0.029
6323	0.028	35377	0.005	108590	0.029	13670	0.029
11430	0.028	101230	0.005	17428	0.030	16079	0.029
12969	0.028	10778	0.005	25557	0.030	100343	0.029
13870	0.028	17863	0.005	102712	0.030	4042	0.029
100231	0.028	15942	0.006	5623	0.033	4080	0.029
1380	0.029	6252	0.006	100400	0.033	4710	0.029
1304	0.029	7154	0.006	6755	0.034	9540	0.029
101187	0.029	10983	0.006	100103	0.034	11686	0.029
20438	0.029	15829	0.006	102021	0.034	23327	0.029
3114	0.029	15872	0.006	10014	0.034	100000	0.029
23845	0.029	20506	0.006	100863	0.034	8410	0.030
100050	0.029	101324	0.006	108801	0.034	9090	0.033
100916	0.029	3784	0.007	522	0.037	5128	0.034
16657	0.030	4666	0.007	5306	0.037	12124	0.034
9506	0.033	5474	0.007	646	0.038	13458	0.034
1232	0.033	7534	0.007	4877	0.038	13819	0.034
2637	0.033	7891	0.007	5030	0.038	15755	0.034
9111	0.034	10013	0.007	5682	0.038	17548	0.034
9186	0.034	10472	0.007	7299	0.038	101272	0.034
7154	0.037	10683	0.007	7819	0.038	102640	0.034
100240	0.037	13960	0.007	7910	0.038	1304	0.037
4379	0.038	15042	0.007	8332	0.038	5460	0.037
4586	0.038	17594	0.007	8420	0.038	5699	0.037
4828	0.038	21320	0.007	9658	0.038	2684	0.038
5030	0.038	33803	0.007	12020	0.038	12426	0.038
6395	0.038	100913	0.007	13213	0.038	13878	0.038
8343	0.038	35447	0.007	14405	0.038	11810	0.039
8643	0.038	102776	0.008	14830	0.038	35697	0.039
11115	0.038	2116	0.008	20549	0.038	17522	0.039
16685	0.038	13822	0.009	20566	0.038	33097	0.039

100015	0.038	107577	0.009	21160	0.038	100542	0.039
3599	0.039	109230	0.009	21880	0.038	11288	0.040
8752	0.040	8591	0.010	34909	0.038	5396	0.041
2061	0.041	13270	0.010	34927	0.038	9131	0.041
16320	0.041	100744	0.010	105750	0.038	20589	0.041
7451	0.041	101148	0.010	100141	0.039	100240	0.041
15198	0.041	101261	0.010	107909	0.039	6739	0.041
3628	0.041	101798	0.010	102309	0.039	34216	0.041
9647	0.041	105083	0.010	108359	0.039	3791	0.041
15755	0.041	101166	0.010	108412	0.039	4524	0.045
3255	0.048	4895	0.010	35575	0.040	12969	0.045
4768	0.048	13347	0.010	9601	0.040	14390	0.045
5744	0.048	101733	0.010	4438	0.041	13154	0.048
5623	0.048	4389	0.010	6545	0.041	27499	0.048
20062	0.048	4843	0.010	6611	0.041	100263	0.048
100045	0.048	7320	0.010	10393	0.041	100725	0.048
107165	0.048	14661	0.010	100112	0.041	1054	0.050
36481	0.050	17142	0.010	10563	0.041	6312	0.050
100118	0.050	105953	0.010	11487	0.041	7982	0.050
		15786	0.010	16121	0.041	8170	0.050
		101667	0.010	22216	0.041	10958	0.050
		5396	0.010	100100	0.041	16385	0.050
		10077	0.010	13442	0.041	17878	0.050
		9546	0.010	16657	0.041	109230	0.050
		8178	0.047	13994	0.045		
		100353	0.048	4455	0.045		
		4549	0.050	10625	0.045		
		9646	0.050	101017	0.050		

Appendix IV: 123 urinary peptides altered between WKY and SHRSP at all time points (NP, GD12 and GD18) or GD12 & GD18 only

PeptideID	Mass	Migration time	Log2 peptide intensity						Fold change (WKY/ SHRSP)		
			WKY NP	SHRSP NP	WKY GD12	SHRSP GD12	WKY GD18	SHRSP GD18	NP	GD12	GD18
929	857.4815	28.15	5.93	6.28	6.35	7.03	5.97	7.12	0.94	0.90	0.84
1054	862.4315	22.67	6.57	8.10	8.11	6.86	6.86	6.36	0.81	1.18	1.08
1304	874.4576	34.49	7.49	6.14	7.73	5.75	6.64	3.95	1.22	1.34	1.68
4119	1009.498	37.80	12.33	13.33	12.23	12.91	11.82	13.09	0.92	0.95	0.90
4706	1046.479	47.56	5.75	6.67	5.57	7.32	6.13	4.75	0.86	0.76	1.29
5098	1073.363	46.52	13.04	13.67	13.11	13.83	13.28	14.25	0.95	0.95	0.93
5254	1083.533	36.50	11.96	11.35	12.24	11.21	12.08	11.42	1.05	1.09	1.06
5474	1099.53	36.52	8.98	7.83	9.31	7.72	9.86	8.23	1.15	1.21	1.20
5497	1100.587	28.83	7.31	5.11	8.58	7.67	8.52	6.09	1.43	1.12	1.40
5661	1111.608	30.47	7.52	4.06	8.29	5.98	7.90	5.15	1.85	1.39	1.53
6367	1155.575	29.05	6.57	4.10	7.14	3.41	8.39	4.48	1.60	2.09	1.87
6546	1167.54	47.90	4.49	5.59	4.63	3.92	5.08	4.30	0.80	1.18	1.18
7006	1196.367	47.02	12.07	12.79	12.42	13.09	12.91	13.48	0.94	0.95	0.96
7982	1255.65	26.25	6.73	4.55	7.88	3.90	6.75	5.44	1.48	2.02	1.24
8591	1295.622	29.62	8.05	3.67	8.18	3.00	9.73	4.23	2.19	2.73	2.30
9325	1341.649	38.48	6.65	5.63	6.62	5.30	7.52	5.21	1.18	1.25	1.44
10270	1407.682	48.28	7.91	9.23	8.50	9.14	8.91	6.45	0.86	0.93	1.38
10772	1444.684	40.04	4.60	5.84	4.28	3.39	7.37	4.59	0.79	1.26	1.61
11141	1471.739	39.49	4.27	4.30	4.99	4.22	5.34	4.74	0.99	1.18	1.13
12407	1564.769	39.41	7.19	5.89	8.34	6.64	8.90	5.66	1.22	1.26	1.57
12582	1579.76	26.34	8.60	7.18	10.10	8.95	9.86	6.87	1.20	1.13	1.44
12628	1584.553	47.97	10.32	12.13	11.42	12.12	11.48	12.24	0.85	0.94	0.94
12969	1611.795	40.17	5.59	7.54	5.92	6.83	5.78	7.19	0.74	0.87	0.80
13270	1635.838	33.09	6.11	4.45	6.30	3.66	7.01	4.56	1.37	1.72	1.53
13543	1659.818	39.66	8.96	6.90	9.43	6.79	9.41	5.46	1.30	1.39	1.72
13580	1663.806	40.59	8.70	5.54	9.39	4.19	8.92	4.80	1.57	2.24	1.86

13742	1679.814	40.76	7.82	6.23	8.45	5.75	7.40	5.22	1.25	1.47	1.42
14788	1780.881	28.09	6.98	4.44	9.02	2.89	9.26	4.33	1.57	3.12	2.14
14896	1790.854	33.26	6.62	4.42	8.29	5.42	8.28	4.66	1.50	1.53	1.78
15819	1885.854	28.11	9.79	4.57	10.90	3.50	11.42	4.68	2.14	3.12	2.44
100383	1139.544	28.69	9.92	6.65	10.46	7.06	10.89	6.37	1.49	1.48	1.71
100433	1173.604	26.22	6.30	4.47	7.69	3.67	6.06	4.87	1.41	2.10	1.24
100744	1417.721	26.35	5.87	4.27	7.21	4.15	6.42	4.65	1.37	1.74	1.38
100773	1433.684	32.66	7.07	5.52	7.79	6.11	7.93	6.28	1.28	1.28	1.26
100916	1532.692	39.51	6.33	8.34	8.62	9.19	7.00	9.06	0.76	0.94	0.77
100954	1554.759	26.62	6.33	4.60	7.18	3.57	6.80	4.57	1.38	2.01	1.49
100964	1561.754	28.12	7.59	4.19	8.80	3.89	8.20	4.91	1.81	2.26	1.67
101001	1584.787	27.29	7.10	4.52	8.12	3.52	8.32	4.83	1.57	2.31	1.72
101201	1713.872	28.25	7.19	4.43	8.82	3.54	9.03	4.84	1.62	2.49	1.87
101224	1726.832	28.14	5.34	4.55	5.81	3.76	6.37	4.69	1.17	1.54	1.36
101391	1832.94	33.34	6.33	4.54	6.28	3.54	7.78	4.94	1.39	1.77	1.57
101392	1833.646	48.36	5.17	6.55	4.94	6.58	6.78	4.81	0.79	0.75	1.41
101695	2013.958	25.17	8.05	4.63	8.93	3.74	9.39	5.05	1.74	2.39	1.86
102001	2196.056	25.43	7.54	4.18	9.66	3.76	9.26	4.61	1.80	2.57	2.01
102056	2239.077	26.87	8.01	4.65	9.33	3.52	8.34	5.06	1.72	2.65	1.65
106356	1418.602	48.47	7.81	4.70	7.40	3.86	8.73	5.14	1.66	1.92	1.70
880	855.4258	35.91	9.61	10.94	9.42	10.64	8.86	11.32	0.88	0.88	0.78
1512	883.4193	35.35	7.59	8.27	7.77	6.69	8.43	6.66	0.92	1.16	1.27
1615	888.4502	34.67	7.05	6.27	8.22	5.97	7.04	4.86	1.13	1.38	1.45
2684	931.5043	27.26	7.97	7.67	7.49	9.31	7.82	8.83	1.04	0.80	0.89
2981	947.4504	34.20	7.66	7.31	7.23	5.09	7.51	5.79	1.05	1.42	1.30
3258	960.5006	29.69	5.54	6.03	7.14	5.88	5.93	4.99	0.92	1.21	1.19
3668	982.5227	36.14	10.42	10.22	10.41	9.58	10.30	8.68	1.02	1.09	1.19
3784	989.4635	47.52	6.51	6.42	6.74	7.99	7.02	5.54	1.01	0.84	1.27
3791	989.5253	28.87	8.40	9.05	7.80	9.24	6.99	8.98	0.93	0.84	0.78
3930	998.4752	34.70	10.08	9.68	9.56	8.17	9.43	6.41	1.04	1.17	1.47
4042	1004.478	47.47	7.44	8.21	7.72	8.92	8.85	6.97	0.91	0.87	1.27
4680	1044.505	36.33	6.11	7.63	6.18	5.59	6.53	5.53	0.80	1.11	1.18
4824	1055.523	36.37	9.66	9.55	9.44	8.94	9.49	8.91	1.01	1.06	1.06
5014	1068.567	29.18	5.30	4.67	5.62	3.91	5.66	4.84	1.14	1.44	1.17

5114	1073.515	36.41	6.52	5.76	5.98	3.96	6.25	5.09	1.13	1.51	1.23
5789	1119.531	48.01	4.82	5.38	4.67	5.91	6.64	5.91	0.90	0.79	1.12
6058	1134.515	47.95	6.16	4.69	4.99	5.56	7.18	5.16	1.31	0.90	1.39
6252	1148.544	48.13	4.93	4.99	4.94	5.90	6.36	5.00	0.99	0.84	1.27
6545	1167.564	29.66	8.30	5.88	5.88	7.50	5.67	9.18	1.41	0.78	0.62
7181	1206.626	25.61	6.64	5.38	6.25	7.93	7.04	5.14	1.23	0.79	1.37
7302	1214.566	37.03	11.12	11.34	11.69	11.14	11.60	12.04	0.98	1.05	0.96
7534	1227.606	37.47	10.57	10.37	10.26	9.45	10.65	9.95	1.02	1.09	1.07
8404	1283.405	47.36	6.44	6.77	7.21	3.99	8.16	6.39	0.95	1.81	1.28
8590	1295.61	37.80	5.85	5.95	6.53	4.29	7.54	5.62	0.98	1.52	1.34
8661	1300.715	39.78	5.99	4.46	7.22	3.86	8.35	4.88	1.34	1.87	1.71
9006	1321.704	32.99	6.65	6.20	6.63	5.18	7.11	5.92	1.07	1.28	1.20
9090	1324.681	29.94	7.57	7.03	9.26	7.61	9.05	6.34	1.08	1.22	1.43
9131	1326.631	39.17	8.23	9.06	8.20	5.14	7.11	5.30	0.91	1.60	1.34
9601	1358.66	32.35	7.02	7.36	5.34	6.53	6.96	5.43	0.95	0.82	1.28
9863	1378.668	39.11	10.44	10.55	10.86	10.08	10.22	9.15	0.99	1.08	1.12
9871	1378.731	31.31	6.94	6.50	8.40	7.60	8.35	6.65	1.07	1.11	1.26
10013	1388.717	39.15	9.66	9.21	10.47	9.54	9.82	8.04	1.05	1.10	1.22
10393	1415.706	39.41	5.71	5.70	5.80	6.85	6.18	5.72	1.00	0.85	1.08
10625	1434.691	48.95	4.71	7.65	6.15	8.04	7.28	7.07	0.62	0.76	1.03
11179	1474.77	26.54	4.98	4.51	5.79	4.18	5.51	4.64	1.10	1.38	1.19
11487	1497.745	31.62	4.91	4.49	5.23	3.61	5.03	4.42	1.09	1.45	1.14
11667	1511.678	39.29	5.95	6.83	6.13	5.35	6.38	5.45	0.87	1.14	1.17
11737	1515.825	32.86	4.71	6.21	6.72	5.36	4.86	5.78	0.76	1.25	0.84
12757	1594.92	33.72	6.04	5.80	4.70	6.45	5.86	8.83	1.04	0.73	0.66
12958	1610.734	38.89	6.83	6.16	8.06	4.90	7.45	4.53	1.11	1.65	1.65
13079	1620.735	32.13	5.06	4.48	5.99	3.96	6.87	4.57	1.13	1.51	1.50
13290	1636.792	40.73	10.05	10.03	10.51	9.77	9.67	8.59	1.00	1.08	1.13
13458	1650.839	33.29	5.19	4.89	6.68	4.79	5.98	4.59	1.06	1.39	1.30
13670	1671.9	28.18	7.11	6.31	8.28	6.70	6.81	4.66	1.13	1.24	1.46
13740	1679.77	32.30	9.18	9.20	9.07	8.01	9.78	8.75	1.00	1.13	1.12
13819	1687.84	41.42	5.26	4.85	5.32	4.24	5.58	4.59	1.08	1.25	1.22
14020	1706.866	41.37	7.12	8.04	8.11	7.12	7.37	5.42	0.89	1.14	1.36
14404	1743.872	33.58	6.88	6.17	7.60	6.29	6.51	5.11	1.11	1.21	1.27

15228	1825.811	40.93	6.65	7.42	7.23	6.53	6.96	5.55	0.90	1.11	1.25
16047	1905.941	34.11	8.35	7.80	9.16	7.25	6.44	5.27	1.07	1.26	1.22
16054	1906.927	42.64	8.95	9.25	8.80	7.90	8.12	5.89	0.97	1.11	1.38
16851	1992.943	42.36	8.77	9.29	9.21	8.36	8.20	7.30	0.94	1.10	1.12
16914	2000.106	35.84	8.97	9.41	7.33	9.83	7.61	11.52	0.95	0.75	0.66
17594	2072.013	40.74	6.32	6.90	7.02	5.83	6.98	5.04	0.92	1.20	1.38
17878	2099.082	42.32	6.14	7.02	6.11	4.23	5.76	5.15	0.88	1.45	1.12
20566	2420.078	44.61	7.04	7.68	7.16	5.77	6.39	4.77	0.92	1.24	1.34
21602	2566.11	44.92	5.86	6.61	6.42	5.13	5.45	4.77	0.89	1.25	1.14
29610	3981.973	38.00	5.17	4.45	7.19	4.64	6.16	4.40	1.16	1.55	1.40
33289	5452.868	24.75	11.77	11.77	10.45	12.70	12.27	8.41	1.00	0.82	1.46
100000	800.3959	33.34	8.16	7.23	7.97	6.08	8.15	6.32	1.13	1.31	1.29
100026	828.4175	33.50	6.76	7.59	7.67	6.31	7.10	5.33	0.89	1.22	1.33
100111	902.4517	29.35	6.53	5.56	5.89	4.96	5.69	4.71	1.18	1.19	1.21
100343	1095.353	47.05	7.70	5.81	5.62	8.58	7.54	5.58	1.32	0.66	1.35
100542	1253.576	37.28	6.04	5.74	6.71	3.38	7.61	5.45	1.05	1.98	1.40
100572	1274.494	47.99	5.81	5.64	7.80	5.10	7.87	5.09	1.03	1.53	1.55
100806	1456.767	27.87	4.88	4.34	6.49	3.77	6.23	4.55	1.12	1.72	1.37
100913	1529.64	29.08	5.58	5.96	7.43	9.05	7.38	8.35	0.94	0.82	0.88
101148	1675.841	41.45	5.90	5.66	6.60	3.80	6.44	4.69	1.04	1.74	1.37
101272	1753.899	50.19	5.49	5.94	5.60	3.57	7.09	4.92	0.92	1.57	1.44
101403	1837.903	28.25	5.91	4.33	8.18	3.73	8.58	4.47	1.37	2.19	1.92
101420	1849.971	29.18	5.92	4.96	7.31	5.51	5.86	4.90	1.19	1.33	1.20
101782	2060.054	42.88	5.29	6.96	6.97	4.05	6.43	4.22	0.76	1.72	1.52
101946	2165.127	30.74	5.07	4.46	5.74	3.55	5.90	5.22	1.14	1.62	1.13
102676	3411.458	28.83	5.13	5.84	5.77	5.83	5.64	4.81	0.88	0.99	1.17
102804	4113.821	47.13	4.65	4.25	6.77	3.70	4.98	4.50	1.09	1.83	1.11
102868	4816.223	32.08	5.01	4.66	5.19	3.56	5.06	4.41	1.08	1.46	1.15
107005	1694.835	33.02	5.52	4.25	6.85	4.44	6.47	4.44	1.30	1.54	1.46

Appendix V: Sequenced peptides list

PeptideID	Mass	Sequence	Protein name	Theoretical Mass	Start	Stop	Rat Protein Accessions
12757	1594.92	IDQTRVLNLGPITR	Uromodulin	1594.91549	596	609	P27590
16914	2000.106	SGNFIDQTRVLNLGPITR	Uromodulin	2000.080323	592	609	P27590
9131	1326.631	TVDETYVPKEF	Serum albumin precursor	1326.634348	516	526	P02770
11179	1474.77	SVIHEDVYEEKK	RCG32337, isoform CRA_a	1474.730374	47	58	D3ZJA4
14788	1780.881	DKTEKELLDSYIDGR	Prothrombin precursor (Fragment)	1780.884309	345	359	IPI:IPI00189981.1
3668	982.5227	VPSYPGPpGP	Protein Col19a1	982.569898	76	84	D3ZCQ0
8590	1295.61	DPVESKIYFAQ	Pro-epidermal growth factor precursor	1295.639768	522	532	P07522
11667	1511.678	AGPpGPpGpPGSIGHpG	procollagen, type IX, alpha 3 (predicted), isoform CRA_a	1511.700471	555	571	D3ZX71
12958	1610.734	LAQLmANEWPHSQA	NACHT, leucine rich repeat and PYD containing 5	1610.751105	69.00	82.00	D3ZDM5
9006	1321.704	DGILGRDTLPHE	Contrapsin-like protease inhibitor 1 precursor	1321.662629	21	32	P05545
11141	1471.739	ALYQAEAFVADFK	Contrapsin-like protease inhibitor 1 precursor	1471.734731	155	167	P05545
11487	1497.745	GPPGpPGDPGKPGAPGK	Collagen alpha-1(IX) chain	1497.757592	68	84	IPI:IPI00192793.6
13742	1679.814	GMpGSpGGPGNDGKPGPpG	Collagen alpha-1(III) chain	1679.720948	536	554	IPI:IPI00366944.2
14896	1790.854	GESGRpGPpGPSGPRGQpG	Collagen alpha-1(III) chain	1790.829588	557	575	P13941

16851	1992.943	QGIpGTSGPpGENGKpGEpGP	Collagen alpha-1(III) chain	1992.902478	640	660	P13941
4706	1046.479	GppGPpGPpGPG	Collagen alpha-1(II) chain	1046.466889	1139	1150	P05539
9863	1378.668	ApGEDGRpGPpGPQ	Collagen alpha-1(II) chain	1378.611322	512	525	P05539
10625	1434.691	GPpGPpGPpGPPSGGY	Collagen alpha-1(I) chain precursor	1434.641559	1170	1185	P02454
3784	989.4635	GppGPpGPpGP	Collagen alpha-1(I) chain	989.445425	131	141	P02454
4042	1004.478	GPpGPpGPPSGG	Collagen alpha-1(I) chain	1004.456324	1173	1184	P02454
4119	1009.498	GRVGPpGPSGN	Collagen alpha-1(I) chain	1009.494075	870.00	880.00	P02454
6546	1167.54	GPpGPpGPPSGGY	Collagen alpha-1(I) chain	1167.519653	1173	1185	P02454
4680	1044.505	ApGFpGARGPS	Collagen alpha-1(I) chain	1044.498815	397.00	407.00	P02454
5254	1083.533	GVVGLpGQRGE	Collagen alpha-1(I) chain	1083.483267	828.00	839	P02454
5789	1119.531	GPpGPTGPTGPpG	Collagen alpha-1(I) chain	1119.519653	-	-	P02454
6252	1148.544	GLpGPpGApGPQG	Collagen alpha-1(I) chain	1148.546202	-	-	P02454
9090	1324.681	GLpGpKGDRGDAGP	Collagen alpha-1(I) chain	1324.637142	-	-	P02454
10013	1388.717	RpGEVGPpGPpGPAG	Collagen alpha-1(I) chain	1388.668442	907	921	P02454
11737	1515.825	GPpGPpGPVGKEGGKGP	Collagen alpha-1(I) chain	1515.768157	882	898	P02454
13079	1620.735	DGVAGPKGPAGERGSpGP	Collagen alpha-1(I) chain	1620.785598	488	505	IPI:IPI00188909.3
13290	1636.792	GSpGSpGPDGKTGPpGPAG	Collagen alpha-1(I) chain	1636.732893	531	549	P02454
13670	1671.9	PpGPpGPVGKEGGKGPRG	Collagen alpha-1(I) chain	1671.869268	882	899	P02454

14020	1706.866	TGPIGPpGPAGApGDKGET	Collagen alpha-1(I) chain	1706.811144	755	773	P02455
13543	1659.818	GAPGAKGNVGppGEPGPpG	Alpha 4 type V collagen	1659.785263	620	638	P68136
4824	1055.523	NELRVAPEE	Actin, alpha skeletal muscle	1055.524738	94	102	IPI:IPI00960053.1

References

1. Levik JR. An Introduction to Cardiovascular Physiology. 5 ed. London: Hodder Arnold; 2009.
2. Fletcher GF, Balady G, Froelicher VF, Hartley LH, Haskell WL, Pollock ML. Exercise Standards: A Statement for Healthcare Professionals From the American Heart Association. Circulation. 1995;91(2):580-615.
3. Valler-Jones T, Wedgbury K. Measuring blood pressure using the mercury sphygmomanometer. British Journal of Nursing. 2005;14(3):145-50.
4. Parati G, Ochoa JE, Lombardi C, Bilo G. Assessment and management of blood-pressure variability. Nature reviews Cardiology. 2013;10(3):143-55.
5. Whitaker S. Flow in Porous-Media .1. A Theoretical Derivation of Darcys-Law. Transport Porous Med. 1986;1(1):3-25.
6. Charkoudian N, Rabbitts JA. Sympathetic neural mechanisms in human cardiovascular health and disease. Mayo Clinic proceedings. 2009;84(9):822-30.
7. Nattie E, Li A. Central chemoreceptors: locations and functions. Comprehensive Physiology. 2012;2(1):221-54.
8. Willie CK, Tzeng YC, Fisher JA, Ainslie PN. Integrative regulation of human brain blood flow. The Journal of physiology. 2014;592(5):841-59.
9. Krause T, Lovibond K, Caulfield M, McCormack T, Williams B, Guideline Development G. Management of hypertension: summary of NICE guidance. Bmj. 2011;343:d4891.
10. Simonetti GD, Mohaupt MG, Bianchetti MG. Monogenic forms of hypertension. Eur J Pediatr. 2012;171(10):1433-9.
11. Freel EM, Connell JMC. Mechanisms of hypertension: The expanding role of aldosterone. Journal of the American Society of Nephrology. 2004;15(8):1993-2001.
12. de Bold AJ, Borenstein HB, Veress AT, Sonnenberg H. A rapid and potent natriuretic response to intravenous injection of atrial myocardial extract in rats. Life sciences. 1981;28(1):89-94.
13. Sudoh T, Kangawa K, Minamino N, Matsuo H. A new natriuretic peptide in porcine brain. Nature. 1988;332(6159):78-81.
14. Ogawa Y, Nakao K, Mukoyama M, Hosoda K, Shirakami G, Arai H, et al. Natriuretic Peptides as Cardiac Hormones in Normotensive and Spontaneously Hypertensive Rats - the Ventricle Is a Major Site of Synthesis and Secretion of Brain Natriuretic Peptide. Circulation Research. 1991;69(2):491-500.
15. Holtwick R, Gotthardt M, Skryabin B, Steinmetz M, Potthast R, Zetsche B, et al. Smooth muscle-selective deletion of guanylyl cyclase-A prevents the acute but not chronic effects of ANP on blood pressure. Proceedings of the National Academy of Sciences. 2002;99(10):7142-7.
16. Harris PJ, Thomas D, Morgan TO. Atrial natriuretic peptide inhibits angiotensin-stimulated proximal tubular sodium and water reabsorption. Nature. 1987;326(6114):697-8.
17. Bricca G, Lantelme P. Natriuretic peptides: ready for prime-time in hypertension? Arch Cardiovasc Dis. 2011;104(6-7):403-9.
18. Paravicini TM, Touyz RM. NADPH oxidases, reactive oxygen species, and hypertension: clinical implications and therapeutic possibilities. Diabetes care. 2008;31 Suppl 2:S170-80.
19. Virdis A, Neves MF, Amiri F, Touyz RM, Schiffrin EL. Role of NAD(P)H oxidase on vascular alterations in angiotensin II-infused mice. J Hypertens. 2004;22(3):535-42.

20. Sedeek M, Nasrallah R, Touyz RM, Hebert RL. NADPH oxidases, reactive oxygen species, and the kidney: friend and foe. J Am Soc Nephrol. 2013;24(10):1512-8.
21. Cai H, Harrison DG. Endothelial dysfunction in cardiovascular diseases: the role of oxidant stress. Circ Res. 2000;87(10):840-4.
22. Shimokawa H, Matoba T. Hydrogen peroxide as an endothelium-derived hyperpolarizing factor. Pharmacol Res. 2004;49(6):543-9.
23. Touyz RM. Reactive oxygen species, vascular oxidative stress, and redox signaling in hypertension: what is the clinical significance? Hypertension. 2004;44(3):248-52.
24. Somlyo AP, Wu X, Walker LA, Somlyo AV. Pharmacomechanical coupling: the role of calcium, G-proteins, kinases and phosphatases. Reviews of physiology, biochemistry and pharmacology. 1999;134:201-34.
25. VanBavel E, Wesselman JP, Spaan JA. Myogenic activation and calcium sensitivity of cannulated rat mesenteric small arteries. Circ Res. 1998;82(2):210-20.
26. Hilgers RH, Webb RC. Molecular aspects of arterial smooth muscle contraction: focus on Rho. Experimental biology and medicine. 2005;230(11):829-35.
27. Durand MJ, Gutterman DD. Diversity in mechanisms of endothelium-dependent vasodilation in health and disease. Microcirculation. 2013;20(3):239-47.
28. Huang A, Sun D, Shesely EG, Levee EM, Koller A, Kaley G. Neuronal NOS-dependent dilation to flow in coronary arteries of male eNOS-KO mice. American journal of physiology Heart and circulatory physiology. 2002;282(2):H429-36.
29. Wilcox JN, Subramanian RR, Sundell CL, Tracey WR, Pollock JS, Harrison DG, et al. Expression of multiple isoforms of nitric oxide synthase in normal and atherosclerotic vessels. Arteriosclerosis, thrombosis, and vascular biology. 1997;17(11):2479-88.
30. Schachinger V, Britten MB, Zeiher AM. Prognostic impact of coronary vasodilator dysfunction on adverse long-term outcome of coronary heart disease. Circulation. 2000;101(16):1899-906.
31. Dharmashankar K, Widlansky ME. Vascular endothelial function and hypertension: insights and directions. Current hypertension reports. 2010;12(6):448-55.
32. THE GLOBAL BURDEN OF DISEASE 2004 UPDATE Introduction. Global Burden of Disease: 2004 Update. 2008.
33. Ali A, Becker E, Chaudhury M, Fuller E, Harris J, Heeks F, et al. Volume 1: Cardiovascular disease and risk factors in adults. In: Craig R, Mindell J, editors. Health Survey for England 2006. 1. London: The Information Centre; 2008.
34. Khattar RS, Senior R, Lahiri A. Cardiovascular outcome in white-coat versus sustained mild hypertension: a 10-year follow-up study. Circulation. 1998;98(18):1892-7.
35. Luft FC, Mervaala E, Muller DN, Gross V, Schmidt F, Park JK, et al. Hypertension-induced end-organ damage : A new transgenic approach to an old problem. Hypertension. 1999;33(1 Pt 2):212-8.
36. Lawes CM, Vander Hoorn S, Rodgers A, International Society of H. Global burden of blood-pressure-related disease, 2001. Lancet. 2008;371(9623):1513-8.
37. Ibrahim MM, Damasceno A. Hypertension in developing countries. Lancet. 2012;380(9841):611-9.
38. Rapsomaniki E, Timmis A, George J, Pujades-Rodriguez M, Shah AD, Denaxas S, et al. Blood pressure and incidence of twelve cardiovascular diseases:

lifetime risks, healthy life-years lost, and age-specific associations in 1.25 million people. Lancet. 2014;383(9932):1899-911.
39. Pater C. The Blood Pressure "Uncertainty Range" - a pragmatic approach to overcome current diagnostic uncertainties (II). Curr Contr Trials C. 2005;6.
40. Timberlake DS, O'Connor DT, Parmer RJ. Molecular genetics of essential hypertension: recent results and emerging strategies. Curr Opin Nephrol Hy. 2001;10(1):71-9.
41. Williams RR, Hunt SC, Hasstedt SJ, Hopkins PN, Wu LL, Berry TD, et al. Are There Interactions and Relations between Genetic and Environmental-Factors Predisposing to High Blood-Pressure. Hypertension. 1991;18(3):29-37.
42. Feinleib M, Garrison RJ, Fabsitz R, Christian JC, Hrubec Z, Borhani NO, et al. The NHLBI twin study of cardiovascular disease risk factors: methodology and summary of results. Am J Epidemiol. 1977;106(4):284-5.
43. Mongeau JG, Biron P, Sing CF. The Influence of Genetics and Household Environment Upon the Variability of Normal Blood-Pressure - the Montreal Adoption Survey. Clin Exp Hypertens A. 1986;8(4-5):653-60.
44. Levy D, DeStefano AL, Larson MG, O'Donnell CJ, Lifton RP, Gavras H, et al. Evidence for a gene influencing blood pressure on chromosome 17 - Genome scan linkage results for longitudinal blood pressure phenotypes in subjects from the Framingham Heart Study. Hypertension. 2000;36(4):477-83.
45. Simonetti GD, Mohaupt MG, Bianchetti MG. Monogenic forms of hypertension. European Journal of Pediatrics. 2012;171(10):1433-9.
46. Shimkets RA, Warnock DG, Bositis CM, Nelson-Williams C, Hansson JH, Schambelan M, et al. Liddle's syndrome: heritable human hypertension caused by mutations in the beta subunit of the epithelial sodium channel. Cell. 1994;79(3):407-14.
47. Caulfield M, Farrall M, Clark AJL. Linkage of the Angiotensinogen Gene to Essential-Hypertension - Reply. New Engl J Med. 1994;331(16):1096-7.
48. Cusi D, Barlassina C, Azzani T, Casari G, Citterio L, Devoto M, et al. Polymorphisms of alpha-adducin and salt sensitivity in patients with essential hypertension. Lancet. 1997;349(9062):1353-7.
49. Frohlich ED, Dustan HP, Bumpus FM. Page,Irvine,H. - 1901-1991 - the Celebration of a Leader. Hypertension. 1991;18(4):443-5.
50. Padmanabhan S, Caulfield M, Dominiczak AF. Genetic and Molecular Aspects of Hypertension. Circulation Research. 2015;116(6):937-59.
51. International Consortium for Blood Pressure Genome-Wide Association S, Ehret GB, Munroe PB, Rice KM, Bochud M, Johnson AD, et al. Genetic variants in novel pathways influence blood pressure and cardiovascular disease risk. Nature. 2011;478(7367):103-9.
52. Padmanabhan S, Melander O, Johnson T, Di Blasio AM, Lee WK, Gentilini D, et al. Genome-wide association study of blood pressure extremes identifies variant near UMOD associated with hypertension. PLoS genetics. 2010;6(10):e1001177.
53. Hamet P. Environmentally-regulated genes of hypertension. Clinical and experimental hypertension. 1996;18(3-4):267-78.
54. Geller DS, Farhi A, Pinkerton N, Fradley M, Moritz M, Spitzer A, et al. Activating mineralocorticoid receptor mutation in hypertension exacerbated by pregnancy. Science. 2000;289(5476):119-23.
55. Hamet P, Pausova Z, Adarichev V, Adaricheva K, Tremblay J. Hypertension: genes and environment. J Hypertens. 1998;16(4):397-418.
56. Barker DJ. The origins of the developmental origins theory. Journal of internal medicine. 2007;261(5):412-7.

57. Geelhoed JJ, Fraser A, Tilling K, Benfield L, Davey Smith G, Sattar N, et al. Preeclampsia and gestational hypertension are associated with childhood blood pressure independently of family adiposity measures: the Avon Longitudinal Study of Parents and Children. Circulation. 2010;122(12):1192-9.
58. Staley JR, Bradley J, Silverwood RJ, Howe LD, Tilling K, Lawlor DA, et al. Associations of blood pressure in pregnancy with offspring blood pressure trajectories during childhood and adolescence: findings from a prospective study. Journal of the American Heart Association. 2015;4(5).
59. Yanes LL, Reckelhoff JF. Postmenopausal hypertension. American journal of hypertension. 2011;24(7):740-9.
60. Mosca L, Manson JE, Sutherland SE, Langer RD, Manolio T, Barrett-Connor E. Cardiovascular disease in women: a statement for healthcare professionals from the American Heart Association. Writing Group. Circulation. 1997;96(7):2468-82.
61. Feldman RD, Gros R. Rapid vascular effects of steroids - a question of balance? The Canadian journal of cardiology. 2010;26 Suppl A:22A-6A.
62. Chinnathambi V, Yallampalli C, Sathishkumar K. Prenatal testosterone induces sex-specific dysfunction in endothelium-dependent relaxation pathways in adult male and female rats. Biology of reproduction. 2013;89(4):97.
63. Gopalakrishnan K, Mishra JS, Chinnathambi V, Vincent KL, Patrikeev I, Motamedi M, et al. Elevated Testosterone Reduces Uterine Blood Flow, Spiral Artery Elongation, and Placental Oxygenation in Pregnant Rats. Hypertension. 2016;67(3):630-9.
64. Burt VL, Whelton P, Roccella EJ, Brown C, Cutler JA, Higgins M, et al. Prevalence of hypertension in the US adult population. Results from the Third National Health and Nutrition Examination Survey, 1988-1991. Hypertension. 1995;25(3):305-13.
65. Grady D, Herrington D, Bittner V, Blumenthal R, Davidson M, Hlatky M, et al. Cardiovascular disease outcomes during 6.8 years of hormone therapy: Heart and Estrogen/progestin Replacement Study follow-up (HERS II). Jama. 2002;288(1):49-57.
66. Rossouw JE, Anderson GL, Prentice RL, LaCroix AZ, Kooperberg C, Stefanick ML, et al. Risks and benefits of estrogen plus progestin in healthy postmenopausal women: principal results From the Women's Health Initiative randomized controlled trial. Jama. 2002;288(3):321-33.
67. Liu PY, Death AK, Handelsman DJ. Androgens and cardiovascular disease. Endocrine reviews. 2003;24(3):313-40.
68. Harrison DG, Guzik TJ, Lob HE, Madhur MS, Marvar PJ, Thabet SR, et al. Inflammation, Immunity, and Hypertension. Hypertension. 2011;57(2):132-40.
69. White FN, Grollman A. Autoimmune Factors Associated with Infarction of the Kidney. Nephron. 1964;1:93-102.
70. Svendsen UG. Evidence for an initial, thymus independent and a chronic, thymus dependent phase of DOCA and salt hypertension in mice. Acta pathologica et microbiologica Scandinavica Section A, Pathology. 1976;84(6):523-8.
71. Olsen F. Transfer of arterial hypertension by splenic cells from DOCA-salt hypertensive and renal hypertensive rats to normotensive recipients. Acta pathologica et microbiologica Scandinavica Section C, Immunology. 1980;88(1):1-5.
72. Schiffrin EL. Immune mechanisms in hypertension and vascular injury. Clinical science. 2014;126(3-4):267-74.

73. Verlohren S, Muller DN, Luft FC, Dechend R. Immunology in Hypertension, Preeclampsia, and Target-Organ Damage. Hypertension. 2009;54(3):439-43.
74. Crowley SD, Song YS, Lin EE, Griffiths R, Kim HS, Ruiz P. Lymphocyte responses exacerbate angiotensin II-dependent hypertension. American journal of physiology Regulatory, integrative and comparative physiology. 2010;298(4):R1089-97.
75. Guzik TJ, Hoch NE, Brown KA, McCann LA, Rahman A, Dikalov S, et al. Role of the T cell in the genesis of angiotensin II induced hypertension and vascular dysfunction. The Journal of experimental medicine. 2007;204(10):2449-60.
76. Mian MO, Paradis P, Schiffrin EL. Innate immunity in hypertension. Current hypertension reports. 2014;16(2):413.
77. De Ciuceis C, Amiri F, Brassard P, Endemann DH, Touyz RM, Schiffrin EL. Reduced vascular remodeling, endothelial dysfunction, and oxidative stress in resistance arteries of angiotensin II-infused macrophage colony-stimulating factor-deficient mice - Evidence for a role in inflammation in angiotensin-induced vascular injury. Arterioscl Throm Vas. 2005;25(10):2106-13.
78. Ko EA, Amiri F, Pandey NR, Javeshghani D, Leibovitz E, Touyz RM, et al. Resistance artery remodeling in deoxycorticosterone acetate-salt hypertension is dependent on vascular inflammation: evidence from m-CSF-deficient mice. Am J Physiol-Heart C. 2007;292(4):H1789-H95.
79. Wenzel P, Knorr M, Kossmann S, Stratmann J, Hausding M, Schuhmacher S, et al. Lysozyme M-Positive Monocytes Mediate Angiotensin II-Induced Arterial Hypertension and Vascular Dysfunction. Circulation. 2011;124(12):1370-U177.
80. Liu JH, Yang F, Yang XP, Jankowski M, Pagano PJ. NAD(P)H oxidase mediates angiotensin II-induced vascular macrophage infiltration and medial hypertrophy. Arterioscl Throm Vas. 2003;23(5):776-82.
81. Vinh A, Chen W, Blinder Y, Weiss D, Taylor WR, Goronzy JJ, et al. Inhibition and Genetic Ablation of the B7/CD28 T-Cell Costimulation Axis Prevents Experimental Hypertension. Circulation. 2010;122(24):2529-37.
82. Granger JP. An emerging role for inflammatory cytokines in hypertension. Am J Physiol-Heart C. 2006;290(3):H923-H4.
83. Lee DL, Sturgis LC, Labazi H, Osborne JB, Fleming C, Pollock JS, et al. Angiotensin II hypertension is attenuated in interleukin-6 knockout mice. Am J Physiol-Heart C. 2006;290(3):H935-H40.
84. Chae CU, Lee RT, Rifai N, Ridker PM. Blood pressure and inflammation in apparently healthy men. Hypertension. 2001;38(3):399-403.
85. Marko L, Kvakan H, Park JK, Qadri F, Spallek B, Binger KJ, et al. Interferon-gamma Signaling Inhibition Ameliorates Angiotensin II-Induced Cardiac Damage. Hypertension. 2012;60(6):1430-U154.
86. Trinchieri G. Biology of natural killer cells. Advances in immunology. 1989;47:187-376.
87. Vivier E, Tomasello E, Baratin M, Walzer T, Ugolini S. Functions of natural killer cells. Nature immunology. 2008;9(5):503-10.
88. Whiteside TL, Herberman RB. Role of human natural killer cells in health and disease. Clinical and diagnostic laboratory immunology. 1994;1(2):125-33.
89. Orr MT, Lanier LL. Natural killer cell education and tolerance. Cell. 2010;142(6):847-56.
90. Barrow AD, Trowsdale J. You say ITAM and I say ITIM, let's call the whole thing off: the ambiguity of immunoreceptor signalling. European journal of immunology. 2006;36(7):1646-53.

91. Fehniger TA, Cai SF, Cao X, Bredemeyer AJ, Presti RM, French AR, et al. Acquisition of murine NK cell cytotoxicity requires the translation of a pre-existing pool of granzyme B and perforin mRNAs. Immunity. 2007;26(6):798-811.
92. Walzer T, Dalod M, Robbins SH, Zitvogel L, Vivier E. Natural-killer cells and dendritic cells: "l' union fait la force". Blood. 2005;106(7):2252-8.
93. Long EO. Ready for prime time: NK cell priming by dendritic cells. Immunity. 2007;26(4):385-7.
94. Knorr M, Munzel T, Wenzel P. Interplay of NK cells and monocytes in vascular inflammation and myocardial infarction. Frontiers in physiology. 2014;5:295.
95. Kerdiles Y, Ugolini S, Vivier E. T cell regulation of natural killer cells. The Journal of experimental medicine. 2013;210(6):1065-8.
96. Carlyle JR, Mesci A, Ljutic B, Belanger S, Tai LH, Rousselle E, et al. Molecular and genetic basis for strain-dependent NK1.1 alloreactivity of mouse NK cells. Journal of Immunology. 2006;176(12):7511-24.
97. Dissen E, Ryan JC, Seaman WE, Fossum S. An autosomal dominant locus, Nka, mapping to the Ly-49 region of a rat natural killer (NK) gene complex, controls NK cell lysis of allogeneic lymphocytes. The Journal of experimental medicine. 1996;183(5):2197-207.
98. Hao L, Klein J, Nei M. Heterogeneous but conserved natural killer receptor gene complexes in four major orders of mammals. Proceedings of the National Academy of Sciences of the United States of America. 2006;103(9):3192-7.
99. Yokoyama WM, Seaman WE. The Ly-49 and NKR-P1 gene families encoding lectin-like receptors on natural killer cells: the NK gene complex. Annual review of immunology. 1993;11:613-35.
100. Huntington ND, Vosshenrich CAJ, Di Santo JP. Developmental pathways that generate natural-killer-cell diversity in mice and humans. Nat Rev Immunol. 2007;7(9):703-14.
101. Iizuka K, Naidenko OV, Plougastel BF, Fremont DH, Yokoyama WM. Genetically linked C-type lectin-related ligands for the NKRP1 family of natural killer cell receptors. Nature immunology. 2003;4(8):801-7.
102. Vogler I, Steinle A. Vis-a-vis in the NKC: genetically linked natural killer cell receptor/ligand pairs in the natural killer gene complex (NKC). Journal of innate immunity. 2011;3(3):227-35.
103. Takahashi T, Dejbakhsh-Jones S, Strober S. Expression of CD161 (NKR-P1A) defines subsets of human CD4 and CD8 T cells with different functional activities. J Immunol. 2006;176(1):211-6.
104. Brissette-Storkus CS, Kettel JC, Whitham TF, Giezeman-Smits KM, Villa LA, Potter DM, et al. Flt-3 ligand (FL) drives differentiation of rat bone marrow-derived dendritic cells expressing OX62 and/or CD161 (NKR-P1). Journal of leukocyte biology. 2002;71(6):941-9.
105. Kveberg L, Sudworth A, Todros-Dawda I, Inngjerdingen M, Vaage JT. Functional characterization of a conserved pair of NKR-P1 receptors expressed by NK cells and T lymphocytes in liver and gut. European journal of immunology. 2015;45(2):501-12.
106. Aust JG, Gays F, Mickiewicz KM, Buchanan E, Brooks CG. The expression and function of the NKRP1 receptor family in C57BL/6 mice. J Immunol. 2009;183(1):106-16.
107. Kirkham CL, Carlyle JR. Complexity and Diversity of the NKR-P1:Clr (Klrb1:Clec2) Recognition Systems. Frontiers in immunology. 2014;5:214.

108. Lanier LL, Chang C, Phillips JH. Human NKR-P1A. A disulfide-linked homodimer of the C-type lectin superfamily expressed by a subset of NK and T lymphocytes. J Immunol. 1994;153(6):2417-28.
109. Poggi A, Costa P, Tomasello E, Moretta L. IL-12-induced up-regulation of NKRP1A expression in human NK cells and consequent NKRP1A-mediated down-regulation of NK cell activation. European journal of immunology. 1998;28(5):1611-6.
110. Rosen DB, Bettadapura J, Alsharifi M, Mathew PA, Warren HS, Lanier LL. Cutting edge: lectin-like transcript-1 is a ligand for the inhibitory human NKR-P1A receptor. J Immunol. 2005;175(12):7796-9.
111. Aldemir H, Prod'homme V, Dumaurier MJ, Retiere C, Poupon G, Cazareth J, et al. Cutting edge: lectin-like transcript 1 is a ligand for the CD161 receptor. J Immunol. 2005;175(12):7791-5.
112. Chambers WH, Vujanovic NL, Deleo AB, Olszowy MW, Herberman RB, Hiserodt JC. Monoclonal-Antibody to a Triggering Structure Expressed on Rat Natural-Killer Cells and Adherent Lymphokine-Activated Killer Cells. Journal of Experimental Medicine. 1989;169(4):1373-89.
113. Ryan JC, Niemi EC, Goldfien RD, Hiserodt JC, Seaman WE. Nkr-P1, an Activating Molecule on Rat Natural-Killer-Cells, Stimulates Phosphoinositide Turnover and a Rise in Intracellular Calcium. Journal of Immunology. 1991;147(9):3244-50.
114. Ryan JC, Niemi EC, Nakamura MC, Seaman WE. Nkr-P1a Is a Target-Specific Receptor That Activates Natural-Killer-Cell Cytotoxicity. Journal of Experimental Medicine. 1995;181(5):1911-5.
115. Li J, Rabinovich BA, Hurren R, Shannon J, Miller RG. Expression cloning and function of the rat NK activating and inhibitory receptors NKR-P1A and -P1B. International immunology. 2003;15(3):411-6.
116. Fine JH, Chen P, Mesci A, Allan DS, Gasser S, Raulet DH, et al. Chemotherapy-induced genotoxic stress promotes sensitivity to natural killer cell cytotoxicity by enabling missing-self recognition. Cancer research. 2010;70(18):7102-13.
117. Kveberg L, Dai KZ, Inngjerdingen M, Brooks CG, Fossum S, Vaage JT. Phylogenetic and functional conservation of the NKR-P1F and NKR-P1G receptors in rat and mouse. Immunogenetics. 2011;63(7):429-36.
118. Matzinger P. The danger model: a renewed sense of self. Science. 2002;296(5566):301-5.
119. Blasius AL, Beutler B. Intracellular toll-like receptors. Immunity. 2010;32(3):305-15.
120. Adib-Conquy M, Scott-Algara D, Cavaillon JM, Souza-Fonseca-Guimaraes F. TLR-mediated activation of NK cells and their role in bacterial/viral immune responses in mammals. Immunology and cell biology. 2014;92(3):256-62.
121. Biron CA, Nguyen KB, Pien GC, Cousens LP, Salazar-Mather TP. Natural killer cells in antiviral defense: Function and regulation by innate cytokines. Annual review of immunology. 1999;17:189-220.
122. Wang RP, Jaw JJ, Stutzman NC, Zou ZC, Sun PD. Natural killer cell-produced IFN-gamma and TNF-alpha induce target cell cytolysis through up-regulation of ICAM-1. Journal of leukocyte biology. 2012;91(2):299-309.
123. Bradley JR. TNF-mediated inflammatory disease. J Pathol. 2008;214(2):149-60.
124. Reinhardt RL, Liang HE, Bao K, Price AE, Mohrs M, Kelly BL, et al. A Novel Model for IFN-gamma-Mediated Autoinflammatory Syndromes. Journal of Immunology. 2015;194(5):2358-68.

125. Bolovan-Fritts CA, Spector SA. Endothelial damage from cytomegalovirus-specific host immune response can be prevented by targeted disruption of fractalkine-CX(3)CR1 interaction. Blood. 2008;111(1):175-82.
126. Rieben R, Seebach JD. Xenograft rejection: IgG1, complement and NK cells team up to activate and destroy the endothelium. Trends in immunology. 2005;26(1):2-5.
127. Kossmann S, Schwenk M, Hausding M, Karbach SH, Schmidgen MI, Brandt M, et al. Angiotensin II-Induced Vascular Dysfunction Depends on Interferon-gamma- Driven Immune Cell Recruitment and Mutual Activation of Monocytes and NK-Cells. Arterioscl Throm Vas. 2013;33(6):1313-+.
128. Wang Y, Li Y, Wu Y, Jia L, Wang J, Xie B, et al. 5TNF-alpha and IL-1beta neutralization ameliorates angiotensin II-induced cardiac damage in male mice. Endocrinology. 2014;155(7):2677-87.
129. Sriramula S, Francis J. Tumor Necrosis Factor - Alpha Is Essential for Angiotensin II-Induced Ventricular Remodeling: Role for Oxidative Stress. Plos One. 2015;10(9).
130. Taherzadeh Z, VanBavel E, de Vos J, Matlung HL, van Montfrans G, Brewster LM, et al. Strain-dependent susceptibility for hypertension in mice resides in the natural killer gene complex. American journal of physiology Heart and circulatory physiology. 2010;298(4):H1273-82.
131. de Vries MR, Seghers L, van Bergen J, Peters HAB, de Jong RCM, Hamming JF, et al. C57BL/6 NK cell gene complex is crucially involved in vascular remodeling. J Mol Cell Cardiol. 2013;64:51-8.
132. Takeichi N, Suzuki K, Kobayashi H. Characterization of immunological depression in spontaneously hypertensive rats. European journal of immunology. 1981;11(6):483-7.
133. Bradley JR. TNF-mediated inflammatory disease. J Pathol. 2008;214(2):149-60.
134. Perez C, Albert I, DeFay K, Zachariades N, Gooding L, Kriegler M. A nonsecretable cell surface mutant of tumor necrosis factor (TNF) kills by cell-to-cell contact. Cell. 1990;63(2):251-8.
135. Wajant H, Pfizenmaier K, Scheurich P. Tumor necrosis factor signaling. Cell death and differentiation. 2003;10(1):45-65.
136. Tartaglia LA, Ayres TM, Wong GHW, Goeddel DV. A Novel Domain within the 55 Kd Tnf Receptor Signals Cell-Death. Cell. 1993;74(5):845-53.
137. Lawrence T. The nuclear factor NF-kappaB pathway in inflammation. Cold Spring Harbor perspectives in biology. 2009;1(6):a001651.
138. Bautista LE, Vera LM, Arenas IA, Gamarra G. Independent association between inflammatory markers (C-reactive protein, interleukin-6, and TNF-alpha) and essential hypertension. J Hum Hypertens. 2005;19(2):149-54.
139. Chamarthi B, Williams GH, Ricchiuti V, Srikumar N, Hopkins PN, Luther JM, et al. Inflammation and Hypertension: The Interplay of Interleukin-6, Dietary Sodium, and the Renin-Angiotensin System in Humans. American journal of hypertension. 2011;24(10):1143-8.
140. Fisher CJ, Jr., Agosti JM, Opal SM, Lowry SF, Balk RA, Sadoff JC, et al. Treatment of septic shock with the tumor necrosis factor receptor:Fc fusion protein. The Soluble TNF Receptor Sepsis Study Group. N Engl J Med. 1996;334(26):1697-702.
141. Ramseyer VD, Garvin JL. Tumor necrosis factor-alpha: regulation of renal function and blood pressure. Am J Physiol-Renal. 2013;304(10):F1231-F42.
142. Satou R, Miyata K, Katsurada A, Navar LG, Kobori H. Tumor necrosis factor-alpha suppresses angiotensinogen expression through formation of a

p50/p50 homodimer in human renal proximal tubular cells. Am J Physiol-Cell Ph. 2010;299(4):C750-C9.
143. Todorov V, Muller M, Schweda F, Kurtz A. Tumor necrosis factor-alpha inhibits renin gene expression. Am J Physiol-Reg I. 2002;283(5):R1046-R51.
144. Schmidt C, Hocherl K, Schweda F, Kurtz A, Bucher M. Regulation of renal sodium transporters during severe inflammation. J Am Soc Nephrol. 2007;18(4):1072-83.
145. Zhang H, Park Y, Wu J, Chen X, Lee S, Yang J, et al. Role of TNF-alpha in vascular dysfunction. Clinical science. 2009;116(3):219-30.
146. Chia S, Qadan M, Newton R, Ludlam CA, Fox KA, Newby DE. Intra-arterial tumor necrosis factor-alpha impairs endothelium-dependent vasodilatation and stimulates local tissue plasminogen activator release in humans. Arteriosclerosis, thrombosis, and vascular biology. 2003;23(4):695-701.
147. Picchi A, Gao X, Belmadani S, Potter BJ, Focardi M, Chilian WM, et al. Tumor necrosis factor-alpha induces endothelial dysfunction in the prediabetic metabolic syndrome. Circ Res. 2006;99(1):69-77.
148. Wimalasundera R, Fexby S, Regan L, Hughes AD. Effect of tumour necrosis factor-alpha and interleukin 1 beta on endothelium-dependent relaxation in rat mesenteric resistance arteries in vitro. Brit J Pharmacol. 2003;138(7):1285-94.
149. Goodwin BL, Pendleton LC, Levy MM, Solomonson LP, Eichler DC. Tumor necrosis factor-alpha reduces argininosuccinate synthase expression and nitric oxide production in aortic endothelial cells. American journal of physiology Heart and circulatory physiology. 2007;293(2):H1115-21.
150. Yoshizumi M, Perrella MA, Burnett JC, Jr., Lee ME. Tumor necrosis factor downregulates an endothelial nitric oxide synthase mRNA by shortening its half-life. Circ Res. 1993;73(1):205-9.
151. Grunfeld S, Hamilton CA, Mesaros S, McClain SW, Dominiczak AF, Bohr DF, et al. Role of superoxide in the depressed nitric oxide production by the endothelium of genetically hypertensive rats. Hypertension. 1995;26(6 Pt 1):854-7.
152. Gillham JC, Myers JE, Baker PN, Taggart MJ. TNF-alpha alters nitric oxide- and endothelium-derived hyperpolarizing factor-mediated vasodilatation in human omental arteries. Hypertension in pregnancy. 2008;27(1):29-38.
153. Kessler P, Popp R, Busse R, Schini-Kerth VB. Proinflammatory mediators chronically downregulate the formation of the endothelium-derived hyperpolarizing factor in arteries via a nitric oxide/cyclic GMP-dependent mechanism. Circulation. 1999;99(14):1878-84.
154. Marsden PA, Brenner BM. Transcriptional regulation of the endothelin-1 gene by TNF-alpha. The American journal of physiology. 1992;262(4 Pt 1):C854-61.
155. Wilkinson MF, Earle ML, Triggle CR, Barnes S. Interleukin-1beta, tumor necrosis factor-alpha, and LPS enhance calcium channel current in isolated vascular smooth muscle cells of rat tail artery. Faseb J. 1996;10(7):785-91.
156. Sprague AH, Khalil RA. Inflammatory cytokines in vascular dysfunction and vascular disease. Biochemical pharmacology. 2009;78(6):539-52.
157. Torjesen I. Number of animals used in science increased slightly in 2013, Home Office reports. Bmj-Brit Med J. 2014;349.
158. Clayton JA, Collins FS. Policy: NIH to balance sex in cell and animal studies. Nature. 2014;509(7500):282-3.
159. Leong XF, Ng CY, Jaarin K. Animal Models in Cardiovascular Research: Hypertension and Atherosclerosis. BioMed research international. 2015;2015:528757.

160. Goldblatt H, Lynch J, Hanzal RF, Summerville WW. Studies on Experimental Hypertension : I. The Production of Persistent Elevation of Systolic Blood Pressure by Means of Renal Ischemia. The Journal of experimental medicine. 1934;59(3):347-79.
161. Dobrian AD, Davies MJ, Prewitt RL, Lauterio TJ. Development of hypertension in a rat model of diet-induced obesity. Hypertension. 2000;35(4):1009-15.
162. Selye H, Hall CE, Rowley EM. Malignant Hypertension Produced by Treatment with Desoxycorticosterone Acetate and Sodium Chloride. Can Med Assoc J. 1943;49(2):88-92.
163. Krieger EM. Neurogenic Hypertension in the Rat. Circ Res. 1964;15:511-21.
164. Hatton DC, DeMerritt J, Coste SC, McCarron DA. Stress-induced hypertension in the borderline hypertensive rat: stimulus duration. Physiology & behavior. 1993;53(4):635-41.
165. Rego A, Vargas R, Cathapermal S, Kuwahara M, Foegh ML, Ramwell PW. Systemic vascular effects of cyclosporin A treatment in normotensive rats. The Journal of pharmacology and experimental therapeutics. 1991;259(2):905-15.
166. Ohkubo H, Kawakami H, Kakehi Y, Takumi T, Arai H, Yokota Y, et al. Generation of transgenic mice with elevated blood pressure by introduction of the rat renin and angiotensinogen genes. Proceedings of the National Academy of Sciences of the United States of America. 1990;87(13):5153-7.
167. Jinek M, Chylinski K, Fonfara I, Hauer M, Doudna JA, Charpentier E. A programmable dual-RNA-guided DNA endonuclease in adaptive bacterial immunity. Science. 2012;337(6096):816-21.
168. Brown DM, Provoost AP, Daly MJ, Lander ES, Jacob HJ. Renal disease susceptibility and hypertension are under independent genetic control in the fawn-hooded rat. Nat Genet. 1996;12(1):44-51.
169. Harris EL, Dene H, Rapp JP. SA Gene and Blood Pressure Cosegregation Using Dahl Salt-Sensitive Rats. American journal of hypertension. 1993;6(4):330-4.
170. Iwai N, Inagami T. Identification of a candidate gene responsible for the high blood pressure of spontaneously hypertensive rats. J Hypertens. 1992;10(10):1155-7.
171. Kovacs P, Voigt B, Kloting I. Novel quantitative trait loci for blood pressure and related traits on rat chromosomes 1, 10, and 18. Biochem Bioph Res Co. 1997;235(2):343-8.
172. Okamoto K, Aoki K. Development of a strain of spontaneously hypertensive rats. Japanese circulation journal. 1963;27:282-93.
173. Luo Y, Owens D, Mulder G, McVey A, Fisher T. Blood Pressure Characterization of Hypertensive and Control Rats for Cardiovascular Studies. AHA, Atlanta: Charles River.
174. Yamori Y, Tomimoto K, Ooshima A, Hazama F, Okamoto K. Proceedings: Developmental course of hypertension in the SHR-substrains susceptible to hypertensive cerebrovascular lesions. Japanese heart journal. 1974;15(2):209-10.
175. Davidson AO, Schork N, Jaques BC, Kelman AW, Sutcliffe RG, Reid JL, et al. Blood pressure in genetically hypertensive rats. Influence of the Y chromosome. Hypertension. 1995;26(3):452-9.
176. Bianchi G, Fox U, Imbasciati E. The development of a new strain of spontaneously hypertensive rats. Life sciences. 1974;14(2):339-47.

177. Zagato L, Modica R, Florio M, Torielli L, Bihoreau MT, Bianchi G, et al. Genetic mapping of blood pressure quantitative trait loci in Milan hypertensive rats. Hypertension. 2000;36(5):734-9.
178. Dahl LK, Heine M, Tassinari L. Effects of Chronic Excess Salt Ingestion - Evidence That Genetic Factors Play an Important Role in Susceptibility to Experimental Hypertension. Journal of Experimental Medicine. 1962;115(6):1173-&.
179. Hinojosa-Laborde C, Lange DL, Haywood JR. Role of female sex hormones in the development and reversal of Dahl hypertension. Hypertension. 2000;35(1):484-9.
180. Dupont J, Dupont JC, Froment A, Milon H, Vincent M. Selection of three strains of rats with spontaneously different levels of blood pressure. Biomedicine / [publiee pour l'AAICIG]. 1973;19(1):36-41.
181. Vincent M, Samani NJ, Gauguier D, Thompson JR, Lathrop GM, Sassard J. A pharmacogenetic approach to blood pressure in Lyon hypertensive rats - A chromosome 2 locus influences the response to a calcium antagonist. Journal of Clinical Investigation. 1997;100(8):2000-6.
182. Ben-Ishay D, Saliternik R, Welner A. Separation of two strains of rats with inbred dissimilar sensitivity to Doca-salt hypertension. Experientia. 1972;28(11):1321-2.
183. Yagil C, Sapojnikov M, Kreutz R, Katni G, Lindpaintner K, Ganten D, et al. Salt susceptibility maps to chromosomes 1 and 17 with sex specificity in the Sabra rat model of hypertension. Hypertension. 1998;31(1):119-24.
184. Phelan EL. The New Zealand strain of rats with genetic hypertension. The New Zealand medical journal. 1968;67(429):334-44.
185. Ashton N, Balment RJ. Sexual dimorphism in renal function and hormonal status of New Zealand genetically hypertensive rats. Acta endocrinologica. 1991;124(1):91-7.
186. Dickhout JG, Lee RM. Blood pressure and heart rate development in young spontaneously hypertensive rats. The American journal of physiology. 1998;274(3 Pt 2):H794-800.
187. Yamori Y, Nara Y, Kihara M, Horie R, Ooshima A. Sodium and Other Dietary Factors in Experimental and Human Hypertension: The Japanese Experience. In: Laragh J, Bühler F, Seldin D, editors. Frontiers in Hypertension Research: Springer New York; 1981. p. 46-8.
188. Nagura J, Hui C, Yamamoto M, Yasuda S, Abe M, Hachisu M, et al. Effect of chronic treatment with ME3221 on blood pressure and mortality in aged stroke-prone spontaneously hypertensive rats. Clinical and experimental pharmacology & physiology Supplement. 1995;22(1):S363-5.
189. Vacher E, Richer C, Fornes P, Clozel JP, Giudicelli. Mibefradil, a selective calcium T-channel blocker, in stroke-prone spontaneously hypertensive rats. J Cardiovasc Pharmacol. 1996;27(5):686-94.
190. Doggrell SA, Brown L. Rat models of hypertension, cardiac hypertrophy and failure. Cardiovascular research. 1998;39(1):89-105.
191. Bubb KJ, Khambata RS, Ahluwalia A. Sexual dimorphism in rodent models of hypertension and atherosclerosis. Br J Pharmacol. 2012;167(2):298-312.
192. Ganten U, Schroder G, Witt M, Zimmermann F, Ganten D, Stock G. Sexual dimorphism of blood pressure in spontaneously hypertensive rats: effects of anti-androgen treatment. J Hypertens. 1989;7(9):721-6.
193. Reckelhoff JF, Zhang H, Srivastava K. Gender differences in development of hypertension in spontaneously hypertensive rats: role of the renin-angiotensin system. Hypertension. 2000;35(1 Pt 2):480-3.

194. Stier CT, Jr., Chander PN, Rosenfeld L, Powers CA. Estrogen promotes microvascular pathology in female stroke-prone spontaneously hypertensive rats. Am J Physiol Endocrinol Metab. 2003;285(1):E232-9.
195. McIntyre M, Hamilton CA, Rees DD, Reid JL, Dominiczak AF. Sex differences in the abundance of endothelial nitric oxide in a model of genetic hypertension. Hypertension. 1997;30(6):1517-24.
196. Giachini FR, Lima VV, Filgueira FP, Dorrance AM, Carvalho MH, Fortes ZB, et al. STIM1/Orai1 contributes to sex differences in vascular responses to calcium in spontaneously hypertensive rats. Clinical science. 2012;122(5):215-26.
197. Bacakova L, Kunes J. Gender differences in growth of vascular smooth muscle cells isolated from hypertensive and normotensive rats. Clinical and experimental hypertension. 2000;22(1):33-44.
198. Wang X, Desai K, Juurlink BHJ, de Champlain J, Wu L. Gender-related differences in advanced glycation endproducts, oxidative stress markers and nitric oxide synthases in rats. Kidney Int. 2006;69(2):281-7.
199. Singh G, Masineni SN, Chander PN, Ranaudo JM, Hassan IR, Stier CT. Gender differences in proteinuria in aged stroke-prone spontaneously hypertensive rats are independent of blood pressure. American journal of hypertension. 2004;17(5):76a-a.
200. Tipton AJ, Baban B, Sullivan JC. Female Spontaneously Hypertensive Rats Have a Compensatory Increase in Renal Regulatory T Cells in Response to Elevations in Blood Pressure. Hypertension. 2014;64(3):557-+.
201. Ballerio R, Gianazza E, Mussoni L, Miller I, Gelosa P, Guerrini U, et al. Gender differences in endothelial function and inflammatory markers along the occurrence of pathological events in stroke-prone rats. Exp Mol Pathol. 2007;82(1):33-41.
202. Chapman AB, Abraham WT, Zamudio S, Coffin C, Merouani A, Young D, et al. Temporal relationships between hormonal and hemodynamic changes in early human pregnancy. Kidney Int. 1998;54(6):2056-63.
203. Robson SC, Hunter S, Moore M, Dunlop W. Haemodynamic changes during the puerperium: a Doppler and M-mode echocardiographic study. British journal of obstetrics and gynaecology. 1987;94(11):1028-39.
204. Wong AYH, Kulandavelu S, Whiteley KJ, Qu DW, Langille BL, Adamson SL. Maternal cardiovascular changes during pregnancy and postpartum in mice. Am J Physiol-Heart C. 2002;282(3):H918-H25.
205. Kulandavelu S, Qu DW, Adamson SL. Cardiovascular function in mice during normal pregnancy and in the absence of endothelial NO synthase. Hypertension. 2006;47(6):1175-82.
206. Dowell RT, Kauer CD. Maternal hemodynamics and uteroplacental blood flow throughout gestation in conscious rats. Methods Find Exp Clin Pharmacol. 1997;19(9):613-25.
207. Aasa KL, Zavan B, Luna RL, Wong PG, Ventura NM, Tse MY, et al. Placental growth factor influences maternal cardiovascular adaptation to pregnancy in mice. Biology of reproduction. 2015;92(2):44.
208. Hunter S, Robson SC. Adaptation of the maternal heart in pregnancy. Br Heart J. 1992;68(6):540-3.
209. Sanghavi M, Rutherford JD. Cardiovascular physiology of pregnancy. Circulation. 2014;130(12):1003-8.
210. Arbab-Zadeh A, Perhonen M, Howden E, Peshock RM, Zhang R, Adams-Huet B, et al. Cardiac remodeling in response to 1 year of intensive endurance training. Circulation. 2014;130(24):2152-61.

211. Melchiorre K, Sharma R, Thilaganathan B. Cardiac structure and function in normal pregnancy. Current opinion in obstetrics & gynecology. 2012;24(6):413-21.
212. Greenwood JP, Scott EM, Stoker JB, Walker JJ, Mary DA. Sympathetic neural mechanisms in normal and hypertensive pregnancy in humans. Circulation. 2001;104(18):2200-4.
213. Hytten F. Blood volume changes in normal pregnancy. Clinics in haematology. 1985;14(3):601-12.
214. Abbassi-Ghanavati M, Greer LG, Cunningham FG. Pregnancy and laboratory studies: a reference table for clinicians. Obstetrics and gynecology. 2009;114(6):1326-31.
215. Ducas RA, Elliott JE, Melnyk SF, Premecz S, daSilva M, Cleverley K, et al. Cardiovascular magnetic resonance in pregnancy: insights from the cardiac hemodynamic imaging and remodeling in pregnancy (CHIRP) study. Journal of cardiovascular magnetic resonance : official journal of the Society for Cardiovascular Magnetic Resonance. 2014;16:1.
216. Melchiorre K, Sharma R, Khalil A, Thilaganathan B. Maternal Cardiovascular Function in Normal Pregnancy: Evidence of Maladaptation to Chronic Volume Overload. Hypertension. 2016;67(4):754-62.
217. Mahendru AA, Everett TR, Wilkinson IB, Lees CC, McEniery CM. A longitudinal study of maternal cardiovascular function from preconception to the postpartum period. J Hypertens. 2014;32(4):849-56.
218. Cheung KL, Lafayette RA. Renal physiology of pregnancy. Advances in chronic kidney disease. 2013;20(3):209-14.
219. Baylis C. Immediate and long-term effects of pregnancy on glomerular function in the SHR. The American journal of physiology. 1989;257(6 Pt 2):F1140-5.
220. Irani RA, Xia Y. The functional role of the renin-angiotensin system in pregnancy and preeclampsia. Placenta. 2008;29(9):763-71.
221. Xia Y, Wen H, Prashner HR, Chen R, Inagami T, Catanzaro DF, et al. Pregnancy-induced changes in renin gene expression in mice. Biology of reproduction. 2002;66(1):135-43.
222. Jarvis SS, Shibata S, Bivens TB, Okada Y, Casey BM, Levine BD, et al. Sympathetic activation during early pregnancy in humans. The Journal of physiology. 2012;590(Pt 15):3535-43.
223. Leduc L, Wasserstrum N, Spillman T, Cotton DB. Baroreflex function in normal pregnancy. American journal of obstetrics and gynecology. 1991;165(4 Pt 1):886-90.
224. Silver HM, Tahvanainen KU, Kuusela TA, Eckberg DL. Comparison of vagal baroreflex function in nonpregnant women and in women with normal pregnancy, preeclampsia, or gestational hypertension. American journal of obstetrics and gynecology. 2001;184(6):1189-95.
225. Gant NF, Daley GL, Chand S, Whalley PJ, MacDonald PC. A study of angiotensin II pressor response throughout primigravid pregnancy. The Journal of clinical investigation. 1973;52(11):2682-9.
226. Nelson SH, Steinsland OS, Johnson RL, Suresh MS, Gifford A, Ehardt JS. Pregnancy-induced alterations of neurogenic constriction and dilation of human uterine artery. The American journal of physiology. 1995;268(4 Pt 2):H1694-701.
227. Shi Z, Cassaglia PA, Gotthardt LC, Brooks VL. Hypothalamic Paraventricular and Arcuate Nuclei Contribute to Elevated Sympathetic Nerve Activity in Pregnant Rats: Roles of Neuropeptide Y and alpha-Melanocyte-Stimulating Hormone. Hypertension. 2015.

228. Paller MS. Mechanism of decreased pressor responsiveness to ANG II, NE, and vasopressin in pregnant rats. The American journal of physiology. 1984;247(1 Pt 2):H100-8.
229. Coelho EB, Ballejo G, Salgado MC. Nitric oxide blunts sympathetic response of pregnant normotensive and hypertensive rat arteries. Hypertension. 1997;30(3 Pt 2):585-8.
230. Walters WA, Lim YL. Cardiovascular dynamics in women receiving oral contraceptive therapy. Lancet. 1969;2(7626):879-81.
231. Hettiaratchi ES, Pickford M. The effect of oestrogen and progesterone on the pressor action of angiotensin in the rat. The Journal of physiology. 1968;196(2):447-51.
232. Gross ML, Ritz E, Korsch M, Adamczak M, Weckbach M, Mall G, et al. Effects of estrogens on cardiovascular structure in uninephrectomized SHRsp rats. Kidney Int. 2005;67(3):849-57.
233. Rylance PB, Brincat M, Lafferty K, De Trafford JC, Brincat S, Parsons V, et al. Natural progesterone and antihypertensive action. Br Med J (Clin Res Ed). 1985;290(6461):13-4.
234. Regensteiner JG, Hiatt WR, Byyny RL, Pickett CK, Woodard WD, Moore LG. Short-term effects of estrogen and progestin on blood pressure of normotensive postmenopausal women. Journal of clinical pharmacology. 1991;31(6):543-8.
235. Barbagallo M, Dominguez LJ, Licata G, Shan J, Bing L, Karpinski E, et al. Vascular Effects of Progesterone : Role of Cellular Calcium Regulation. Hypertension. 2001;37(1):142-7.
236. Conrad KP. Emerging role of relaxin in the maternal adaptations to normal pregnancy: implications for preeclampsia. Seminars in nephrology. 2011;31(1):15-32.
237. Debrah DO, Conrad KP, Danielson LA, Shroff SG. Effects of relaxin on systemic arterial hemodynamics and mechanical properties in conscious rats: sex dependency and dose response. Journal of applied physiology. 2005;98(3):1013-20.
238. Debrah DO, Conrad KP, Jeyabalan A, Danielson LA, Shroff SG. Relaxin increases cardiac output and reduces systemic arterial load in hypertensive rats. Hypertension. 2005;46(4):745-50.
239. Debrah DO, Novak J, Matthews JE, Ramirez RJ, Shroff SG, Conrad KP. Relaxin is essential for systemic vasodilation and increased global arterial compliance during early pregnancy in conscious rats. Endocrinology. 2006;147(11):5126-31.
240. Danielson LA, Sherwood OD, Conrad KP. Relaxin is a potent renal vasodilator in conscious rats. Journal of Clinical Investigation. 1999;103(4):525-33.
241. Chappell LC, Duckworth S, Seed PT, Griffin M, Myers J, Mackillop L, et al. Diagnostic accuracy of placental growth factor in women with suspected preeclampsia: a prospective multicenter study. Circulation. 2013;128(19):2121-31.
242. Spradley FT, Tan AY, Joo WS, Daniels G, Kussie P, Karumanchi SA, et al. Placental Growth Factor Administration Abolishes Placental Ischemia-Induced Hypertension. Hypertension. 2016;67(4):740-7.
243. Hermida RC, Ayala DE, Mojon A, Fernandez JR, Alonso I, Aguilar MF, et al. Differences in circadian blood pressure variability during gestation between healthy and complicated pregnancies. American journal of hypertension. 2003;16(3):200-8.

244. Ayala DE, Hermida RC, Mojon A, Fernandez JR, Iglesias M. Circadian blood pressure variability in healthy and complicated pregnancies. Hypertension. 1997;30(3 Pt 2):603-10.
245. Kubota T, Yamada T. Circulating hypotensive factor in pregnant spontaneously hypertensive rats. Clinical and experimental pharmacology & physiology. 1981;8(2):125-32.
246. de Rijk EPCT, van Esch E, Flik G. Pregnancy dating in the rat: Placental morphology and maternal blood parameters. Toxicologic pathology. 2002;30(2):271-82.
247. Soares MJ, Chakraborty D, Karim Rumi MA, Konno T, Renaud SJ. Rat placentation: an experimental model for investigating the hemochorial maternal-fetal interface. Placenta. 2012;33(4):233-43.
248. Osol G, Mandala M. Maternal uterine vascular remodeling during pregnancy. Physiology. 2009;24:58-71.
249. Burton GJ, Woods AW, Jauniaux E, Kingdom JC. Rheological and physiological consequences of conversion of the maternal spiral arteries for uteroplacental blood flow during human pregnancy. Placenta. 2009;30(6):473-82.
250. Pijnenborg R, Vercruysse L, Hanssens M. The uterine spiral arteries in human pregnancy: facts and controversies. Placenta. 2006;27(9-10):939-58.
251. Brar AK, Frank GR, Kessler CA, Cedars MI, Handwerger S. Progesterone-dependent decidualization of the human endometrium is mediated by cAMP. Endocrine. 1997;6(3):301-7.
252. Pijnenborg R, Robertson WB, Brosens I, Dixon G. Review article: trophoblast invasion and the establishment of haemochorial placentation in man and laboratory animals. Placenta. 1981;2(1):71-91.
253. Gellersen B, Brosens IA, Brosens JJ. Decidualization of the human endometrium: mechanisms, functions, and clinical perspectives. Seminars in reproductive medicine. 2007;25(6):445-53.
254. Ain R, Trinh ML, Soares MJ. Interleukin-11 signaling is required for the differentiation of natural killer cells at the maternal-fetal interface. Dev Dynam. 2004;231(4):700-8.
255. Dunn CL, Kelly RW, Critchley HO. Decidualization of the human endometrial stromal cell: an enigmatic transformation. Reproductive biomedicine online. 2003;7(2):151-61.
256. Moffett-King A. Natural killer cells and pregnancy. Nat Rev Immunol. 2002;2(9):656-63.
257. Loke YW, King A. Immunological aspects of human implantation. Journal of reproduction and fertility Supplement. 2000;55:83-90.
258. Vercruysse L, Caluwaerts S, Luyten C, Pijnenborg R. Interstitial trophoblast invasion in the decidua and mesometrial triangle during the last third of pregnancy in the rat. Placenta. 2006;27(1):22-33.
259. Cartwright JE, Fraser R, Leslie K, Wallace AE, James JL. Remodelling at the maternal-fetal interface: relevance to human pregnancy disorders. Reproduction. 2010;140(6):803-13.
260. Adamson SL, Lu Y, Whiteley KJ, Holmyard D, Hemberger M, Pfarrer C, et al. Interactions between trophoblast cells and the maternal and fetal circulation in the mouse placenta. Developmental biology. 2002;250(2):358-73.
261. Greenwood JD, Minhas K, di Santo JP, Makita M, Kiso Y, Croy BA. Ultrastructural studies of implantation sites from mice deficient in uterine natural killer cells. Placenta. 2000;21(7):693-702.

262. Lash GE, Schiessl B, Kirkley M, Innes BA, Cooper A, Searle RF, et al. Expression of angiogenic growth factors by uterine natural killer cells during early pregnancy. Journal of leukocyte biology. 2006;80(3):572-80.
263. Naruse K, Lash GE, Innes BA, Otun HA, Searle RF, Robson SC, et al. Localization of matrix metalloproteinase (MMP)-2, MMP-9 and tissue inhibitors for MMPs (TIMPs) in uterine natural killer cells in early human pregnancy. Hum Reprod. 2009;24(3):553-61.
264. Lyall F, Bulmer JN, Duffie E, Cousins F, Theriault A, Robson SC. Human trophoblast invasion and spiral artery transformation: the role of PECAM-1 in normal pregnancy, preeclampsia, and fetal growth restriction. The American journal of pathology. 2001;158(5):1713-21.
265. Palmer SK, Zamudio S, Coffin C, Parker S, Stamm E, Moore LG. Quantitative estimation of human uterine artery blood flow and pelvic blood flow redistribution in pregnancy. Obstetrics and gynecology. 1992;80(6):1000-6.
266. Nienartowicz A, Link S, Moll W. Adaptation of the uterine arcade in rats to pregnancy. Journal of developmental physiology. 1989;12(2):101-8.
267. Osol G, Moore LG. Maternal uterine vascular remodeling during pregnancy. Microcirculation. 2014;21(1):38-47.
268. van der Heijden OW, Essers YP, Fazzi G, Peeters LL, De Mey JG, van Eys GJ. Uterine artery remodeling and reproductive performance are impaired in endothelial nitric oxide synthase-deficient mice. Biology of reproduction. 2005;72(5):1161-8.
269. Cipolla M, Osol G. Hypertrophic and hyperplastic effects of pregnancy on the rat uterine arterial wall. American journal of obstetrics and gynecology. 1994;171(3):805-11.
270. Metcalfe J, Romney SL, Ramsey LH, Reid DE, Burwell CS. Estimation of Uterine Blood Flow in Normal Human Pregnancy at Term. Journal of Clinical Investigation. 1955;34(11):1632-8.
271. Bruce NW. The distribution of blood flow to the reproductive organs of rats near term. Journal of reproduction and fertility. 1976;46(2):359-62.
272. Konje JC, Kaufmann P, Bell SC, Taylor DJ. A longitudinal study of quantitative uterine blood flow with the use of color power angiography in appropriate for gestational age pregnancies. American journal of obstetrics and gynecology. 2001;185(3):608-13.
273. Dowell RT, Kauer CD. Maternal hemodynamics and uteroplacental blood flow throughout gestation in conscious rats. Method Find Exp Clin. 1997;19(9):613-25.
274. van der Heijden OWH, Essers YPG, Spaanderman MEA, De Mey JGR, van Eys GJJM, Peeters LLH. Uterine artery remodeling in pseudopregnancy is comparable to that in early pregnancy. Biology of reproduction. 2005;73(6):1289-93.
275. Ford SP, Chenault JR. Blood-Flow to the Corpus Luteum-Bearing Ovary and Ipsilateral Uterine Horn of Cows during the Estrous-Cycle and Early-Pregnancy. Journal of reproduction and fertility. 1981;62(2):555-62.
276. Ford SP, Chenault JR, Echternkamp SE. Uterine Blood-Flow of Cows during the Estrous-Cycle and Early-Pregnancy - Effect of the Conceptus on the Uterine Blood-Supply. Journal of reproduction and fertility. 1979;56(1):53-62.
277. Waddell BJ, Burton PJ. Full induction of rat myometrial 11 beta-hydroxysteroid dehydrogenase type 1 in late pregnancy is dependent on intrauterine occupancy. Biology of reproduction. 2000;62(4):1005-9.

278. Makinoda S, Moll W. Deoxyribonucleic-Acid Synthesis in Mesometrial Arteries of Guinea-Pigs during Estrous-Cycle, Pregnancy and Treatment with Estradiol Benzoate. Placenta. 1986;7(3):189-98.
279. Tarhouni K, Guihot AL, Freidja ML, Toutain B, Henrion B, Baufreton C, et al. Key Role of Estrogens and Endothelial Estrogen Receptor alpha in Blood Flow-Mediated Remodeling of Resistance Arteries. Arterioscl Throm Vas. 2013;33(3):605-+.
280. Berg CJ, Callaghan WM, Syverson C, Henderson Z. Pregnancy-related mortality in the United States, 1998 to 2005. Obstetrics and gynecology. 2010;116(6):1302-9.
281. Burns H. Saving Mothers' Lives: Reviewing maternal deaths to make motherhood safer: 2006-2008. Bjog-Int J Obstet Gy. 2011;118:5-6.
282. Easterling TR. Post-Control of Hypertension in Pregnancy Study (CHIPS): What Is the Optimal Strategy to Manage Hypertension During Pregnancy? Hypertension. 2016.
283. Sattar N, Greer IA. Pregnancy complications and maternal cardiovascular risk: opportunities for intervention and screening? Brit Med J. 2002;325(7356):157-60.
284. Craici I, Wagner S, Garovic VD. Preeclampsia and future cardiovascular risk: formal risk factor or failed stress test? Therapeutic advances in cardiovascular disease. 2008;2(4):249-59.
285. Cuevas AM, Germain AM. A Failed Pregnancy Stress Test: A New and Under-Recognized Cardiovascular Risk Factor. Curr Atheroscler Rep. 2011;13(4):285-6.
286. Bellamy L, Casas JP, Hingorani AD, Williams DJ. Pre-eclampsia and risk of cardiovascular disease and cancer in later life: systematic review and meta-analysis. Brit Med J. 2007;335(7627):974-7.
287. Hannaford P, Ferry S, Hirsch S. Cardiovascular sequelae of toxaemia of pregnancy. Heart. 1997;77(2):154-8.
288. Magnussen EB, Vatten LJ, Smith GD, Romundstad PR. Hypertensive Disorders in Pregnancy and Subsequently Measured Cardiovascular Risk Factors. Obstetrics and gynecology. 2009;114(5):961-70.
289. Wang IK, Muo CH, Chang YC, Liang CC, Chang CT, Lin SY, et al. Association between hypertensive disorders during pregnancy and end-stage renal disease: a population-based study. Can Med Assoc J. 2013;185(3):207-13.
290. Smith GCS, Pell JP, Walsh D. Pregnancy complications and maternal risk of ischaemic heart disease: a retrospective cohort study of 129,290 births. Lancet. 2001;357(9273):2002-6.
291. Pell JP, Smith GCS, Wash D. Pregnancy complications and subsequent maternal cerebrovascular events: A retrospective cohort study of 119,668 births. Am J Epidemiol. 2004;159(4):336-42.
292. Vikse BE, Irgens LM, Leivestad T, Skjaerven R, Iversen BM. Preeclampsia and the risk of end-stage renal disease. N Engl J Med. 2008;359(8):800-9.
293. Vikse BE, Hallan S, Bostad L, Leivestad T, Iversen BM. Previous preeclampsia and risk for progression of biopsy-verified kidney disease to end-stage renal disease. Nephrology, dialysis, transplantation : official publication of the European Dialysis and Transplant Association - European Renal Association. 2010;25(10):3289-96.
294. Kestenbaum B, Seliger SL, Easterling TR, Gillen DL, Critchlow CW, Stehman-Breen CO, et al. Cardiovascular and thromboembolic events following hypertensive pregnancy. Am J Kidney Dis. 2003;42(5):982-9.

295. Ray JG, Vermeulen MJ, Schull MJ, Redelmeier DA. Cardiovascular health after maternal placental syndromes (CHAMPS): population-based retrospective cohort study. Lancet. 2005;366(9499):1797-803.
296. Steegers EAP, von Dadelszen P, Duvekot JJ, Pijnenborg R. Pre-eclampsia. The Lancet.376(9741):631-44.
297. Khan KS, Wojdyla D, Say L, Gulmezoglu AM, Van Look PF. WHO analysis of causes of maternal death: a systematic review. Lancet. 2006;367(9516):1066-74.
298. Powe CE, Levine RJ, Karumanchi SA. Preeclampsia, a disease of the maternal endothelium: the role of antiangiogenic factors and implications for later cardiovascular disease. Circulation. 2011;123(24):2856-69.
299. Schlembach D. Pre-eclampsia--still a disease of theories. Fukushima journal of medical science. 2003;49(2):69-115.
300. American College of O, Gynecologists. ACOG Practice Bulletin No. 125: Chronic hypertension in pregnancy. Obstetrics and gynecology. 2012;119(2 Pt 1):396-407.
301. Sibai BM. Chronic hypertension in pregnancy. Obstetrics and gynecology. 2002;100(2):369-77.
302. Lawler J, Osman M, Shelton JA, Yeh J. Population-based analysis of hypertensive disorders in pregnancy. Hypertension in pregnancy. 2007;26(1):67-76.
303. Roberts CL, Ford JB, Algert CS, Antonsen S, Chalmers J, Cnattingius S, et al. Population-based trends in pregnancy hypertension and pre-eclampsia: an international comparative study. BMJ open. 2011;1(1):e000101.
304. Bateman BT, Bansil P, Hernandez-Diaz S, Mhyre JM, Callaghan WM, Kuklina EV. Prevalence, trends, and outcomes of chronic hypertension: a nationwide sample of delivery admissions. American journal of obstetrics and gynecology. 2012;206(2):134 e1-8.
305. Seely EW, Ecker J. Chronic hypertension in pregnancy. Circulation. 2014;129(11):1254-61.
306. Bramham K, Parnell B, Nelson-Piercy C, Seed PT, Poston L, Chappell LC. Chronic hypertension and pregnancy outcomes: systematic review and meta-analysis. Bmj. 2014;348:g2301.
307. Matthews TJ, Hamilton BE. Delayed childbearing: more women are having their first child later in life. NCHS data brief. 2009(21):1-8.
308. Wang YC, McPherson K, Marsh T, Gortmaker SL, Brown M. Health and economic burden of the projected obesity trends in the USA and the UK. Lancet. 2011;378(9793):815-25.
309. Ramos RG, Olden K. The prevalence of metabolic syndrome among US women of childbearing age. Am J Public Health. 2008;98(6):1122-7.
310. Nabel EG. Heart Disease Prevention in Young Women: Sounding an Alarm. Circulation. 2015;132(11):989-91.
311. Wellings K, Jones KG, Mercer CH, Tanton C, Clifton S, Datta J, et al. The prevalence of unplanned pregnancy and associated factors in Britain: findings from the third National Survey of Sexual Attitudes and Lifestyles (Natsal-3). Lancet. 2013;382(9907):1807-16.
312. Finer LB, Henshaw SK. Disparities in rates of unintended pregnancy in the United States, 1994 and 2001. Perspectives on sexual and reproductive health. 2006;38(2):90-6.
313. Catov JM, Nohr EA, Olsen J, Ness RB. Chronic hypertension related to risk for preterm and term small for gestational age births. Obstetrics and gynecology. 2008;112(2):290-6.

314. Catov JM, Nohr EA, Olsen J, Ness RB. Chronic hypertension related to risk for preterm and term small for gestational age births. Obstetrics and gynecology. 2008;112(2 Pt 1):290-6.
315. Bateman BT, Huybrechts KF, Fischer MA, Seely EW, Ecker JL, Oberg AS, et al. Chronic hypertension in pregnancy and the risk of congenital malformations: a cohort study. American journal of obstetrics and gynecology. 2015;212(3):337 e1-14.
316. Hink E, Bolte AC. Pregnancy outcomes in women with heart disease: Experience of a tertiary center in the Netherlands. Pregnancy hypertension. 2015;5(2):165-70.
317. Marcolan Quitete CM, Marcolan Salvany A, de Andrade Martins W, Mesquita ET. Left ventricular remodeling and diastolic function in chronic hypertensive pregnant women. Pregnancy hypertension. 2015;5(2):187-92.
318. Seely EW, Ecker J. Clinical practice. Chronic hypertension in pregnancy. N Engl J Med. 2011;365(5):439-46.
319. Sibai BM, Lindheimer M, Hauth J, Caritis S, VanDorsten P, Klebanoff M, et al. Risk factors for preeclampsia, abruptio placentae, and adverse neonatal outcomes among women with chronic hypertension. New Engl J Med. 1998;339(10):667-71.
320. Brent RL, Beckman DA. Angiotensin-converting enzyme inhibitors, an embryopathic class of drugs with unique properties: information for clinical teratology counselors. Teratology. 1991;43(6):543-6.
321. Chevalier RL. Mechanisms of fetal and neonatal renal impairment by pharmacologic inhibition of angiotensin. Current medicinal chemistry. 2012;19(27):4572-80.
322. Cockburn J, Moar VA, Ounsted M, Redman CW. Final report of study on hypertension during pregnancy: the effects of specific treatment on the growth and development of the children. Lancet. 1982;1(8273):647-9.
323. Lip GY, Beevers M, Churchill D, Shaffer LM, Beevers DG. Effect of atenolol on birth weight. The American journal of cardiology. 1997;79(10):1436-8.
324. Nifedipine versus expectant management in mild to moderate hypertension in pregnancy. Gruppo di Studio Ipertensione in Gravidanza. British journal of obstetrics and gynaecology. 1998;105(7):718-22.
325. Abalos E, Duley L, Steyn DW. Antihypertensive drug therapy for mild to moderate hypertension during pregnancy. Cochrane Db Syst Rev. 2014(2).
326. Magee LA, Singer J, von Dadelszen P, Group CS. Less-tight versus tight control of hypertension in pregnancy. N Engl J Med. 2015;372(24):2367-8.
327. McCarthy FP, Kingdom JC, Kenny LC, Walsh SK. Animal models of preeclampsia; uses and limitations. Placenta. 2011;32(6):413-9.
328. Granger JP, LaMarca BB, Cockrell K, Sedeek M, Balzi C, Chandler D, et al. Reduced uterine perfusion pressure (RUPP) model for studying cardiovascular-renal dysfunction in response to placental ischemia. Methods in molecular medicine. 2006;122:383-92.
329. Gilbert JS, Babcock SA, Granger JP. Hypertension produced by reduced uterine perfusion in pregnant rats is associated with increased soluble fms-like tyrosine kinase-1 expression. Hypertension. 2007;50(6):1142-7.
330. Llinas MT, Alexander BT, Seedek M, Abram SR, Crell A, Granger JP. Enhanced thromboxane synthesis during chronic reductions in uterine perfusion pressure in pregnant rats. American journal of hypertension. 2002;15(9):793-7.
331. Walsh SK, English FA, Johns EJ, Kenny LC. Plasma-mediated vascular dysfunction in the reduced uterine perfusion pressure model of preeclampsia: a microvascular characterization. Hypertension. 2009;54(2):345-51.

332. Schenone MH, Mari G, Schlabritz-Loutsevitch N, Ahokas R. Effects of selective reduced uterine perfusion pressure in pregnant rats. Placenta. 2015;36(12):1450-4.
333. Huang PL, Huang Z, Mashimo H, Bloch KD, Moskowitz MA, Bevan JA, et al. Hypertension in mice lacking the gene for endothelial nitric oxide synthase. Nature. 1995;377(6546):239-42.
334. Kanasaki K, Palmsten K, Sugimoto H, Ahmad S, Hamano Y, Xie L, et al. Deficiency in catechol-O-methyltransferase and 2-methoxyoestradiol is associated with pre-eclampsia. Nature. 2008;453(7198):1117-U12.
335. Shesely EG, Gilbert C, Granderson G, Carretero CD, Carretero OA, Beierwaltes WH. Nitric oxide synthase gene knockout mice do not become hypertensive during pregnancy. American journal of obstetrics and gynecology. 2001;185(5):1198-203.
336. Palmer K, Saglam B, Whitehead C, Stock O, Lappas M, Tong S. Severe Early-Onset Preeclampsia Is Not Associated with a Change in Placental Catechol O-Methyltransferase (COMT) Expression. The American journal of pathology. 2011;178(6):2484-8.
337. Bohlender J, Ganten D, Luft FC. Rats transgenic for human renin and human angiotensinogen as a model for gestational hypertension. Journal of the American Society of Nephrology. 2000;11(11):2056-61.
338. Geusens N, Verlohren S, Luyten C, Taube M, Hering L, Vercruysse L, et al. Endovascular trophoblast invasion, spiral artery remodelling and uteroplacental haemodynamics in a transgenic rat model of pre-eclampsia. Placenta. 2008;29(7):614-23.
339. Ramesar SV, Mackraj I, Gathiram P, Moodley J. Sildenafil citrate improves fetal outcomes in pregnant, L-NAME treated, Sprague-Dawley rats. Eur J Obstet Gynecol Reprod Biol. 2010;149(1):22-6.
340. Samangaya RA, Mires G, Shennan A, Skillern L, Howe D, McLeod A, et al. A Randomised, Double-Blinded, Placebo-Controlled Study of the Phosphodiesterase Type 5 Inhibitor Sildenafil for the Treatment of Preeclampsia. Hypertension in pregnancy. 2009;28(4):369-82.
341. Maynard SE, Min J-Y, Merchan J, Lim K-H, Li J, Mondal S, et al. Excess placental soluble fms-like tyrosine kinase 1 (sFlt1) may contribute to endothelial dysfunction, hypertension, and proteinuria in preeclampsia. Journal of Clinical Investigation. 2003;111(5):649-58.
342. Venkatesha S, Toporsian M, Lam C, Hanai J, Mammoto T, Kim YM, et al. Soluble endoglin contributes to the pathogenesis of preeclampsia. Nat Med. 2006;12(6):642-9.
343. LaMarca B, Speed J, Fournier L, Babcock SA, Berry H, Cockrell K, et al. Hypertension in Response to Chronic Reductions in Uterine Perfusion in Pregnant Rats Effect of Tumor Necrosis Factor-alpha Blockade. Hypertension. 2008;52(6):1161-7.
344. Davisson RL, Hoffmann DS, Butz GM, Aldape G, Schlager G, Merrill DC, et al. Discovery of a spontaneous genetic mouse model of preeclampsia. Hypertension. 2002;39(2 Pt 2):337-42.
345. Gillis EE, Williams JM, Garrett MR, Mooney JN, Sasser JM. The Dahl salt-sensitive rat is a spontaneous model of superimposed preeclampsia. Am J Physiol-Reg I. 2015;309(1):R62-R70.
346. Gillis EE, Mooney JN, Garrett MR, Granger JP, Sasser JM. Sildenafil Treatment Ameliorates the Maternal Syndrome of Preeclampsia and Rescues Fetal Growth in the Dahl Salt-Sensitive Rat. Hypertension. 2016;67(3):647-53.

347. Fuchi I, Higashino H, Noda K, Suzuki A, Matsubara Y. Placental Na+, K+ activated ATP-ase activity in SHRSP in connection with pregnancy induced hypertension and intra-uterine growth retardation. Clinical and experimental pharmacology & physiology Supplement. 1995;22(1):S283-5.
348. Yamada N, Kido K, Tamai T, Mukai M, Hayashi S. Hypertensive effects on pregnancy in spontaneously hypertensive rats (SHR) and stroke-prone SHR (SHRSP). International journal of biological research in pregnancy. 1981;2(2):80-4.
349. Small HY, Morgan H, Beattie E, Griffin S, Indahl M, Delles C, et al. Abnormal uterine artery remodelling in the stroke prone spontaneously hypertensive rat. Placenta. 2016;37:34-44.
350. Robertson WB, Brosens I, Dixon G. Uteroplacental vascular pathology. Eur J Obstet Gynecol Reprod Biol. 1975;5(1-2):47-65.
351. Pourageaud F, De Mey JG. Structural properties of rat mesenteric small arteries after 4-wk exposure to elevated or reduced blood flow. The American journal of physiology. 1997;273(4 Pt 2):H1699-706.
352. Schroeder A, Mueller O, Stocker S, Salowsky R, Leiber M, Gassmann M, et al. The RIN: an RNA integrity number for assigning integrity values to RNA measurements. BMC molecular biology. 2006;7:3.
353. Freeman WM, Walker SJ, Vrana KE. Quantitative RT-PCR: pitfalls and potential. BioTechniques. 1999;26(1):112-22, 24-5.
354. Livak KJ, Schmittgen TD. Analysis of relative gene expression data using real-time quantitative PCR and the 2(T)(-Delta Delta C) method. Methods. 2001;25(4):402-8.
355. Kilkenny C, Browne WJ, Cuthill IC, Emerson M, Altman DG. Improving bioscience research reporting: the ARRIVE guidelines for reporting animal research. Osteoarthritis and cartilage / OARS, Osteoarthritis Research Society. 2012;20(4):256-60.
356. Nabika T, Nara Y, Ikeda K, Endo J, Yamori Y. Genetic heterogeneity of the spontaneously hypertensive rat. Hypertension. 1991;18(1):12-6.
357. Untergasser A, Cutcutache I, Koressaar T, Ye J, Faircloth BC, Remm M, et al. Primer3--new capabilities and interfaces. Nucleic acids research. 2012;40(15):e115.
358. Chung E, Leinwand LA. Pregnancy as a cardiac stress model. Cardiovascular research. 2014;101(4):561-70.
359. Sala C, Campise M, Ambrose G, Motta T, Zanchetti A, Morganti A. Atrial-Natriuretic-Peptide and Hemodynamic-Changes during Normal Human-Pregnancy. Hypertension. 1995;25(4):631-6.
360. Andersen LB, Przybyl L, Haase N, von Versen-Hoynck F, Qadri F, Jorgensen JS, et al. Vitamin D depletion aggravates hypertension and target-organ damage. Journal of the American Heart Association. 2015;4(2).
361. Resnik JL, Hong C, Resnik R, Kazanegra R, Beede J, Bhalla V, et al. Evaluation of B-type natriuretic peptide (BNP) levels in normal and preeclamptic women. American journal of obstetrics and gynecology. 2005;193(2):450-4.
362. Hameed AB, Chan K, Ghamsary M, Elkayam U. Longitudinal changes in the B-type natriuretic peptide levels in normal pregnancy and postpartum. Clinical cardiology. 2009;32(8):E60-2.
363. Schiffrin EL. Role of endothelin-1 in hypertension. Hypertension. 1999;34(4):876-81.
364. George EM, Granger JP. Endothelin: Key Mediator of Hypertension in Preeclampsia. American journal of hypertension. 2011;24(9):964-9.

365. Zeisler H, Llurba E, Chantraine F, Vatish M, Staff AC, Sennstrom M, et al. Predictive Value of the sFlt-1:PlGF Ratio in Women with Suspected Preeclampsia. N Engl J Med. 2016;374(1):13-22.
366. Bramham K, Seed PT, Lightstone L, Nelson-Piercy C, Gill C, Webster P, et al. Diagnostic and predictive biomarkers for pre-eclampsia in patients with established hypertension and chronic kidney disease. Kidney Int. 2016;89(4):874-85.
367. Banek CT, Bauer AJ, Needham KM, Dreyer HC, Gilbert JS. AICAR administration ameliorates hypertension and angiogenic imbalance in a model of preeclampsia in the rat. American journal of physiology Heart and circulatory physiology. 2013;304(8):H1159-65.
368. Zamudio S, Kovalenko O, Echalar L, Torricos T, Al-Khan A, Alvarez M, et al. Evidence for extraplacental sources of circulating angiogenic growth effectors in human pregnancy. Placenta. 2013;34(12):1170-6.
369. Weissgerber TL, McConico A, Knudsen BE, Butters KA, Hayman SR, White WM, et al. Methodological differences account for inconsistencies in reported free VEGF concentrations in pregnant rats. American journal of physiology Regulatory, integrative and comparative physiology. 2014;306(11):R796-803.
370. Leung DN, Smith SC, To KF, Sahota DS, Baker PN. Increased placental apoptosis in pregnancies complicated by preeclampsia. American journal of obstetrics and gynecology. 2001;184(6):1249-50.
371. Hung TH, Skepper JN, Charnock-Jones DS, Burton GJ. Hypoxia-reoxygenation - A potent inducer of apoptotic changes in the human placenta and possible etiological factor in preeclampsia. Circulation Research. 2002;90(12):1274-81.
372. Coan PM, Conroy N, Burton GJ, Ferguson-Smith AC. Origin and characteristics of glycogen cells in the developing murine placenta. Developmental dynamics : an official publication of the American Association of Anatomists. 2006;235(12):3280-94.
373. Collison M, Glazier AM, Graham D, Morton JJ, Dominiczak MH, Aitman TJ, et al. Cd36 and molecular mechanisms of insulin resistance in the stroke-prone spontaneously hypertensive rat. Diabetes. 2000;49(12):2222-6.
374. Faulkner J, Murphy S, Lee N, Moseley J, LaMarca B. Inhibition of 20-HETE Synthesis Attenuates Elevations in Blood Pressure and Uterine Artery Resistance Index in the RUPP Rat Model of Preeclampsia. Faseb J. 2015;29.
375. Li ZH, Zhang Y, Ma JY, Kapoun AM, Shao Q, Kerr I, et al. Recombinant vascular endothelial growth factor 121 attenuates hypertension and improves kidney damage in a rat model of preeclampsia. Hypertension. 2007;50(4):686-92.
376. Johnston BM. Fetal growth retardation and increased placental weight in the spontaneously hypertensive rat. Reproduction, fertility, and development. 1995;7(3):639-45.
377. Cotechini T, Graham CH. Aberrant maternal inflammation as a cause of pregnancy complications: A potential therapeutic target? Placenta. 2015;36(8):960-6.
378. Mor G, Cardenas I, Abrahams V, Guller S. Inflammation and pregnancy: the role of the immune system at the implantation site. Ann Ny Acad Sci. 2011;1221:80-7.
379. Dekel N, Gnainsky Y, Granot I, Mor G. Inflammation and Implantation. Am J Reprod Immunol. 2010;63(1):17-21.
380. Thomson AJ, Telfer JF, Young A, Campbell S, Stewart CJR, Cameron IT, et al. Leukocytes infiltrate the myometrium during human parturition: further

evidence that labour is an inflammatory process. Hum Reprod. 1999;14(1):229-36.
381. Staun-Ram E, Shalev E. Human trophoblast function during the implantation process. Reproductive biology and endocrinology : RB&E. 2005;3:56.
382. Basu J, Agamasu E, Bendek B, Salafia CM, Mishra A, Benfield N, et al. Placental tumor necrosis factor-alpha protein expression during normal human gestation. The journal of maternal-fetal & neonatal medicine : the official journal of the European Association of Perinatal Medicine, the Federation of Asia and Oceania Perinatal Societies, the International Society of Perinatal Obstet. 2016:1-5.
383. Meisser A, Chardonnens D, Campana A, Bischof P. Effects of tumour necrosis factor-α, interleukin-1 α, macrophage colony stimulating factor and transforming growth factor ß on trophoblastic matrix metalloproteinases. Molecular Human Reproduction. 1999;5(3):252-60.
384. Monzon-Bordonaba F, Vadillo-Ortega F, Feinberg RF. Modulation of trophoblast function by tumor necrosis factor-alpha: a role in pregnancy establishment and maintenance? American journal of obstetrics and gynecology. 2002;187(6):1574-80.
385. Cotechini T, Komisarenko M, Sperou A, Macdonald-Goodfellow S, Adams MA, Graham CH. Inflammation in rat pregnancy inhibits spiral artery remodeling leading to fetal growth restriction and features of preeclampsia. The Journal of experimental medicine. 2014;211(1):165-79.
386. Elovitz MA, Wang Z, Chien EK, Rychlik DF, Phillippe M. A new model for inflammation-induced preterm birth: the role of platelet-activating factor and Toll-like receptor-4. The American journal of pathology. 2003;163(5):2103-11.
387. Falcon BJ, Cotechini T, Macdonald-Goodfellow SK, Othman M, Graham CH. Abnormal inflammation leads to maternal coagulopathies associated with placental haemostatic alterations in a rat model of foetal loss. Thromb Haemostasis. 2012;107(3):438-47.
388. Renaud SJ, Cotechini T, Quirt JS, Macdonald-Goodfellow SK, Othman M, Graham CH. Spontaneous Pregnancy Loss Mediated by Abnormal Maternal Inflammation in Rats Is Linked to Deficient Uteroplacental Perfusion. Journal of Immunology. 2011;186(3):1799-808.
389. LaMarca BB, Cockrell K, Sullivan E, Bennett W, Granger JP. Role of endothelin in mediating tumor necrosis factor-induced hypertension in pregnant rats. Hypertension. 2005;46(1):82-6.
390. Kupferminc MJ, Peaceman AM, Wigton TR, Rehnberg KA, Socol ML. Tumor-Necrosis-Factor-Alpha Is Elevated in Plasma and Amniotic-Fluid of Patients with Severe Preeclampsia. American journal of obstetrics and gynecology. 1994;170(6):1752-9.
391. Szarka A, Rigo J, Jr., Lazar L, Beko G, Molvarec A. Circulating cytokines, chemokines and adhesion molecules in normal pregnancy and preeclampsia determined by multiplex suspension array. BMC immunology. 2010;11:59.
392. Tosun M, Celik H, Avci B, Yavuz E, Alper T, Malatyalioglu E. Maternal and umbilical serum levels of interleukin-6, interleukin-8, and tumor necrosis factor-alpha in normal pregnancies and in pregnancies complicated by preeclampsia. The journal of maternal-fetal & neonatal medicine : the official journal of the European Association of Perinatal Medicine, the Federation of Asia and Oceania Perinatal Societies, the International Society of Perinatal Obstet. 2010;23(8):880-6.

393. Benyo DF, Smarason A, Redman CW, Sims C, Conrad KP. Expression of inflammatory cytokines in placentas from women with preeclampsia. The Journal of clinical endocrinology and metabolism. 2001;86(6):2505-12.
394. Wang Y, Walsh SW. TNF alpha concentrations and mRNA expression are increased in preeclamptic placentas. Journal of reproductive immunology. 1996;32(2):157-69.
395. Zubor P, Dokus K, Zigo I, Skerenova M, Pullmann R, Danko J. TNF-alpha G308A Gene Polymorphism Has an Impact on Renal Function, Microvascular Permeability, Organ Involvement and Severity of Preeclampsia. Gynecol Obstet Inves. 2014;78(3):150-61.
396. Stonek F, Hafner E, Metzenbauer M, Katharina S, Stumpflen I, Schneeberger C, et al. Absence of an association of tumor necrosis factor (TNF)-alpha G308A, interleukin-6 (IL-6) G174C and interleukin-10 (IL-10) G1082A polymorphism in women with preeclampsia. Journal of reproductive immunology. 2008;77(1):85-90.
397. Anderson NH, Devlin AM, Graham D, Morton JJ, Hamilton CA, Reid JL, et al. Telemetry for cardiovascular monitoring in a pharmacological study: new approaches to data analysis. Hypertension. 1999;33(1 Pt 2):248-55.
398. Spiers A, Padmanabhan N. A guide to wire myography. Methods in molecular medicine. 2005;108:91-104.
399. Gutkowska J, Granger JP, Lamarca BB, Danalache BA, Wang DH, Jankowski M. Changes in cardiac structure in hypertension produced by placental ischemia in pregnant rats: effect of tumor necrosis factor blockade. J Hypertens. 2011;29(6):1203-12.
400. Tran LT, MacLeod KM, McNeill JH. Chronic etanercept treatment prevents the development of hypertension in fructose-fed rats. Mol Cell Biochem. 2009;330(1-2):219-28.
401. Venegas-Pont M, Manigrasso MB, Grifoni SC, LaMarca BB, Maric C, Racusen LC, et al. Tumor Necrosis Factor-alpha Antagonist Etanercept Decreases Blood Pressure and Protects the Kidney in a Mouse Model of Systemic Lupus Erythematosus. Hypertension. 2010;56(4):643-9.
402. Elmarakby AA, Quigley JE, Imig JD, Pollock JS, Pollock DM. TNF-alpha inhibition reduces renal injury in DOCA-salt hypertensive rats. Am J Physiol-Reg I. 2008;294(1):R76-R83.
403. Berthelsen BG, Fjeldsoe-Nielsen H, Nielsen CT, Hellmuth E. Etanercept concentrations in maternal serum, umbilical cord serum, breast milk and child serum during breastfeeding. Rheumatology. 2010;49(11):2225-7.
404. Murashima A, Watanabe N, Ozawa N, Saito H, Yamaguchi K. Etanercept during pregnancy and lactation in a patient with rheumatoid arthritis: drug levels in maternal serum, cord blood, breast milk and the infant's serum. Ann Rheum Dis. 2009;68(11):1793-4.
405. Ma R, Gu Y, Groome LJ, Wang Y. ADAM17 regulates TNF alpha production by placental trophoblasts. Placenta. 2011;32(12):975-80.
406. Warrington JP, Drummond HA, Granger JP, Ryan MJ. Placental ischemia-induced increases in brain water content and cerebrovascular permeability: role of TNF-alpha. Am J Physiol-Reg I. 2015;309(11):R1425-R31.
407. Murphy SR, LaMarca BBD, Parrish M, Cockrell K, Granger JP. Control of soluble fms-like tyrosine-1 (sFlt-1) production response to placental ischemia/hypoxia: role of tumor necrosis factor-alpha. Am J Physiol-Reg I. 2013;304(2):R130-R5.
408. Gelber SE, Brent E, Redecha P, Perino G, Tomlinson S, Davisson RL, et al. Prevention of Defective Placentation and Pregnancy Loss by Blocking Innate

Immune Pathways in a Syngeneic Model of Placental Insufficiency. Journal of Immunology. 2015;195(3):1129-38.
409. Murdaca G, Colombo BM, Cagnati P, Gulli R, Spano F, Puppo F. Update upon efficacy and safety of TNF-alpha inhibitors. Expert Opin Drug Saf. 2012;11(1):1-5.
410. Winger EE, Reed JL. Treatment with tumor necrosis factor inhibitors and intravenous immunoglobulin improves live birth rates in women with recurrent spontaneous abortion. Am J Reprod Immunol. 2008;60(1):8-16.
411. Jerzak M, Ohams M, Gorski A, Baranowski W. Etanercept immunotherapy in women with a history of recurrent reproductive failure. Ginekologia polska. 2012;83(4):260-4.
412. Johnson DL, Jones KL, Chambers C, Grp OCR. Pregnancy outcomes in women exposed to etanercept: The OTIS autoimmune diseases in pregnancy project. Arthritis Rheum-Us. 2008;58(9):S682-S.
413. Mor G, Cardenas I. The immune system in pregnancy: a unique complexity. Am J Reprod Immunol. 2010;63(6):425-33.
414. Branch DW. Physiologic adaptations of pregnancy. Am J Reprod Immunol. 1992;28(3-4):120-2.
415. Hartley JD, Ferguson BJ, Moffett A. The role of shed placental DNA in the systemic inflammatory syndrome of preeclampsia. American journal of obstetrics and gynecology. 2015;213(3):268-77.
416. Sacks G, Sargent I, Redman C. An innate view of human pregnancy. Immunology today. 1999;20(3):114-8.
417. Somerset DA, Zheng Y, Kilby MD, Sansom DM, Drayson MT. Normal human pregnancy is associated with an elevation in the immune suppressive CD25(+) CD4(+) regulatory T-cell subset. Immunology. 2004;112(1):38-43.
418. Tilburgs T, Roelen DL, van der Mast BJ, van Schip JJ, Kleijburg C, de Groot-Swings GM, et al. Differential distribution of CD4(+)CD25(bright) and CD8(+)CD28(-) T-cells in decidua and maternal blood during human pregnancy. Placenta. 2006;27 Suppl A:S47-53.
419. Mjösberg J, Svensson J, Johansson E, Hellström L, Casas R, Jenmalm MC, et al. Systemic Reduction of Functionally Suppressive CD4dimCD25highFoxp3+ Tregs in Human Second Trimester Pregnancy Is Induced by Progesterone and 17β-Estradiol. The Journal of Immunology. 2009;183(1):759-69.
420. Shibuya T, Izuchi K, Kuroiwa A, Okabe N, Shirakawa K. Study on nonspecific immunity in pregnant women: increased chemiluminescence response of peripheral blood phagocytes. American journal of reproductive immunology and microbiology : AJRIM. 1987;15(1):19-23.
421. Cordeau M, Herblot S, Charrier E, Audibert F, Cordeiro P, Harnois M, et al. Defects in CD54 and CD86 up-regulation by plasmacytoid dendritic cells during pregnancy. Immunological investigations. 2012;41(5):497-506.
422. Fukui A, Funamizu A, Yokota M, Yamada K, Nakamua R, Fukuhara R, et al. Uterine and circulating natural killer cells and their roles in women with recurrent pregnancy loss, implantation failure and preeclampsia. Journal of reproductive immunology. 2011;90(1):105-10.
423. Robson A, Harris LK, Innes BA, Lash GE, Aljunaidy MM, Aplin JD, et al. Uterine natural killer cells initiate spiral artery remodeling in human pregnancy. Faseb J. 2012;26(12):4876-85.
424. Moffett A, Regan L, Braude P. Natural killer cells, miscarriage, and infertility. Bmj. 2004;329(7477):1283-5.
425. Hidaka Y, Amino N, Iwatani Y, Kaneda T, Mitsuda N, Morimoto Y, et al. Changes in natural killer cell activity in normal pregnant and postpartum

women: increases in the first trimester and postpartum period and decrease in late pregnancy. Journal of reproductive immunology. 1991;20(1):73-83.
426. Fukui A, Yokota M, Funamizu A, Nakamua R, Fukuhara R, Yamada K, et al. Changes of NK Cells in Preeclampsia. Am J Reprod Immunol. 2012;67(4):278-86.
427. Burke SD, Barrette VF, Carter AL, Gravel J, Adams MA, Croy BA. Cardiovascular adaptations of pregnancy in T and B cell-deficient mice. Biology of reproduction. 2011;85(3):605-14.
428. Darmochwal-Kolarz D, Rolinski J, Leszczynska-Gorzelak B, Oleszczuk J. The expressions of intracellular cytokines in the lymphocytes of preeclamptic patients. Am J Reprod Immunol. 2002;48(6):381-6.
429. Molvarec A, Ito M, Shima T, Yoneda S, Toldi G, Stenczer B, et al. Decreased proportion of peripheral blood vascular endothelial growth factor-expressing T and natural killer cells in preeclampsia. American journal of obstetrics and gynecology. 2010;203(6).
430. Hanna J, Goldman-Wohl D, Hamani Y, Avraham I, Greenfield C, Natanson-Yaron S, et al. Decidual NK cells regulate key developmental processes at the human fetal-maternal interface. Nat Med. 2006;12(9):1065-74.
431. Ain R, Canham LN, Soares MJ. Gestation stage-dependent intrauterine trophoblast cell invasion in the rat and mouse: novel endocrine phenotype and regulation. Developmental biology. 2003;260(1):176-90.
432. Yu TK, Caudell EG, Smid C, Grimm EA. IL-2 activation of NK cells: involvement of MKK1/2/ERK but not p38 kinase pathway. J Immunol. 2000;164(12):6244-51.
433. Ikejima T, Okusawa S, Ghezzi P, van der Meer JW, Dinarello CA. Interleukin-1 induces tumor necrosis factor (TNF) in human peripheral blood mononuclear cells in vitro and a circulating TNF-like activity in rabbits. The Journal of infectious diseases. 1990;162(1):215-23.
434. Hunter CA, Timans J, Pisacane P, Menon S, Cai G, Walker W, et al. Comparison of the effects of interleukin-1 alpha, interleukin-1 beta and interferon-gamma-inducing factor on the production of interferon-gamma by natural killer. European journal of immunology. 1997;27(11):2787-92.
435. Luster AD, Unkeless JC, Ravetch JV. Gamma-interferon transcriptionally regulates an early-response gene containing homology to platelet proteins. Nature. 1985;315(6021):672-6.
436. Farber JM. A macrophage mRNA selectively induced by gamma-interferon encodes a member of the platelet factor 4 family of cytokines. Proceedings of the National Academy of Sciences of the United States of America. 1990;87(14):5238-42.
437. Moore MP, Carter NP, Redman CW. Lymphocyte subsets defined by monoclonal antibodies in human pregnancy. Am J Reprod Immunol. 1983;3(4):161-4.
438. Redman CWG, Tannetta DS, Dragovic RA, Gardiner C, Southcombe JH, Collett GP, et al. Review: Does size matter? Placental debris and the pathophysiology of pre-eclampsia. Placenta. 2012;33, Supplement:S48-S54.
439. Tannetta DS, Dragovic RA, Gardiner C, Redman CW, Sargent IL. Characterisation of syncytiotrophoblast vesicles in normal pregnancy and pre-eclampsia: expression of Flt-1 and endoglin. Plos One. 2013;8(2):e56754.
440. Gardiner C, Tannetta DS, Simms CA, Harrison P, Redman CW, Sargent IL. Syncytiotrophoblast microvesicles released from pre-eclampsia placentae exhibit increased tissue factor activity. Plos One. 2011;6(10):e26313.

441. Kambe S, Yoshitake H, Yuge K, Ishida Y, Ali MM, Takizawa T, et al. Human exosomal placenta-associated miR-517a-3p modulates the expression of PRKG1 mRNA in Jurkat cells. Biology of reproduction. 2014;91(5):129.
442. Sabapatha A, Gercel-Taylor C, Taylor DD. Specific isolation of placenta-derived exosomes from the circulation of pregnant women and their immunoregulatory consequences. Am J Reprod Immunol. 2006;56(5-6):345-55.
443. Hedlund M, Stenqvist AC, Nagaeva O, Kjellberg L, Wulff M, Baranov V, et al. Human Placenta Expresses and Secretes NKG2D Ligands via Exosomes that Down-Modulate the Cognate Receptor Expression: Evidence for Immunosuppressive Function. Journal of Immunology. 2009;183(1):340-51.
444. Jones DC, Hayslett JP. Outcome of pregnancy in women with moderate or severe renal insufficiency. N Engl J Med. 1996;335(4):226-32.
445. Imbasciati E, Gregorini G, Cabiddu G, Gammaro L, Ambroso G, Del Giudice A, et al. Pregnancy in CKD stages 3 to 5: fetal and maternal outcomes. Am J Kidney Dis. 2007;49(6):753-62.
446. Dunlop W. Serial Changes in Renal Hemodynamics during Normal Human-Pregnancy. British journal of obstetrics and gynaecology. 1981;88(1):1-9.
447. Cheung KL, Lafayette RA. Renal Physiology of Pregnancy. Advances in chronic kidney disease. 2013;20(3):209-14.
448. Davison JM, Lindheimer MD. Changes in renal haemodynamics and kidney weight during pregnancy in the unanaesthetized rat. The Journal of physiology. 1980;301:129-36.
449. Odutayo A, Hladunewich M. Obstetric nephrology: renal hemodynamic and metabolic physiology in normal pregnancy. Clinical journal of the American Society of Nephrology : CJASN. 2012;7(12):2073-80.
450. Bidani AK, Griffin KA. Pathophysiology of hypertensive renal damage: implications for therapy. Hypertension. 2004;44(5):595-601.
451. Hladunewich M, Karumanchi SA, Lafayette R. Pathophysiology of the clinical manifestations of preeclampsia. Clinical journal of the American Society of Nephrology : CJASN. 2007;2(3):543-9.
452. Lafayette RA, Druzin M, Sibley R, Derby G, Malik T, Huie P, et al. Nature of glomerular dysfunction in pre-eclampsia. Kidney Int. 1998;54(4):1240-9.
453. Dechend R, Gratze P, Wallukat G, Shagdarsuren E, Plehm R, Brasen JH, et al. Agonistic autoantibodies to the AT1 receptor in a transgenic rat model of preeclampsia. Hypertension. 2005;45(4):742-6.
454. Norden AGW, Rodriguez-Cutillas P, Unwin RJ. Clinical urinary peptidomics: Learning to walk before we can run. Clinical chemistry. 2007;53(3):375-6.
455. Decramer S, de Peredo AG, Breuil B, Mischak H, Monsarrat B, Bascands JL, et al. Urine in Clinical Proteomics. Mol Cell Proteomics. 2008;7(10):1850-62.
456. Theodorescu D, Wittke S, Ross MM, Walden M, Conaway M, Just I, et al. Discovery and validation of new protein biomarkers for 4 urothelial cancer: a prospective analysis. Lancet Oncol. 2006;7(3):230-40.
457. Delles C, Diez J, Dominiczak AF. Urinary proteomics in cardiovascular disease: Achievements, limits and hopes. Proteom Clin Appl. 2011;5(5-6):222-32.
458. Carty DM, Schiffer E, Delles C. Proteomics in hypertension. J Hum Hypertens. 2013;27(4):211-6.
459. Kolialexi A, Mavreli D, Tounta G, Mavrou A, Papantoniou N. Urine proteomic studies in preeclampsia. Proteom Clin Appl. 2015;9(5-6):501-6.
460. Albalat A, Bitsika V, Zurbig P, Siwy J, Mullen W. High-Resolution Proteome/Peptidome Analysis of Body Fluids by Capillary Electrophoresis Coupled with MS. In: Volpi N, Maccari F, editors. Capillary Electrophoresis of

Biomolecules: Methods and Protocols. Totowa, NJ: Humana Press; 2013. p. 153-65.
461. Neuhoff N, Kaiser T, Wittke S, Krebs R, Pitt A, Burchard A, et al. Mass spectrometry for the detection of differentially expressed proteins: a comparison of surface-enhanced laser desorption/ionization and capillary electrophoresis/mass spectrometry. Rapid communications in mass spectrometry : RCM. 2004;18(2):149-56.
462. Rouse R, Siwy J, Mullen W, Mischak H, Metzger J, Hanig J. Proteomic candidate biomarkers of drug-induced nephrotoxicity in the rat. Plos One. 2012;7(4):e34606.
463. Graf C, Maser-Gluth C, de Muinck Keizer W, Rettig R. Sodium retention and hypertension after kidney transplantation in rats. Hypertension. 1993;21(5):724-30.
464. Griffin KA, Churchill PC, Picken M, Webb RC, Kurtz TW, Bidani AK. Differential salt-sensitivity in the pathogenesis of renal damage in SHR and stroke prone SHR. American journal of hypertension. 2001;14(4):311-20.
465. Padmanabhan S, Graham L, Ferreri NR, Graham D, McBride M, Dominiczak AF. Uromodulin, an emerging novel pathway for blood pressure regulation and hypertension. Hypertension. 2014;64(5):918-23.
466. Muchmore AV, Decker JM. Uromodulin - a Unique 85-Kilodalton Immunosuppressive Glycoprotein Isolated from Urine of Pregnant-Women. Science. 1985;229(4712):479-81.
467. Brown MA, Wang MX, Buddle ML, Carlton MA, Cario GM, Zammit VC, et al. Albumin Excretory Rate in Normal and Hypertensive Pregnancy. Clinical science. 1994;86(3):251-5.
468. Kononikhin AS, Starodubtseva NL, Bugrova AE, Shirokova VA, Chagovets VV, Indeykina MI, et al. An untargeted approach for the analysis of the urine peptidome of women with preeclampsia. Journal of proteomics. 2016.
469. Matafora V, Zagato L, Ferrandi M, Molinari I, Zerbini G, Casamassima N, et al. Quantitative proteomics reveals novel therapeutic and diagnostic markers in hypertension. BBA clinical. 2014;2:79-87.
470. Rioux JD, Abbas AK. Paths to understanding the genetic basis of autoimmune disease. Nature. 2005;435(7042):584-9.
471. Ruchat SM, Despres JP, Weisnagel SJ, Chagnon YC, Bouchard C, Perusse L. Genome-wide linkage analysis for circulating levels of adipokines and C-reactive protein in the Quebec family study (QFS). J Hum Genet. 2008;53(7):629-36.
472. Kreutz R, Struk B, Stock P, Hubner N, Ganten D, Lindpaintner K. Evidence for primary genetic determination of heart rate regulation - Chromosomal mapping of a genetic locus in the rat. Circulation. 1997;96(4):1078-81.
473. Grabowski K, Koplin G, Aliu B, Schulte L, Schulz A, Kreutz R. Mapping and confirmation of a major left ventricular mass QTL on rat chromosome 1 by contrasting SHRSP and F344 rats. Physiol Genomics. 2013;45(18):827-33.
474. Gu LP, Dene H, Deng AY, Hoebee B, Bihoreau MT, James M, et al. Genetic mapping of two blood pressure quantitative trait loci on rat chromosome 1. Journal of Clinical Investigation. 1996;97(3):777-88.
475. Gigante B, Rubattu S, Stanzione R, Lombardi A, Baldi A, Baldi F, et al. Contribution of genetic factors to renal lesions in the stroke-prone spontaneously hypertensive rat. Hypertension. 2003;42(4):702-6.
476. Schroeder DI, Blair JD, Lott P, Yu HO, Hong D, Crary F, et al. The human placenta methylome. Proceedings of the National Academy of Sciences of the United States of America. 2013;110(15):6037-42.

477. Hemmi H, Takeuchi O, Kawai T, Kaisho T, Sato S, Sanjo H, et al. A Toll-like receptor recognizes bacterial DNA. Nature. 2000;408(6813):740-5.
478. Goulopoulou S, Matsumoto T, Bomfim GF, Webb RC. Toll-like receptor 9 activation: a novel mechanism linking placenta-derived mitochondrial DNA and vascular dysfunction in preeclampsia. Clinical science (London, England : 1979). 2012;123(7):429-35.
479. Fandrich F, Zepernick-Kalinski C, Gebhardt H, Henne-Bruns D, Zavazava N, Lin X. The role of natural killer cell mediated caspases activation in a graft-versus-host disease model of semiallogeneic small bowel transplantation. Transplant immunology. 1999;7(1):1-7.
480. Jian L, Fa X, Zhou Z, Liu S. Functional analysis of UMOD gene and its effect on inflammatory cytokines in serum of essential hypertension patients. International journal of clinical and experimental pathology. 2015;8(9):11356-63.
481. Graham LA, Padmanabhan S, Fraser NJ, Kumar S, Bates JM, Raffi HS, et al. Validation of Uromodulin as a Candidate Gene for Human Essential Hypertension. Hypertension. 2014;63(3):551-8.
482. Scolari F, Izzi C, Ghiggeri GM. Uromodulin: from monogenic to multifactorial diseases. Nephrol Dial Transpl. 2015;30(8):1250-6.
483. Hession C, Decker JM, Sherblom AP, Kumar S, Yue CC, Mattaliano RJ, et al. Uromodulin (Tamm-Horsfall Glycoprotein) - a Renal Ligand for Lymphokines. Science. 1987;237(4821):1479-84.
484. Hoyer JR. Tubulointerstitial Immune-Complex Nephritis in Rats Immunized with Tamm-Horsfall Protein. Kidney Int. 1980;17(3):284-92.
485. Saemann MD, Weichhart T, Zeyda M, Staffler G, Schunn M, Stuhlmeier KM, et al. Tamm-Horsfall glycoprotein links innate immune cell activation with adaptive immunity via a Toll-like receptor-4-dependent mechanism. The Journal of clinical investigation. 2005;115(2):468-75.
486. Ong SS, Baker PN, Mayhew TM, Dunn WR. Remodeling of myometrial radial arteries in preeclampsia. American journal of obstetrics and gynecology. 2005;192(2):572-9.
487. Osol G, Cipolla M. Pregnancy-induced changes in the three-dimensional mechanical properties of pressurized rat uteroplacental (radial) arteries. American journal of obstetrics and gynecology. 1993;168(1 Pt 1):268-74.
488. Gokina NI, Mandala M, Osol G. Induction of localized differences in rat uterine radial artery behavior and structure during gestation. American journal of obstetrics and gynecology. 2003;189(5):1489-93.
489. McCarthy FP, Drewlo S, English FA, Kingdom J, Johns EJ, Kenny LC, et al. Evidence Implicating Peroxisome Proliferator-Activated Receptor-gamma in the Pathogenesis of Preeclampsia. Hypertension. 2011;58(5):882-U447.
490. Gokina NI, Chan SL, Chapman AC, Oppenheimer K, Jetton TL, Cipolla MJ. Inhibition of PPAR gamma during rat pregnancy causes intrauterine growth restriction and attenuation of uterine vasodilation. Frontiers in physiology. 2013;4.
491. Lunghi L, Ferretti ME, Medici S, Biondi C, Vesce F. Control of human trophoblast function. Reproductive biology and endocrinology : RB&E. 2007;5:6.
492. Otun HA, Lash GE, Innes BA, Bulmer JN, Naruse K, Hannon T, et al. Effect of tumour necrosis factor-alpha in combination with interferon-gamma on first trimester extravillous trophoblast invasion. Journal of reproductive immunology. 2011;88(1):1-11.

493. Huber AV, Saleh L, Bauer S, Husslein P, Knofler M. TNFalpha-mediated induction of PAI-1 restricts invasion of HTR-8/SVneo trophoblast cells. Placenta. 2006;27(2-3):127-36.
494. Bauer S, Pollheimer J, Hartmann J, Husslein P, Aplin JD, Knofler M. Tumor necrosis factor-alpha inhibits trophoblast migration through elevation of plasminogen activator inhibitor-1 in first-trimester villous explant cultures. J Clin Endocr Metab. 2004;89(2):812-22.
495. Zhu JY, Pang ZJ, Yu YH. Regulation of trophoblast invasion: the role of matrix metalloproteinases. Reviews in obstetrics & gynecology. 2012;5(3-4):e137-43.
496. Xu B, Nakhla S, Makris A, Hennessy A. TNF-alpha inhibits trophoblast integration into endothelial cellular networks. Placenta. 2011;32(3):241-6.
497. Chen LM, Liu B, Zhao HB, Stone P, Chen Q, Chamley L. IL-6, TNFalpha and TGFbeta promote nonapoptotic trophoblast deportation and subsequently causes endothelial cell activation. Placenta. 2010;31(1):75-80.
498. Tessier DR, Raha S, Holloway AC, Yockell-Lelievre J, Tayade C, Gruslin A. Characterization of immune cells and cytokine localization in the rat utero-placental unit mid- to late gestation. Journal of reproductive immunology. 2015;110:89-101.
499. Groen B, Links TP, Lefrandt JD, van den Berg PP, de Vos P, Faas MM. Aberrant Pregnancy Adaptations in the Peripheral Immune Response in Type 1 Diabetes: A Rat Model. Plos One. 2013;8(6):e65490.
500. Szasz T, Webb RC. Perivascular adipose tissue: more than just structural support. Clinical science. 2012;122(1-2):1-12.
501. Walker JA, Barlow JL, McKenzie ANJ. Innate lymphoid cells - how did we miss them? Nat Rev Immunol. 2013;13(2):75-87.
502. Satoh-Takayama N, Vosshenrich CAJ, Lesjean-Pottier S, Sawa S, Lochner M, Rattis F, et al. Microbial Flora Drives Interleukin 22 Production in Intestinal NKp46(+) Cells that Provide Innate Mucosal Immune Defense. Immunity. 2008;29(6):958-70.
503. Westgaard IH, Berg SF, Vaage JT, Wang LL, Yokoyama WM, Dissen E, et al. Rat NKp46 activates natural killer cell cytotoxicity and is associated with FcεRIγ and CD3ζ. Journal of leukocyte biology. 2004;76(6):1200-6.
504. Beausejour A, Auger K, St-Louis J, Brochu M. High-sodium intake prevents pregnancy-induced decrease of blood pressure in the rat. American journal of physiology Heart and circulatory physiology. 2003;285(1):H375-83.
505. St-Louis J, Sicotte B, Beausejour A, Brochu M. Remodeling and angiotensin II responses of the uterine arcuate arteries of pregnant rats are altered by low- and high-sodium intake. Reproduction. 2006;131(2):331-9.
506. Beausejour A, Bibeau K, Lavoie JC, St-Louis J, Brochu M. Placental oxidative stress in a rat model of preeclampsia. Placenta. 2007;28(1):52-8.
507. Nara Y, Ikeda K, Nabika T, Sawamura M, Mano M, Endo J, et al. Comparison of Salt Sensitivity of Male and Female F2 Progeny from Crosses between Wky and Shrsp Rats. Clin Exp Pharmacol P. 1994;21(11):899-902.
508. Chen J, Delaney KH, Kwiecien JM, Lee RM. The effects of dietary sodium on hypertension and stroke development in female stroke-prone spontaneously hypertensive rats. Exp Mol Pathol. 1997;64(3):173-83.
509. Rakova N, Muller DN, Staff AC, Luft FC, Dechend R. Novel ideas about salt, blood pressure, and pregnancy. Journal of reproductive immunology. 2014;101:135-9.
510. Machnik A, Neuhofer W, Jantsch J, Dahlmann A, Tammela T, Machura K, et al. Macrophages regulate salt-dependent volume and blood pressure by a

vascular endothelial growth factor-C-dependent buffering mechanism. Nat Med. 2009;15(5):545-52.
511. Kleinewietfeld M, Manzel A, Titze J, Kvakan H, Yosef N, Linker RA, et al. Sodium chloride drives autoimmune disease by the induction of pathogenic TH17 cells. Nature. 2013;496(7446):518-22.
512. Fu B, Tian Z, Wei H. TH17 cells in human recurrent pregnancy loss and pre-eclampsia. Cell Mol Immunol. 2014;11(6):564-70.
513. Ananth CV, Keyes KM, Wapner RJ. Pre-eclampsia rates in the United States, 1980-2010: age-period-cohort analysis. Bmj. 2013;347:f6564.